

AN EXPERIMENTAL STUDY ON THE TREATMENT OF  
EXPANSIVE SOILS BY GRANULAR MATERIALS

A THESIS SUBMITTED TO  
THE GRADUATE SCHOOL OF NATURAL AND APPLIED SCIENCES  
OF MIDDLE EAST TECHNICAL UNIVERSITY

BY

TİMUÇİN HERGÜL

IN PARTIAL FULFILLMENT OF THE REQUIREMENTS  
FOR  
THE DEGREE OF DOCTOR OF PHILOSOPHY  
IN  
CIVIL ENGINEERING

SEPTEMBER 2012

Approval of the thesis:

**AN EXPERIMENTAL STUDY ON THE TREATMENT OF  
EXPANSIVE SOILS BY GRANULAR MATERIALS**

submitted by **TİMUÇİN HERGÜL** in partial fulfillment of the requirements for the degree of **Doctor of Philosophy in Civil Engineering Department, Middle East Technical University** by,

Prof. Dr. Canan Özgen  
Dean, Graduate School of **Natural and Applied Sciences**

\_\_\_\_\_

Prof. Dr. Güney Özcebe  
Head of Department, **Civil Engineering**

\_\_\_\_\_

Prof. Dr. Erdal Çokça  
Supervisor, **Civil Engineering Department, METU**

\_\_\_\_\_

**Examining Committee Members:**

Prof. Dr. Orhan Erol  
Civil Engineering Department, METU

\_\_\_\_\_

Prof. Dr. Erdal Çokça  
Civil Engineering Department, METU

\_\_\_\_\_

Prof. Dr. Reşat Ulusay  
Geological Engineering Department, Hacettepe University

\_\_\_\_\_

Prof. Dr. Kemal Önder Çetin  
Civil Engineering Department, METU

\_\_\_\_\_

Asst.Prof. Dr. Nejan Huvaj Sarıhan  
Civil Engineering Department, METU

\_\_\_\_\_

**Date:** 14.09.2012

**I hereby declare that all information in this document has been obtained and presented in accordance with academic rules and ethical conduct. I also declare that, as required by these rules and conduct, I have fully cited and referenced all materials and results that are not original to this work.**

Name, Last Name : Timuçin Hergül

Signature :

## **ABSTRACT**

### **AN EXPERIMENTAL STUDY ON THE TREATMENT OF EXPANSIVE SOILS BY GRANULAR MATERIALS**

Hergül, Timuçin

Ph.D., Department of Civil Engineering

Supervisor: Prof. Dr. Erdal Çokça

September, 2012, 322 pages

Expansive soils are a worldwide problem that possesses various challenges for civil engineers. With increasing water content, they exhibit excessive volume changes, resulting in large horizontal and vertical stresses to the structures located or buried in these regions. The most common method to minimize this effect is to replace these types of clays around the proposed structure with non-expansive soils. For the cases needing larger volume of replacement, either sidewalls or the foundations must be designed to cater for the anticipated pressures or a suitable improvement technique shall be applied in place.

In this experimental study, it is intended to investigate the possible positive effects of trenches backfilled with granular material such as crushed stone or rock on the improvement of swell parameters of expansive soils. Thin-wall oedometer tests, conventional oedometer tests and larger size tests with moulds were performed on artificially compacted untreated and granular fill treated samples for this purpose. The trenches were modeled by opening a hole with a diameter that satisfies the predicted percent trench content at the center of the soil samples, which was then backfilled with granular material. Modified thin-wall oedometer tests were performed to measure the lateral swell pressures of both untreated



and treated samples, whereas the conventional oedometer tests and tests on samples placed in moulds were performed to measure the vertical swell parameters of soils.

It was observed that both the vertical swell percentages as well as the lateral swell pressures reduced considerably as the volume of granular material filled trench was increased. The treatment was observed to be more remarkable under the surcharge effect of a light weight structure or a fill placed on top.

Keywords: Lateral Swell Pressure, Vertical Swell, Thin-Wall Oedometer Ring, Treatment of Expansive Soils, Granular Fill.

## ÖZ

### ŞİŞEN ZEMİNLERİN TANELİ MALZEMEYLE İYİLEŞTİRİLMESİ ÜZERİNE DENEYSEL BİR ÇALIŞMA

Hergül, Timuçin

Doktora, İnşaat Mühendisliği Bölümü

Tez Yöneticisi: Prof. Dr. Erdal Çokça

Eylül, 2012, 322 sayfa

Şişen zeminler tüm dünyada inşaat mühendisleri için sorun teşkil etmeye aday özellikler sergilemektedir. Bu tip zeminler, su içeriklerinin artmasıyla birlikte ciddi oranda hacimsel değişikliklere uğramakta ve üzerlerinde inşa edilmiş yapılarda büyük yatay ve düşey gerilme artışlarına neden olmaktadır. Şişen zeminlerin olumsuz etkilerinin azaltılmasına yönelik en sık kullanılan yöntem, planlanan yapı çevresinde bulunan killerin sahadan uzaklaştırılarak yerine şişmeyen özellikte zeminlerin yerleştirilmesidir. Yapılacak iyileştirmenin büyük hacimli olması durumunda perde duvarlar ve temeller oluşacak şişme basınçlarını güvenli bir biçimde taşıyacak şekilde tasarımlanmalı, ya da şişme basınçlarını düşürmeye yönelik uygun bir yerinde iyileştirme yöntemi seçilerek uygulanmalıdır.

Bu deneysel çalışmada; kırmataş, kırma kaya gibi taneli bir malzemeyle doldurulmuş hendeklerin şişen zeminlerin şişme parametreleri üzerindeki muhtemel olumlu etkilerinin araştırılması amaçlanmıştır. Bu amaçla, hem taneli malzemeyle iyileştirilmiş, hem de iyileştirilmemiş şişen zemin örnekleri üzerinde ince çeperli odometre, klasik odometre ve daha büyük boyutta silindirik kalıpla karşılaştırmalı deneyler yapılmıştır. Hendekler, örneğin ortasında öngörülen hacimsel iyileştirme yüzdesini sağlayacak çapta açılmış deliklere taneli malzeme

doldurulması yöntemiyle modellenmiştir. İnce çeperli odometre deneyleri, iyileştirilmiş ve iyileştirilmemiş örneklerin yanal şişme basınçlarının ölçülmesi; klasik odometre ve silindirik kalıplarda gerçekleştirilen deneyler ise, zeminlerin düşey yöndeki şişme parametrelerinin belirlenmesi için yapılmıştır.

Taneli malzeme doldurulmuş hendek hacminin arttırılmasıyla düşey yöndeki şişme yüzdeleri ve yanal yöndeki şişme basınçlarında kayda değer azalmalar olduğu saptanmıştır. Doğal zemin yüzeyine yerleştirilmiş hafif bir yapı ya da dolguya ait örtü etkisi altında iyileştirmelerin etkisinin daha da arttığı gözlemlenmiştir.

Anahtar Kelimeler: Yanal Şişme Basıncı, Düşey Şişme, İnce Çeperli Odometre Deneyi, Şişen Zeminlerin İyileştirilmesi, Taneli Dolgu.

**To my beloved son Mete  
and my dear wife Mizyal**

## **ACKNOWLEDGEMENTS**

The author would like to express sincere gratitude to Prof. Dr. Erdal Çokça for his guidance, valuable suggestions and patience throughout the research.

Very special thanks are extended to Prof. Dr. Reşat Ulusay and Prof. Dr. Orhan Erol for their suggestions, helpful ideas and encouragement and to the staff of Geotechnical Engineering Laboratory especially to Mr. Ali Bal for their help during testing. I would also like to thank Prof. Dr. İlyas Yılmaz for his incredible and unforgettable efforts during obtaining the samples from site.

I am forever indebted to my beloved son Mete who grew up with this study for his unconditional love.

Finally, the author wishes to express his heartfelt gratitude to his wife Mizyal for her endless love, patience, understanding and encouragement during the last seven years. Without her precious support, this study would never end.

## TABLE OF CONTENTS

ABSTRACT .....	IV
ÖZ .....	VI
ACKNOWLEDGEMENTS.....	IX
TABLE OF CONTENTS .....	X
LIST OF TABLES .....	XIV
LIST OF FIGURES .....	XIX
CHAPTERS	
1. INTRODUCTION .....	1
2. AN OVERVIEW OF RELATED LITERATURE .....	4
2.1 INTRODUCTION .....	4
2.2 SWELL POTENTIAL AND PARAMETERS .....	4
2.3 FACTORS AFFECTING SWELL POTENTIAL .....	5
2.4 CLASSIFICATION OF EXPANSIVE SOILS .....	12
2.4.1 USAEWES Classification.....	13
2.4.2 USBR Classification.....	14
2.4.3 Classification Based on Clay Percent and Activity .....	15
2.5 ASSESSMENT OF SWELL PARAMETERS .....	17
2.5.1 Empirical Methods .....	18
2.5.2 Suction Method.....	18
2.5.3 Potential Volume Change (PVC) .....	19
2.5.4 Oedometer Test Methods .....	21
2.5.4.1 Improved Swell Oedometer (ISO) Test (Method A) .....	22
2.5.4.2 Swell Overburden (SO) Test (Method B).....	24

2.5.4.3 Constant Volume Swell (CVS) Test (Method C) .....	25
2.5.4.4 Comparison of the Oedometer Test Methods .....	26
2.5.5 Modified Oedometer Tests .....	28
2.5.6 Modified Triaxial Tests .....	44
2.5.7 Large Scale Tests and Case Studies .....	77
2.6 COMMONLY USED REHABILITATION METHODS .....	91
2.6.1 Granular Pile Anchors .....	92
2.6.2 Stabilization by Chemicals and Industrial Wastes .....	102
2.6.3 Mechanical Alteration and the Cushion Technique .....	106
3. TEST APPARATUS .....	112
3.1 GENERAL .....	112
3.2 CONVENTIONAL OEDOMETER TESTS .....	113
3.3 THIN-WALL OEDOMETER RING .....	113
3.3.1 Thin-Wall Swell Pressure Oedometer Ring Body .....	114
3.3.2 Instrumentation with Electrical Strain Gauges .....	117
3.3.3 Data Acquisition System .....	119
3.3.4 Calibration of the Swell Pressure Ring .....	121
3.3.5 Verification of Swell Pressure Oedometer Ring .....	124
3.4 MODIFIED CBR MOULD .....	128
4. TEST PROGRAM .....	129
4.1 INTRODUCTION .....	129
4.2 TEST MATERIAL .....	129
4.2.1 Properties of Clays .....	130
4.2.2 Properties of Granular Materials .....	141
4.2.3 Properties of Silt .....	144

4.3	PREPARATION OF TEST SAMPLES.....	145
4.3.1	Preparation of the Samples for the Conventional and Thin Wall Oedometer Tests.....	145
4.3.2	Preparation of the Samples for Modified CBR Mould .....	148
4.4	TEST SCHEDULE .....	153
5.	TEST RESULTS.....	157
5.1	GENERAL.....	157
5.2	EFFICIENCY OF THE METHOD AND EFFECT OF GRADATION ON PERFORMANCE (PHASE 1).....	157
5.2.1	Free Swell Tests .....	158
5.1.2	Swell Overburden Tests .....	161
5.2	EFFECT OF CLAY TYPE AND SAMPLE SIZE (PHASE.2) .....	169
5.2.1	Stage (a) Tests .....	169
5.2.2	Stage (b) Tests .....	172
5.2.3	Stage (c) Tests .....	180
5.3	PERFORMANCE OF SILT AS TREATMENT MATERIAL (PHASE.3).....	186
5.4	LATERAL SWELL PRESSURE MEASUREMENTS (PHASE.4).....	196
5.4.1	Stage (a) Tests .....	196
5.4.2	Stage (b) Tests .....	199
5.4.3	Stage (c) Tests .....	203
5.4.4	Stage (d) Tests .....	206
6.	DISCUSSION OF RESULTS.....	209
6.1	GENERAL.....	209
6.2	INVESTIGATION PHASE 1 .....	209
6.3	INVESTIGATION PHASE 2.....	222



6.4	INVESTIGATION PHASE 3.....	245
6.5	INVESTIGATION PHASE 4.....	250
7.	CONCLUSIONS .....	278
	REFERENCES .....	282
APPENDICES		
A.	RESULTS OF THIN-WALL RING TESTS PERFORMED ON UNTREATED TYPE- 3 AND TYPE 5 SOIL SAMPLES .....	299
B.	RESULTS OF THIN-WALL RING TESTS PERFORMED ON TREATED TYPE- 3 SOIL SAMPLES .....	305
C.	RESULTS OF THIN-WALL RING TESTS PERFORMED ON TREATED TYPE- 5 SOIL SAMPLES .....	310
D.	RESULTS OF THIN-WALL RING TESTS PERFORMED ON TYPE- 5 SOIL SAMPLES TREATED WITH SILT .....	314
E.	COMPARISON OF OEDOMETER AND MODIFIED CBR MOULD TEST RESULTS .....	316
	CURRICULUM VITAE .....	321

## LIST OF TABLES

### TABLES

Table 2. 1	Factors Affecting Swell Potential (adapted from Nelson and Miller, 1992) .....	7
Table 2. 2	USAEWES Classification of Expansive Soils (Snethen et al., 1977) .....	14
Table 2. 3	USBR Classification of Expansive Soils (adapted from Erol, 1987) .....	14
Table 2. 4	Activity of Various Minerals (Skempton, 1953 and Mitchell, 1993) .....	15
Table 2. 5	Empirical Relationships for the Assessment of Swell .....	20
Table 2. 6	Comparative Values of Swelling Pressure by Different Methods of Oedometer Test (adapted from Sridrahan, Rao and Sivapullaiah, 1986) .....	28
Table 2. 7	Results of Swell Pressure Tests, Uniaxial Technique (Kassif and Baker, 1969) .....	47
Table 2. 8	Results of Swell Pressure Tests, Triaxial Technique (Kassif and Baker, 1969) .....	47
Table 2. 9	Results of Swell Pressure Tests, Comparison of Uniaxial and Triaxial Techniques (Kassif and Baker, 1969) .....	48
Table 2. 10	Index Properties of Soil Samples used in the Investigation (Shiming, 1984) .....	52
Table 2. 11	Comparison of Expansion for Monorail Tests (Shiming, 1984) .....	52
Table 2. 12	Swell Pressure Measurements (After Shiming, 1984) .....	53
Table 2. 13	Oedometer and Triaxial Swell Tests Comparison (Shiming, 1984) .....	53
Table 2. 14	Shale Swell Parameters Obtained from Oedometer and Triaxial Swell Tests (Al-Shamrani and Dhowian, 2003) .....	68
Table 2. 15	Heave Data for the Airport Research (McKeen, 1981) .....	82

Table 2. 16	% Heave of Expansive Clay Bed Reinforced by Granular Pile Anchors (Phanikumar et al., 2004) .....	94
Table 2. 17	Improvement Factors for Different Oedometer Tests (Al-Omari and Hamodi, 1991).....	96
Table 2. 18	The Effect of Geopile Diameter and Fill Material Characteristics on % Heave (Sharma and Phanikumar, 2005).....	99
Table 2. 19	The Effect of Spacing between Two Piles with respect to Fill Material Type (d= 50 mm) (Sharma and Phanikumar, 2005).....	99
Table 2. 20	Test Results – GPAF with Base Geosynthetics (Phanikumar and Rao, 2000).....	102
Table 2. 21	Values of Swelling Pressure in Terms of Distance to Column (Tonoz et al., 2003) .....	106
Table 2. 22	Test Program (adapted from Elhady, 2007).....	108
Table 2. 23	Results for Sand-Lime Cushion (adapted from Elhady, 2007).....	108
Table 2. 24	Specifications for CNS Soil (Katti, 1979) .....	110
Table 3. 1	Catalogue Data for the Strain Gauges.....	117
Table 4. 1	Some Index Properties of Soils Used for Tests .....	133
Table 4. 2	Soil Mineralogy and Clay Mineralogy of Gazi Clay (Type-4 Sample) (Özer et al. 2012).....	138
Table 4. 3	Soil Mineralogy and Clay Mineralogy of Esenboğa Clay (Type-5 Sample) .....	138
Table 4. 4	Physical Properties of the Sand Used in the Preparation of Granular Columns for Conventional Oedometer Tests.....	142
Table 4. 5	Some Physical Properties of Fine Gravel Used in the Preparation of Granular Columns for Conventional Oedometer Tests and Thin-Wall Oedometer Tests .....	143
Table 4. 6	Some Physical Properties of Medium Gravel Used in the Preparation of Granular Columns for Modified CBR Moulds .....	144
Table 4. 7	Some Physical Properties of Coarse Silt used in the Oedometer and Thin-Wall Tests .....	145

Table 4. 8	Test Schedule for Phase I and Phase II .....	155
Table 4. 9	Test Schedule for Phase III and Phase IV .....	156
Table 5. 1	Results of Free Swell Tests Performed with Sand Material.....	158
Table 5. 2	Results of Free Swell Tests Performed with Gravel Material.....	159
Table 5. 3	Vertical Swell Pressure, $P_v$ (kPa) with respect to Material Type and Area Replacement Ratio Obtained from Free Swell Tests.....	161
Table 5. 4	Results of Swell Overburden Tests Performed with Sand Material .....	162
Table 5. 5	Results of Swell Overburden Tests Performed with Gravel Material .....	163
Table 5. 6	Vertical Swell Pressure, $P_v$ (kPa) with respect to Material Type and Area Replacement Ratio Obtained from Swell Overburden Tests (Phase-1) .....	163
Table 5. 7	Modified CBR Mould Test Results with Seating Pressure of 1 kPa.....	170
Table 5. 8	Modified CBR Mould Test Results Performed with Free Swell Testing Technique ( $P_s=7$ kPa) (Phase-2, Stage (b)).....	173
Table 5. 9	Oedometer Test Results Performed with Free Swell Testing Technique ( $P_s=7$ kPa) (Phase-2, Stage(b)).....	174
Table 5. 10	Modified CBR Mould Test Results Performed with Swell Overburden Testing Technique ( $P_o=25$ kPa) (Phase-2, Stage (c)) .....	180
Table 5. 11	Oedometer Test Results Performed with Swell Overburden Testing Technique ( $P_o=25$ kPa) (Phase-2, Stage (c)).....	181
Table 5. 12	Oedometer Test Results Performed with Free Swell Testing Technique ( $P_s=7$ kPa) (Phase-3) .....	187
Table 5. 13	Oedometer Test Results Performed with Swell Overburden Testing Technique ( $P_o=25$ kPa) (Phase-3) .....	188
Table 5. 14	Results of Thin-Wall Ring Tests (Ring-1) Performed on Untreated Soil Type-3 (Phase-4, Stage (a)) .....	197
Table 5. 15	Results of Thin-Wall Ring Tests Performed on Untreated Soil Type-5 (Phase-4, Stage (a)) .....	198

Table 5. 16	Results of Thin-Wall Ring Tests Performed on Soil Type-3 (Phase-4, Stage (b)) .....	200
Table 5. 17	Results of Thin-Wall Ring Tests Performed on Soil Type-5 with $P_s=7$ kPa (Phase-4, Stage (c)) .....	203
Table 5. 18	Results of Thin-Wall Ring Tests Performed on Soil Type-5 with $P_o=25$ kPa (Phase-4, Stage (c)) .....	204
Table 5. 19	Results of Thin-Wall Ring Tests Performed on Silt Treated Soil Type-5 with $P_s=7$ kPa (Phase-4, Stage (d)) .....	207
Table 6. 1	Vertical Swell, $S_v$ (%) and Treatment, $TS_v$ (%) with respect to Material and Area Replacement Ratio Obtained from Free Swell Tests (Phase-1) .....	210
Table 6. 2	Vertical Swell Pressure, $P_v$ (kPa) and Treatment, $TP_v$ (%) with respect to Material and Area Replacement Ratio Obtained from Free Swell Tests (Phase-1).....	210
Table 6. 3	Vertical Swell, $S_v$ (%) and Treatment, $TS_v$ (%) with respect to Material and Area Replacement Ratio Obtained from Swell Overburden Tests (Phase-1).....	213
Table 6. 4	Vertical Swell Pressure, $P_v$ (kPa) and Treatment, $TP_v$ (%) with respect to Material and Area Replacement Ratio Obtained from Swell Overburden Tests (Phase-1).....	214
Table 6. 5	Average Vertical Swell, $S_{v(av)}$ (%) and Treatment, $TS_v$ (%) with respect to Area Replacement Ratio and Seating Pressure Obtained from Modified CBR Mould Tests (Phase-2, Stage(a)) .....	223
Table 6. 6	Average Vertical Swell, $S_{v(av)}$ (%) and Treatment, $TS_v$ (%) with respect to Area Replacement Ratio for Free Swell CBR Mould and Oedometer Tests under $P_s=7$ kPa Pressure (Phase-2, Stage(b)).....	226
Table 6. 7	Average Vertical Swell, $S_{v(av)}$ (%) and Treatment, $TS_v$ (%) with respect to Area Replacement Ratio for Swell Overburden CBR Mould and Oedometer Tests under $P_o=25$ kPa Pressure (Phase-2, Stage(c)) .....	233

Table 6. 8	Average Vertical Swell, $S_{v(av)}$ (%) and Treatment, $TS_v$ (%)for Swell Overburden CBR Mould and Oedometer Tests Describing the Combined Effect of Trench and Surcharge (Phase-2, Stage(c)).....	239
Table 6. 9	Average Vertical Swell, $S_{v(av)}$ (%) and Treatment, $TS_v$ (%)for Free Swell and Swell Overburden Oedometer Tests Performed on Gravel, Silt (As Layer), Silt (As Column) and Hole (Phase-3).....	245
Table 6. 10	Comparison of Average Vertical Swell, $S_{v(av)}$ (%) for Free Swell and Swell Overburden Oedometer and Thin-Wall Ring Tests (Phase-4, Stage (a)) .....	251
Table 6. 11	Thin-Wall Ring Test Results (Phase-4, Stage (a)).....	252
Table 6. 12	Thin-Wall Ring Test Results (Phase-4, Stage (b)).....	256
Table 6. 13	Comparison of Average Vertical Swell, $S_{v(av)}$ (%)for Free Swell and Swell Overburden Oedometer and Thin-Wall Ring Tests for Type-3 Soil (Phase-4, Stage (b)).....	261
Table 6. 14	Thin-Wall Ring Test Results (Phase-4, Stage (c)) .....	263
Table 6. 15	Comparison of Average Vertical Swell, $S_{v(av)}$ (%) for Free Swell and Swell Overburden Oedometer and Thin-Wall Ring Tests for Type-5 Soil (Phase-4, Stage (c)).....	269
Table 6. 16	Comparison of Average Lateral Swell Pressure, $P_{h(av)}$ (kPa) for Free Swell Oedometer and Thin-Wall Ring Tests for Type-5 Soil Treated with Gravel and Silt (Phase-4, Stage (d)) .....	273
Table 6. 17	Comparison of Average Vertical Swell, $S_{v(av)}$ (%) for Free Swell Oedometer and Thin-Wall Ring Tests for Type-5 Soil Treated with Gravel and Silt (Phase-4, Stage (d)).....	275
Table 6. 18	Comparison of Test Methods Used during the Investigations.....	277

## LIST OF FIGURES

### FIGURES

Figure 2. 1	Effect of Clay Content on the Swelling Potential of Soils (a) Results of Sand-Clay Soils (b) Results of Silt – Clay Soils (El-Sohby and Rabba, 1981) .....	6
Figure 2. 2	Effect of Clay Content on the Swelling Pressure of Soils (El-Sohby and Rabba, 1981) .....	8
Figure 2. 3	Effect of Initial Dry Density on the Swelling Potential of Soils (a)Results of Sand-Clay Soils (b) Results of Silt – Clay Soils (El-Sohby and Rabba, 1981) .....	9
Figure 2. 4	Effect of Initial Water Content on the Swell Percentage of Soils (El Sohby and Rabba, 1981).....	10
Figure 2. 5	Effect of Initial Water Content on the Swell Pressure of Soils (El-Sohby and Rabba, 1981).....	10
Figure 2. 6	Effect of Initial Surcharge on (a) Lateral Swell Pressure (b) Swell Pressure Ratio (Joshi and Katti, 1984).....	12
Figure 2. 7	Swell Potential Classification (Seed et al., 1962(b)) .....	16
Figure 2. 8	Swell Potential Estimation (Popescu, 1986) .....	17
Figure 2. 9	Swell Index versus Potential Volume Change (FHA, 1974).....	21
Figure 2. 10	Void Ratio versus Log of Pressure Curve for an ISO Test (ASTM D4546-08,2008).....	23
Figure 2. 11	Void Ratio versus Log of Pressure Curve for an SO Test (ASTM D4546-08,2008).....	25
Figure 2. 12	Void Ratio vs. Log of Pressure Curve for a CVS Test (ASTM D4546-08, 2008).....	26
Figure 2. 13	Modified Thin-Wall Oedometer Cell (Komornik and Zeitlen,1965).....	29
Figure 2. 14	Vertical Movements as a Function of Vertical and Lateral Pressures (Komornik and Zeitlen, 1965) .....	29
Figure 2. 15	Lateral Swell Pressure (LSP) Apparatus Cross Section (Ofer, 1980).....	30

Figure 2. 16	Lateral Swell Pressure (LSP) Test Set-Up (Ofer, 1980) .....	31
Figure 2. 17	Vertical and Horizontal Swell Percentages for Different Initial Dry Densities Observed from LSP Tests (Ofer, 1980) .....	31
Figure 2. 18	Lateral Swell Pressure Test-Set Up (Ertekin, 1991) .....	34
Figure 2. 19	Lateral Swell Pressure and Vertical Swell Percent versus Water Content Relationship (Edil and Alanazy, 1992).....	35
Figure 2. 20	Effect of Initial Water Content on Swell Pressure (Erol and Ergun, 1994) .....	36
Figure 2. 21	Effect of Initial Water Content on Swell Pressure Ratio (Erol and Ergun, 1994).....	37
Figure 2. 22	Swelling Tests Performed with the Flexible Ring (a) Evolution of the Axial Strain (b) Evolution of the Lateral Pressure (Windal and Shahrour, 2002) .....	38
Figure 2. 23	Swelling Tests Performed with the Stiff Ring (a) Evolution of the Axial Strain (b) Evolution of the Lateral Pressure (Windal and Shahrour, 2002).....	39
Figure 2. 24	Relationship between the Swelling Pressure and Initial Water Content for Samples with Different Initial Dry Densities (a) Change in Vertical Swell Pressure (b) Change in Lateral Swell Pressure (Sapaz, 2004).....	41
Figure 2. 25	Relationship between the Swelling Pressure and Initial Dry Densities for Samples with Different Initial Water Contents (a) Change in Vertical Swell Pressure (b) Change in Lateral Swell Pressure (Sapaz, 2004) .....	42
Figure 2. 26	VR-LFST Results (Özalp, 2010) .....	44
Figure 2. 27	Swelling Test Apparatus (Parcher and Liu, 1965) .....	45
Figure 2. 28	Volumetric Swell vs. Initial Water Content according to Compaction Method (Parcher and Liu, 1965) .....	46
Figure 2. 29	Swelling vs. Time Curves for Compacted and Undisturbed Samples (Parcher and Liu, 1965) .....	46
Figure 2. 30	Modified Triaxial Cell Apparatus (Dhawan et al., 1982).....	49



Figure 2. 31	Development of Vertical Swell Pressure with Time under Different Lateral Confining Pressures. (Dhawan et al., 1982).....	49
Figure 2. 32	Variation of Vertical Swell Pressure with Lateral Confinement and Accompanied Volume Change. (Dhawan et al., 1982).....	50
Figure 2. 33	Schematic Description of the Modified Triaxial Apparatus (a) The Apparatus (b) Compression Cell (Shiming, 1984).....	51
Figure 2. 34	Lateral Pressure Measurement Test Set-up (Chen and Huang, 1987).....	55
Figure 2. 35	Lateral and Vertical Swell Pressure versus Time (Chen and Huang, 1987).....	55
Figure 2. 36	Schematic Description of the Triaxial Stress Path Cell (Bishop and Wesley, 1975).....	56
Figure 2. 37	Variation of Final Measured Vertical Strain with Applied Vertical Stress (Fourie, 1989).....	58
Figure 2. 38	Variation of Final Measured Lateral Strain with Applied Initial Cell Pressure (After Fourie, 1989).....	59
Figure 2. 39	Vertical Swell under Different Confining Pressures (Al-Shamrani and Al-Mhaidib, 2000).....	61
Figure 2. 40	Vertical Swell versus Time for Different Initial Water Contents (Al-Shamrani and Al-Mhaidib, 2000).....	62
Figure 2. 41	Relationship between Initial Water Content and Vertical Swell for Confining Pressure = 25 kPa (Al-Shamrani and Al-Mhaidib, 2000).....	62
Figure 2. 42	Vertical Swell Percentage from Oedometer and Triaxial Tests (Confining Pressure=35 kPa) (Al-Shamrani and Al-Mhaidib, 2000).....	63
Figure 2. 43	Relationship between Applied Pressure and Ultimate Vertical Swell Measured in Oedometer and Triaxial Swell Tests (Al-Shamrani and Al-Mhaidib, 2000).....	64

Figure 2. 44	Final Water Contents of Triaxial and Oedometer Samples at Different Confining Pressures (Al-Shamrani and Al-Mhaidib, 2000) .....	65
Figure 2. 45	Schematic of the Field Station Instrumentation (Al-Shamrani and Dhowian, 2003) .....	66
Figure 2. 46	Field Data (a) Cumulative Heave (b) Moisture Content (c) Suction (Al-Shamrani and Dhowian, 2003).....	67
Figure 2. 47	(a) Vertical Swell Behaviour under Oedometer and Triaxial Loading Conditions (b) Variation of Oedometer and Triaxial Ultimate Swell with Confining Pressure (Al-Shamrani and Dhowian, 2003).....	69
Figure 2. 48	Measured and Predicted Heave based on Moisture Techniques (Al-Shamrani and Dhowian, 2003) .....	71
Figure 2. 49	Schematic Representation of the Free Lateral Movement Test (Dhowian and Al-Saadon, 2010).....	73
Figure 2. 50	Comparison between Vertical Swell and Average Lateral Swell (Dhowian and Al-Saadon, 2010) .....	74
Figure 2. 51	Comparison of Vertical Swell Percentages Measured in Oedometer Ring and Free Lateral Movement Tests (Dhowian and Al-Saadon, 2010).....	75
Figure 2. 52	Triaxial Swell Test Cell (Thomas , 2008) .....	76
Figure 2. 53	Triaxial Swell Test Apparatus (Thomas, 2008) .....	76
Figure 2. 54	Lateral Pressure versus Depth at Different Locations (Richards and Kurzeme, 1973) .....	78
Figure 2. 55	Instrumented Test Pit (Robertson and Wagener, 1975) .....	80
Figure 2. 56	Vertical and Lateral Pressures for Test Pit 1 (Robertson and Wagener, 1975) .....	81
Figure 2. 57	Vertical and Lateral Pressures for Test Pit 2 (Robertson and Wagener, 1975) .....	81
Figure 2. 58	In-Situ Lateral Swell Measurement Probe (Ofer and Komornik, 1983).....	83
Figure 2. 59	Moisture Content Profile at the end of ISP Probe Test (Ofer, 1980).....	84

Figure 2. 60	Time versus Percent Swell Pressure for ISP Probe (Ofer, 1980).....	84
Figure 2. 61	Large Scale Laboratory Set-Up (Katti et al., 1983).....	86
Figure 2. 62	Tank and Reaction Frame of Large Scale Laboratory Set-Up (Joshi and Katti, 1984) .....	87
Figure 2. 63	Lateral Pressure Development versus Depth (a) Dry Loose State (b) Compacted State (c) Compacted Saturated State (After Katti et al., 1983).....	88
Figure 2. 64	Lateral Swell Pressure vs. Depth for Different Thicknesses of CNS (Katti et al., 1983).....	88
Figure 2. 65	Development of Lateral Pressure with Time (Joshi and Katti, 1984).....	90
Figure 2. 66	Experimental Setup for GPAF System (Phanikumar et al., 2004).....	94
Figure 2. 67	Geopiles for Embankment and Building Foundations (Al-Omari and Hamodi, 1991).....	96
Figure 2. 68	Experimental Set-up for (a) Single and (b) Group Geopiles (Sharma and Phanikumar, 2005).....	98
Figure 2. 69	Experimental Setup for GPAF System with Base Geosynthetics (Phanikumar and Rao, 2000).....	100
Figure 2. 70	Pattern of Lime Columns of 2 cm Diameter Constructed in the Block Clay Sample (Tono et al., 2003).....	105
Figure 2. 71	Section from the Block Illustrating Sampling Distances from Lime Columns (Tono et al., 2003).....	105
Figure 2. 72	Shallow Foundation with CNS and MSM Intercepting Layers (Katti et al., 2002).....	111
Figure 3. 1	Cross - Sectional and Plan View of Thin-Wall Oedometer Ring Ertekin,1991) .....	115
Figure 3. 2	Lateral Swell Pressure Test Set-Up Ready for Instrumentation (Ertekin, 1991).....	116
Figure 3. 3	Lateral Swell Pressure Test Set-Up Ready for Instrumentation (Avşar, 2007).....	116
Figure 3. 4	Installation of the Strain Gauges (Ertekin, 1991) .....	117

Figure 3. 5	Strain Gauge Nomenclature (Ertekin, 1991).....	118
Figure 3. 6	Full Wheaston Bridge Configuration (Ertekin, 1991).....	119
Figure 3. 7	An Active Strain Gauge on the Thin-Wall Ring (Ertekin, 1991).....	119
Figure 3. 8	Data Acquisition Unit.....	121
Figure 3. 9	Bottom Cap (Left) and Top Cap (Right) with Supply (Center) Inlet and Release (Outlet) Points.....	122
Figure 3. 10	Calibration Curve Obtained from the Thin-Wall Cell Developed by (a) Ertekin (1991), (b) Avşar (2007) .....	123
Figure 3. 11	Stress Distribution in the Thin-Wall Oedometer Ring Wall .....	126
Figure 3. 12	Modified CBR Moulds with Inundation Containers.....	128
Figure 4. 1	Test Pit at Gazi University Campus Area.....	130
Figure 4. 2	Cracks Observed on building next to the test pit at Gazi University Campus Area .....	131
Figure 4. 3	Test Pit at Esenboğa.....	131
Figure 4. 4	A View from the Test Pit at Esenboğa .....	132
Figure 4. 5	Damaged Retaining Walls near Test Pit at Esenboğa.....	132
Figure 4. 6	Grain Size Distribution of the Sample Type-1 .....	134
Figure 4. 7	Grain Size Distribution of the Sample Type-2.....	134
Figure 4. 8	Grain Size Distribution of the Sample Type-3.....	135
Figure 4. 9	Grain Size Distribution of the Sample Type-4 .....	135
Figure 4. 10	Grain Size Distribution of the Sample Type-5.....	136
Figure 4. 11	USCS Chart and Classification of the Samples Used for Tests .....	136
Figure 4. 12	Activity Chart for the Determination of Swell Potential of the Soil Samples Used in the Tests.....	137
Figure 4. 13	X-Ray Diffractograms of Soil Type-4 for Bulk (Whole) Sample (Özer et al., 2012).....	139
Figure 4. 14	XRD Pattern for Clay Fraction in Gazi Clay (Özer et al., 2012).....	139
Figure 4. 15	X-Ray Diffractograms of Soil Type-5 for Bulk (Whole) Sample.....	140
Figure 4. 16	XRD Pattern for Clay Fraction in Esenboğa Clay .....	140

Figure 4. 17	Grain Size Distribution of the Sand Used in Oedometer Tests .....	141
Figure 4. 18	Grain Size Distribution of Fine Gravel used in Oedometer Tests and Thin-Wall Tests .....	142
Figure 4. 19	Grain Size Distribution of Medium Gravel used in the Modified CBR Mould .....	143
Figure 4. 20	Grain Size Distribution of Coarse Silt used in the Oedometer and Thin-Wall Tests .....	144
Figure 4. 21	Specimen Transferred into Thin-Wall Ring Ready to be Tested .....	146
Figure 4. 22	Hole Opened inside Specimen to Construct Granular Column.....	147
Figure 4. 23	Placement of Granular Soil inside the Hole .....	147
Figure 4. 24	Hole Filled with Granular Soil.....	148
Figure 4. 25	Placement of Sample inside Modified CBR Mould .....	149
Figure 4. 26	Top Cap Placed inside CBR Mould for Compaction Purposes.....	149
Figure 4. 27	Sample Compacted inside CBR Mould.....	150
Figure 4. 28	Extraction of Cylindrical Mould from the Specimen .....	151
Figure 4. 29	Hole inside CBR Specimen.....	151
Figure 4. 30	Placement of Granular Material into Hole in CBR Sample .....	152
Figure 4. 31	Hole Filled with Granular Material in CBR Sample .....	152
Figure 4. 32	Top Cap Placed on CBR Specimen.....	153
Figure 5. 1	Vertical Swell Percentage vs. Time Relationship for Oedometer Tests Performed with Free Swell Testing Technique on Type-2 Expansive Soil Samples Treated with Sand.....	159
Figure 5. 2	Vertical Swell Percentage vs. Time Relationship for Oedometer Tests Performed with Free Swell Testing Technique on Type-2 Expansive Soil Samples Treated with Gravel .....	160

Figure 5. 3	Void Ratio vs. Overburden Pressure Graphs Determined from the Loading Stage of Free Swell Tests Performed with Type-2 Soil Treated by Sand Material. ....	160
Figure 5. 4	Void Ratio vs. Overburden Pressure Graphs Determined from the Loading Stage of Free Swell Tests Performed with Type-2 Soil Treated by Gravel Material. ....	161
Figure 5. 5	Vertical Swell Percentage vs. Time Relationship for Oedometer Tests Performed with Swell Overburden Testing Technique on Type-2 Expansive Soil Samples Treated with Sand ( $P_o=25$ kPa) .....	164
Figure 5. 6	Vertical Swell Percentage vs. Time Relationship for Oedometer Tests Performed with Swell Overburden Testing Technique on Type-2 Expansive Soil Samples Treated with Sand ( $P_o =50$ kPa) .....	164
Figure 5. 7	Vertical Swell Percentage vs. Time Relationship for Oedometer Tests Performed with Swell Overburden Testing Technique on Type-2 Expansive Soil Samples Treated with Sand ( $P_o =100$ kPa) .....	165
Figure 5. 8	Vertical Swell Percentage vs. Time Relationship for Oedometer Tests Performed with Swell Overburden Testing Technique on Type-2 Expansive Soil Samples Treated with Sand ( $P_o =150$ kPa) .....	165
Figure 5. 9	Vertical Swell Percentage vs. Time Relationship for Oedometer Tests Performed with Swell Overburden Testing Technique on Type-2 Expansive Soil Samples Treated with Gravel ( $P_o =25$ kPa) .....	166
Figure 5. 10	Vertical Swell Percentage vs. Time Relationship for Oedometer Tests Performed with Swell Overburden Testing Technique on Type-2 Expansive Soil Samples Treated with Gravel ( $P_o =50$ kPa) .....	166
Figure 5. 11	Vertical Swell Percentage vs. Time Relationship for Oedometer Tests Performed with Swell Overburden	

	Testing Technique on Type-2 Expansive Soil Samples Treated with Gravel ( $P_o = 100$ kPa) .....	167
Figure 5. 12	Vertical Swell Percentage vs. Time Relationship for Oedometer Tests Performed with Swell Overburden Testing Technique on Type-2 Expansive Soil Samples Treated with Gravel ( $P_o = 150$ kPa) .....	167
Figure 5. 13	Vertical Swell Percentage vs. Overburden Pressure for Oedometer Tests Performed with Swell Overburden Testing Technique on Type-2 Expansive Soil Samples Improved by Sand .....	168
Figure 5. 14	Vertical Swell Percentage vs. Overburden Pressure for Oedometer Tests Performed with Swell Overburden Testing Technique on Type-2 Expansive Soil Samples Improved by Gravel .....	168
Figure 5. 15	Vertical Swell Percentage vs. Time Relationship for Modified CBR Mould Tests Performed with Free Swell Testing Technique ( $P_s = 1$ kPa) on Type-1 Expansive Soil Samples Treated with Gravel .....	171
Figure 5. 16	Vertical Swell Percentage vs. Time Relationship for Modified CBR Mould Tests Performed with Free Swell Testing Technique ( $P_s = 1$ kPa) on Type-2 Expansive Soil Samples Treated with Gravel .....	171
Figure 5. 17	Vertical Swell Percentage vs. Time Relationship for Modified CBR Mould Tests Performed with Free Swell Testing Technique ( $P_s = 1$ kPa) on Type-3 Expansive Soil Samples Treated with Gravel .....	172
Figure 5. 18	Vertical Swell Percentage vs. Time Relationship for Modified CBR Mould Tests Performed with Free Swell Testing Technique ( $P_s = 7$ kPa) on Type-1 Expansive Soil Samples Treated with Gravel .....	175
Figure 5. 19	Vertical Swell Percentage vs. Time Relationship for Modified CBR Mould Tests Performed with Free Swell	

	Testing Technique ( $P_s=7$ kPa) on Type-2 Expansive Soil Samples Treated with Gravel.....	175
Figure 5. 20	Vertical Swell Percentage vs. Time Relationship for Modified CBR Mould Tests Performed with Free Swell Testing Technique ( $P_s=7$ kPa) on Type-3 Expansive Soil Samples Treated with Gravel.....	176
Figure 5. 21	Vertical Swell Percentage vs. Time Relationship for Modified CBR Mould Tests Performed with Free Swell Testing Technique ( $P_s=7$ kPa) on Type-4 Expansive Soil Samples Treated with Gravel.....	176
Figure 5. 22	Vertical Swell Percentage vs. Time Relationship for Modified CBR Mould Tests Performed with Free Swell Testing Technique ( $P_s=7$ kPa) on Type-5 Expansive Soil Samples Treated with Gravel.....	177
Figure 5. 23	Vertical Swell Percentage vs. Time Relationship for Oedometer Tests Performed with Free Swell Testing Technique ( $P_s=7$ kPa) on Type-1 Expansive Soil Samples Treated with Gravel.....	177
Figure 5. 24	Vertical Swell Percentage vs. Time Relationship for Oedometer Tests Performed with Free Swell Testing Technique ( $P_s=7$ kPa) on Type-2 Expansive Soil Samples Treated with Gravel.....	178
Figure 5. 25	Vertical Swell Percentage vs. Time Relationship for Oedometer Tests Performed with Free Swell Testing Technique ( $P_s=7$ kPa) on Type-3 Expansive Soil Samples Treated with Gravel.....	178
Figure 5. 26	Vertical Swell Percentage vs. Time Relationship for Oedometer Tests Performed with Free Swell Testing Technique ( $P_s=7$ kPa) on Type-4 Expansive Soil Samples Treated with Gravel.....	179
Figure 5. 27	Vertical Swell Percentage vs. Time Relationship for Oedometer Tests Performed with Free Swell Testing	



	Technique ( $P_s=7$ kPa) on Type-5 Expansive Soil Samples Treated with Gravel.....	179
Figure 5. 28	Vertical Swell Percentage vs. Time Relationship for Modified CBR Mould Tests Performed with Swell Overburden Testing Technique ( $P_o=25$ kPa) on Type-1 Soil Samples Treated with Gravel.....	182
Figure 5. 29	Vertical Swell Percentage vs. Time Relationship for Modified CBR Mould Tests Performed with Swell Overburden Testing Technique ( $P_o=25$ kPa) on Type-2 Soil Samples Treated with Gravel.....	182
Figure 5. 30	Vertical Swell Percentage vs. Time Relationship for Modified CBR Mould Tests Performed with Swell Overburden Testing Technique ( $P_o=25$ kPa) on Type-3 Soil Samples Treated with Gravel.....	183
Figure 5. 31	Vertical Swell Percentage vs. Time Relationship for Modified CBR Mould Tests Performed with Swell Overburden Testing Technique ( $P_o=25$ kPa) on Type-5 Soil Samples Treated with Gravel.....	183
Figure 5. 32	Vertical Swell Percentage vs. Time Relationship for Oedometer Tests Performed with Swell Overburden Testing Technique ( $P_o=25$ kPa) on Type-1 Expansive Soil Samples Treated with Gravel.....	184
Figure 5. 33	Vertical Swell Percentage vs. Time Relationship for Oedometer Tests Performed with Swell Overburden Testing Technique ( $P_o=25$ kPa) on Type-2 Expansive Soil Samples Treated with Gravel.....	184
Figure 5. 34	Vertical Swell Percentage vs. Time Relationship for Oedometer Tests Performed with Swell Overburden Testing Technique ( $P_o=25$ kPa) on Type-3 Expansive Soil Samples Treated with Gravel.....	185
Figure 5. 35	Vertical Swell Percentage vs. Time Relationship for Oedometer Tests Performed with Swell Overburden	

	Testing Technique ( $P_o=25$ kPa) on Type-5 Expansive Soil Samples Treated with Gravel.....	185
Figure 5. 36	Vertical Swell Percentage vs. Time Relationship for Oedometer Tests Performed with Free Swell Testing Technique ( $P_s=7$ kPa) on Type-5 Expansive Soil Samples Treated with 10% Silt.....	189
Figure 5. 37	Vertical Swell Percentage vs. Time Relationship for Oedometer Tests Performed with Free Swell Testing Technique ( $P_s=7$ kPa) on Type-5 Expansive Soil Samples Treated with 20% Silt.....	189
Figure 5. 38	Vertical Swell Percentage vs. Time Relationship for Oedometer Tests Performed with Free Swell Testing Technique ( $P_s=7$ kPa) on Type-5 Expansive Soil Samples Treated with 30% Silt.....	190
Figure 5. 39	Vertical Swell Percentage vs. Time Relationship for Oedometer Tests Performed with Swell Overburden Testing Technique ( $P_o=25$ kPa) on Type-5 Expansive Soil Samples Treated with 10% Silt.....	190
Figure 5. 40	Vertical Swell Percentage vs. Time Relationship for Oedometer Tests Performed with Swell Overburden Testing Technique ( $P_o=25$ kPa) on Type-5 Expansive Soil Samples Treated with 20% Silt.....	191
Figure 5. 41	Vertical Swell Percentage vs. Time Relationship for Oedometer Tests Performed with Swell Overburden Testing Technique ( $P_o=25$ kPa) on Type-5 Expansive Soil Samples Treated with 30% Silt.....	191
Figure 5. 42	Vertical Swell Percentage vs. Time Relationship for Oedometer Tests Performed with Free Swell Testing Technique ( $P_s=7$ kPa) on Type-5 Expansive Soil for 10% ARR (Silt, Gravel and Empty Hole).....	193
Figure 5. 43	Vertical Swell Percentage vs. Time Relationship for Oedometer Tests Performed with Free Swell Testing	

	Technique ( $P_s=7$ kPa) on Type-5 Expansive Soil for 20% ARR (Silt, Gravel and Empty Hole).....	193
Figure 5. 44	Vertical Swell Percentage vs. Time Relationship for Oedometer Tests Performed with Free Swell Testing Technique ( $P_s=7$ kPa) on Type-5 Expansive Soil for 30% ARR (Silt, Gravel and Empty Hole).....	194
Figure 5. 45	Vertical Swell Percentage vs. Time Relationship for Oedometer Tests Performed with Swell Overburden Tests ( $P_o=25$ kPa) on Type-5 Expansive Soil for 10% ARR (Silt, Gravel and Empty Hole).....	194
Figure 5. 46	Vertical Swell Percentage vs. Time Relationship for Oedometer Tests Performed with Swell Overburden Tests ( $P_o=25$ kPa) on Type-5 Expansive Soil for 20% ARR (Silt, Gravel and Empty Hole).....	195
Figure 5. 47	Vertical Swell Percentage vs. Time Relationship for Oedometer Tests Performed with Swell Overburden Tests ( $P_o=25$ kPa) on Type-5 Expansive Soil for 30% ARR (Silt, Gravel and Empty Hole).....	195
Figure 5. 48	Lateral Swell Pressure vs. Time Relationship for Thin-Wall Ring Tests (Ring-1) Performed on Type-3 Untreated Soil Samples .....	197
Figure 5. 49	Lateral Swell Pressure vs. Time Relationship for Thin-Wall Ring Tests (Ring-1) Performed on Type-5 Untreated Soil Samples .....	198
Figure 5. 50	Lateral Swell Pressure vs. Time Relationship for Thin-Wall Ring Tests (Ring-2) Performed on Type-5 Untreated Soil Samples .....	199
Figure 5. 51	Lateral Swell Pressure vs. Time Relationship for Thin-Wall Ring Tests (Ring-1) Performed on Type-3 Soil Samples for Different Treatment Percentages ( $P_s=7$ kPa).....	201
Figure 5. 52	Lateral Swell Pressure vs. Time Relationship for Thin-Wall Ring Tests (Ring-1) Performed on Type-3 Soil Samples for Different Treatment Percentages ( $P_o=25$ kPa) .....	201

Figure 5. 53	Lateral Swell Pressure vs. Time Relationship for Thin-Wall Ring Tests (Ring-1) Performed on Type-3 Soil Samples for Different Treatment Percentages ( $P_o=50$ kPa) .....	202
Figure 5. 54	Lateral Swell Pressure vs. Time Relationship for Thin-Wall Ring Tests (Ring-1) Performed on Type-3 Soil Samples for Different Treatment Percentages ( $P_o=100$ kPa) .....	202
Figure 5. 55	Lateral Swell Pressure vs. Time Relationship for Thin-Wall Ring Tests (Ring-1) Performed on Type-5 Soil Samples for Different Treatment Percentages ( $P_s=7$ kPa).....	204
Figure 5. 56	Lateral Swell Pressure vs. Time Relationship for Thin-Wall Ring Tests (Ring-2) Performed on Type-5 Soil Samples for Different Treatment Percentages ( $P_s=7$ kPa).....	205
Figure 5. 57	Lateral Swell Pressure vs. Time Relationship for Thin-Wall Ring Tests (Ring-1) Performed on Type-5 Soil Samples for Different Treatment Percentages ( $P_o=25$ kPa) .....	205
Figure 5. 58	Lateral Swell Pressure vs. Time Relationship for Thin-Wall Ring Tests (Ring-2) Performed on Type-5 Soil Samples for Different Treatment Percentages ( $P_o=25$ kPa) .....	206
Figure 5. 59	Lateral Swell Pressure vs. Time Relationship for Thin-Wall Ring Tests (Ring-1) Performed on Type-5 Soil Samples for Different Treatment Percentages with Silt ( $P_s=7$ kPa) .....	207
Figure 5. 60	Lateral Swell Pressure vs. Time Relationship for Thin-Wall Ring Tests (Ring-2) Performed on Type-5 Soil Samples for Different Treatment Percentages with Silt ( $P_s=7$ kPa) .....	208
Figure 6. 1	Treatment Percentage in Vertical Swell vs. Area Replacement Ratio for Free Swell Oedometer Tests Performed on Type-2 Soil Samples .....	211
Figure 6. 2	Treatment Percentage in Vertical Swell Pressure vs. Area Replacement Ratio for Free Swell Oedometer Tests Performed on Type-2 Soil Samples .....	212
Figure 6. 3	Treatment Percentage in Vertical Swell vs. Area Replacement Ratio for Swell Overburden Oedometer Tests Performed on Type-2 Soil (Sand Treated).....	214

Figure 6. 4	Treatment Percentage in Vertical Swell vs. Area Replacement Ratio for Swell Overburden Oedometer Tests Performed on Type-2 Soil (Gravel Treated).....	215
Figure 6. 5	Treatment Percentage in Vertical Swell Pressure vs. Area Replacement Ratio for Swell Overburden Oedometer Tests Performed on Type-2 Soil .....	215
Figure 6. 6	Plan View of Soil Sample Intruded into Granular Material after Expanding.....	217
Figure 6. 7	A-A Cross Sectional View of Soil Sample Intruded into Granular Material after Expanding .....	217
Figure 6. 8	Average Final Water Content vs. Vertical Overburden Pressure for Oedometer Tests Performed on Type-2 Soil Treated with Sand.....	220
Figure 6. 9	Average Final Water Content vs. Vertical Overburden Pressure for Oedometer Tests Performed on Type-2 Soil Treated with Gravel.....	220
Figure 6. 10	Average Final Water Content vs. Area Replacement Ratio for Oedometer Tests Performed on Type-2 Soil Treated with Sand .....	221
Figure 6. 11	Average Final Water Content vs. Area Replacement Ratio for Oedometer Tests Performed on Type-2 Soil Treated with Gravel.....	221
Figure 6. 12	Vertical Swell vs. Area Replacement Ratio for Modified CBR Mould Tests Performed with 1 kPa and 7 kPa Seating Pressures (Phase-2, Stage(a)) .....	224
Figure 6. 13	Treatment Percentage in Vertical Swell vs. Area Replacement Ratio for Modified CBR Mould Tests Performed with 1 kPa and 7 kPa Seating Pressures (Phase-2, Stage(a)) .....	224
Figure 6. 14	Vertical Swell Percentage vs. Time Relationship for Oedometer Tests and Modified CBR Mould Tests on Type-5 Soil Samples ( $P_s=7$ kPa).....	227

Figure 6. 15	Vertical Swell vs. Area Replacement Ratio for Modified CBR Mould Tests Performed with 7 kPa Seating Pressure (Phase-2, Stage(b)) .....	228
Figure 6. 16	Vertical Swell vs. Area Replacement Ratio for Oedometer Tests Performed with 7 kPa Seating Pressure (Phase-2, Stage(b)).....	229
Figure 6. 17	Vertical Swell vs. Area Replacement Ratio for Modified CBR Mould and Oedometer Tests Performed with 7 kPa Seating Pressure (Phase-2, Stage(b)).....	229
Figure 6. 18	Treatment Percentage in Vertical Swell vs. Area Replacement Ratio for Modified CBR Mould and Oedometer Tests Performed with 7 kPa Seating Pressure (Phase-2, Stage(b)) .....	230
Figure 6. 19	Scatter of the Predicted versus Measured Vertical Swell Percentages for Oedometer Tests and Modified CBR Mould Tests on Type-5 Soil Samples ( $P_s=7$ kPa).....	232
Figure 6. 20	Vertical Swell Percentage vs. Time Relationship for Oedometer Tests and Modified CBR Mould Tests on Type-5 Soil Samples ( $P_o=25$ kPa).....	234
Figure 6. 21	Vertical Swell vs. Area Replacement Ratio for Modified CBR Mould Tests Performed with 25 kPa Overburden Pressure (Phase-2, Stage(c)) .....	235
Figure 6. 22	Vertical Swell vs. Area Replacement Ratio for Oedometer Tests Performed with 25 kPa Overburden Pressure (Phase-2, Stage(c)).....	235
Figure 6. 23	Vertical Swell vs. Area Replacement Ratio for Modified CBR Mould and Oedometer Tests Performed with 25 kPa Overburden Pressure (Phase-2, Stage(c)) .....	236
Figure 6. 24	Treatment Percentage in Vertical Swell vs. Area Replacement Ratio for Modified CBR Mould and Oedometer Tests Performed with 25 kPa Overburden Pressure (Phase-2, Stage(c)) .....	236

Figure 6. 25	Scatter of the Predicted versus Measured Vertical Swell Percentages for Oedometer Tests and Modified CBR Mould Tests on Type-5 Soil Samples ( $P_o=25$ kPa).....	238
Figure 6. 26	Final Water Content vs. Area Replacement Ratio for Modified CBR Mould Tests Performed with 7 kPa Seating Pressure.....	241
Figure 6. 27	Final Water Content vs. Area Replacement Ratio for Modified CBR Mould Tests Performed with 25 kPa Overburden Pressure.....	241
Figure 6. 28	Final Water Content vs. Area Replacement Ratio for Oedometer Tests Performed with 7 kPa Seating Pressure .....	242
Figure 6. 29	Final Water Content vs. Area Replacement Ratio for Oedometer Tests Performed with 25 kPa Overburden Pressure.....	242
Figure 6. 30	Final Water Content vs. Area Replacement Ratio (Type-1 Soil).....	243
Figure 6. 31	Final Water Content vs. Area Replacement Ratio (Type-2 Soil).....	243
Figure 6. 32	Final Water Content vs. Area Replacement Ratio (Type-3 Soil).....	244
Figure 6. 33	Final Water Content vs. Area Replacement Ratio (Type-5 Soil).....	244
Figure 6. 34	Vertical Swell vs. Area Replacement Ratio for Oedometer Tests Performed on Type -5 Soil, Treated with Gravel, Silt Layer and Silt Column with 7 kPa Seating Pressure (Phase-3) .....	246
Figure 6. 35	Vertical Swell vs. Area Replacement Ratio for Oedometer Tests Performed on Type -5 Soil, Treated with Gravel, Silt Layer and Silt Column with 25 kPa Overburden Pressure (Phase-3) .....	246
Figure 6. 36	Treatment Percentage in Vertical Swell vs. Area Replacement Ratio for Oedometer Tests Performed on	

	Type -5 Soil, Treated with Gravel, Silt Layer and Silt Column with 7 kPa Seating Pressure (Phase-3).....	247
Figure 6. 37	Treatment Percentage in Vertical Swell vs. Area Replacement Ratio for Oedometer Tests Performed on Type -5 Soil, Treated with Gravel, Silt Layer and Silt Column with 25 kPa Seating Pressure (Phase-3).....	247
Figure 6. 38	Final Water Content vs. Area Replacement Ratio for Type-5 Soil under Overburden Pressures of 7 kPa and 25 kPa (Phase-3) .....	249
Figure 6. 39	Vertical Swell Percentage vs. Overburden Pressure for Thin-Wall Ring Tests (Phase-4, Stage (a)) .....	250
Figure 6. 40	Effect of Overburden Pressure on Lateral Swell Pressure (Present Study) .....	253
Figure 6. 41	Effect of Overburden Pressure on Lateral Swell Pressure (Comparison with Previous Research) .....	254
Figure 6. 42	The Lateral Swell Pressure vs. Area Replacement Ratio Relationships for Type-3 Soil ( $P_s=7$ kPa).....	257
Figure 6. 43	The Lateral Swell Pressure vs. Area Replacement Ratio Relationships for Type-3 Soil ( $P_o=25$ kPa).....	258
Figure 6. 44	The Lateral Swell Pressure vs. Area Replacement Ratio Relationships for Type-3 Soil ( $P_o=50$ kPa).....	258
Figure 6. 45	The Lateral Swell Pressure vs. Area Replacement Ratio Relationships for Type-3 Soil ( $P_o=100$ kPa).....	259
Figure 6. 46	The Treatment in Lateral Swell Pressure vs. Area Replacement Ratio Relationships for Type-3 Soil .....	260
Figure 6. 47	Vertical Swell Percentage vs. Overburden Pressure for Different Area Replacement Ratios for Type-3 Soil .....	260
Figure 6. 48	Final Water Content vs. Area Replacement Ratio for Type-3 Soil under Different Overburden Pressures (Phase-4, Stage (b)).....	262
Figure 6. 49	The Lateral Swell Pressure vs. Area Replacement Ratio Relationships for Type-5 Soil and Ring-1 ( $P_s=7$ kPa) .....	263



Figure 6. 50	The Lateral Swell Pressure vs. Area Replacement Ratio Relationships for Type-5 Soil and Ring-2 ( $P_s=7$ kPa) .....	264
Figure 6. 51	The Lateral Swell Pressure vs. Area Replacement Ratio Relationships for Type-5 Soil and Ring-1 ( $P_o=25$ kPa) .....	264
Figure 6. 52	The Lateral Swell Pressure vs. Area Replacement Ratio Relationships for Type-5 Soil and Ring-2 ( $P_o=25$ kPa) .....	265
Figure 6. 53	The Lateral Swell Pressure vs. Area Replacement Ratio Relationships for Type-5 Soil .....	265
Figure 6. 54	Schematic Description of the Decrease in Peak Horizontal Swell Pressure as Area Replacement Ratio is Increased.....	266
Figure 6. 55	The Treatment Percentage vs. Area Replacement Ratio Relationships for Type-5 Soil .....	268
Figure 6. 56	Vertical Swell Percentage vs. Area Replacement Ratios for Type-5 Soil under Vertical Pressure of 7 kPa .....	269
Figure 6. 57	Vertical Swell Percentage vs. Area Replacement Ratios for Type-5 Soil under Vertical Pressure of 25 kPa .....	270
Figure 6. 58	Final Water Content vs. Area Replacement Ratio for Type-5 Soil under Vertical Pressure of 7 kPa (Phase-4, Stage (c)).....	271
Figure 6. 59	Final Water Content vs. Area Replacement Ratio for Type-5 Soil under Vertical Pressure of 7 kPa (Phase-4, Stage (c)).....	272
Figure 6. 60	The Lateral Swell Pressure vs. Area Replacement Ratio Relationships for Thin-Wall Ring Tests Performed on Type-5 Soil under Vertical Pressure of 7 kPa (Phase-4, Stage (d)) .....	273
Figure 6. 61	Vertical Swell Percentage vs. Area Replacement Ratios for Type-5 Soil under Vertical Pressure of 7 kPa for Gravel and Silt Treatment (Phase-4, Stage (d)) .....	275
Figure 6. 62	Final Water Content vs. Area Replacement Ratio for Type-5 Soil under Vertical Pressure of 7 kPa (Phase-4, Stage (d)) .....	276

Figure A. 1	Vertical Swell Percentage vs. Time Relationship for Thin-Wall Ring Tests (Ring-1) Performed on Type-3 Untreated Soil Samples .....	299
Figure A. 2	Lateral Swell Pressure vs. Time Relationship for Thin-Wall Ring Tests (Ring-1) Performed on Type-3 Untreated Soil Samples .....	300
Figure A. 3	Lateral Swell Pressure vs. Time Relationship for Thin-Wall Ring Tests (Ring-1) Performed on Type-3 Untreated Soil Samples ( $P_o=25$ kPa).....	300
Figure A. 4	Lateral Swell Pressure vs. Time Relationship for Thin-Wall Ring Tests (Ring-1) Performed on Type-3 Untreated Soil Samples ( $P_o=50$ kPa).....	301
Figure A. 5	Lateral Swell Pressure vs. Time Relationship for Thin-Wall Ring Tests (Ring-1) Performed on Type-3 Untreated Soil Samples ( $P_o=100$ kPa).....	301
Figure A. 6	Lateral Swell Pressure vs. Time Relationship for Thin-Wall Ring Tests Performed on Type-5 Untreated Soil Samples ( $P_s=7$ kPa).....	302
Figure A. 7	Lateral Swell Pressure vs. Time Relationship for Thin-Wall Ring Tests Performed on Type-5 Untreated Soil Samples ( $P_o=25$ kPa).....	302
Figure A. 8	Lateral Swell Pressure vs. Time Relationship for Thin-Wall Ring Tests Performed on Type-5 Untreated Soil Samples ( $P_o=50$ kPa).....	303
Figure A. 9	Lateral Swell Pressure vs. Time Relationship for Thin-Wall Ring Tests Performed on Type-5 Untreated Soil Samples ( $P_o=100$ kPa).....	303
Figure A. 10	Lateral Swell Pressure vs. Time Relationship for Thin-Wall Ring Tests Performed on Type-5 Untreated Soil Samples ( $P_o=150$ kPa).....	304
Figure B. 1	Vertical Swell Percentage vs. Time Relationship for Thin-Wall Ring Tests (Ring-1) Performed on Type-3 Soil with Different Treatment Percentages ( $P_o=25$ kPa) .....	305

Figure B. 2	Vertical Swell Percentage vs. Time Relationship for Thin-Wall Ring Tests (Ring-1) Performed on Type-3 Soil with Different Treatment Percentages ( $P_o=50$ kPa) .....	306
Figure B. 3	Vertical Swell Percentage vs. Time Relationship for Thin-Wall Ring Tests (Ring-1) Performed on Type-3 Soil with Different Treatment Percentages ( $P_o=100$ kPa) .....	306
Figure B. 4	Lateral Swell Pressure vs. Time Relationship for Thin-Wall Ring Tests (Ring-1) Performed on Type-3 Soil Samples with ARR=5% ( $P_o=25$ kPa) .....	307
Figure B. 5	Lateral Swell Pressure vs. Time Relationship for Thin-Wall Ring Tests (Ring-1) Performed on Type-3 Soil Samples with ARR=10% ( $P_o=25$ kPa) .....	307
Figure B. 6	Lateral Swell Pressure vs. Time Relationship for Thin-Wall Ring Tests (Ring-1) Performed on Type-3 Soil Samples with ARR=5% ( $P_o=50$ kPa) .....	308
Figure B. 7	Lateral Swell Pressure vs. Time Relationship for Thin-Wall Ring Tests (Ring-1) Performed on Type-3 Soil Samples with ARR=10% ( $P_o=50$ kPa) .....	308
Figure B. 8	Lateral Swell Pressure vs. Time Relationship for Thin-Wall Ring Tests (Ring-1) Performed on Type-3 Soil Samples with ARR=5% ( $P_o=100$ kPa) .....	309
Figure B. 9	Lateral Swell Pressure vs. Time Relationship for Thin-Wall Ring Tests (Ring-1) Performed on Type-3 Soil Samples with ARR=10% ( $P_o=100$ kPa) .....	309
Figure C. 1	Lateral Swell Pressure vs. Time Relationship for Thin-Wall Ring Tests Performed on Type-5 Soil (10% Treated ; $P_s=7$ kPa).....	310
Figure C. 2	Lateral Swell Pressure vs. Time Relationship for Thin-Wall Ring Tests Performed on Type-5 Soil (20% Treated ; $P_s=7$ kPa).....	311
Figure C. 3	Lateral Swell Pressure vs. Time Relationship for Thin-Wall Ring Tests Performed on Type-5 Soil (30% Treated ; $P_s=7$ kPa).....	311

Figure C. 4	Lateral Swell Pressure vs. Time Relationship for Thin-Wall Ring Tests Performed on Type-5 Soil (10% Treated ; $P_0=25$ kPa).....	312
Figure C. 5	Lateral Swell Pressure vs. Time Relationship for Thin-Wall Ring Tests Performed on Type-5 Soil (20% Treated ; $P_0=25$ kPa).....	312
Figure C. 6	Lateral Swell Pressure vs. Time Relationship for Thin-Wall Ring Tests Performed on Type-5 Soil (30% Treated ; $P_0=25$ kPa).....	313
Figure D. 1	Lateral Swell Pressure vs. Time Relationship for Thin-Wall Ring Tests Performed on Type-5 Soil (10% Treated with Silt ; $P_s=7$ kPa).....	314
Figure D. 2	Lateral Swell Pressure vs. Time Relationship for Thin-Wall Ring Tests Performed on Type-5 Soil (20% Treated with Silt ; $P_s=7$ kPa).....	315
Figure D. 3	Lateral Swell Pressure vs. Time Relationship for Thin-Wall Ring Tests Performed on Type-5 Soil (30% Treated with Silt ; $P_s=7$ kPa).....	315
Figure E. 1	Vertical Swell Percentage vs. Time Relationship for Oedometer Tests and Modified CBR Mould Tests on Type-1 Soil Samples ( $P_s=7$ kPa).....	316
Figure E. 2	Vertical Swell Percentage vs. Time Relationship for Oedometer Tests and Modified CBR Mould Tests on Type-2 Soil Samples ( $P_s=7$ kPa).....	317
Figure E. 3	Vertical Swell Percentage vs. Time Relationship for Oedometer Tests and Modified CBR Mould Tests on Type-3 Soil Samples ( $P_s=7$ kPa).....	317
Figure E. 4	Vertical Swell Percentage vs. Time Relationship for Oedometer Tests and Modified CBR Mould Tests on Type-4 Soil Samples ( $P_s=7$ kPa).....	318
Figure E. 5	Vertical Swell Percentage vs. Time Relationship for Oedometer Tests and Modified CBR Mould Tests on Type-5 Soil Samples ( $P_s=7$ kPa).....	318

Figure E. 6	Vertical Swell Percentage vs. Time Relationship for Oedometer Tests and Modified CBR Mould Tests on Type- 1 Soil Samples ( $P_o=25$ kPa).....	319
Figure E. 7	Vertical Swell Percentage vs. Time Relationship for Oedometer Tests and Modified CBR Mould Tests on Type- 2 Soil Samples ( $P_o=25$ kPa).....	319
Figure E. 8	Vertical Swell Percentage vs. Time Relationship for Oedometer Tests and Modified CBR Mould Tests on Type- 3 Soil Samples ( $P_o=25$ kPa).....	320
Figure E. 9	Vertical Swell Percentage vs. Time Relationship for Oedometer Tests and Modified CBR Mould Tests on Type- 5 Soil Samples ( $P_o=25$ kPa).....	320

## **CHAPTER I**

### **INTRODUCTION**

Most of clayey soils in arid or semi-arid regions more or less have a tendency to swell. The magnitude of expansion depends mostly upon the kind and amount of clay minerals present, hydration of cations on clay surfaces and release of intrinsic stresses caused by overconsolidation. Deformational behaviour of clay, under changes of moisture content and state of stress, is therefore a complex function of both the physiochemical and the effective strength characteristics of clay.

Since it was recognized that any structure constructed on or in expansive soils may be threatened by large vertical and horizontal stresses, many attempts have been made to assess their extent both in the field and laboratory conditions. These investigations were mainly focused on two swell parameters which are namely the swell pressure and swell percentage. Today, based on its availability and simplicity, conventional oedometer test is the most widely used testing technique for the determination of these parameters and there are three alternative laboratory oedometer test methods approved by ASTM and designated as D 4546 – 08 (2008) for determining the swell potential of relatively undisturbed or compacted cohesive soils.

At the very early stages of investigations about the expansive soils, it was clearly recognized that their behaviour can best fit the deformation in the 3D space, and simulating the behaviour by means of a one dimensional test can lead to unrealistic results (McDowell, 1956). The results of the case histories and more complicated laboratory tests revealed that conventional oedometer tests overpredict vertical deformations by a factor of 3 (McDowell, 1956 ; Richards, 1967 ; Erol et. al., 1987, Dhowian, 1990, Al-Shamrani and Dhowian, 2003).

Realizing the limitations of the conventional oedometer tests for the assessment of swell potential and swell parameters, alternative methods have been devised by several researchers to simulate the actual field conditions in a more rational manner.

The expansive soils are a worldwide problem and the unattended swell and shrink cycles of expansive soils lead to serious damage to civil engineering structures, the cost of which sums up to several billion dollars annually. As a consequence, engineering practice is continuously searching for effective rehabilitation solutions to control, if not totally prevent, the ground movement resulting from the expansive soils.

In this experimental study, it is intended to investigate the possible positive outcomes of forming trenches in expansive soils and backfilling them with granular material, and hence to follow up the variations in the swell parameters. For this purpose, a comprehensive laboratory test program was conducted, including conventional oedometer tests, modified thin-wall oedometer tests and larger sized laboratory scale tests on modified CBR moulds were performed both on untreated samples and on samples treated with granular materials. In a group of tests, the granular backfill material was interchanged with silt, which is also used as a blanket layer for CNS (Cohesive Non-Swelling Soil) effect in another set of experiments.

To give a better understanding of the concept of expansive clays and the solutions offered to overcome its hazardous nature, a literature survey is performed on past research for the assessment of vertical and lateral swell parameters as well as the common methods used for the stabilization of expansive soils and the outcomes are presented in Chapter II.

Chapter III involves assembly details for the three test apparatus to be used during the investigations mainly focusing on their specific features. The calibration procedure for relevant devices is also presented in this chapter.

In Chapter IV, the details of the test program are given, mainly concentrating on the test material to be used and the preparation of the test specimens. This chapter also focuses on the development of the test schedule.

In Chapter V, the results of experiments are enlisted, with emphasis on cause and effect of the phased progress of the test program. The explanations of the test outcomes and comparisons with previous research are presented in Chapter VI, with comprehensive discussion of the test results.

Finally in Chapter VII, an overall coverage of the conclusions drawn at the end of each phase of the experimental program is given.



## **CHAPTER II**

### **AN OVERVIEW OF RELATED LITERATURE**

#### **2.1 INTRODUCTION**

The present investigation involves a comprehensive research activity performed to assess the efficiency of treatment of the vertical and lateral swelling parameters of expansive soils by introducing trenches or holes in the soil and filling them with granular material. Therefore, this chapter is dedicated to an extensive literature survey on the assessment of vertical and lateral swell parameters, and the common methods used for the stabilization of expansive soils.

#### **2.2 SWELL POTENTIAL AND PARAMETERS**

Swell potential can be defined as the vertical or volumetric percent swell where lateral deformations are prevented by means of lateral restraint. A more comprehensive definition of swell potential was given by Seed et al. (1962(a)), who offered the determination of the percentage of swell on a laterally restrained soil sample that is soaked with a surcharge of 7 kPa following its compaction to its maximum dry density at its optimum water content as outlined in the AASHTO compaction test procedure.

As a matter of fact, to make an effective definition of swell potential, one shall incorporate into the explanation the effects of site conditions including the ones pertaining to the stress conditions i.e., the present overburden pressure and the confinement degree as well as other properties of soil such as its initial water content and dry density. A definition that embraces all these factors is introduced

by Snethen (1984), who portrays the swell potential as “the vertical volume change obtained from a conventional oedometer test and can be expressed as the percentage of the original height of an undisturbed sample at its initial water content and dry density to the height of the sample saturated under the applied load equivalent to present overburden pressure”.

In case the overburden pressure is high enough to restrict the swelling, then, the swell potential of a particular soil is governed by the magnitude and extent of vertical and lateral soil pressures imposed by the named boundary conditions. Swell pressure is simply the overburden to be applied on the soil sample and is needed to keep the soil volume at its initial magnitude even after the water content of the sample is increased. As a consequence of this fact, either the percent free swell or the swell pressure can be used as the swell parameters to predict the swell potential of a clayey soil sample.

### **2.3 FACTORS AFFECTING SWELL POTENTIAL**

The swell potential of a clayey soil is mainly affected by the properties of the soil in question, the environmental factors acting on the system and the state of stress present on the soil. These factors are summarized in Table 2.1.

Among the factors given below, the mineralogical composition and clay content of the soil in question are obviously the most important factors influencing the extent of swell of clayey soils. Past research has proved that the magnitude of swell potential of a clayey soil varies with the kind of clay mineral present dominating the soil mass, where montmorillonite and illite demonstrate higher swelling tendency compared to kaolinite (Lambe and Whitman, 1969).

This behaviour is mainly a result of variations in the electrical field with each clay mineral type, which in turn yield distinguishing swelling features. As a result, not only the amount but also the variety of clay present in the soil mass can be said to have a major influence on the swell potential. El-Sohby and Rabba (1981)

presented similar conclusions, reporting that the swell potential or swell pressure of a definite soil mass increase as its clay content is increased as represented in Figure 2.1 and Figure 2.2. The authors also investigated the effect of initial dry density and initial water content on the swell potential. Their findings are consistent with that is enlisted in Table 2.1 as they concluded that the swell potential increases with increasing initial dry density but decreases with increasing initial water content. The named correlations are given in Figure 2.3, Figure 2.4 and Figure.2.5.

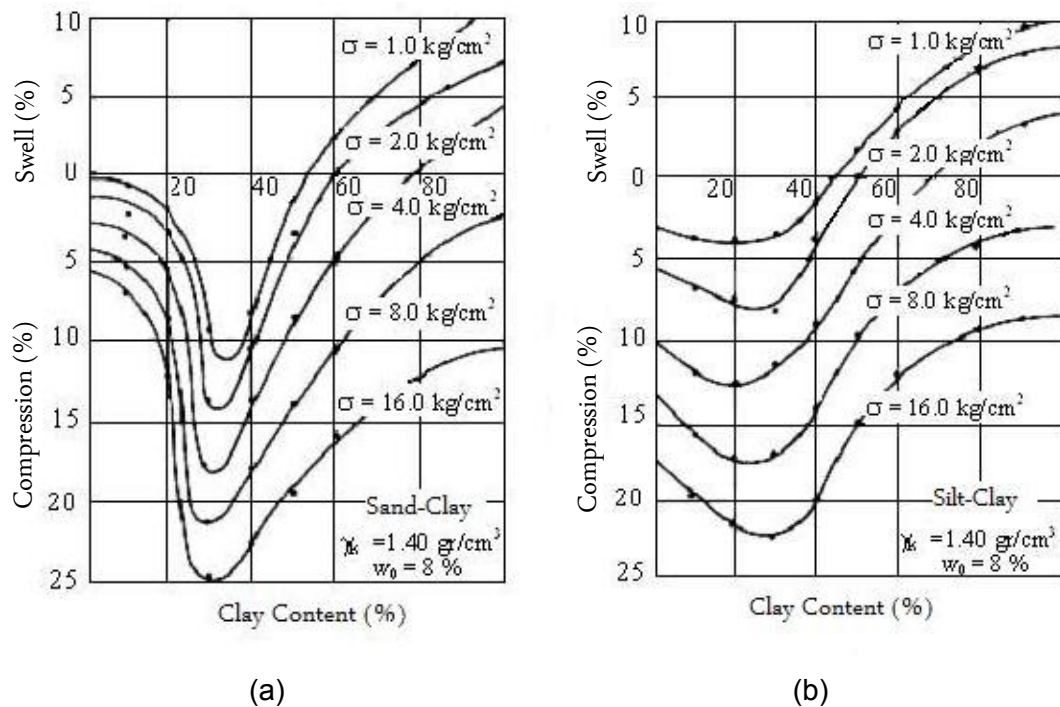


Figure 2. 1 Effect of Clay Content on the Swelling Potential of Soils (a) Results of Sand-Clay Soils (b) Results of Silt – Clay Soils (El-Sohby and Rabba, 1981)

Table 2. 1 Factors Affecting Swell Potential (adapted from Nelson and Miller, 1992)

Soil Properties	Environmental Factors	State of Stress
<p><b>Mineralogical Composition of Clay</b></p> <p>Montmorillonites and their mixed layers with other clay minerals are potentially expansive. Very fine particles of illites and kaolinites may also cause volumetric changes.</p> <p><b>Structure of Clay</b></p> <p>Flocculated clay particles have a greater tendency to swell compared to clays with dispersed particles.</p> <p>In addition, cementation reduces swell tendency</p> <p><b>Mineralogical Composition of Pore Water</b></p> <p>High concentration of cations as well as increased cation valences reduce the tendency to swell. In other words, presence of divalent and trivalent cations in the pore water suppress swelling, whereas monovalent cations increase it.</p> <p><b>Suction</b></p> <p>Suction (<math>u_a - u_w</math>) refers to difference value between pore air pressure <math>u_a</math> and pore water pressure <math>u_w</math> in unsaturated soils. It reflects the capacity of the soil matrix to hold water and is a function of soil structure, granular components, pore size and particle distribution.</p> <p><b>Plasticity</b></p> <p>Plasticity is an indication for swell potential. Clays that have high liquid limit generally exhibit a tendency to swell.</p> <p><b>Dry Density</b></p> <p>The larger the dry density, the closer the particle spacing, that in turn facilitates repellent forces and hence swell potential.</p>	<p><b>Climate</b></p> <p>The problem of expansive clays is very common in arid and semi-arid regions of the world, as well as at places where periods of droughts are followed by an intensive rainy season.</p> <p><b>Temperature Variations</b></p> <p>An increase in ambient temperature causes soil moisture to dissipate towards cooler areas, mostly under foundations or pavement slabs, causing expansion underneath.</p> <p><b>Initial Moisture Content and its Variations</b></p> <p>Natural clayey soils with smaller initial moisture content and with high liquid limit have a potency to swell. The active zone close to the upper boundary of the profile is highly moisture sensitive.</p> <p><b>Location of Water Table</b></p> <p>Superficial and fluctuating water tables promote heave.</p> <p><b>Surface Drainage and Artificial Water Sources</b></p> <p>Water accumulation from surface drainage or seepage from manmade hydraulic construction contribute to swell.</p> <p><b>Field Permeability</b></p> <p>Fissures and cracks cause high permeability of the soil, thus leading to higher rates of heave.</p> <p><b>Vegetation</b></p> <p>Alternating vegetation type or density lead to differential wetting of soil and cause depleted and wetted areas.</p>	<p><b>Stress History</b></p> <p>Overconsolidation of a clay causes an increase in swell potential compared to the same clay with the same void ratio under normal consolidation conditions.</p> <p><b>Initial In-Situ Stress State</b></p> <p>The initial in-situ effective stresses acting on the soil must be known to assess the outcomes of loading the soil or changing its water content.</p> <p><b>Surcharge</b></p> <p>External loading, if large enough, counteracts the repulsive forces and eliminates swell.</p> <p><b>Soil Profile</b></p> <p>Superficial expansive layers reaching down below the active zone have a greater tendency to swell than the ones that are covered by a nonexpansive layer.</p>

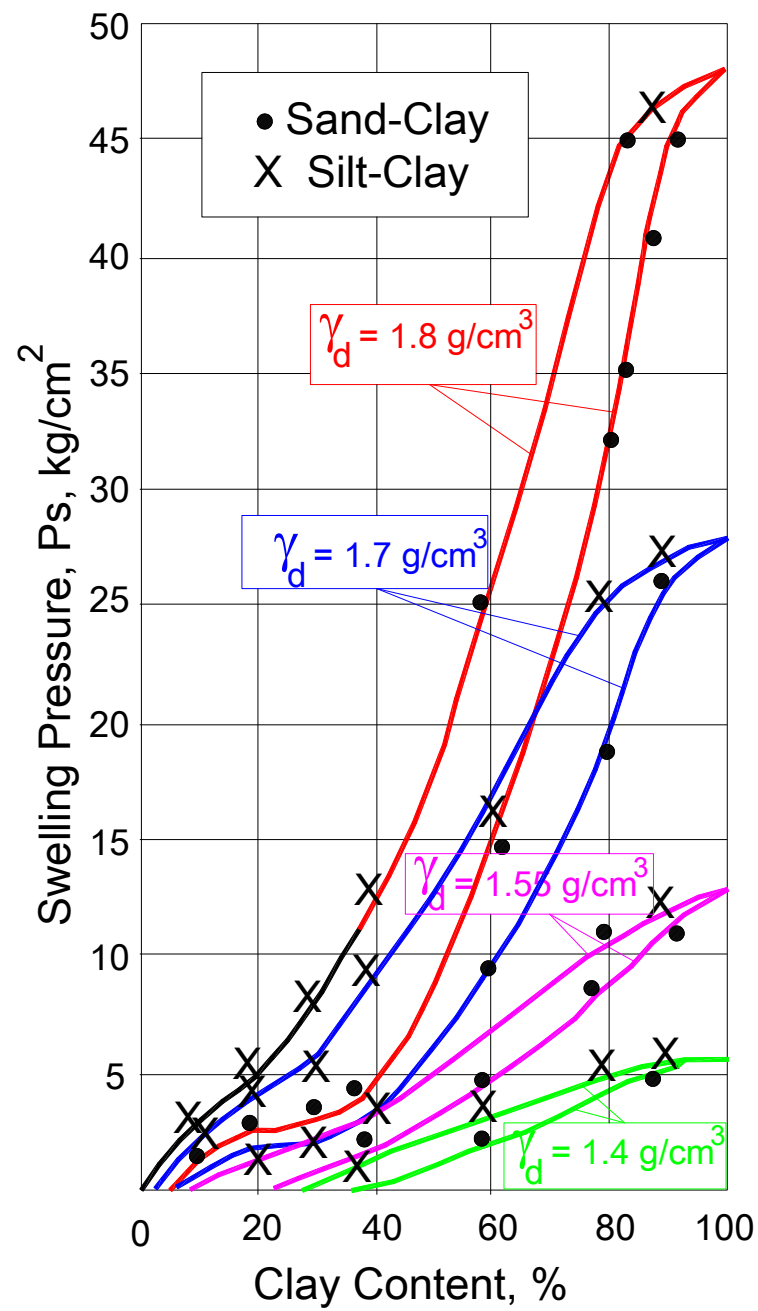


Figure 2. 2 Effect of Clay Content on the Swelling Pressure of Soils (El-Sohby and Rabba, 1981)

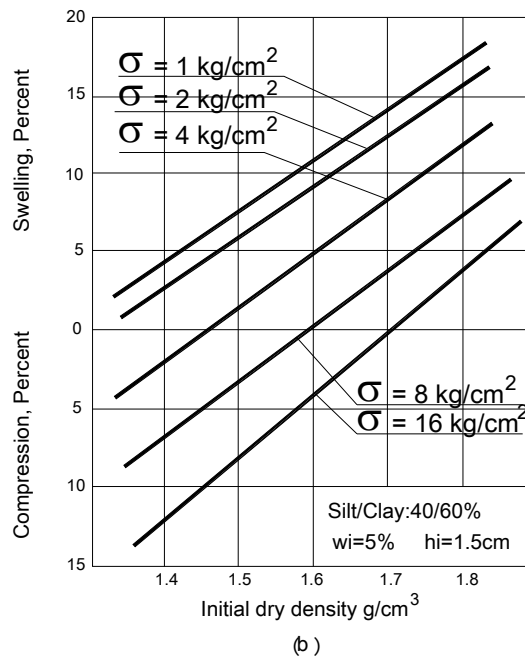
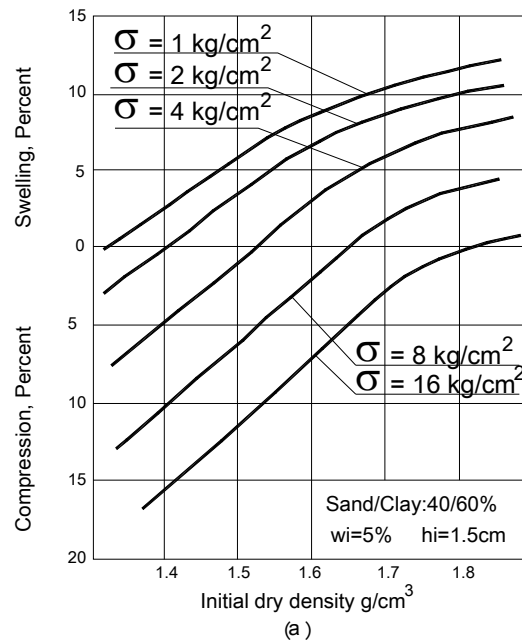


Figure 2. 3 Effect of Initial Dry Density on the Swelling Potential of Soils  
 (a)Results of Sand-Clay Soils (b) Results of Silt – Clay Soils (El-Sohby and Rabba, 1981)

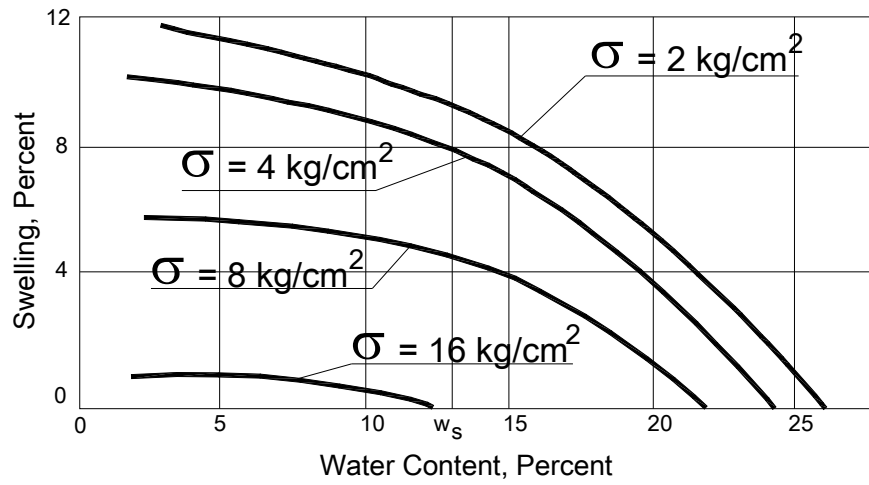


Figure 2. 4 Effect of Initial Water Content on the Swell Percentage of Soils (El Sohby and Rabba, 1981)

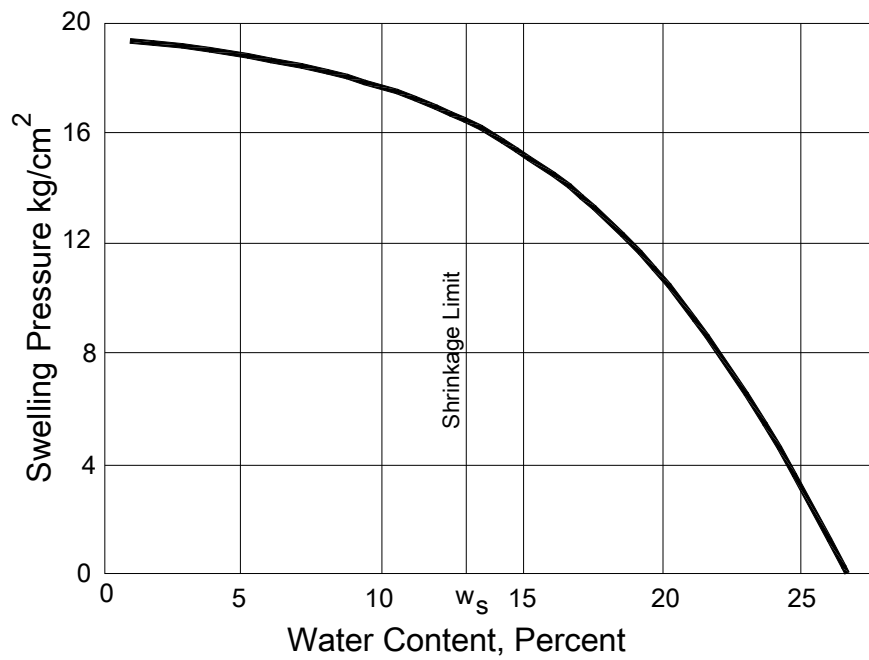


Figure 2. 5 Effect of Initial Water Content on the Swell Pressure of Soils (El-Sohby and Rabba, 1981)

The inverse relationship between the initial water content and the swelling potential is in fact foreseeable, as the likelihood of the soil to absorb excess water decreases while the initial degree of saturation increases, thus leading to a decrease in the swelling ability. From Figures 2.4 and 2.5, it can be seen that the reaction of swelling parameters to initial water content becomes more pronounced after the water content exceeds the shrinkage limit. Parallel results were obtained from the investigations of various researchers including but not limited to Edil and Alanazy (1992), and, Erol and Ergun (1994). Similarly, thin-wall oedometer tests conducted by Sapaz (2004) yielded that (a) for a group of samples with identical dry unit weights, increasing the initial water content leads to a decrease in both the vertical and lateral swell pressures; (b) for a group of samples with identical initial water contents, increasing the initial dry unit weights leads to an increase in both the vertical and lateral swell pressures.

Joshi and Katti (1984) isolated their designated research to study the effect of surcharge loads and depth on lateral swell pressures. The authors reported that higher lateral pressures develop when a sample is saturated under a preliminary high surcharge which is then lowered, compared to the lateral pressure developed under initially lower surcharges. The time elapsed to reach the equilibrium lateral swelling pressure, i.e. the constant value of lateral swelling pressure achieved under a given initial surcharge load, depends on the magnitude of initial surcharge load. Raising the initial surcharge causes a prompt increase in the lateral swell pressures. However, the ratio of the lateral swell pressure to the vertical swell pressure, namely the swell ratio, decreases when the initial surcharge is increased. The above mentioned behaviors are given in Figure 2.6. Joshi and Katti (1984) also worked on large scale laboratory tests to model field conditions in terms of the effect of depth factor. The authors concluded that (a) the lateral pressure just below the ground level was insignificant; (b) at 1.00 meters of depth the lateral swelling pressure increased up to  $287 \text{ kN/m}^2$ , which was nearly equal to the vertical swelling pressure and (c) after this point the lateral swell pressure remained constant up to where the weight of the soil above was equal to the swelling pressure.



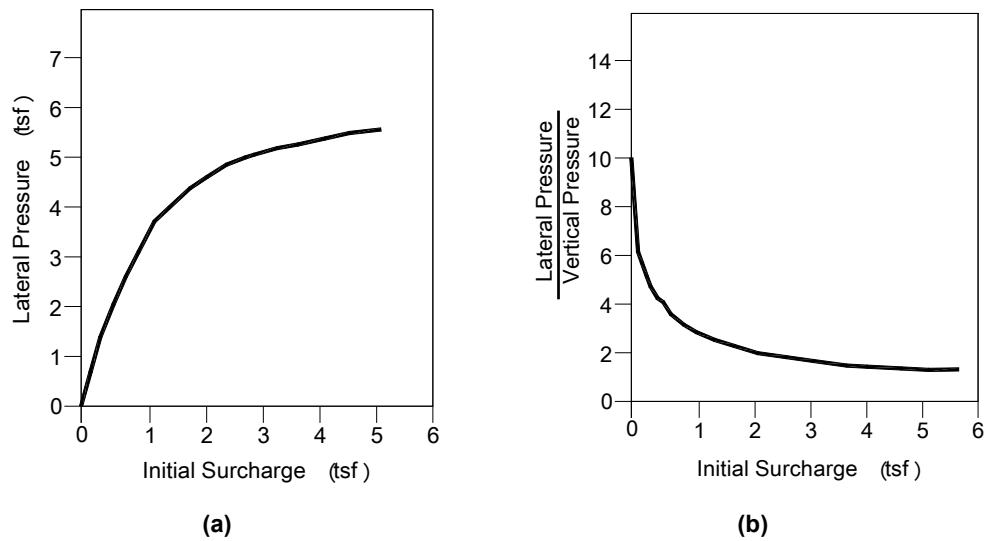


Figure 2. 6 Effect of Initial Surcharge on (a) Lateral Swell Pressure (b) Swell Pressure Ratio (Joshi and Katti, 1984)

## 2.4 CLASSIFICATION OF EXPANSIVE SOILS

Construction on expansive soils necessitates a comprehensive engineering analysis and design work to prevent any potential damage, to which the structures may be encountered, not only during construction but also during the life span of the structure. The improper design criteria proposed as a result of inadequate engineering analysis may lead to catastrophic results therefore a suitable evaluation of expansive soil classification shall be incorporated in the very early phases of the analysis and design stages.

Various direct and indirect test methods, to characterize expansive soils and to predict the anticipated level of volumetric change, are available in the literature. In addition, visual inspection of surface appearance as well as mineralogical identification procedures such as X-Ray Diffraction or Differential Thermal Analysis may also be used although they are expensive and uncommon. Lately, concentrated efforts have been made to utilize remote sensing technology to

model volumetric change potential and related index properties of expansive soils (Goetz et al., 2001; Chabrilat et al., 2002; Kariuki et al., 2004; Yitagesu et al., 2009; Ben-Dor et al., 2009).

As far as the direct measuring methods are concerned, the most commonly used procedures are measurement of the swell pressure, i.e. the pressure needed to resist the expansion of soil, via the oedometer and triaxial testing apparatus to simulate actual conditions on site.

There also exist a number of indirect methods to determine the swelling potential of expansive methods. The indirect classification of expansive soils generally offers a qualitative rating, which evaluates expansive soils from non-critical to highly critical in terms expected expansions. However, as it was stated by Seed et al. (1962(a)), any two soils with similar ratings of probable swell, may in turn demonstrate very different swell characteristics. Therefore, a satisfactory classification shall also encompass soil properties, i.e. the index properties or mineralogical properties along with actual stress data and the qualitative rating. Some of the popular classification models for expansive soils are explained in the following subsections.

#### **2.4.1 USAEWES Classification**

A classification scheme involving the plasticity index, in-situ soil suction and potential swell is recommended by Snethen et al. (1977) in the referred publication of the United States Army Engineer Waterways Experiment Station (USAEWES). The classification given in Table 2.2 assumes the potential swell as the swell percentage obtained from a free swell test under an initial surcharge of 2.5 kPa.

Table 2. 2      USAEWES Classification of Expansive Soils (Snethen et al., 1977)

Liquid Limit	Plasticity Index	In-situ Soil Suction	Potential Swell (% Swell)	Potential Swell Classification
(LL, %)	(I <sub>p</sub> , %)	( $\sigma_{ini}$ , tons/sq.ft)		
< 50	< 25	< 1.5	< 0.5	LOW
50 - 60	25 - 35	1.5 – 4.0	0.5 – 1.5	MARGINAL
> 60	> 35	> 4.0	> 1.5	HIGH

#### 2.4.2 USBR Classification

Another method suggested by the United States Bureau of Reclamation (USBR) on the other hand, uses the clay size fraction less than 2 $\mu$ m (percent by weight) along with the shrinkage limit, plasticity index and percent swell as the classification parameters. The classification criteria are listed in Table 2.3, as cited in Erol (1987).

Table 2. 3      USBR Classification of Expansive Soils (adapted from Erol, 1987)

Clay-size Fraction	Plasticity Index	Shrinkage Limit	Percent Swell	Classification of Expansiveness
(<2 $\mu$ m, %)	(I <sub>p</sub> , %)	(SL, %)	(%)	
> 15	< 18	> 15	< 10	LOW
13 – 23	15 – 28	10 – 16	10 – 20	MEDIUM
20 – 31	25 – 41	7 – 12	20 – 30	HIGH
> 28	> 35	< 11	> 30	VERY HIGH

### 2.4.3 Classification Based on Clay Percent and Activity

Plasticity of a clayey soil mainly depends on its mineral types and relative quantities of these minerals present in the soil sample. Skempton (1953) realized that plasticity of soil mass increased with the increase in clay fraction, and defined the term activity as:

$$A = \frac{I_p}{C} \dots\dots\dots (2.1)$$

where, A: Activity

$I_p$ : Plasticity Index, (%)

C:Percent Clay Fraction finer than 2 $\mu$ m

Typical activity values of various minerals are given in Table.2.4.

Table 2. 4 Activity of Various Minerals (Skempton, 1953 and Mitchell, 1993)

Mineral	Activity
Na-montmorillonite	4-7
Ca-montmorillonite	1-5
Illite	0.5-1.3
Kaolinite	0.3-0.5
Halloysite (dehydrated)	0.5
Halloysite (hydrated)	0.1
Attapulgit	0.5-1.2
Allophane	0.5-1.2
Mica (muscovite)	0.2
Calcite	0.2
Quartz	0

Seed et al. (1962(b)) proposed an activity based classification in which the soil samples were remolded and artificially compacted in standard AASHTO compaction test under a surcharge of 1 psi. Another relationship was defined by Popescu (1986), who proposed the utilization of the plasticity index, clay content and the activity of the soil in expansiveness classification. The two methods are consecutively displayed in Figure 2.7 and Figure 2.8. Based on the original data determined by Seed et al. (1962(b)), Mitchell (1993) developed another relationship for the swell potential of soils by using the activity and clay fraction of soils as:

$$S = (3.6 \times 10^{-5}) \times A^{2.44} \times C^{3.44} \quad \dots\dots\dots (2.2)$$

where, S: Swell Potential (%)

A: Activity

C: Percent Clay Fraction finer than 2µm

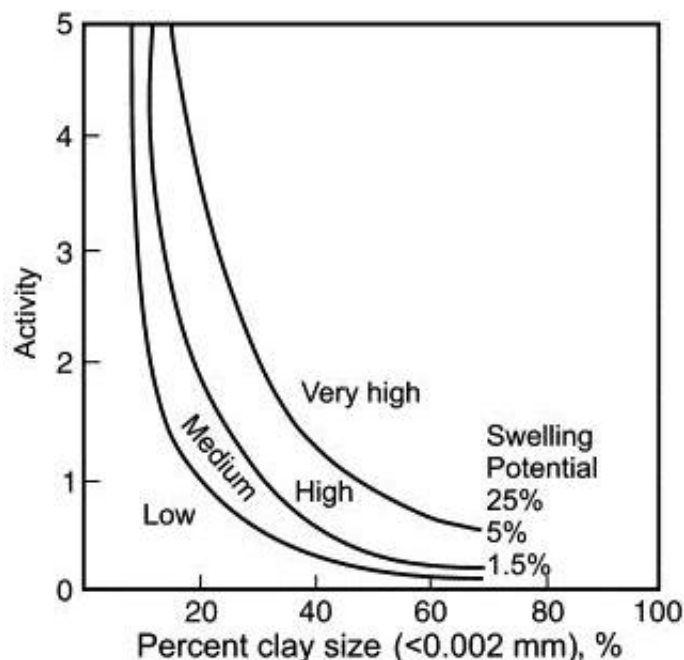


Figure 2. 7 Swell Potential Classification (Seed et al., 1962(b))

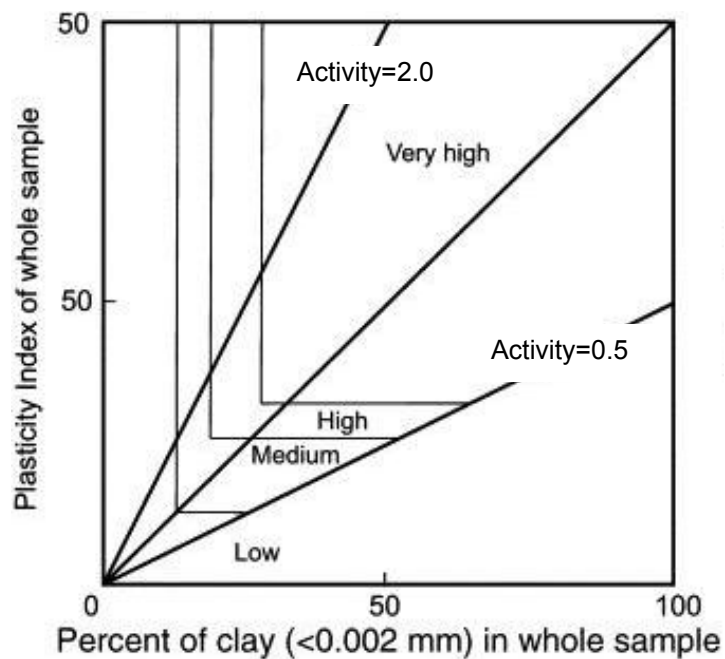


Figure 2. 8 Swell Potential Estimation (Popescu, 1986)

## 2.5 ASSESSMENT OF SWELL PARAMETERS

As it has already been mentioned in the previous section, percent swell and swell pressure can be assessed by means of various methods. While empirical relationships, involving charts and tables developed by various researchers, offer the opportunity to estimate the approximate values of these parameters, standardized oedometer test methods and three dimensional laboratory as well as site tests, exhibit the effort to assess these parameters in a more rational manner.

### **2.5.1 Empirical Methods**

The empirical methods used to assess the swell parameters of clayey soils mostly depend on experience related with certain geographical and climatic conditions. These methods give the opportunity to the engineers to assess the swell parameters by using simple apparatus and well defined indices such as Atterberg limits, clay content, initial water content and dry density. Though these methods are widely used to anticipate the swell parameters rapidly, it should always be kept in mind that; relationships were developed for a particular case study and may not reflect the actual behaviour present at the subject site. Some empirical formulae reported by various researchers are presented in Table 2.5.

### **2.5.2 Suction Method**

Soil suction phenomenon was first developed for agricultural purposes. Its extent to geotechnics can be seen in the 1950's at the Road Research Laboratory in England (Croney and Coleman, 1948). From geotechnical engineering point of view, total suction can be divided into two components, i.e.; "matric suction" which is defined as the difference between pore air and pore water pressure, and "osmotic suction" that is directly related with the salt content in the pore water of soil mass. Based on the assumption that osmotic suction remains constant, total suction is mainly affected from the change in matric suction (Fredlund and Rahardjo, 1993). Capillary phenomenon and capillarity observed in unsaturated soil masses due to surface tension developed between water, soil particles and air are essentially the matric suction of the soil mass. Matric suction, in more general terms, can be described as the ability of soil mass to absorb and hold water. According to Snethen (1980) the physical behaviour of any soil mass, which mainly consists of the interaction between soil particles and water, can be described by using the soil suction phenomenon.

Measurement of soil suction (or the negative pore water pressure) by either a pressure plate or a thermocouple psychrometer test apparatus, in turn allows the

verification of the influence of presence of moisture on the volume and strength parameters of partially saturated soils. A psychrometer is an instrument commonly used in laboratories to measure relative humidity, from which the soil suction can be estimated. This method is recommended by Erol et al. (1987) as a superior method to the oedometer test, with shorter test durations as well as better representation of environmental conditions.

### **2.5.3 Potential Volume Change (PVC)**

The PVC test that was developed by T.W Lambe in the 1960's for the U.S. Department of Housing and Development (FHA in short), is essentially the measurement of the pressure exerted by a sample of compacted soil when it swells against a restraining force after being wetted. The pressure reading thus taken is called the "swell index", which is then converted to potential volume change by using the chart given in Figure 2.9 (FHA, 1974).



Table 2. 5 Empirical Relationships for the Assessment of Swell

Researchers	Relationships Based on	Proposed Empirical Equation
Seed et al., 1962(b)	Activity (A) and Clay Content (C)	$S_p = 3.6 \times 10^{-5} (A^{2.44}) (C^{3.44})$
	Plasticity Index (PI)	$S_p = 3.6 \times 10^{-5} (M) (PI^{2.44})$ where M=60 for natural and M=100 for artificial soils
Van der Merve, 1964	Correction Factor (F), Thickness of Non-Expansive Layer (D), Thickness of Expansive Layer (H)	$\Delta H = F \times e^{-0.377D} \times (e^{-0.377H} - 1)$
Komornik and David, 1969	Liquid Limit (LL), Initial Water Content ( $w_0$ ) and Dry Unit Weight ( $\gamma_d$ ) ( $\gamma_d$ in kg/m <sup>3</sup> )	$\log P_s = -2.132 + 0.0208LL + 0.000665\gamma_d - 0.0269 w_0$
Nayak and Christensen, 1971	Plasticity Index (PI), Initial Water Content ( $w_0$ ) and Clay Content (C)	$S_p = (0.00229PI)(1.45C)/w_0 + 6.38$
		$P_s = (3.58 \times 10^{-2}) PI^{1.12} C^2/w_0^2 + 3.79 (P_s \text{ in psi})$
Vijayvergia anf Ghazzaly, 1973	Liquid Limit (LL), Initial Water Content ( $w_0$ ) and Dry Unit Weight ( $\gamma_d$ ) ( $\gamma_d$ in lb/ft <sup>3</sup> )	$\log S_p = (0.44LL - w_0 + 5.5) / 12$
		$\log S_p = 0.0526 \gamma_d + 0.033LL - 6.8$
Schnider et al., 1974	Plasticity Index (PI) and Initial Water Content ( $w_0$ )	$\log S_p = 0.9(PI/w_0) - 1.19$
Johnson and Snethen, 1978	Thickness of Expansive Layer (H), Plasticity Index (PI), Initial Water Content ( $w_0$ )	$S_p = 23.82 + 0.7346PI - 0.1458H - 1.7w_0 + 0.00225PIw_0 - 0.0088PIH$
		$S_p = -9.18 + 1.5546PI + 0.08424H + 0.1w_0 - 0.0432 PI w_0 - 0.0215 PIH$
Weston, 1980	Weighted Liquid Limit ( $LL_w$ ), Surcharge Load ( $\sigma_v$ ), Initial Water Content ( $w_0$ )	$S_p = 0.00411(LL_w)^{4.17} \sigma_v^{-3.86} w_0^{-2.33}$
Chen, 1988	Plasticity Index (PI)	$S_p = 0.2558e^{0.383(PI)}$
TxDOT, 1999	Plasticity Index (PI)	$S_p = 0.217(PI) - 2.9$ (For Optimum Conditions) $S_p = 0.294(PI) - 2.9$ (For Average Conditions with $PI < 60$ )
Thomas et al., 2000	Clay Content (C), Cation Exchange Capacity (CEC), Liquid Limit (LL), Swell Index ( $C_s$ )	Unified Expansive Soil Index (ESI) Estimation
Ergüler and Ulusay, 2003	Liquid Limit (LL), Methylene Blue Value (MBV), Clay Content (C), Plastic Limit (PL), Plasticity Index (PI), Water Content at 24 h ( $w_{max24}$ ), Water Content at 72 h ( $w_{max72}$ ), Percent of Smectite ( $S_m$ )	$S_p$ and $P_s$ Values Estimated from Various Equations
Kariuki and van der Meer, 2004	Activity (A), Cation Exchange Activity (CEA), Saturated Standard Moisture (SSP), Linear Extensibility Percentage (LEP)	Unified Expansive Soil Index (ESI) Estimation
Avşar, Ulusay and Ergüler, 2005	Liquid Limit (LL), Methylene Blue Value (MBV), Clay Content (C), Plasticity Index (PI)	$S_p$ and $P_s$ Values Estimated from Various Equations
Yılmaz, 2009	Liquidity Index (LI)	$S_p = 2.0981e^{(-1.7196LI)}$
Yılmaz and Kaynar, 2011	Liquid Limit, Cation Exchange Capacity (CEC), Activity (A)	$S_p = 9.223 \times 10^{-2} LL + 2.041 \times 10^{-2} A + 5.535 \times 10^{-2} CEC - 0.153$

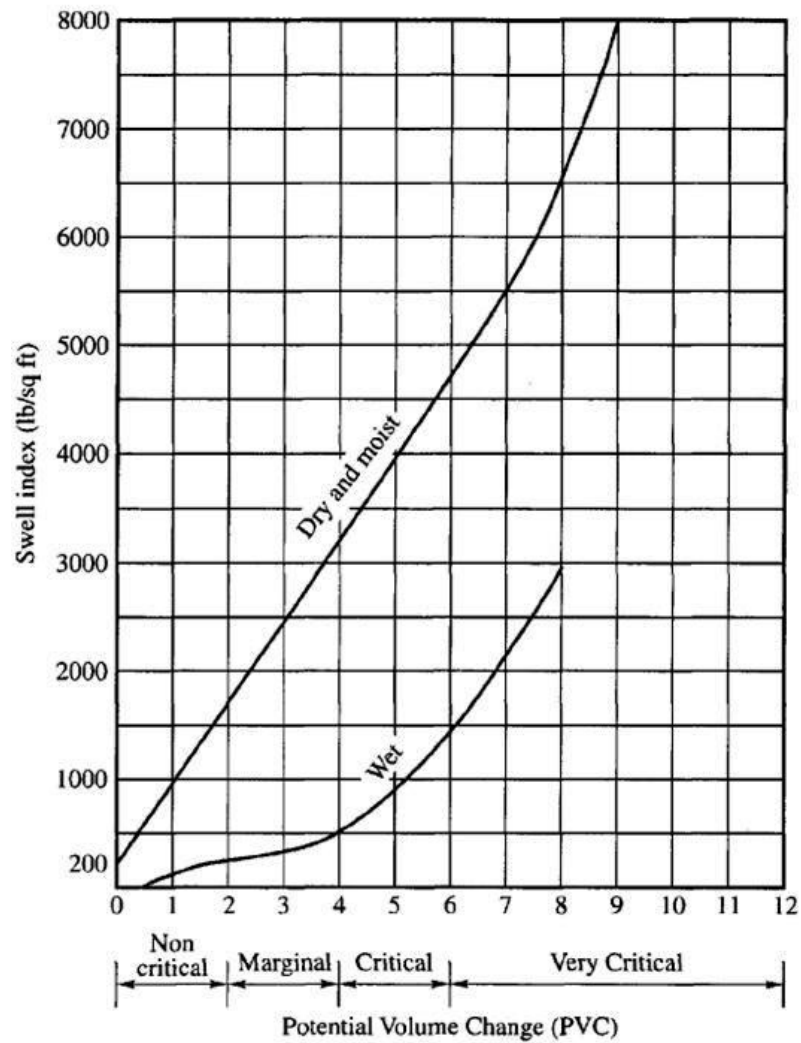


Figure 2. 9 Swell Index versus Potential Volume Change (FHA, 1974)

#### 2.5.4 Oedometer Test Methods

There are three alternative laboratory oedometer test methods approved by ASTM and designated as D 4546 – 08 for determining the swell behaviour and swell parameters of relatively undisturbed or compacted cohesive soils. Based on the fact that relatively small variations in initial water content and void ratio of the

in situ soil may significantly alter the swell behaviour and its parameters, the test method, loading, and inundation sequences should be selected in accordance with the wetting and drying effects and changes in loading conditions expected at site. Besides, the compaction method used for artificially prepared soil samples could also significantly change soil's behaviour by changing its soil fabric.

#### ***2.5.4.1 Improved Swell Oedometer (ISO) Test (Method A)***

This test method has the capability to measure

- (a) the free swell,
- (b) the percent heave for vertical confining pressures up to swell pressure,
- (c) the swell pressure

At the beginning of the test, a vertical seating pressure of at least 1 kPa is applied on the soil sample for half an hour. Then, an initial vertical stress equivalent to the estimated vertical pressure on the in-situ soil is applied and held on the soil sample for another half an hour. The void ratio observed at this stage of loading is recorded as the in-situ void ratio of the sample. The initial vertical stress is then removed except the seating load and the soil sample is held another half an hour. After these loading and unloading stages, the specimen is inundated and deformations are recorded after various elapsed times. Readings at 0.1, 0.2, 0.5, 1.0, 2.0, 4.0, 8.0, 15.0, 30.0 minutes followed by 1, 2, 4, 8, 24, 48 and 72 hours are usually satisfactory. The primary swell, which corresponds to nearly 90-95 % of the ultimate swell, is realized promptly, while the remaining swell deformations spread over a long period and are negligible in magnitude. Therefore, after the primary swell is accomplished, the specimen is loaded in accordance with the pressure increments as performed in conventional oedometer tests until specimen is recompressed to its initial void ratio or height. The pressure corresponding to the initial void ratio on  $e$  vs.  $\log P$  curve is defined as the swell pressure  $P_s$  as illustrated in Figure.2.10 (Erol et al., 1987).

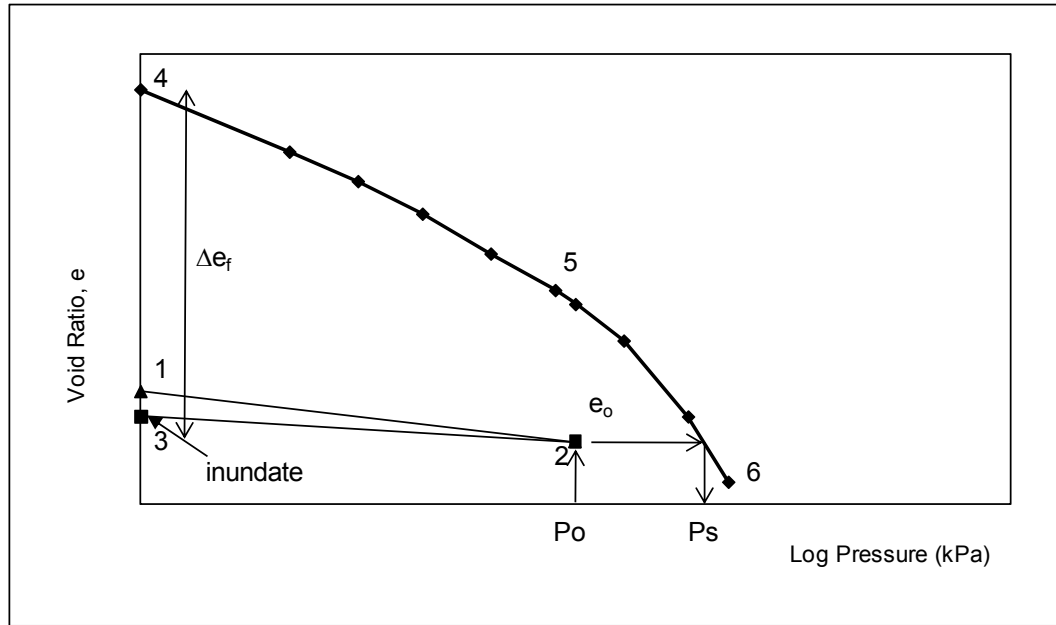


Figure 2. 10 Void Ratio versus Log of Pressure Curve for an ISO Test (ASTM D4546-08,2008)

The free swell at the seating pressure relative to the initial void ratio,  $e_0$ , can be calculated as:

$$\frac{\Delta h}{h_o} \times 100 = \frac{e_{se} - e_o}{1 + e_o} \times 100 = \left( \frac{\gamma_{do}}{\gamma_{dse}} - 1 \right) \times 100 \quad \dots\dots\dots (2.3)$$

where,  $\Delta h$  : change in specimen height,  
 $h_o$  : initial specimen height,  
 $e_{se}$  : void ratio after stabilized swell at the seating pressure  $\sigma_{se}$   
 $e_0$  : initial void ratio,  
 $\Delta e_f$  :  $e_{se} - e_0$  (void ratio at point 4 – void ratio at point 2)  
 $\gamma_{d0}$  : dry unit weight at void ratio  $e_0$  and  
 $\gamma_{dse}$  : dry unit weight at void ratio  $e_{se}$

Similarly, the percent heave at a vertical pressure,  $\sigma_{v0}$ , up to the swell pressure  $\sigma_{sp}$ , relative to  $e_0$  is as follows;

$$\frac{\Delta h}{h_o} \times 100 = \frac{e_{0s} - e_o}{1 + e_o} \times 100 = \left( \frac{\gamma_{do}}{\gamma_{dos}} - 1 \right) \times 100 \quad \dots\dots\dots (2.4)$$

where,  $e_{0s}$  : void ratio at the vertical pressure, and  
 $\gamma_{dos}$  : dry unit weight at void ratio  $e$

#### **2.5.4.2 Swell Overburden (SO) Test (Method B)**

This test method has the capability to measure

- (a) the percent heave or settlement for vertical pressure that is usually equivalent to the estimated in-situ vertical overburden and other vertical pressure up to the swell pressure, and
- (b) the swell pressure.

In this version of the oedometer test, a predetermined vertical overburden pressure exceeding the seating pressure is applied at the start of the test. After a waiting period of half an hour, specimen is inundated and deformations are recorded at various intervals until the primary swell is completed. The remaining portion of the test is similar to ISO test and rebound can be achieved by unloading the specimen up to the equilibrium swell. A representative void ratio versus logarithm of pressure curve for Method B is given in Figure.2.11.

The percent heave at the vertical pressure  $\sigma_{v0}$ , applied following the seating pressure, relative to the initial void ratio,  $e_0$ , can be calculated from Formula (2.4) presented in the previous subsection.

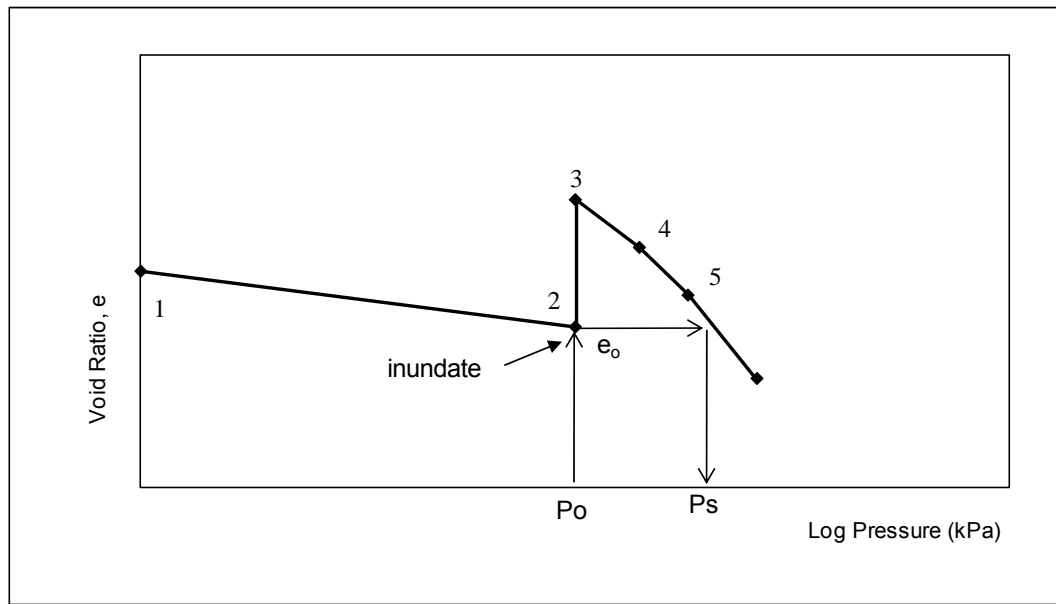


Figure 2. 11 Void Ratio versus Log of Pressure Curve for an SO Test (ASTM D4546-08,2008)

#### 2.5.4.3 Constant Volume Swell (CVS) Test (Method C)

This test method has the capability to measure

- (a) the swell pressure,
- (b) preconsolidation pressure, and
- (c) the percent heave or settlement within the range of applied vertical pressures.

This method follows a procedure similar to ISO test up to the inundation phase except the initial vertical stress removal. At the beginning, a vertical seating pressure of at least 1 kPa is applied on the soil sample for half an hour. Then, an initial vertical stress equivalent to the estimated vertical pressure on the in-situ soil is applied and held on the soil sample for another half an hour. The void ratio observed at this stage of loading is recorded as the in-situ void ratio of the sample. The specimen is immediately inundated and vertical stress increments are applied to prevent swell. Variations from the deformation reading, at the time

the specimen is inundated at initial stress level, shall be kept preferably within 0.005 mm and not more than 0.01 mm. The specimen is loaded following no further tendency to swell is observed. The submerged specimen is then loaded in increments that are sufficient to evaluate the maximum curvature on the curve and to calculate the slope of the virgin compression curve. From void ratio vs. logarithm of pressure curve, swell pressure can be determined (Figure.2.12). The free swell percentage can be reached by unloading of the specimen until equilibrium swell. It is proposed by Erol et al. (1987) that when compared with the ISO test, the CVS method may yield lower values for the free swell.

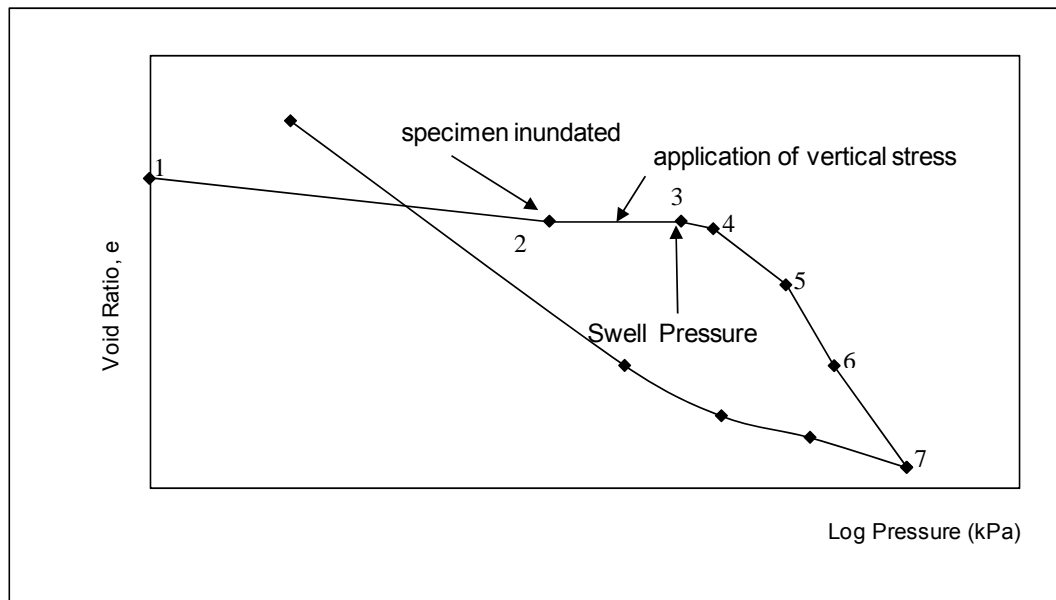


Figure 2. 12 Void Ratio vs. Log of Pressure Curve for a CVS Test (ASTM D4546-08, 2008)

#### **2.5.4.4 Comparison of the Oedometer Test Methods**

Sridrahan, Rao and Sivapullaiah (1986) investigated the results of three conventional oedometer test methods performed on black cotton soil. The

experiments incorporated the effects of time, stress path, initial density, moisture content and compactive energy employed during specimen preparation.

Table 2.6 presents the results of tests by different methods for some of the soils used during the investigations. From these results, investigators concluded that the three test methods yielded significantly different values for similar testing conditions.

Free swell test (Method A), which permitted complete swelling of the specimen upon saturation at seating pressure and then subsequent loading to bring it back to its original volume, yielded the maximum value of swelling pressure. For Method A, one specimen was sufficient but the method was time consuming.

In Method B, three or more samples were loaded to different pressures around estimated swelling pressure, allowing the specimens to imbibe water, and swell or compress to reach equilibrium points. The results of the tests showed that for different consolidation loads (Method B) resulted in the least value of swelling pressure. Compared to Method A, Method B required at least three specimens but it was less time consuming.

Continuous loading was done in Method C allowing water to be absorbed by the specimen and keeping the volume change nearly zero. It was observed that; Method C gave swelling pressures in between Method A and Method B. Compared to the other methods; Method C required only one specimen and it was quick. However, from the test results the investigators concluded that this method was sensitive to load increment and rate of loading. As a consequence, they concluded that, when constant volume tests are to be performed for the determination of swelling pressure and if the initial rate of swelling is found to be rapid, the first load increments should be added quickly, and gradually slowing down at later stages (Sridrahan, Rao and Sivapullaiah, 1986). Based on the results of their investigations, Sridrahan, Rao and Sivapullaiah (1986) reported that the swelling pressure of black cotton soil was primarily dependent on the initial dry unit weight. The effect of initial water content was found to be less.



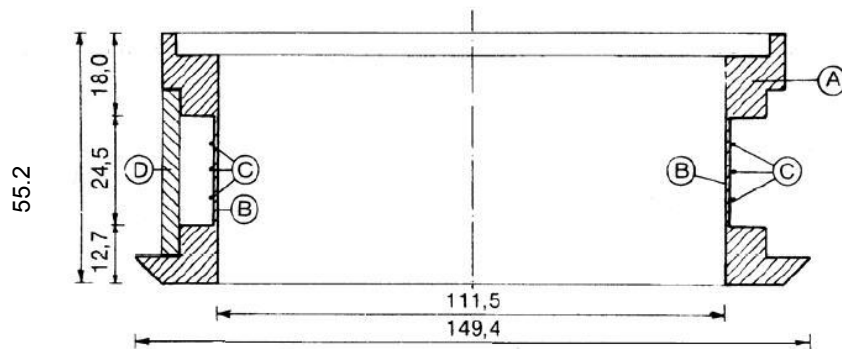
Table 2. 6      Comparative Values of Swelling Pressure by Different Methods of Oedometer Test (adapted from Sridrahan, Rao and Sivapullaiah, 1986)

Soil	Initial Conditions		Swell Pressure, kg/cm <sup>2</sup> , by Method		
	e <sub>i</sub>	w, %	A	B	C
BC1	0.893	0	3	1.6	1.9
BC4	1.002	0	3.9	1.6	2.2
BC5	0.742	0	5.1	1.4	3.1
BC7	0.572	0	13	3.4	3.8
BC8	0.656	20.8	1.5	-	0.7

### 2.5.5 Modified Oedometer Tests

The first attempt to measure the lateral swell pressure of expansive soils by means of a modified oedometer cell was performed by Komornik and Zeitlen in 1965. They modified the conventional oedometer ring for this purpose and manufactured a special ring with thin-wall section in its central portion equipped with electrical strain gages for the measurement of lateral pressures (Figure 2.13). The lateral swell pressures were measured by determining the hoop strain of the ring and converting it to pressure units via using the elastic properties of the ring. The results of the tests performed by Komornik and Zeitlen (1965) are presented in Figure 2.14.

Realizing that even small amounts of lateral strains led to significant differences in lateral swell pressure measurements, Ofer (1980) developed a new testing method that had the capability to measure the lateral swell pressures by compensating the lateral strain and thus minimizing the effect of deformations on lateral swell pressures. Although the new lateral swelling pressure ring (LSP) was very similar to that developed by Komornik and Zeitlen (1965), air pressure was introduced to simulate the direct measurement of lateral swell pressure to counterbalance the lateral strains observed during swelling.



#### LEGEND

- A — Main ring
- B — Thin wall section, 0.3mm thick
- C — Circumference strain wires
- D — Stiffening member

Figure 2. 13 Modified Thin-Wall Oedometer Cell (Komornik and Zeitlen,1965)

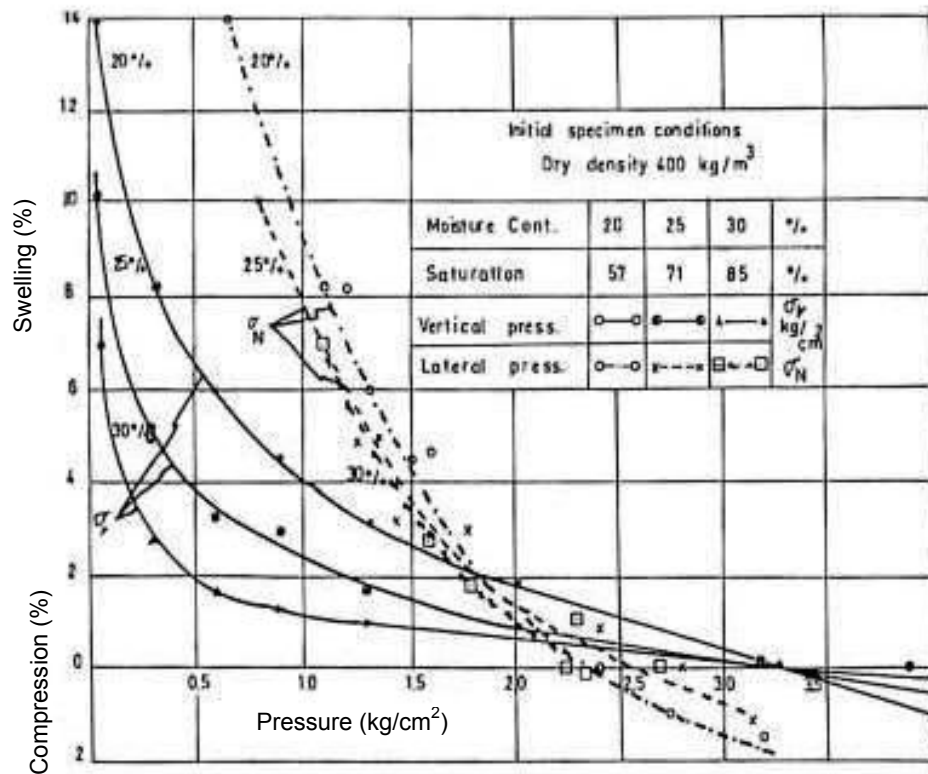


Figure 2. 14 Vertical Movements as a Function of Vertical and Lateral Pressures (Komornik and Zeitlen, 1965)

The cross-section and the important parts of the LSP apparatus are consecutively given in Figure 2.15 and 2.16. In order to record the corresponding strains by a digital strain indicator and a strain recorder, Ofer (1980) introduced pressurized air to the inner part of the ring that was clamped between the end plates. The thin-wall ring was manufactured from stainless steel with a thickness of 0.7 mm. The experiments yielded that long term loading had no substantial effect on the calibration of the apparatus. The test program involved clay samples compacted to different initial dry densities, on which a constant vertical pressure of 19 kPa were applied. The measured vertical and lateral swell pressures for different initial dry densities are presented in Figure.2.17.

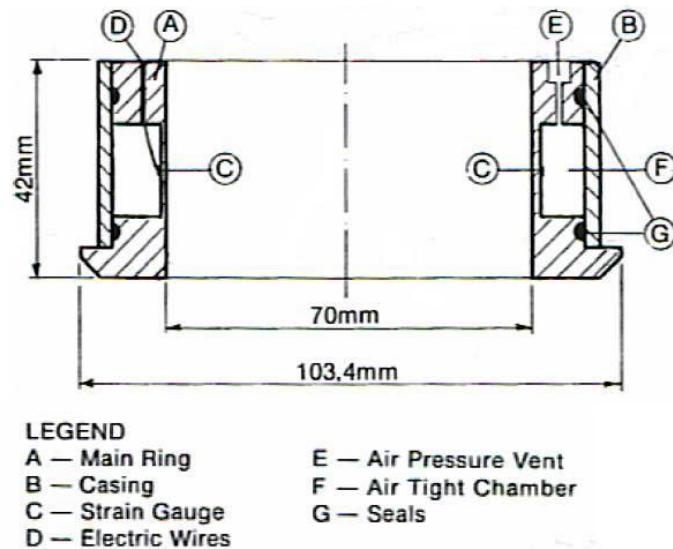


Figure 2. 15 Lateral Swell Pressure (LSP) Apparatus Cross Section (Ofer, 1980)

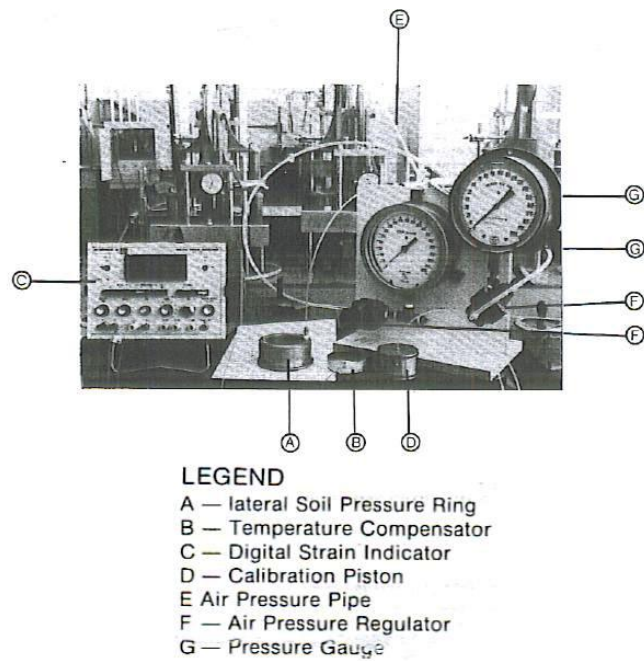


Figure 2. 16 Lateral Swell Pressure (LSP) Test Set-Up (Ofer, 1980)

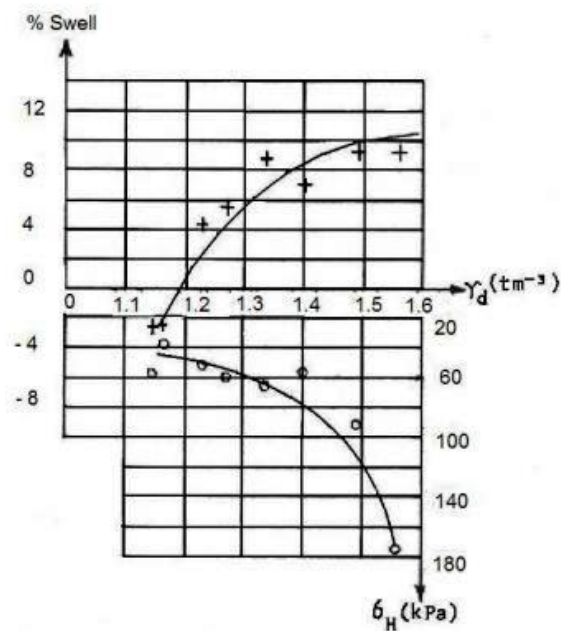


Figure 2. 17 Vertical and Horizontal Swell Percentages for Different Initial Dry Densities Observed from LSP Tests (Ofer, 1980)

On a further study based on the outcomes of Ofer's research, Ofer and Komornik (1983) noted that the development of vertical swell strain and lateral pressure were time-dependent where their response times were mainly governed by the extent of vertical pressures exerted during the tests. The specimens that exhibited the maximum lateral swell pressures were the ones which were compacted at their optimum moisture contents and maximum dry densities. Consecutively, a decrease or an increase in moisture content accompanied by a decrease in density resulted in a drop in the developed lateral swelling pressure. Ofer and Komornik (1983) also reported that the mobilization of even minor lateral strains caused a considerable reduction in the lateral swell pressures. Therefore, the authors reported that the lateral swell pressures were much greater for samples restrained from lateral strain compared to samples where small amounts of lateral strain were permitted. Finally, Ofer and Komornik (1983) found out that independent of differences in their location, origin and history, testing of clays of similar mineralogy and physical properties under similar testing conditions generated similar lateral swelling characteristics.

Yanıkömeroğlu (1990) performed a study to investigate the effect of lateral confinement on swell behaviour of expansive soils. A conventional oedometer cell was used to develop the necessary boundary conditions to investigate the influence of lateral confinement on (a) no lateral restraint, (b) partial lateral restraint and (c) full lateral restraint cases. The fully restraint condition was exactly the conventional oedometer test condition where the soil sample was in direct contact with the ring. Partial restraint condition was simulated by opening specific number of holes in the specimen. No lateral restraint condition was satisfied by placing the specimen over a block in between two porous stones and the sample was enclosed within a polyethylene bag to prevent moisture loss. All the three test methods defined in Section 2.4.4, namely free swell, constant volume swell and swell overburden tests, were performed for the three boundary conditions. The test program yielded that the amount of swell as well as swell pressures increased with increasing values of dry densities. It was observed that the swell and swell pressures were reduced with an increase in the macropore percent. This outcome was ascribed to the sealing of these macropores during

the test procedure leading to a possible reduction in lateral swell pressures. Furthermore, rate of swell was found to increase under the existence of macropores which in turn caused an increase in the permeability and therefore the rate of water absorption. During his study, Yanıkömeroğlu (1990) has made an attempt to correlate a lateral restraint factor with percent macropore content and surcharge pressure. Accordingly, the investigator recommended that the predicted heave based on experimental swell data obtained should be corrected by multiplying with a lateral restraint factor, in case such a factor can be reasonably estimated to represent a real soil profile.

Similar to the previous works of Komornik and Zeitlen (1965) and Ofer (1980), Ertekin (1991) developed a modified thin-wall oedometer to obtain the highest level of lateral pressure applied by the soil sample to the walls of the test instrument. As noted by the researcher, this was only possible in the case of generating a  $K_0$  condition with strictly prohibiting any lateral movement during swelling. The apparatus for the test program was therefore designed accordingly. The main ring was made up of high quality alloy steel for this purpose. The wall thickness and the height of the ring were manufactured as 0.35 mm and 78 mm respectively. The outer diameter was selected to be 140.2 mm. In order to eliminate the internal stresses and avoid permanent deformations during the tests, the ring body was exposed to the heat treatment and hardening process. A cross sectional diagram of the complete test set-up is shown in Figure 2.18. Electrical strain gauges were installed on the outer surface of the thin-wall cylinder. Calibration of the lateral pressure measurement ring was made by applying water pressure in it. As explained in detail by the researcher, the thickness of the thin-wall was tried to be selected to satisfy that the ring was sufficiently thin so that the hoop deformations would be sensed by the strain gauge and also sufficiently thick to satisfy the  $K_0$  condition. According to mechanics of materials and theory of elasticity, the anticipated design proved to be satisfactory for the expected swell pressure ranges of the soil specimen.

The test schedule involved constant volume swell (CVS), free swell (ISO) and swell overburden (SO) tests to be performed on disturbed soil samples

compacted to predetermined initial dry densities and water contents. The preliminary tests performed with different sample thicknesses showed that the magnitude of swell pressures were higher for thicker soil samples. The effect of macropores on the magnitude of lateral swell pressures was also investigated by opening holes inside the soil specimen. From the test results, it was noted that the magnitude of vertical swell was significantly reduced due to lateral expansion arising from the presence of macropores. It was observed that the lateral swell pressure reached to a peak value at early stages of swell, and then decreased to an ultimate value in fully saturated state, which was attributed to a passive failure condition under very high lateral stresses. For the tested soil properties, the lateral swell pressures measured in constant volume tests were determined to be higher than the vertical swell pressures by a factor of 1.5 to 1.8. Finally, it was noted that lateral swell pressure was strongly dependent on surcharge pressure, showing a sharp decrease when the overburden is increased.

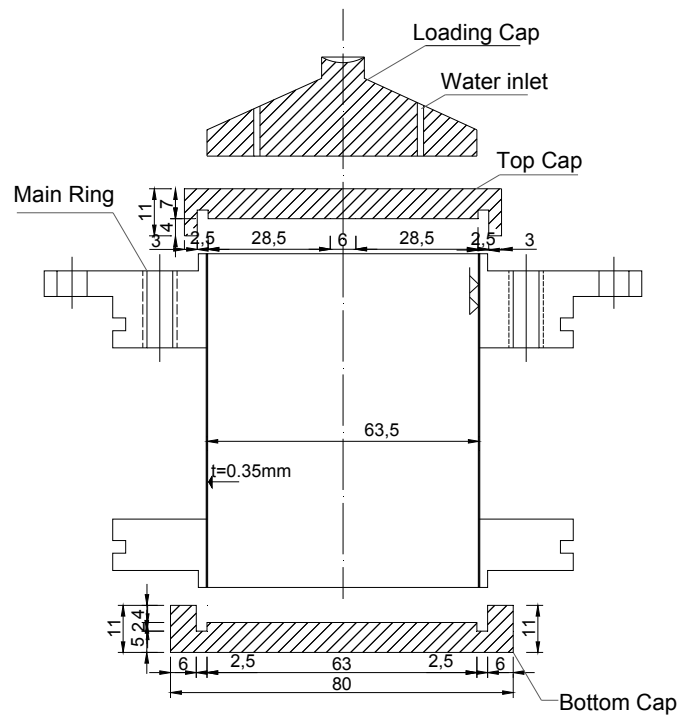


Figure 2. 18 Lateral Swell Pressure Test-Set Up (Ertekin, 1991)

Edil and Alanazy (1992), constructed a lateral swell pressure test set-up similar to the one developed by Ofer (1980). Their apparatus had similar dimensions with a standard oedometer and contained an exclusively manufactured hollow ring equipped with strain gauges. The thickness of the modified thin-wall was selected to be 1 mm, around which a sealed outer ring was used to create a chamber of lateral pressure. This chamber was exposed to air pressure to keep lateral displacements at minimum during vertical stress application. From the results of this investigation, the researchers concluded that lateral swell pressure decreased as the initial water content of the specimen was increased. However the decrease in vertical swell pressure with increasing water content was more pronounced (Figure.2.19). In addition, they have observed that the lateral swell pressure was highly influenced from the method of compaction i.e. statically compacted samples were found to generate higher swelling pressures compared to samples compacted by kneading effort although the specimens were compacted to same initial dry densities and water contents.

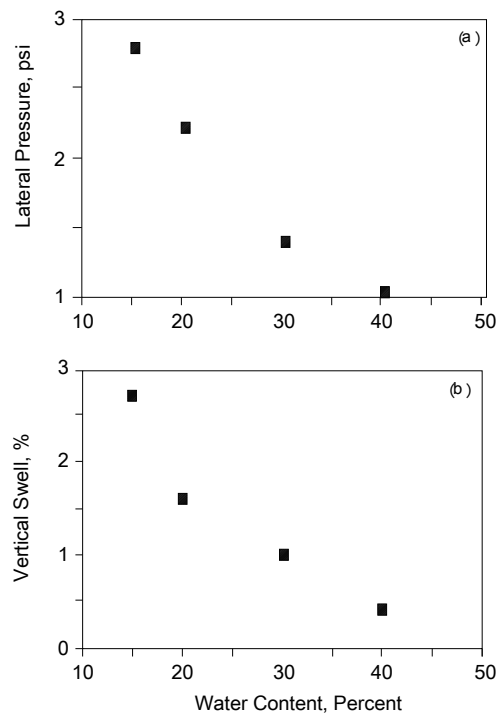


Figure 2. 19 Lateral Swell Pressure and Vertical Swell Percent versus Water Content Relationship (Edil and Alanazy, 1992)



Hatipoğlu (1993) used the same modified lateral pressure test set-up previously developed by Ertekin (1991) and reached to the similar finding that the lateral swell pressure reached to a peak value at early stages of swell and then decreased to an ultimate value in fully saturated state. This behaviour was once more attributed to a passive failure condition under very high lateral stresses.

From the results of the constant volume swell tests they performed by thin-wall oedometer, Erol and Ergun (1994) concluded that both the lateral and vertical swell pressures decreased with increasing initial water contents (Figure 2.20) revealing larger swell pressure ratios at higher initial water contents (Figure 2.21). The main findings of Ertekin (1991) and Hatipoglu (1993) related with the observed peak lateral swell pressures at the early stages of tests, and the decrease of lateral pressures to an ultimate value in fully saturated state was once more noted by the study of Erol and Ergun (1994).

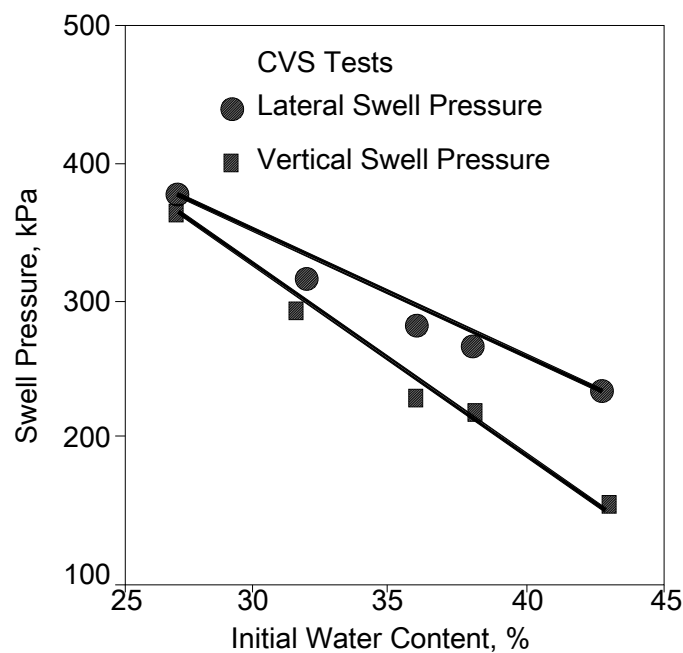


Figure 2. 20 Effect of Initial Water Content on Swell Pressure (Erol and Ergun, 1994)

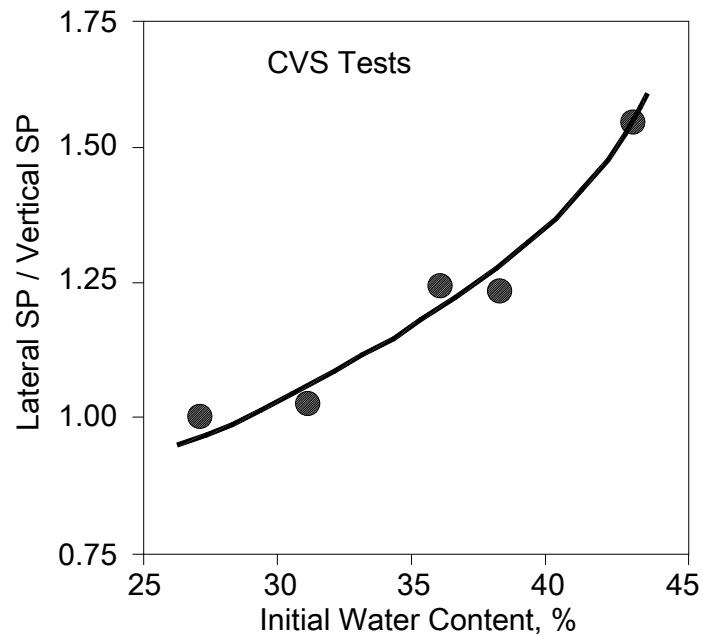


Figure 2. 21 Effect of Initial Water Content on Swell Pressure Ratio (Erol and Ergun, 1994)

Windal and Shahrour (2002), performed tests on soil samples placed in thin-wall oedometer rings manufactured from different metals with varying stiffness to control various degrees of lateral movements. In this study, aluminum was used to simulate the behaviour of stiffer ring whereas an alloy of copper and beryllium was used for the flexible rings. The thickness of the aluminum ring was manufactured as 1 mm and the thickness of the copper ring was selected as 0.15 mm. The rings were instrumented with strain gauges to measure the lateral strains. The lateral swell pressure was derived from the lateral strain measurement using a calibration curve established for each ring.

Results of free swelling tests indicated that the development of the axial strain as well as the lateral pressure resulting from the soil expansion were dependent not only on the axial stress but also on the stiffness of the oedometer ring. Furthermore, at low axial stresses, the lateral swell pressure was found to reach

a peak value and then decrease with the increase in axial stress (Figure 2.22 and Figure 2.23). This outcome was parallel with the results of the laboratory investigations of Erol and Ergun (1994) and large scale tests of (Chen and Huang, 1987; Joshi and Katti, 1980). Chen and Huang (1987) attributed this to a gradual change in the soil structure and clay particle orientation associated with the saturation process. According to Windal and Shahrour (2002), this can also be attributed to stress relaxation phenomena in the soil.

The experiments performed by Windal and Shahrour (2002) showed that an increase in the stiffness of the oedometer ring lead to significant increase in both lateral swell pressure and the axial swell strain. Furthermore, reducing the soil swelling in one direction led to a notable increase in the soil swelling in the other directions.

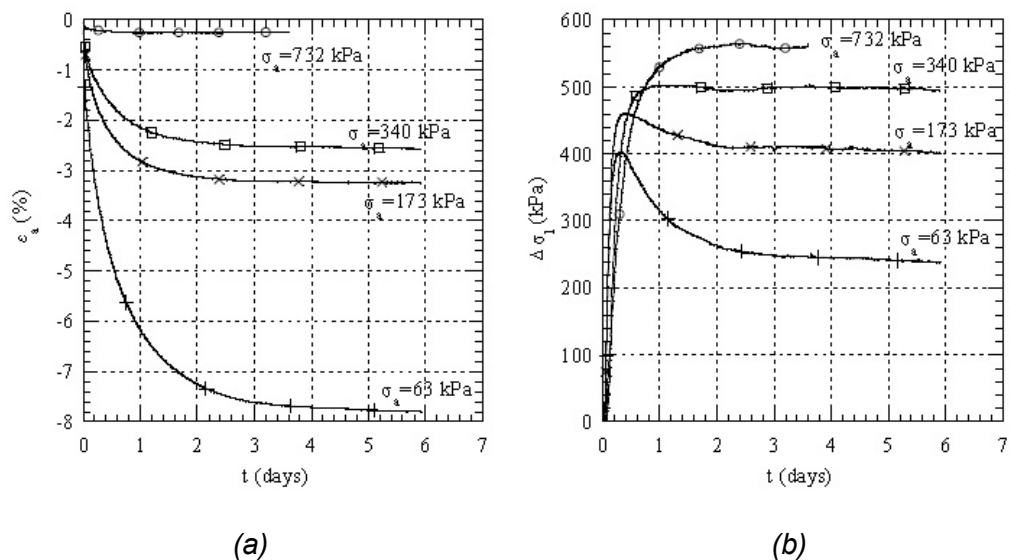


Figure 2. 22 Swelling Tests Performed with the Flexible Ring (a) Evolution of the Axial Strain (b) Evolution of the Lateral Pressure (Windal and Shahrour, 2002)

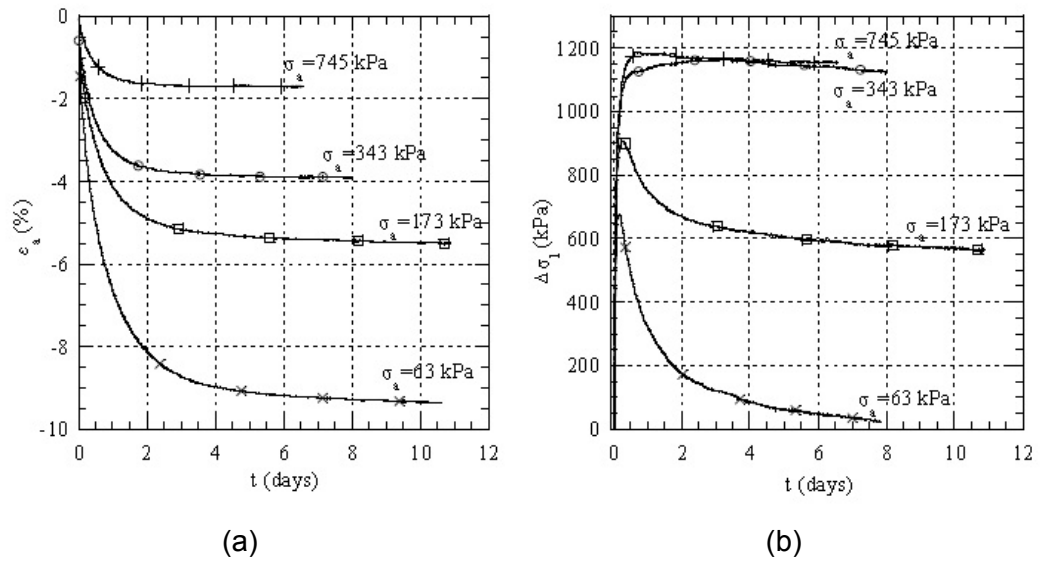


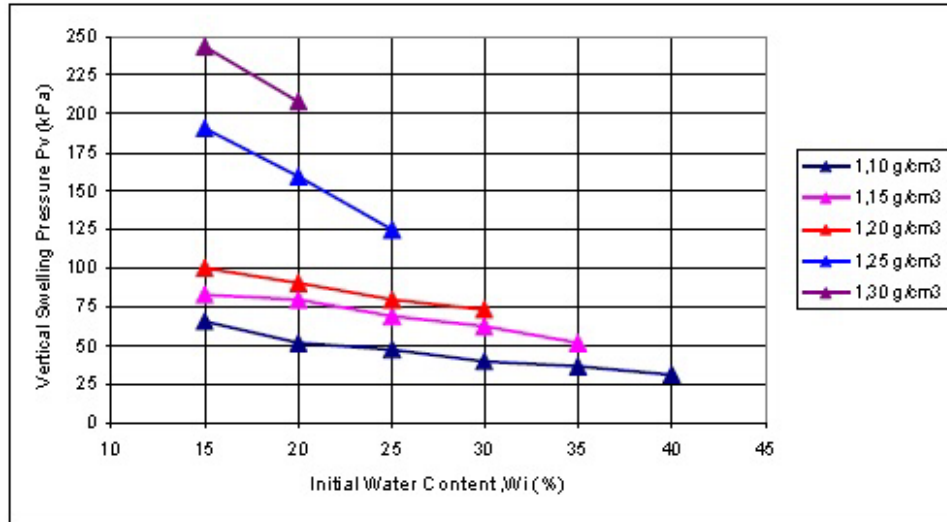
Figure 2. 23 Swelling Tests Performed with the Stiff Ring (a) Evolution of the Axial Strain (b) Evolution of the Lateral Pressure (Windal and Shahrour, 2002)

The thin-wall oedometer test set – up previously developed by Ertekin (1991) and used during the investigations of Hatipoglu (1993) and Erol and Ergun (1994) was once more used by Sapaz (2004) for further investigations of the lateral swelling pressure phenomena. The thin-wall oedometer apparatus with strain gauges installed at the mid height of a 0.35 mm thick ring was used for this purpose. Vertical swelling pressures were also determined during this investigation. Constant volume swell (CVS) tests were carried out and the tests also involved unloading steps. The tested soils with different initial water contents and different initial dry densities were statically compacted for sample preparation.

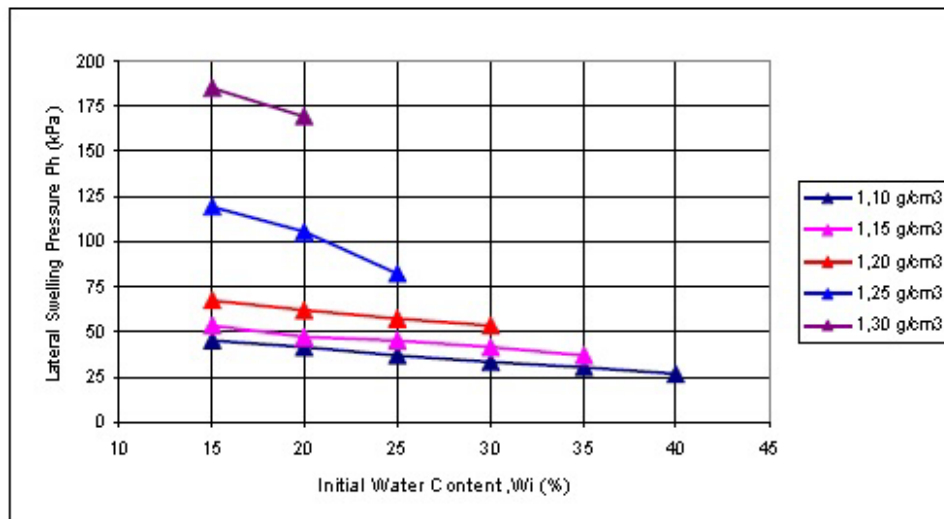
On the basis of his experimental program, Sapaz (2004) reported that the lateral and vertical swelling pressures decreased with increasing initial water content for the samples having the same initial dry unit weight (Figure 2.24), whereas they increased with increasing initial dry unit weight for the samples having the same initial water contents (Figure 2.25).

Sapaz (2004) also noted that the magnitude of lateral swelling pressures developed in CVS tests were smaller compared to the vertical swelling pressures, with swell pressure ratios varying over a range between 0.59-0.86 for the conditions of the present experimental work. The researcher reminded that although they worked in similar testing conditions, Erol and Ergun (1994) reported the swell pressure ratios between 1.00 and 1.55 for their CVS tests with thin-wall oedometer technique. Sapaz (2004) attributed this difference to different swelling characteristics of soil samples. Finally, the researcher emphasized that the vertical swelling pressures reached to equilibrium state earlier than the lateral swelling pressures and linked this outcome to characteristics of the test apparatus.

Avşar (2007) investigated the swelling pressures and swelling percentages by using both the conventional oedometer tests and the thin-wall oedometer ring. Undisturbed samples, obtained from the predetermined sites were tested for this purpose. Avşar (2007) reported that the swelling parameters measured in both directions by the two test methods were in harmony whereas the parameters obtained for vertical directions were greater than those determined in lateral direction. The ratio of lateral to vertical swell pressures were found in between 0.34 and 0.98 for thin-wall oedometer ring and 0.41 and 1.10 for conventional oedometer tests. It was also determined that the swelling pressure and percentage in vertical direction increased with an increase in preconsolidation pressure of clay sample. The study also involved the scanning of the undisturbed samples by electron microscope analysis, and this phase of the study suggested that the tested clay grains were layered in horizontal or almost horizontal orientation with a stepped face to face surface which was probably a consequence of the preconsolidation pressure leading to higher swelling pressures in the vertical direction than those in the lateral direction.

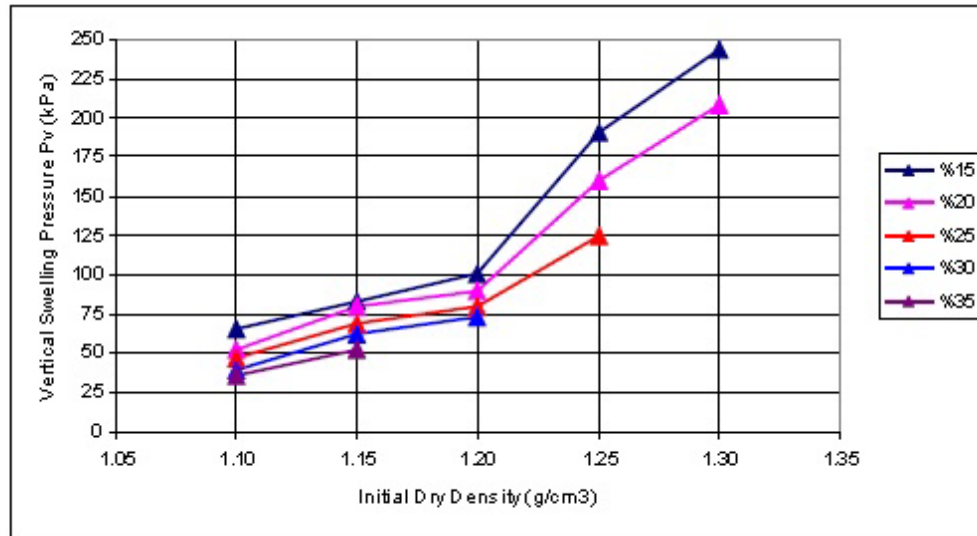


(a)

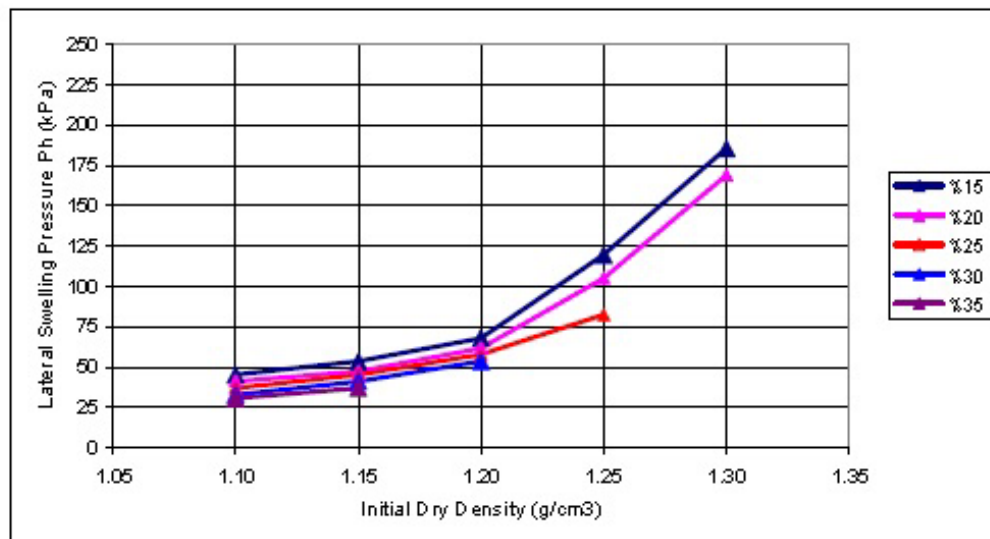


(b)

Figure 2. 24 Relationship between the Swelling Pressure and Initial Water Content for Samples with Different Initial Dry Densities (a) Change in Vertical Swell Pressure (b) Change in Lateral Swell Pressure (Sapaz, 2004)



(a)



(b)

Figure 2. 25 Relationship between the Swelling Pressure and Initial Dry Densities for Samples with Different Initial Water Contents (a) Change in Vertical Swell Pressure (b) Change in Lateral Swell Pressure (Sapaz, 2004)

Özalp (2010) studied the dependency of lateral swelling pressures on depth and the rigidity of the support system for deep excavations and tunnel constructions in expansive soils. A special lateral swell pressure apparatus based on the thin-wall oedometer of Komornick and Zeitlen (1965), Ofer (1981) and Ertekin (1991) was constructed; however, with a taller and more flexible ring. Furthermore, the mechanism preventing lateral movements was attained by hydraulic pressure rather than air pressure in the Ofer (1981) ring. Three strain gauges were used on the ring to supervise any non-homogenous tendency on the horizontal plane. Swelling tests were conducted on samples of the same clay compacted to the same initial water content. The investigation encompassed lateral swelling tests that were grouped in accordance with different stress-strain conditions, i.e.

- a) VR-LFST: Zero vertical strain – lateral free swell tests ( $\varepsilon_v=0$ ,  $\varepsilon_h \neq 0$ )
- b) VR-CVS: Zero vertical strain – constant volume tests ( $\varepsilon_v=0$ ,  $\varepsilon_h=0$ )
- c) CS-LFST: Constant vertical surcharge – lateral free swell tests ( $\varepsilon_h \neq 0$ )
- d) CS-ZLST: Constant vertical surcharge – zero lateral strain tests ( $\varepsilon_h=0$ )

Both the vertical and the lateral swelling pressures attained fitted in the range of 80 to 150 kPa, not only for the “zero vertical strain (VR)” tests, but also for the “constant vertical surcharge (CS)” tests. The swelling pressure ratio for the VR-LFST tests ranged between 1.0 and 2.0, whereas, the ratio for the VR-CVS tests was slightly higher than but not as high as it was anticipated. These findings were conflicting with the previous findings of Ofer (1981) as well as Windal and Shahrour (2002), who acclaimed that the lateral swelling pressures for the constant volume and zero lateral strain tests where  $\varepsilon_h=0$ , should be greater. Özalp (2010) attributed this contradiction to the manual application of the cell pressure. The comparison of the VR-LFST tests with the previous research findings are illustrated in Figure 2.26. As far as the CS-LFST and the CS-ZLST tests were concerned, the swell pressure ratio remained in the range of 0.9 – 1.0, with no significant difference between the two test methods.



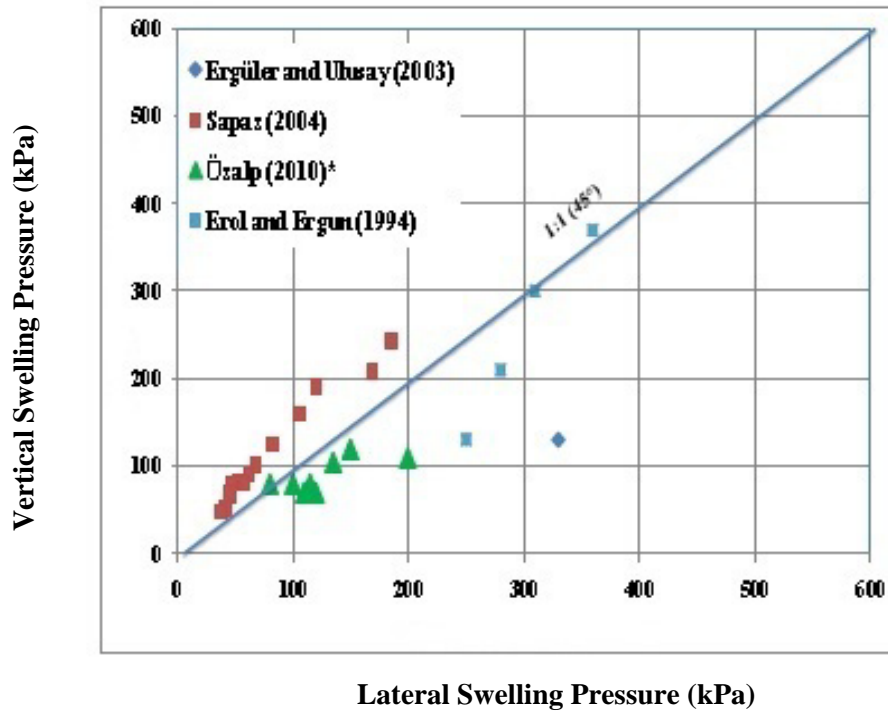


Figure 2. 26 VR-LFST Results

### 2.5.6 Modified Triaxial Tests

After it was understood that using three dimensional deformations might have been a more rational method of simulating the behaviour of expansive soils, alternative procedures have been devised by several researchers for the assessment of swell parameters.

The research performed by Parcher and Liu (1965) was the first investigation encountered in literature that aimed to measure the vertical and lateral swell of expansive soils independently with a triaxial cell apparatus. The schematic diagram of the apparatus developed for this purpose is presented in Figure 2.27. During the tests, a dial gage was used to measure the vertical swelling, while the change in volume as the result of lateral swelling was measured as the movement of water in a small tube going from the cell to a meter stick. The quantity of water, imbibed by the specimen as it swelled, was followed from

readings of a surface gage located at the water reservoir. Based on the fact that both the plexiglass chamber and the measurement tube had a tendency to absorb small quantities of water, calibration curves were prepared to comprise the effect of this lost water. Parcher and Liu (1965) reported that generation of volumetric swell was affected both by the initial water content and the type of construction procedure. The soil samples compacted statically were noted to show higher volumetric swell percentages compared to the samples compacted by kneading. Furthermore, as the initial water content was increased, the volumetric swell percentage of the soil mass was tending to decrease accordingly (Figure 2.28). The results of the tests indicated that the horizontal swell was almost invariably exceeding the swell in the vertical direction. It was also reported from this investigation that the compacted soil samples swelled approximately four times as much, both vertically and horizontally, as did the undisturbed soil samples (Figure 2.29). The investigators attributed this behaviour to the existence and importance of bonds of cementation present in the undisturbed soil mass.

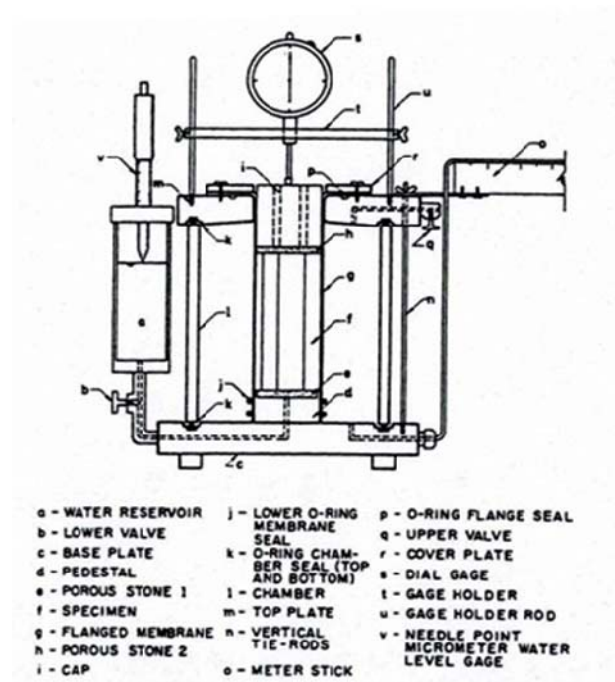


Figure 2. 27 Swelling Test Apparatus (Parcher and Liu, 1965)

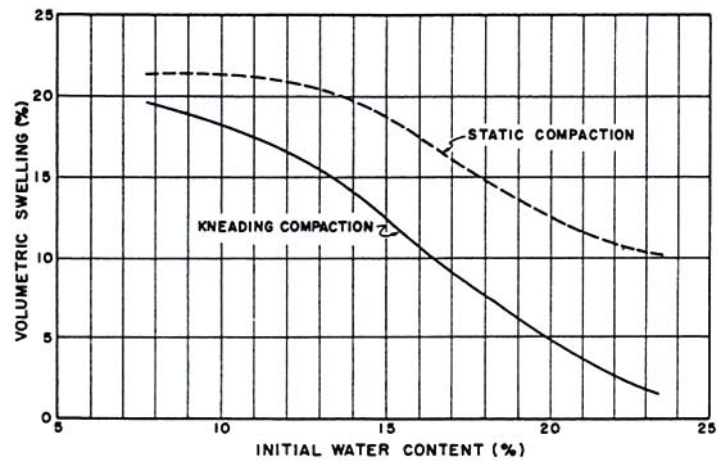


Figure 2. 28 Volumetric Swell vs. Initial Water Content according to Compaction Method (Parcher and Liu, 1965)

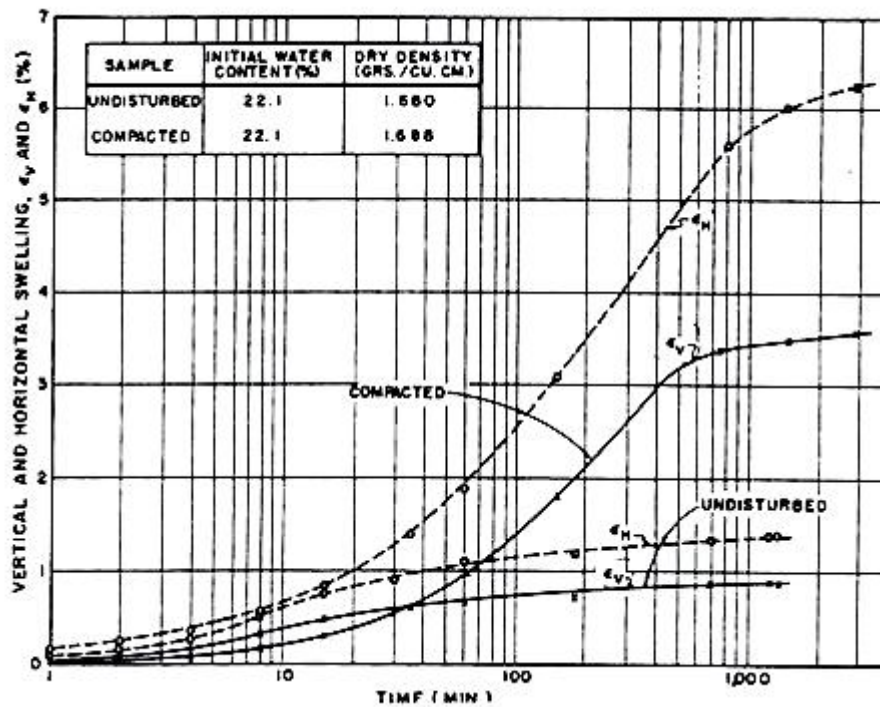


Figure 2. 29 Swelling vs. Time Curves for Compacted and Undisturbed Samples (Parcher and Liu, 1965)

In his particular work, Komornik (1962) had presented the results of a consolidometer technique. Baker (1968) conducted a study of swell pressures of the same clay under comparable placement conditions using triaxial technique. Kassif and Baker (1969) presented a research on the experimental results of Komornik (1962) and Baker (1968). The aim of the study was to measure the lateral pressures that makes possible the determination of  $(K_o)_s$ , where  $(K_o)_s$  was defined as the ratio of change in lateral pressure to vertical pressure under various combinations of the vertical swell pressure  $\sigma_1'$  and lateral swell pressure  $\sigma_3'$ . The results of the tests in terms of vertical swell pressures for zero volume change are presented in Table 2.7 and in terms of all-round cell pressure  $\sigma_a'$ , for no volume change in Table 2.8. Kassif and Baker (1969) reported that the swell pressures obtained by both techniques at comparable placement ratios yielded a pressure ratio  $(\sigma_a' / \sigma_1')$  around 1.00 as given in Table.2.9.

Table 2. 7      Results of Swell Pressure Tests, Uniaxial Technique (Kassif and Baker, 1969)

Moisture Content %	Dry Density = 1.4 g/cm <sup>3</sup>			Dry Density = 1.3 g/cm <sup>3</sup>			Dry Density = 1.2 g/cm <sup>3</sup>		
	$\sigma_1'$ kg/cm <sup>2</sup>	$\sigma_3'$ kg/cm <sup>2</sup>	$(K_o)_s$	$\sigma_1'$ kg/cm <sup>2</sup>	$\sigma_3'$ kg/cm <sup>2</sup>	$(K_o)_s$	$\sigma_1'$ kg/cm <sup>2</sup>	$\sigma_3'$ kg/cm <sup>2</sup>	$(K_o)_s$
20	3.3	2.4	0.73	1.2	1.4	1.15	0.7	0.8	1.14
25	3.3	2.6	0.8	1.25	1.3	1.04	0.65	0.75	1.15
30	3.2	2.3	0.72	1.5	1.4	0.94	0.6	0.6	1

Table 2. 8      Results of Swell Pressure Tests, Triaxial Technique (Kassif and Baker, 1969)

Moisture Content (%)	$\sigma_a'$ (kg/cm <sup>2</sup> ) for $\gamma_d = 1.45$ g/cm <sup>3</sup>	$\sigma_a'$ (kg/cm <sup>2</sup> ) for $\gamma_d = 1.31$ g/cm <sup>3</sup>
25.4	3.7	1.4
27.3	3.4	1.3
30.7	3.25	1.25

Table 2. 9      Results of Swell Pressure Tests, Comparison of Uniaxial and Triaxial Techniques (Kassif and Baker, 1969)

Moisture Content (%)	$\sigma_a' / \sigma_1'$ for $\gamma_d \approx 1.4 \text{ g/cm}^3$	$\sigma_a' / \sigma_1'$ for $\gamma_d \approx 1.3 \text{ g/cm}^3$
$\approx 25$	1.12	1.12
$\approx 30$	1.01	0.84

Another modified triaxial apparatus (Figure 2.30), which had previously been developed during the investigations of Lal and Palit (1969), was used by Dhawan et al (1982), to determine the vertical swell pressure and accompanied volume changes for various lateral confinement levels. The equipment involved a hollow loading plunger with an outside diameter equal to that of the soil sample to prevent any confining pressure acting at the top of soil samples. The ring hollow shaped samples used in this study were cast in a special mold and compacted to desired density and the water content. They were then placed into the triaxial cell and confining pressure was applied following an initial vertical seating load. The samples were left to imbibe water and the vertical swell pressures were recorded for the next 48 hours. No significant vertical swelling pressure change after 24 hours was observed so the all-round cell pressure at which no volume change takes place was accepted as the maximum lateral swell pressure. The vertical swell pressures versus time for different confining pressures are presented in Figure 2.31. Dhawan et al. (1982) also reported that the vertical pressure increased as swell was decreasing with the increase in lateral confinement simulating the depth of expansive soil strata at which the foundation rests (Figure 2.32).

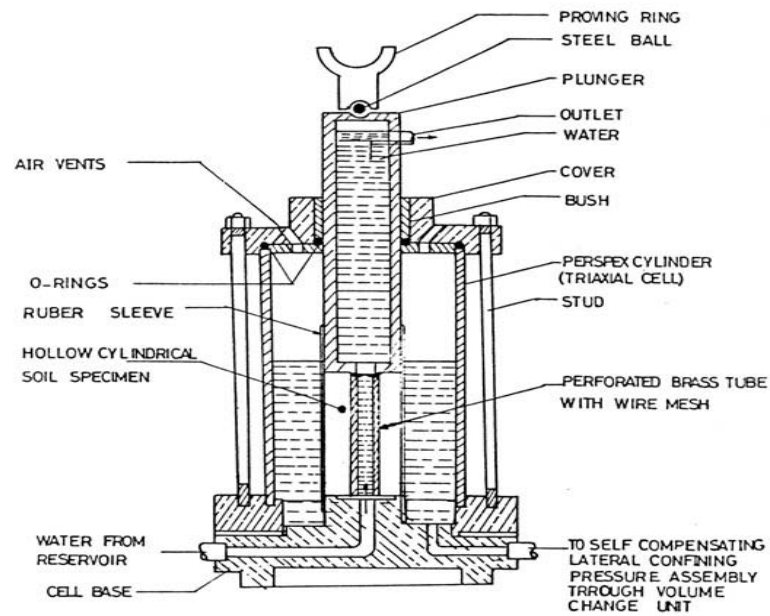


Figure 2. 30 Modified Triaxial Cell Apparatus (Dhawan et al., 1982)

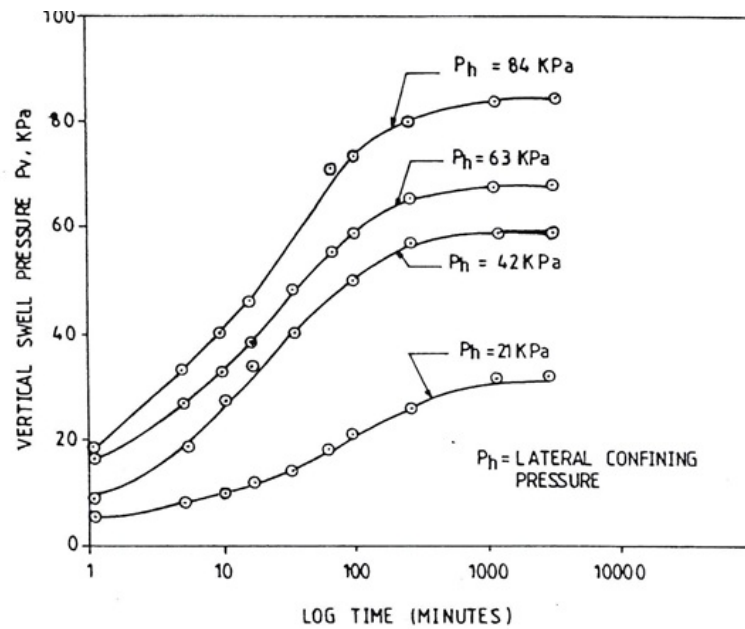


Figure 2. 31 Development of Vertical Swell Pressure with Time under Different Lateral Confining Pressures. (Dhawan et al., 1982)

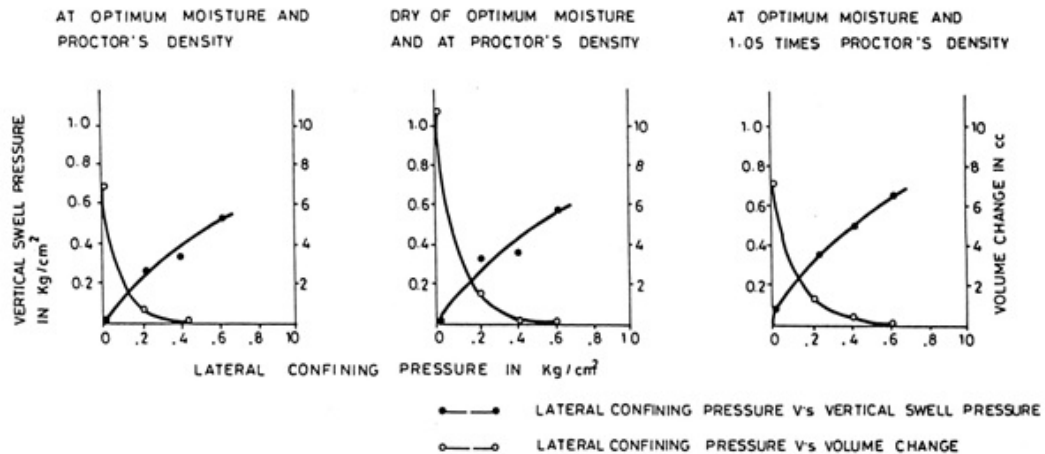


Figure 2. 32 Variation of Vertical Swell Pressure with Lateral Confinement and Accompanied Volume Change. (Dhawan et al., 1982)

Shiming (1984) carried out a research on three types of expansive soils in a modified triaxial apparatus that was capable of controlling  $\sigma_1$ ,  $\sigma_3$  and lateral pressure independently. The vertical and lateral swelling pressures as well as strains could be obtained by this experimental apparatus. The apparatus used in the investigations is presented in Figure 2.33. Samples tested in the investigations were undisturbed samples obtained from three different sites and in-situ depths, and were 6.5 cm in diameter and 7 cm in height. The soil properties used in these tests are presented in Table 2.10. Conventional oedometer swell tests, i.e. monoaxial tests, were performed on undisturbed samples taken as both horizontal and vertical with the axis of the cutting ring. The results of these tests are presented in Table 2.11. As it can be seen from these results, the vertical expansion was determined to be higher compared to lateral expansion though the swell potential of the samples differed considerably. In the next stage of investigations, three dimensional swell tests were performed by the modified triaxial apparatus. Comparison of the pressure measurements for two types of tests is presented in Table 2.12. The tests revealed lateral swell pressures which were smaller than the vertical swell pressures for all cases. Another comparison of the results showed that the expansion in each direction

was different (Table 2.13), and this trait was explained by the anisotropic nature of the expansive soil. The test program also included a small number of expansion tests, conducted on remoulded samples that gave larger swell potential compared to undisturbed samples tested at the same initial dry density and overburden stress.

At a former work of his own, Shiming (1979) stated that soil blocks of different sizes were formed in the soil mass due to the growth of fissures. Based on this fact, Shiming (1984) concluded that, the laboratory tests were not expected to reflect the situation of the soil mass in-situ, but only give an approximation to the properties of the samples.

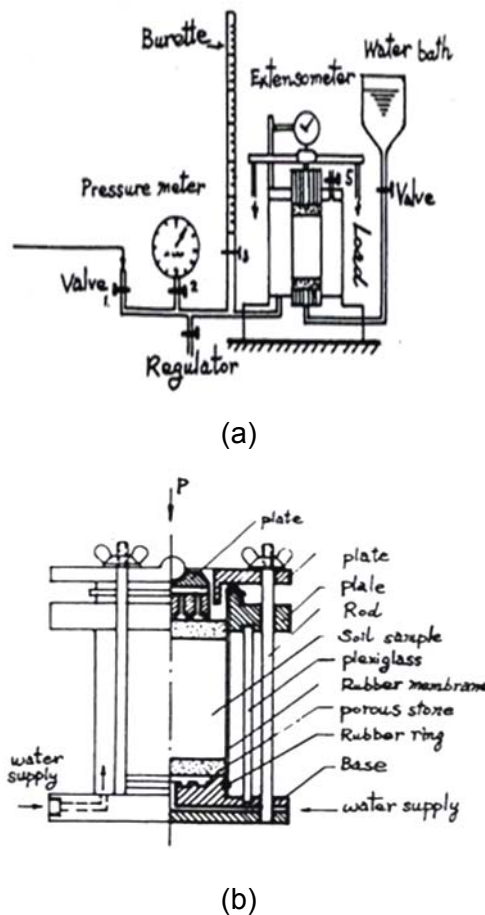


Figure 2. 33 Schematic Description of the Modified Triaxial Apparatus  
(a) The Apparatus (b) Compression Cell (Shiming, 1984)



Table 2. 10 Index Properties of Soil Samples used in the Investigation  
(Shiming, 1984)

Sample No	W (%)	$\gamma_d$ (g/cm <sup>3</sup> )	Void Ratio	LL (%)	PI (%)	Linear Shrinkage (%)	<0.005mm (%)
W <sub>1</sub>	31.8	1.36	1.015	51.5	27.3	17.6	67
	47.4	1.15	1.4	72	31	37.6	
H <sub>2</sub>	21.7	1.6	0.721	43.8	20.7	18.4	41
	20.7	1.66	0.652	45.5	21	14.4	
N <sub>3</sub>	23.6	1.63	0.68	34	18	6.8	34

Table 2. 11 Comparison of Expansion for Monorail Tests (Shiming, 1984)

No. of Sample	Before Testing		Expansion Direction	Expansion (%)	After Testing		LL (%)	PI (%)
	Moisture Content (%)	Dry Bulk Density (g/cm <sup>3</sup> )			Moisture Content (%)	Dry Bulk Density (g/cm <sup>3</sup> )		
W <sub>1</sub> (1.15m)	28.1	1.43	Vertical	3.5	37.5	1.95	47	20
			Lateral	0.585	34	1.88		
H <sub>2</sub> (2.0m)	17.6	1.69	Vertical	5.585	25	2.12	42	22
			Lateral	4.45	22.7	2.09		
N <sub>3</sub> (2.5m)	19.7	1.65	Vertical	0.565	22.1	2	36	19
			Lateral	0.45	21.3	2		
N <sub>3</sub> (2.5m)	9.5	1.73	Vertical	27.11	34.8	2.09	36	17
			Lateral	24.1	36.2	2.09		

Table 2. 12 Swell Pressure Measurements (After Shiming, 1984)

No of Sample	Before Testing		Conventional Oedometer (kg/cm <sup>2</sup> )	Triaxial		Remarks
	Moisture Content (%)	Dry Bulk Density (g/cm <sup>3</sup> )		Vertical (kg/cm <sup>2</sup> )	Lateral (kg/cm <sup>2</sup> )	
W <sub>1</sub>	45.1	1.15	0.5	0.21	0.15	
				0.12	0.12	
H <sub>2</sub>	20.8	1.66	0.8	0.81	0.7	
				0.66	0.3	
S <sub>4</sub>	32.2	1.44	0.85	0.51	0.23	Remolded Clay

Table 2. 13 Oedometer and Triaxial Swell Tests Comparison (Shiming, 1984)

No. of Sample	Initial Moisture Content (%)	Dry Bulk Density (g/cm <sup>3</sup> )	Test Method	Expansion Direction	Expansion (%)	Final Moisture Content (%)	LL (%)	PI (%)
W <sub>1</sub> (1.2 m)	32.5	1.35	Triaxial	Vertical	3.61	38.8	51.6	24.3
				Lateral	5.64			
	31.8	1.35	Monoaxial	Vertical	17.37	47.5		
H <sub>2</sub> (0.8m)	21.8	1.6	Triaxial	Vertical	1.44	26.2	43.8	23.1
				Lateral	2.73			
	21.7	1.6	Monoaxial	Vertical	5.58	26.2		

The multi-dimensional behaviour of expansive soils on cubic soil samples were investigated by Shanker, Ratnam and Rao (1987), who allowed swell to occur in one, two or three dimensions respectively under a given surcharge pressure. The soil sample that was allowed to swell in three directions expanded most, while the sample which was permitted to swell in vertical direction only swelled the least. Similar results supporting this behaviour was also observed at samples that were allowed to swell freely from their top and bottom faces, which showed greater swell compared to samples allowed to swell from one face only. Shanker et al. (1987) also observed that the percent swell decreased with the decrease in specimen dimensions for samples of same thickness. This behaviour was linked to side friction which was constraining the swelling mechanism.

Chen and Huang (1987) developed a small scale testing set-up with application principles very similar to a modified triaxial apparatus, although it was not a real one (Figure 2.34). The aim of the research was to investigate the magnitude of lateral expansion pressure exerted on a rigid wall, so that the walls surrounding the sample box were designed to be rigid to secure minimal deflection occurrence during expansion. The clay sample taken from U.S. Denver area was mixed with some bentonite and compacted into the sample box to maximum proctor density at one inch layers, between which filter papers were placed to sustain proper infiltration of water during compaction. The box used in the model test was 15" x 15" x 12" (L x W x H). The initial water content at beginning of the test was slightly lower than the optimum moisture content. The sample that was initially loaded with a seating surcharge of 0.04 kPa was then maintained at constant volume. The lateral swell pressures were measured by three load cells that were installed at top, mid-height and bottom of the box along its height. An adjustable plate was mounted at the top to control the constant volume requirements. Two additional load cells were installed at the top to measure the vertical swell pressure. The movement of the container was monitored by means of strain gauges. Water was given to the sample through a steel mesh plate located at the back of the sample. The peak lateral swell pressures recorded were higher than the vertical pressure as given in Figure 2.35.

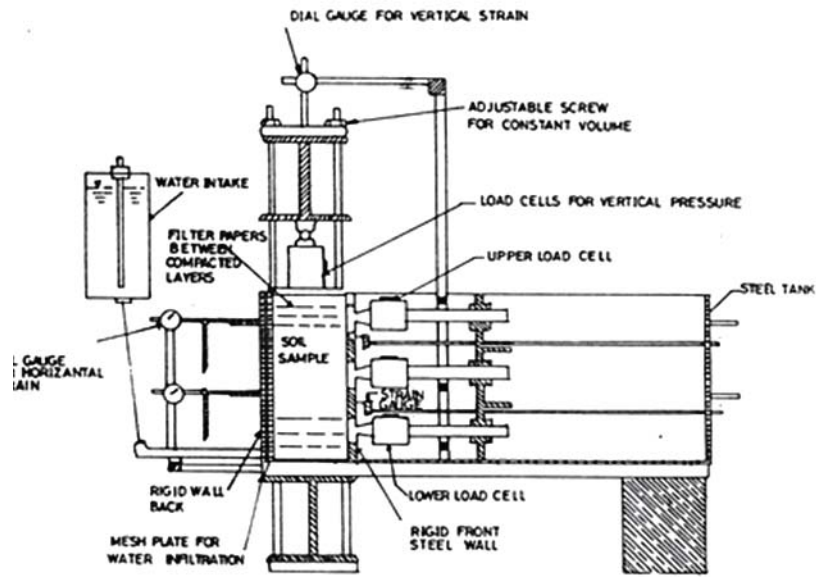


Figure 2. 34 Lateral Pressure Measurement Test Set-up (Chen and Huang, 1987)

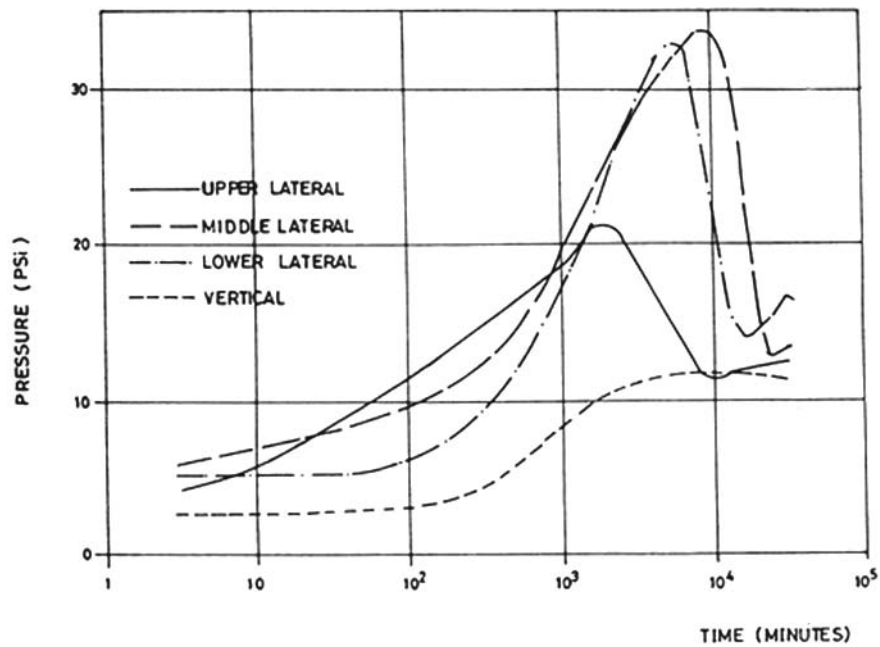


Figure 2. 35 Lateral and Vertical Swell Pressure versus Time (Chen and Huang, 1987)

Fourie (1989) investigated the lateral swelling pressure of expansive soils by using the hydraulic triaxial apparatus originally developed by Bishop and Wesley (1975) for controlled stress path testing (Figure 2.36). Different from the conventional triaxial cell, stress path cell was an independent, convenient and compact unit. Pressure is applied to the lower chamber mounted at the bottom of the cell. The piston pushed up the loading ram, moving the sample towards a fixed submersible load cell, thus applying axial load to the sample. This was an important feature of the stress path cell that made it possible to measure the vertical swell in contrast with the conventional triaxial cell for which volumetric swell was the only deformation component that could be measured.

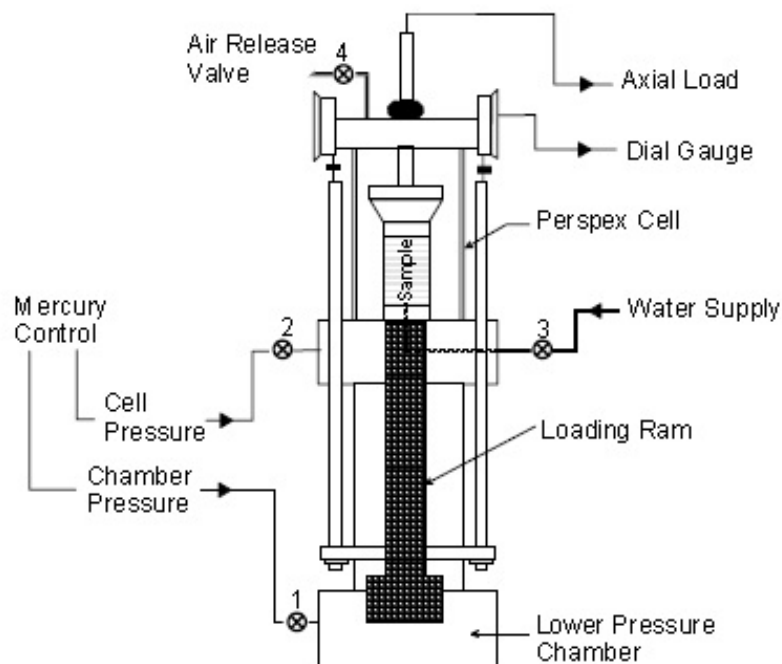


Figure 2. 36 Schematic Description of the Triaxial Stress Path Cell (Bishop and Wesley, 1975)

In the first stage of the investigations, oedometer samples at a moisture content of 22% and dry unit weight of  $14.2 \text{ kN/m}^3$  were prepared and tested according to “Method of Equilibrium Void Ratios” as defined by Sridrahan (1986), under different vertical stresses and the change in sample thickness was measured (Figure 2.37). Then, additional samples were prepared with the same initial water content and dry density and tested as for a conventional triaxial sample with provision for radial as well as top and bottom drainage. A lateral strain belt described by Bishop and Henkel (1962) was then assembled around the sample. After filling and pressurizing the triaxial cell, any desired ratio of vertical to horizontal total stress could thus be imposed on the sample prior to wetting up. The soil sample was simultaneously fed with water through the top and bottom loading plates as well as the radial drains. The technique consisted of continuously increasing the cell pressure. If any increase in diameter upon ingress of water to the sample was detected by the lateral strain belt, the test proved unsatisfactory based on the fact that it was impossible to compress the sample back to its original diameter. Due to unsatisfactory results, an alternative approach based on “Method of Equilibrium Void Ratios” was adopted for the rest of the work. A series of identically prepared samples were set up in the hydraulic triaxial cell and were subjected to different values of initial cell pressures. A back pressure of 50 kPa was applied to the samples and they were allowed to change volume until equilibrium had been reached. An equilibrium state was assumed to have occurred when the lateral strain belt reading settled at a constant value for a minimum of three days. Because of the extremely low permeability of clay samples, each of the tests was reported to take three to four weeks for completion.

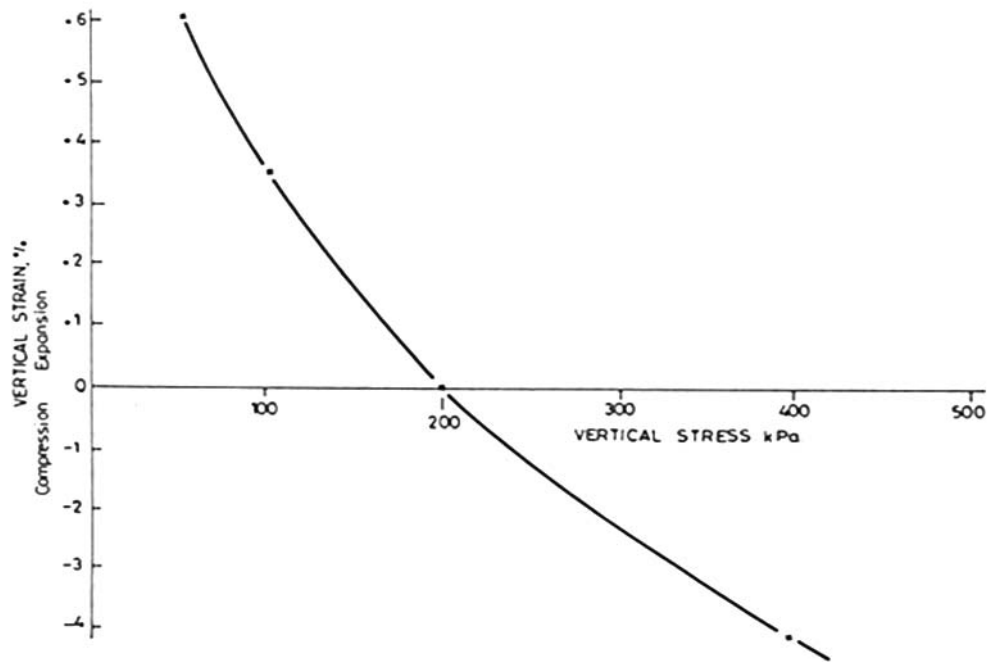


Figure 2. 37 Variation of Final Measured Vertical Strain with Applied Vertical Stress (Fourie, 1989)

The results of the tests obtained by this technique are presented in Figure 2.38. The vertical axis shows the ultimate lateral strain values given by the lateral strain belt. The point at which the curve intersects the horizontal axis, namely the zero lateral strain line, depicts the lateral swelling pressure developed under zero lateral strain conditions. From the comparison of Figure 2.37 and Figure 2.38, Fourie (1989) concluded that the lateral pressure estimated by the hydraulic triaxial cell was almost two times greater than the vertical swell pressure obtained from the conventional oedometer test for zero lateral strain condition. Since the "Method of Equilibrium Void Ratios" technique used in this investigation gives the lowest estimate for swell pressures (Sridrahan et al., 1986), Fourie (1989) recommended that this method would obviously provide a lower-bound estimate of lateral swelling pressures in the field. Pointing out the possible errors on the measurement of axial strain using conventional triaxial cell (Jardine et al., 1984), Fourie (1989) concluded that this test method has a significant advantage based on its direct lateral strain measurement capability, which is more preferable for

the determination of lateral swell pressures. One other important advantage of hydraulic triaxial cell over conventional oedometer cell is its capability of allowance for swell in both directions.

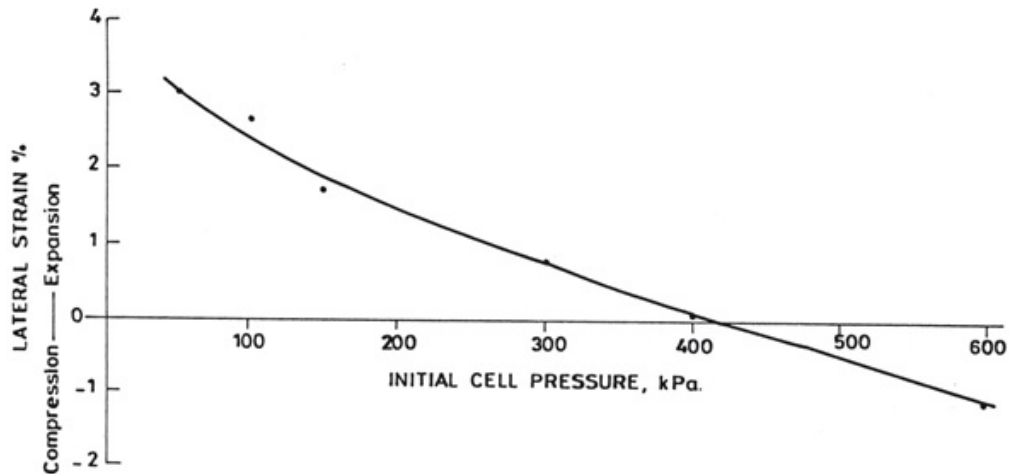


Figure 2. 38 Variation of Final Measured Lateral Strain with Applied Initial Cell Pressure (After Fourie, 1989)

Michel, Beaumont and Tessier (2000), performed an investigation on the measurement of swell parameters of expansive soils by using the hydraulic triaxial cell originally developed by Bishop and Wesley (1975). Unlike Fourie (1989), they used a computer controlled hydraulic triaxial testing system (Menzies, 1988) for this purpose which had the capability to measure the lateral and axial confining pressures as well as the deformations. Three microprocessors controlling hydraulic actuators were used in the experiments. Two of these probes were used to measure the axial and lateral pressures and deformations and the third one was used to generate a constant rate of water intake into the soil sample. Undisturbed soil samples were obtained from the site in winter and dried very slowly at room temperature. Samples were then placed



into triaxial cell and tests were carried out at different confining pressures by saturating them at a constant rate of inflow into the sample. The radial and axial volume changes were simultaneously measured by means of the probes. From the test results, it was observed that two of the samples tested swelled anisotropically, whereas the other three samples showed isotropic swell behaviour.

Al-Shamrani and Al-Mhaidib (2000) used a stress path triaxial testing apparatus to assess the vertical swell of expansive soils under multi-dimensional loading conditions. The effect of boundary conditions as well as the initial moisture content on the vertical swell was investigated. The results from the triaxial tests were then compared with the swell characteristics obtained from monoaxial loading test performed in an oedometer apparatus on samples having identical initial conditions. The soil samples were obtained from the town of Al-Ghatt in Saudi Arabia, and were remoulded prior to testing in order to avoid undesirable deviations in the test results. The aim of the initial group of triaxial tests was to assess the relationship between the amount of vertical swell and the confinement conditions. It was observed that an increase in the confining pressure resulted in a decrease in the percentage of swell, as illustrated in Figure 2.39. Furthermore, just after the test was started, the rate of expansion was monitored to be relatively low in the case of higher lateral confinement. This observation was linked to the difficulty imposed by larger confinement pressures for the water to penetrate into soil, whereas, the absorption of water by the soil was relatively easier under lower confinements. Additionally, it was noted that the effect of the confining pressure on the vertical swell vs. time relationship was not so pronounced up to a certain level of confinement.

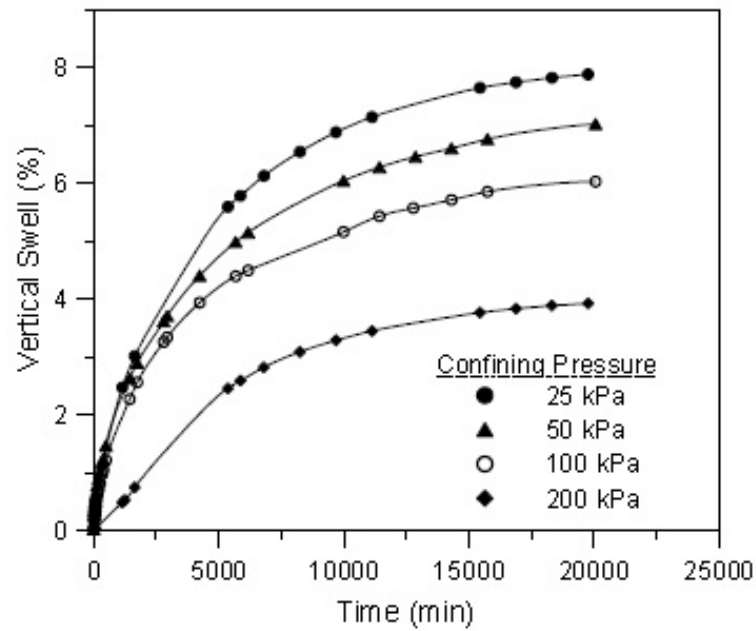


Figure 2. 39 Vertical Swell under Different Confining Pressures (Al-Shamrani and Al-Mhaidib, 2000)

Another group of triaxial swell tests were performed by Al-Shamrani and Al-Mhaidib (2000) to evaluate the effect of initial water content on the magnitude of vertical swell. As it can be seen from Figure 2.40, the vertical swell was significantly influenced by the initial water content regardless of the magnitude of confinement. To depict the correlation between swell and initial water content, tests were conducted with different initial water contents under a confinement of 25 kPa. The trendline obtained is given in Figure 2.41.

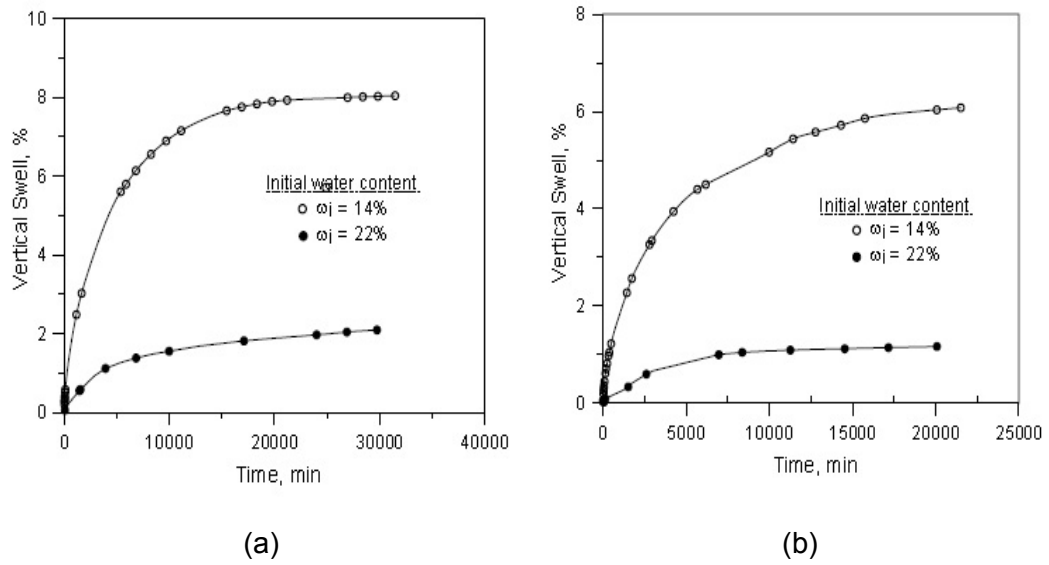


Figure 2. 40 Vertical Swell versus Time for Different Initial Water Contents  
 (a) Confining Pressure=25 kPa (b) Confining Pressure = 100 kPa  
 (Al-Shamrani and Al-Mhaidib, 2000)

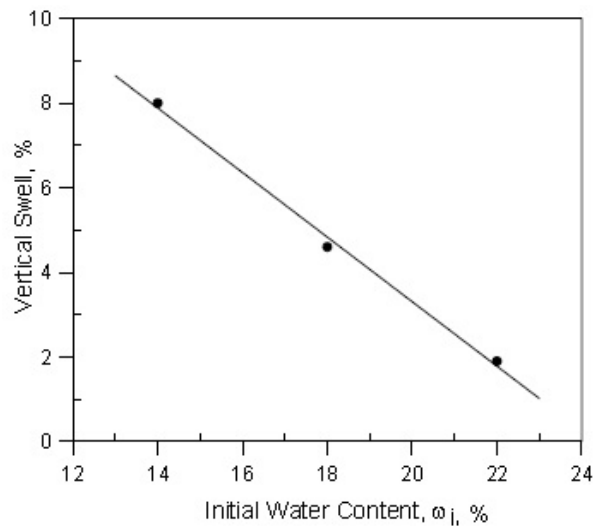


Figure 2. 41 Relationship between Initial Water Content and Vertical Swell for  
 Confining Pressure = 25 kPa (Al-Shamrani and Al-Mhaidib, 2000)

As it can be seen from Figure 2.41, the ultimate vertical swell tended to decrease with increasing initial water content. Al-Shamrani and Al-Mhaidib (2000) extrapolated the linear relationship presented in Figure 2.41 and defined its intersection with the x-axis as the initial moisture content value at which the soil will experience zero vertical swell. This value was found to be around 24 % which was below the plastic limit of 30 %. However, based on the previous statements (Dhowian et al., 1990; Edil and Alanazy, 1992) showing that the water content for swell mobilization was very close to the plastic limit for swell tests performed in the oedometer apparatus, Al-Shamrani and Al-Mhaidib (2000) concluded that the relationship between the vertical swell and the initial moisture content largely depend on the loading conditions of the swell test.

Al-Shamrani and Al-Mhaidib (2000) also conducted a group of tests both on the conventional oedometer and triaxial apparatus to examine the vertical swell under different loading conditions. The vertical swell percentage versus time graph for a confinement of 35 kPa is presented in Figure 2.42. It was reported from the test results that; the vertical swells obtained from oedometer were considerably larger than the triaxial test measurements.

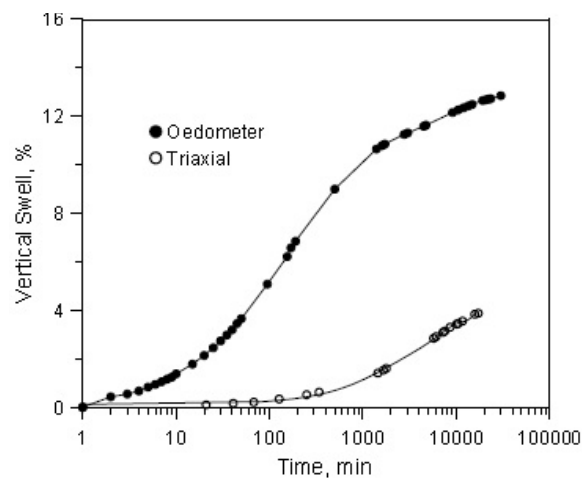


Figure 2. 42 Vertical Swell Percentage from Oedometer and Triaxial Tests  
(Confining Pressure=35 kPa) (Al-Shamrani and Al-Mhaidib, 2000)

Figure 2.43 gives a plot of vertical swell percentages obtained from the two types of tests versus the logarithm of different confining pressures utilized. It was noticed that the rate of decrease in the vertical swell with increasing pressure was higher for the oedometer test than for the triaxial test. It was also reported that in oedometer tests samples had higher final water contents than the triaxial tests. Al-Shamrani and Al-Mhaidib (2000) noted that this observation was supporting the suggestion made by Erol et al. (1987) that utilization of a moisture factor is as important as the factor of lateral restraint while oedometer test results are being used for heave prediction (Figure 2.44).

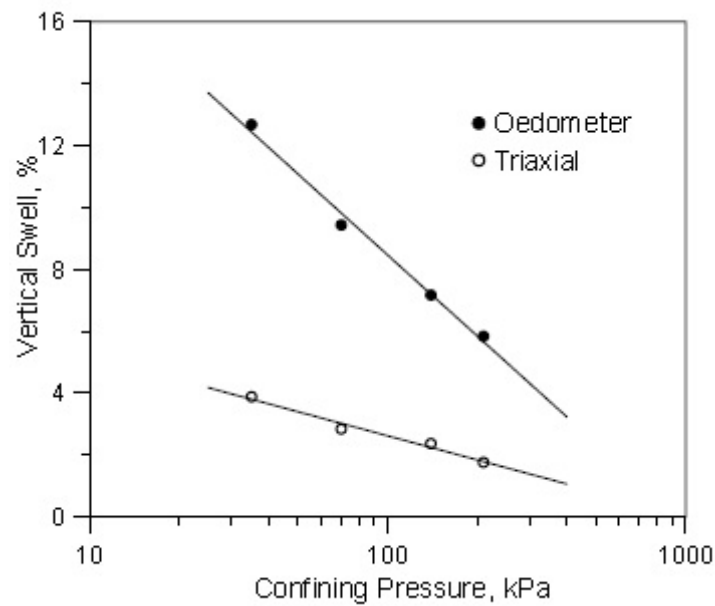


Figure 2. 43 Relationship between Applied Pressure and Ultimate Vertical Swell Measured in Oedometer and Triaxial Swell Tests (Al-Shamrani and Al-Mhaidib, 2000)

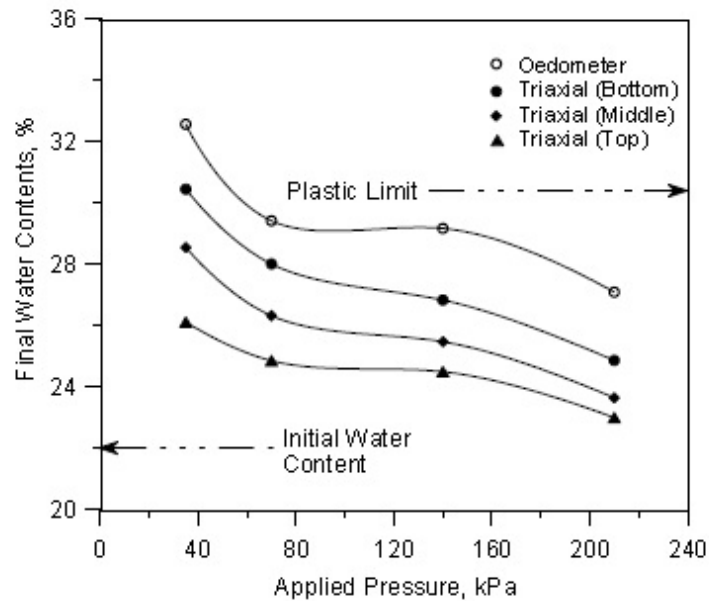


Figure 2. 44 Final Water Contents of Triaxial and Oedometer Samples at Different Confining Pressures (Al-Shamrani and Al-Mhaidib, 2000)

Al-Shamrani and Dhowian (2003) studied the impact of lateral restraint conditions on swell levels of expansive soils from Al-Ghatt town of Saudi Arabia, through a comprehensive laboratory testing program performed on compacted and undisturbed soil samples in a hydraulic triaxial testing apparatus as well as an oedometer test set-up. The swell parameters obtained from the test program were then used to forecast the in-situ heave measurements taken from an instrumentation station in Al-Ghatt region. Pressure, suction, and moisture heave prediction methods were also used to evaluate in-situ heave, and the results were compared with the experimental results. According to the preliminary investigations and past experience, the soil formation in Al-Ghatt was a shale material, having 8 to 10 meters of thickness and high swell parameters. Roughly a 1.5 m of surface soil was stripped off from the station area having plan dimensions of 20 x 20 meters, prior to installation of the saturation system and the instrumentation in order to reach the expansive material. The saturation system consisted of 19 sand drains and there were six instrumented units, each

consisting of a thermocouple psychrometer stack, moisture access tube, surface heave plate, and five deep heave plates. The field instrumentation is illustrated in Figure 2.45.

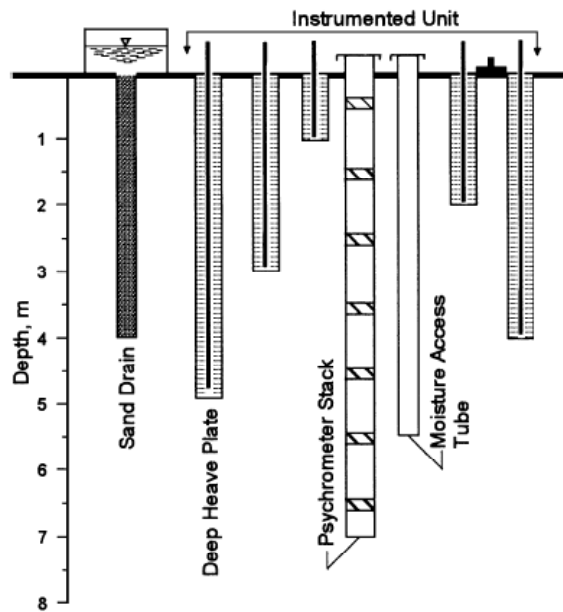


Figure 2. 45 Schematic of the Field Station Instrumentation (Al-Shamrani and Dhowian, 2003)

For a period of 54 weeks, the instrumentation station was irrigated via the drain system to achieve the essential swell conditions. Measurements were made for the surface and subsurface heave while samples were taken for corresponding moisture content determination. The changes in soil moisture content and suction, and the associated heave are illustrated in Figure 2.46.

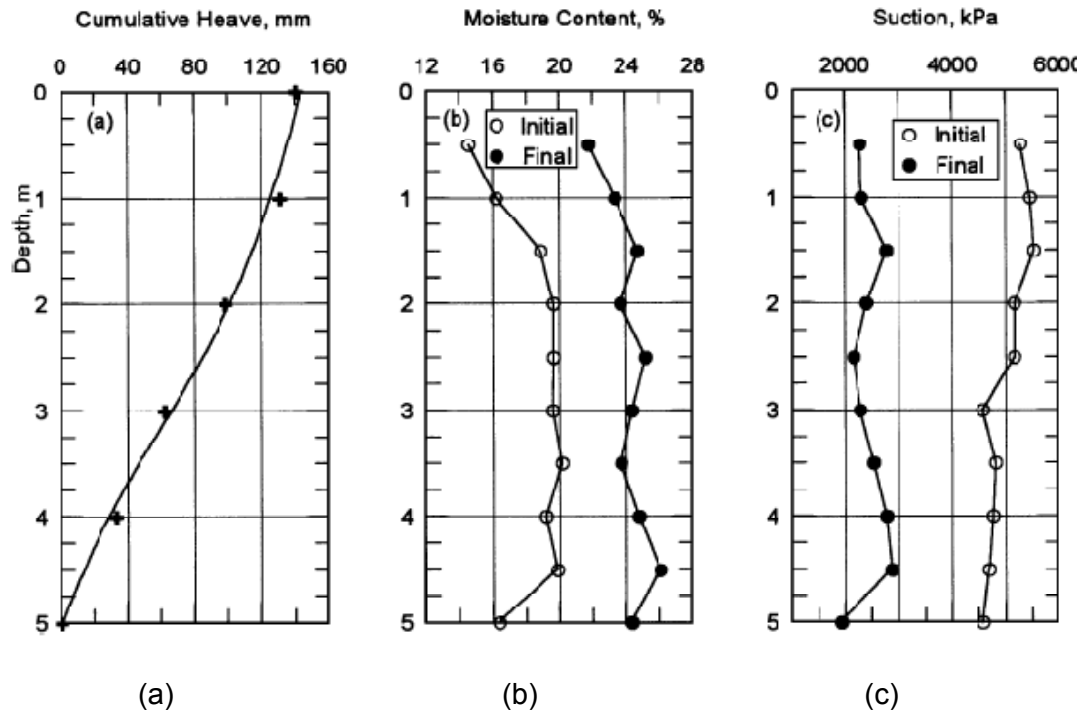


Figure 2. 46 Field Data (a) Cumulative Heave (b) Moisture Content (c) Suction  
(Al-Shamrani and Dhowian, 2003)

As mentioned earlier, Al-Shamrani and Dhowian (2003) used different types of oedometer tests as well as triaxial testing to obtain the swell needed to forecast the field heave. The fissured and laminated structure of the in-situ soil obscured the collection of undisturbed samples having a relatively longer length requirement for triaxial testing. Therefore the triaxial test program was limited to compacted samples only, whereas oedometer tests were performed mainly on undisturbed samples, with a series of the oedometer program reserved to compacted samples for a better comparison of results.

The oedometer test schedule included all the three types of tests, namely the free swell (ISO), swell overburden (SO) and constant volume swell (CVS) tests. The triaxial swell tests were performed in a hydraulic triaxial stress path cell of Bishop and Wesley (1975). Although it is possible to measure the swell parameters by



triaxial loading through a similar procedure to the three oedometer tests, i.e. ISO, SO and CVS methods; it was reported by various researchers (Brackley, 1975; El Sayed and Rabba, 1986) that results from the SO method represented the field conditions better, so Al-Shamrani and Dhowian (2003) limited the triaxial testing schedule to the SO procedure only. In the presentation of their investigations, the triaxial swell overburden tests were labeled as TSO, whereas the corresponding oedometer tests were designated as OSO. The average values for swell pressure and swell index obtained from the test program are presented in Table 2.14.

Table 2. 14 Shale Swell Parameters Obtained from Oedometer and Triaxial Swell Tests (Al-Shamrani and Dhowian, 2003)

<b>Swell Test</b>	<b>Swell Pressure, Ps (kN/m<sup>2</sup>)</b>	<b>Swell index, Cs</b>
Free Swell Test (ISO)	829	0.069
Constant Volume Test (CVS)	586	0.054
Swell Overburden Test (OSO) (Undisturbed Samples)	390	0.156
Swell Overburden Test (OSO) (Compacted Samples)	860	0.145
Triaxial Swell Tests (TSO)	1070	0.041

Parallel to the previous findings of Sridrahan, Rao and Sivapullaiah (1986), it was observed that the ISO tests, among the three types of oedometer tests, gave the highest value of swell pressure. The swell pressure from the SO test was the lowest, whereas the results from the CVS tests fell in between. As far as the swell indices were considered, the results from the ISO and CVS tests were comparable but the results from the OSO tests were significantly higher. Finally, the comparison of undisturbed and compacted OSO tests revealed that the swell indices from the two tests were quite similar in contrast with the outcome that the swell pressures for the compacted samples were more than twice the value obtained for undisturbed samples. Typical variation of the percentage of vertical

swell with elapsed time and variation of vertical swell versus applied pressure is shown in Figure 2.47 for the Oedometer and Triaxial tests for samples compacted to similar initial moisture content and dry unit weight. The vertical swells obtained from the oedometer tests were, as expected, considerably larger than the triaxial test measurements.

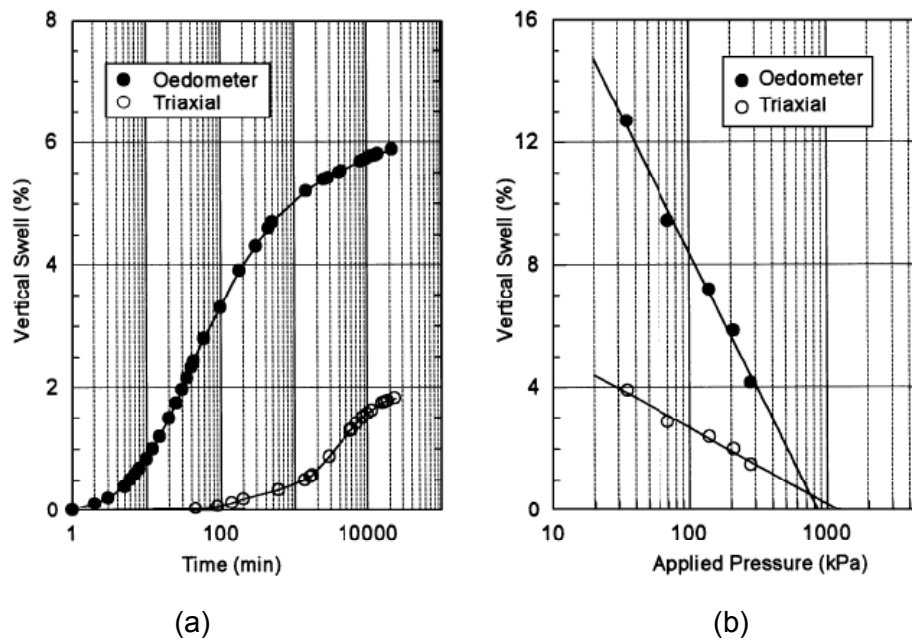


Figure 2. 47 (a) Vertical Swell Behaviour under Oedometer and Triaxial Loading Conditions (b) Variation of Oedometer and Triaxial Ultimate Swell with Confining Pressure (Al-Shamrani and Dhowian, 2003)

Al-Shamrani and Dhowian (2003) concluded that the differences in the results from the two test methods were acceptable, since, the samples were laterally constrained in the oedometer ring, leading to the measurement of volumetric strain as the swell value, whereas, in the triaxial apparatus, only a portion of the volume change of the sample could be reflected as the vertical swell. In addition,

it was noted by Al-Shamrani and Dhowian (2003) that side friction slowed down swelling in the oedometer tests. This was similar to the finding of Shanker et al. (1987) who noted a decrease in the percent swell as the sample diameter decreased. Furthermore, referencing Tisot and Aboushook's (1983) conclusion that oedometer ISO testing gave swell pressures nearly three times the value from the oedometer CVS test, Al-Shamrani and Dhowian (2003) pointed out that the swell pressure obtained from a triaxial CVS test and from a triaxial ISO test differed by less than 10%, attributing the significant disparity of swell pressures from the oedometer methods to the effect of side friction.

In the next stages of their investigations, by using the results of oedometer and triaxial swell tests, Al-Shamrani and Dhowian (2003) made an attempt to forecast the field heave based on the pressure approach, suction data and moisture data and compared them with the actual field measurements. From the results of these investigations, they concluded that; field heave measurements were markedly overpredicted when the results of oedometer tests were used. Triaxial swell parameters however yielded a better approximation. The results of the named test are illustrated in Figure 2.48. The best solution, however, was found to be the utilization of the results of triaxial swell tests in conjunction with the moisture heave prediction method.

Al-Shamrani and Dhowian (2003) explained the large discrepancy between measured and the predicted heave by the effect of lateral restraint conditions of the oedometer test. They proposed the application of a lateral restraint correction factor between 0.31 to 0.33, subject to the type of oedometer test, heave prediction method, and fabric and structure of the soil, to the predicted values to obtain an agreement between measured and predicted heaves. The authors (Al-Shamrani and Dhowian, 2003), also noted that this correction factor not only accounted for the effect of lateral restraint conditions but also for the difference between the perfect soaking circumstances in the oedometer and the insufficient in-situ wetting.

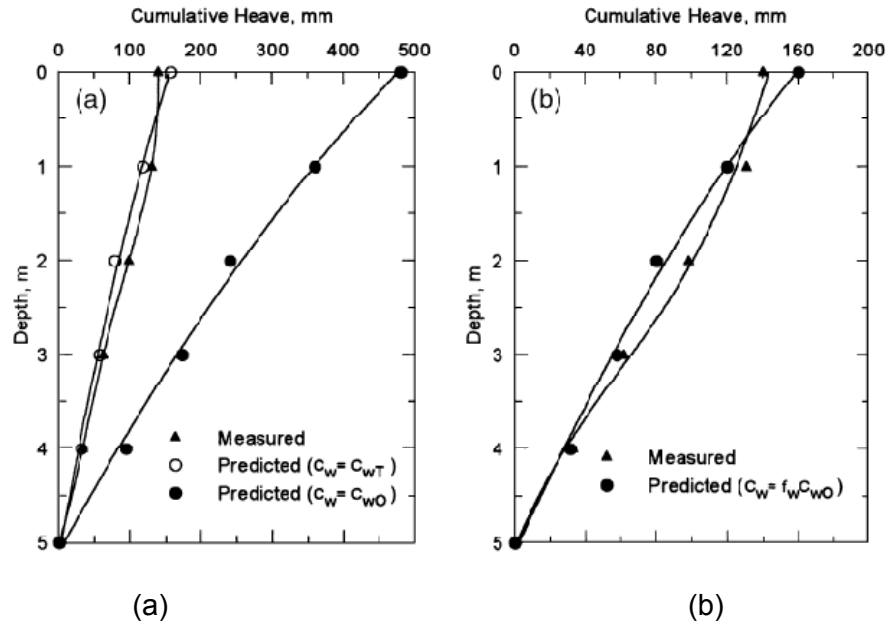


Figure 2. 48 Measured and Predicted Heave based on Moisture Techniques:  
(a) Using Oedometer and Triaxial Moisture Index; (b) Using  
Corrected Oedometer Moisture Index. (Al-Shamrani and Dhowian,  
2003)

Dhowian and Al-Saadon (2010) carried out an experimental testing program on an expansive soil to investigate the effect of lateral confinement on the amount of vertical and lateral swell percentages. In the first part of their investigations, ISO and CVS were performed on undisturbed samples in accordance with ASTM D4546-85, by using the conventional oedometer testing techniques. In the second part of the investigations, a test device that was capable of measuring both the lateral and vertical swells under unconfined testing conditions was developed and the tests were repeated once more.

To achieve this goal, expansive soil samples with 35.5 mm diameter and 76 mm long were artificially prepared by compacting them with the dry densities and natural moisture contents representing their field conditions. Then the soil

samples were placed inside a rubber membrane and put on top of a metal base and a porous stone of 40 mm diameter. Another porous stone was placed on top of the soil sample which was in direct contact with the top metal circular plate. Both the bottom and top plates were manufactured with small holes that allow water to flow through circular tubes of 1.5 mm diameter into the soil. Four dial gages were mounted in direct contact with the lateral side of the soil sample at equal intervals to measure the lateral swell whereas a fifth dial gage was mounted on top of the sample for the purpose of vertical swell measurements. The schematic representation of test set up is presented in Figure 2.49.

Before starting the experiment, a small vertical seating load of 7 kPa was applied to ensure complete contact of the top plate with the soil sample and test was started by allowing water inundating the specimen from its bottom. As expected, expansion was realized starting from the bottom and extending upwards as the time passed. Vertical and lateral deformations were recorded against time until they attained an ultimate value and were stabilized.

For the ISO tests, the average free swell was recorded to be around 11% and the estimated swell pressure ranges were in between 200-300 kPa, with a swell index of about 0.07. In the CVS test, however, the swell pressure was determined to be around 200 kPa, but the free swell was nearly 23% and the swell index was 0.25. The authors (Dhowian and Al-Saadon, 2010) explained this difference in the swell parameters by the variation in the tested soil properties as well as the differences caused by the methods of testing, which have the capability to significantly contribute to swell parameters.

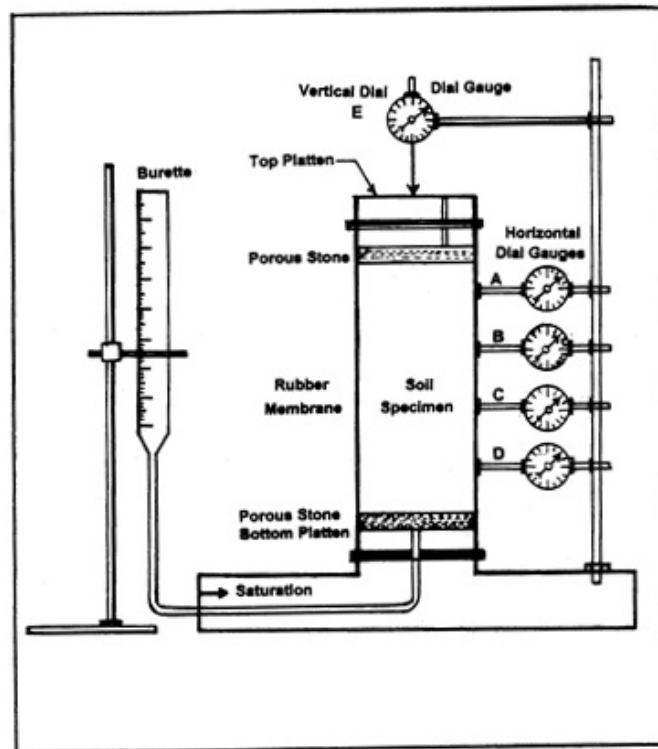


Figure 2. 49 Schematic Representation of the Free Lateral Movement Test (Dhowian and Al-Saadon, 2010)

The typical results of free lateral movement tests showing the relationship between the vertical swell and average lateral swell are presented in Figure 2.50. As it can be seen from this figure, the ratio of average lateral swell to vertical swell was found to be around 26%, which is in agreement with the previous work of Dhowian et al. (1990), in which it was reported that about one third of the soil expansion was in lateral direction. A comparison between ISO test performed in conventional oedometer apparatus and free lateral movement test is presented in Figure 2.51. It can be noticed from the figure that the vertical swell in the ISO test was higher than the vertical swell measured in free lateral movement test, confirming that considerable amount of deformation was consumed in the lateral direction. The vertical swell measured with zero lateral restraint was reported to

be about 8 percent, which in turn was less than the values measured in the oedometer test. The result of expansion with lateral swell was found to be consistent with the findings in the previous study conducted by Shamrani and Dhowian (2003), where triaxial testing technique had been used to measure the vertical and lateral expansion.

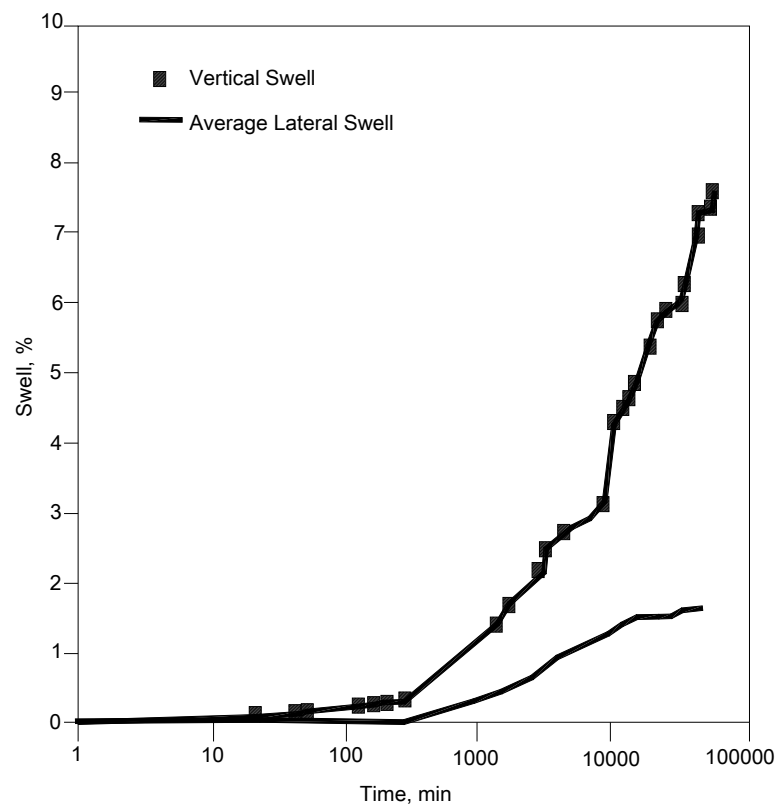


Figure 2. 50 Comparison between Vertical Swell and Average Lateral Swell (Dhowian and Al-Saadon, 2010)

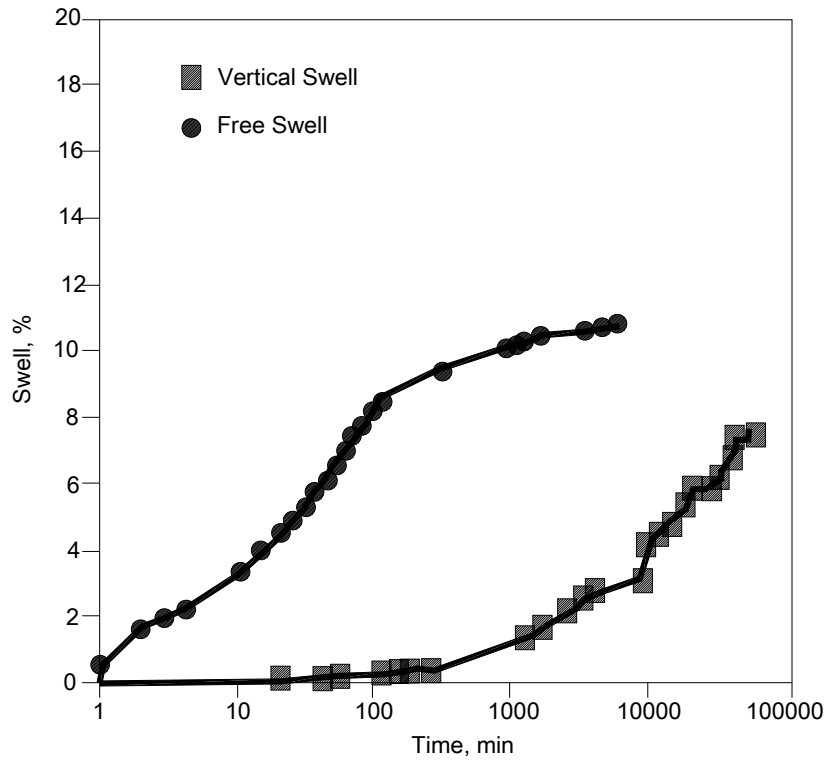


Figure 2. 51 Comparison of Vertical Swell Percentages Measured in Oedometer Ring and Free Lateral Movement Tests (Dhowian and Al-Saadon, 2010)

The results of the expansion tests in laterally restrained and unrestrained conditions performed by Dhowian and Al-Saadon (2010) showed that the contribution of lateral expansion on the volumetric expansion cannot be neglected and the adopted method of testing should reflect the actual field conditions. They concluded that some lateral expansion together with partial restraint does exist and hence, the swell parameters obtained from the conventional oedometer testing method and the method used in their investigation are not expected to produce an accurate heave prediction.

Thomas (2008) described a modified triaxial cell (originally used by Wattanasanticharoen et al., 2007) that was capable of measuring axial and



vertical pressures and strains to model three-dimensional anisotropic state of stress. Confining pressure was simulated by the water pressure applied on the sample placed in the triaxial cell while the vertical pressure was exerted by the classical dead weight system (Figure 2.52 and Figure 2.53).

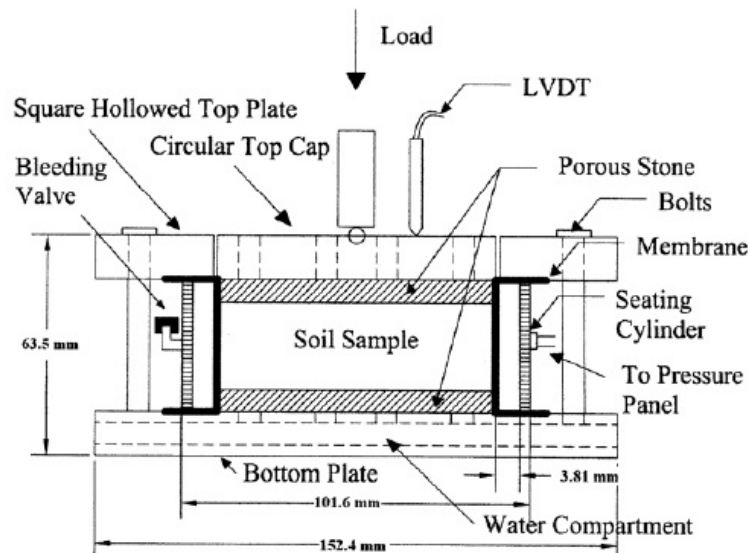


Figure 2. 52 Triaxial Swell Test Cell (Thomas , 2008)

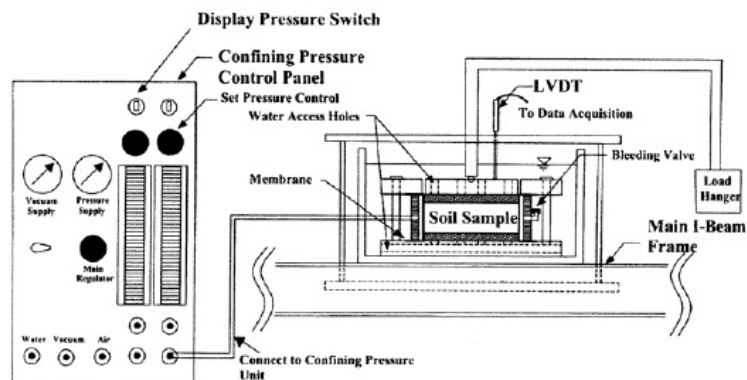


Figure 2. 53 Triaxial Swell Test Apparatus (Thomas, 2008)

Wattanasanticharoen et al. (2007) measured the radial swell strains in the sample using calipers as soon as the test was terminated. Utilization of confining pressures relatively higher compared to the vertical pressures, it was maintained that the original directions of axial and lateral pressure were interchanged, i.e. a 90° rotation in the directions of the vertical and lateral swell was obtained. The authors proposed that this device could be further modified by suction sensors to estimate the effect of matric suction.

### **2.5.7 Large Scale Tests and Case Studies**

Damage to the structures caused by lateral swelling pressures was first introduced in the literature by Kassiff and Zeitlen (1962), discussing the field observations of damage to pipelines buried in expansive clays. They determined inequalities in the lateral and vertical swelling behaviour which resulted in very large stresses in the pipeline.

Richards and Kurzeme (1973) and Richards (1977) presented the case study of a 7.5 m high reinforced concrete retaining wall to be constructed in a highly expansive stiff fissured clay and marl in Adelaide, Australia. Because of the nature of the accommodating soil bed, a 25 m length of the wall was dedicated as a monitoring and testing section along which twelve series of psychrometers as well as six series of earth pressure cells were installed in the vertical direction. Furthermore, lateral pressure readings were assured by additional earth pressure cells mounted at the back side of the wall. The back side instrumentation also included supplementary psychrometers, located at different distances to the wall with the nearest one at two meters of distance, to measure soil suction variations at back of the wall. Regular measurements were recorded against time between 1971 and 1975. The supplementary psychrometers at the back of the wall did not measure substantial decline in soil suction, however the increase in the lateral earth pressures determined by measurements from the lower pressure cells were noteworthy, reaching nearly up to five times of the vertical overburden pressure. The authors explained this trait by the seepage of surface water down from the

back face of the wall, hence causing the swelling action to commence from the bottom of the wall. As the time passed, it was observed that the lateral earth pressures progressed upwards with further wetting of the backfill with free water available (Figure 2.54).

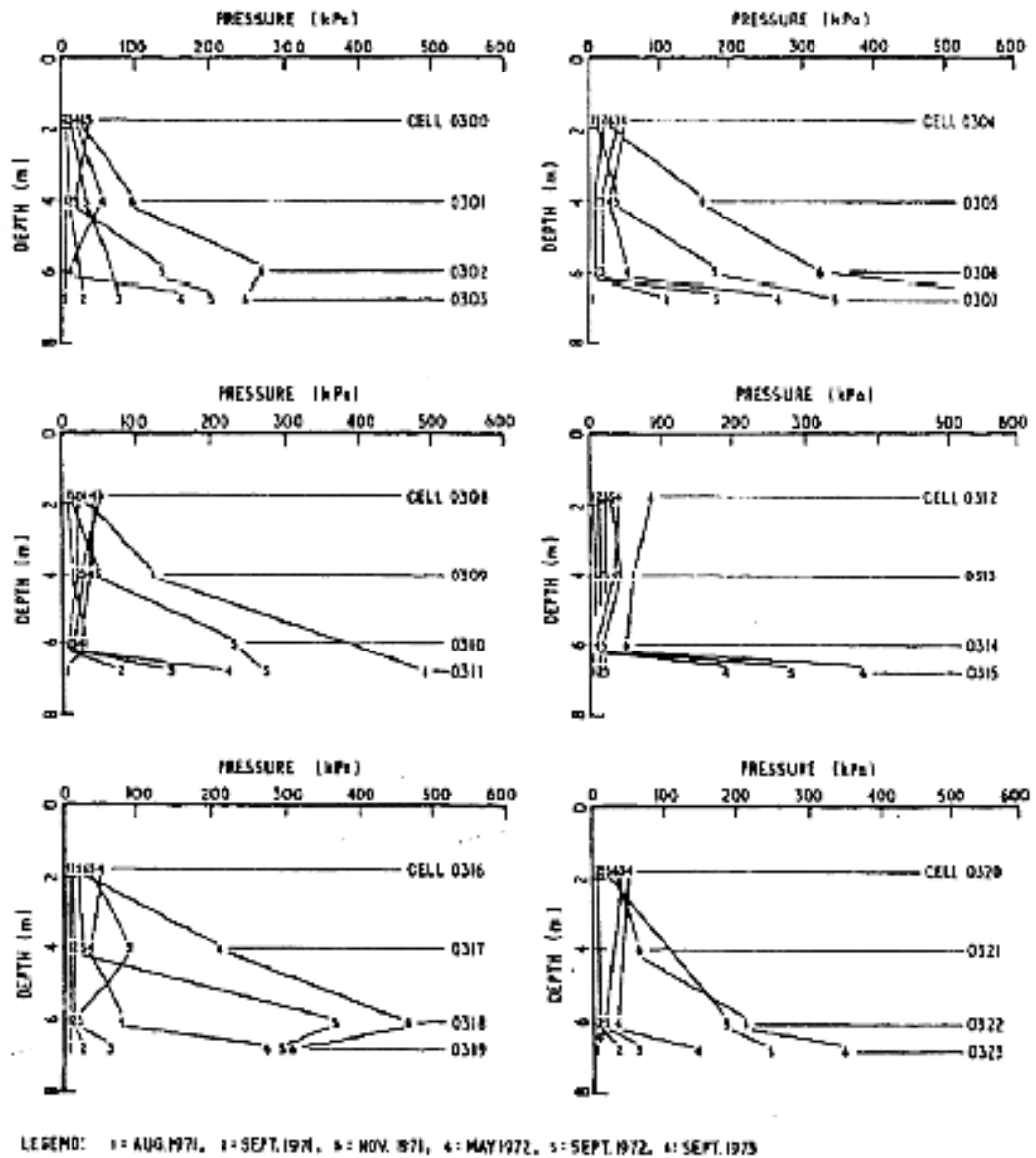


Figure 2. 54 Lateral Pressure versus Depth at Different Locations (Richards and Kurzeme, 1973)

In 1975, Robertson and Wagener introduced a total pressure cell for the in situ measurement of vertical and lateral swelling pressures. Two test pits were formed in medium dense to dense soil for this purpose as illustrated in Figure 2.55. The proper drainage of the tests pits were maintained by a gravel drainage layer placed at the bottom, whereas PVC lining was used all around pit to prevent water intrusion.

For their test program, Robertson and Wagener (1975) formed 50 mm of compacted clay layers within the pits, with 5 mm thick sand layers in between. The test pits were instrumented with pneumatic total pressure cells at 1 meter of depth beneath the final clay layer. In addition, horizontal pressure cells were installed at a shallow depth from the surface. Controlled wetting was performed at the two pits through auger holes opened to intersect the sand layers. A revision of the wetting process for Pit 2 was required after poor wetting conditions were depicted for Pit 1. Pressure cell readings were recorded at predetermined time intervals and the variation the average pressure values from the vertical and horizontal pressure cells for the two pits were plotted against time as given in Figure 2.56 and Figure 2.57.

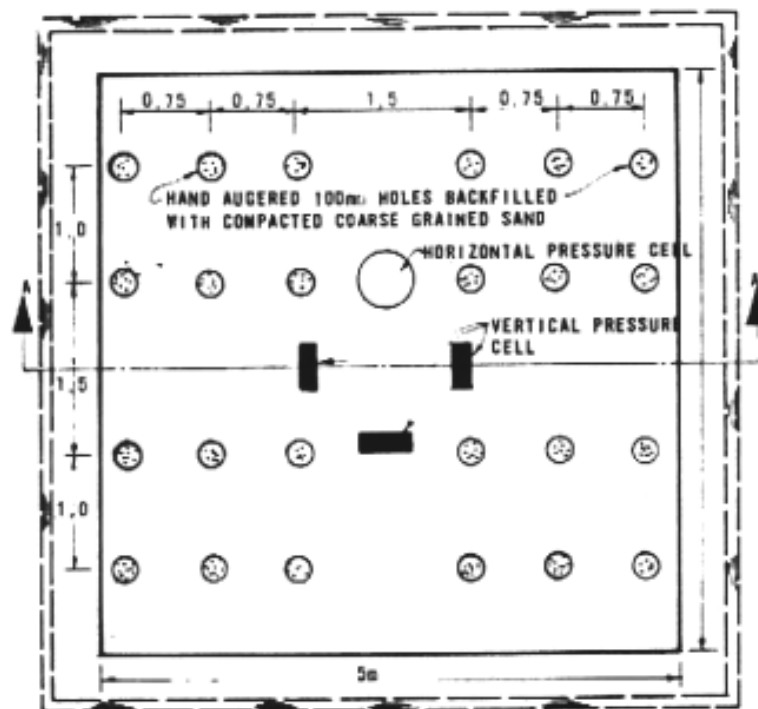
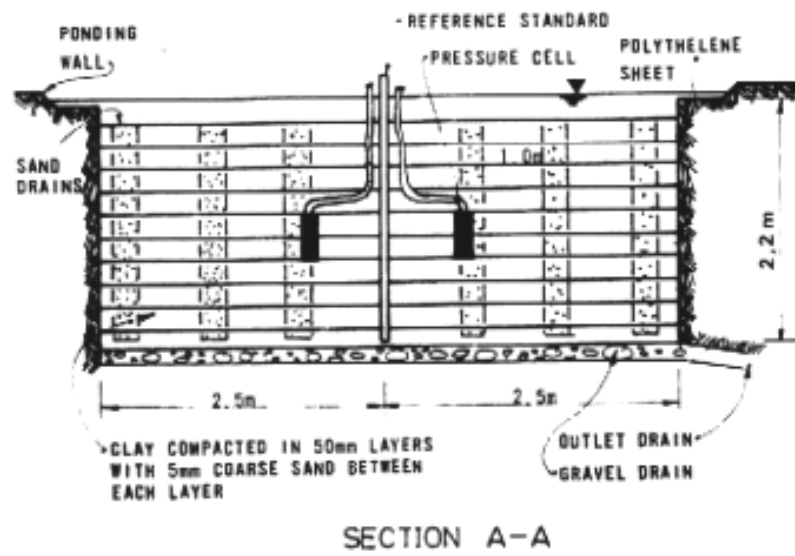


Figure 2. 55 Instrumented Test Pit (Robertson and Wagener, 1975)

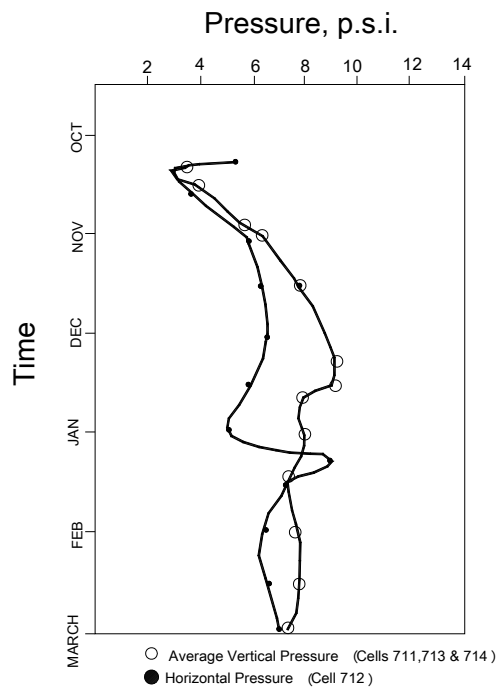


Figure 2. 56 Vertical and Lateral Pressures for Test Pit 1 (Robertson and Wagener, 1975)

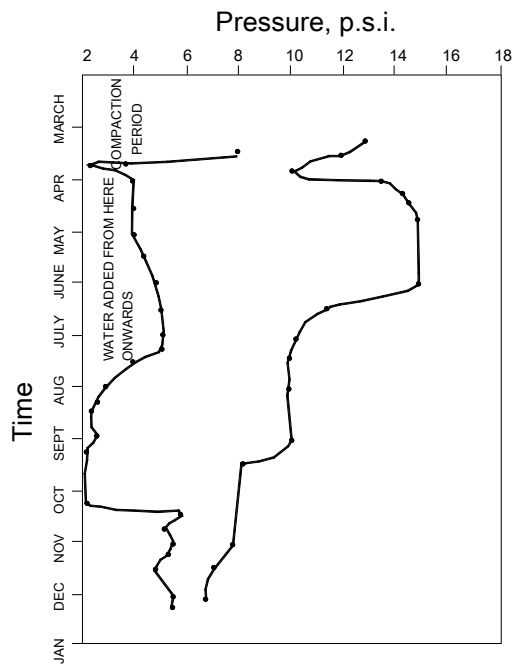


Figure 2. 57 Vertical and Lateral Pressures for Test Pit 2 (Robertson and Wagener, 1975)

During his investigations of an airport pavement on expansive clays, McKeen (1981) reported that the effect of cracks and fissures in a soil mass could be symbolized by the utilization of a lateral strain factor which should be between 0.33 for the unrestraint conditions and 1.00 for the fully restrained case. He defined the “fully restraint case” as being a steady soil mass without any cracks or other discontinuities, and the “unrestrained case” as a very dry soil mass with intensive cracking. During research, the measured heave from two sites were compared with the predicted heave and found that the restraint factors lied between 0.50 and 0.83. The values listed in Table 2.15 were found to be within the expected range. The results showed that the factors were low for the dry season, and began to increase towards 1.00 as the rainy season proceeded.

Table 2. 15 Heave Data for the Airport Research (McKeen, 1981)

<b>Period (Site)</b>	<b>Actual Heave (m)</b>	<b>Predicted Heave (m)</b>	<b>Restraint Factor</b>
Apr-May (Site-1)	0.04	0.048	0.833
May-Jul (Site-1)	-0.07	-0.15	0.503
Sep-Nov (Site-1)	0.02	0.04	0.497
Nov-Mar (Site-2)	0.04	0.06	0.737
May-Jul (Site-2)	-0.02	-0.03	0.829

Ofer (1980) and Ofer and Komornik (1983), introduced an in-situ lateral swelling probe (ISP) for the simultaneous in-situ measurement of lateral swelling pressures of wetted expansive clays. This apparatus, which is illustrated in Figure 2.58, mainly consisted of pressure transducers placed in between wetting rings and a cutting edge, that allowed for the minimum disturbance of soil as the probe was being inserted in. For the in-situ testing, the ISP, which was a cylindrical steel probe with an outside diameter 90 mm and a height of 200 mm, was positioned in a hole drilled for this purpose and lateral swellings were recorded real time while the surrounding clay was being wetted.

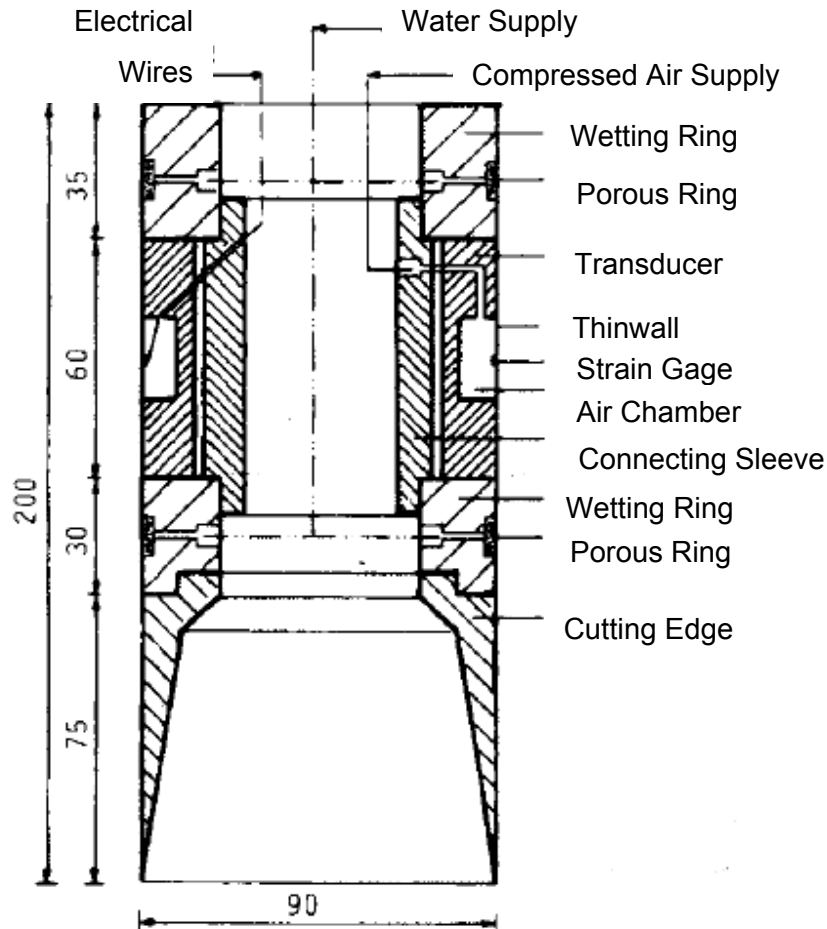


Figure 2. 58 In-Situ Lateral Swell Measurement Probe (Ofer and Komornik, 1983)

Field tests were conducted at two different depths of 0.6 m and 2.0 m, in which the lateral soil pressures obeyed a similar trend of an initial sudden decrease followed by a continuous rise to a peak value succeeded by a reduction in pressure stabilizing at a constant value. Ofer (1980) reported that the pattern of cresting and then stabilizing was similar to what had been observed in previous research, but the initial lateral pressure decrease was uncommon. This trait was attributed to represent the probable stress release or redistribution around the probe developed during insertion. The results of this investigation (Ofer, 1980) tests are presented in Figure 2.59 and Figure 2.60.



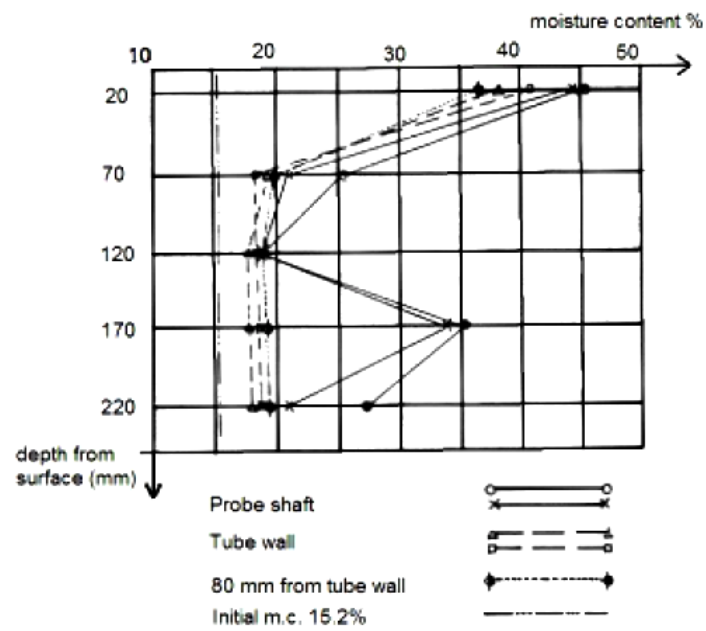


Figure 2. 59 Moisture Content Profile at the end of ISP Probe Test (Ofer, 1980)

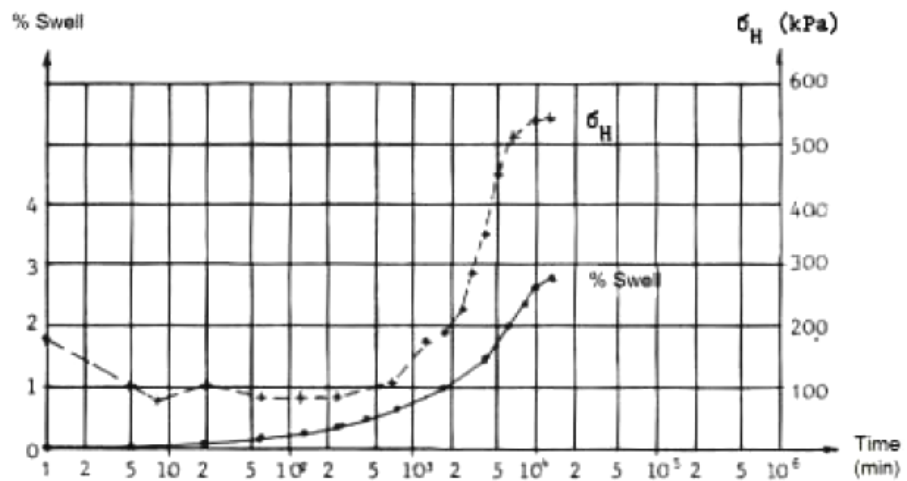


Figure 2. 60 Time versus Percent Swell Pressure for ISP Probe (Ofer, 1980)

Based on the comparison of their laboratory investigations with previous field research, Ofer and Blight (1985) concluded that the lateral swelling pressure obtained from the field tests were substantially less than the corresponding values estimated from laboratory tests. The authors explained this difference partly by the possible scale effects and mostly the biased soil sampling, so that the laboratory tests yielding results on the safe side when compared to the relatively lower field results. In addition, particularly for the investigation mentioned, the in situ soil in question was fissured and fragmented with root residues down to 15 meters causing an increase in the lateral compressibility of soil. The authors concluded that a laboratory test performed on an unfissured specimen should give higher lateral swelling pressure values than the one recorded in-situ (Ofer and Blight, 1985).

Katti, Bhangle and Moza (1983) and Joshi and Katti (1984) investigated the swell behaviour of expansive soils by means of comprehensive large scale laboratory experiments. The former work by Katti et al. (1983) concentrated on pressure developments on retaining structures with and without use of cohesive non-swelling materials, or CNS in short, between the structure and the clay fill. The model wall was not allowed to move, so that the values from the tests represented the conditions of earth pressure at rest, i.e. the  $K_0$  conditions. The state of zero deflection maintained along the vertical axis made the measurement of lateral swelling pressures mobilized after compaction and saturation possible. Preliminary evaluations by Katti et al. (1983) indicated that the complete saturation of the tested soil would last nearly 45 days, however the soil was saturated for 60-70 days to be conservative. The test set-up is presented in Figure 2.61 and Figure 2.62. The lateral pressures developed over the depth of the wall were evaluated for four different conditions, namely;

1. Granular materials (sand), CNS and expansive clayey soils in loose dry, compacted dry and compacted saturated conditions,
2. Expansive clay fill having varying thicknesses of CNS inserted between the wall and the expansive clay fill,

3. Expansive clay fill with varying thicknesses of CNS placed and compacted over the expansive fill,
4. Expansive clay fill having CNS both placed between the wall and the expansive fill, and over the fill.

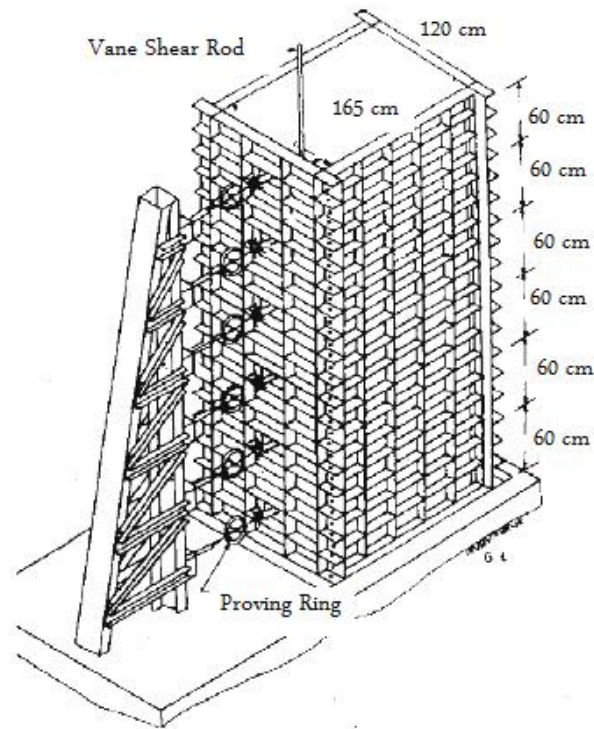


Figure 2. 61 Large Scale Laboratory Set-Up (Katti et al., 1983)

For the first type of experiments, Katti et al. (1983) observed a linear relationship of lateral pressure with depth for the loose dry conditions of all three materials. In other words, the Jacky's equation,  $K_0 = 1 - \sin \phi'$ , was valid for dry, loosely placed soil but it was not accurate for compacted soils. The lateral pressure vs. depth for the compacted dry condition was also linear but the  $K_0$  values were greater than 1, with the sand exhibiting the highest results, which are attributed to compaction load added over the self-weight of the fill at a given depth.

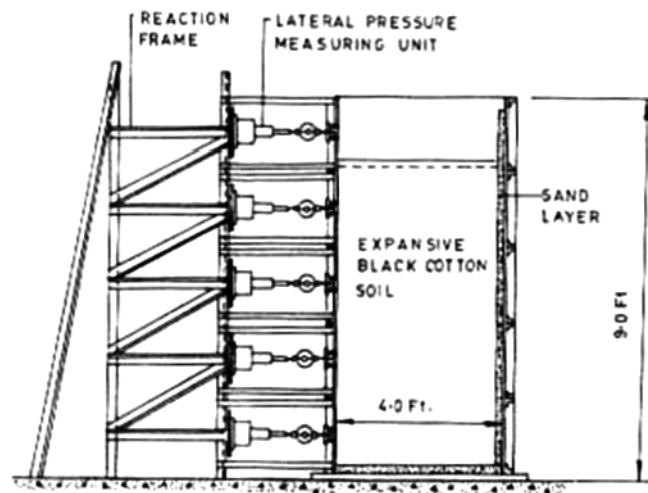


Figure 2. 62 Tank and Reaction Frame of Large Scale Laboratory Set-Up  
(Joshi and Katti, 1984)

Similarly, for the compacted saturated condition of the sand and the CNS, a linear relationship of lateral pressure with depth was observed. Compacted saturated expansive clay materials, however, exhibited a completely different behavior, with the lateral pressures against the wall increasing rapidly with depth to about 1.5 m, then at a milder rate below that depth. Although the sum of the lateral pressures generated by the buoyant weight of soil, the water and the compaction loads only amount to about 19 kPa at 1.5 m depth., the lateral pressures developed were measured to be about 230 kPa, the difference in between coming from the lateral swell pressure generated by the absorption of water by the clay minerals. The results of this test are presented in Figure 2.63 whereas Type 2 test results with CNS inserted between the wall and the expansive clay fill is presented in Figure 2.64. As it can be seen from the figure, lateral swell pressures applied to the back of the wall were decreased as the thicknesses of non-expansive backfill placed between the wall face and the expansive backfill increased (Katti et al., 1983).

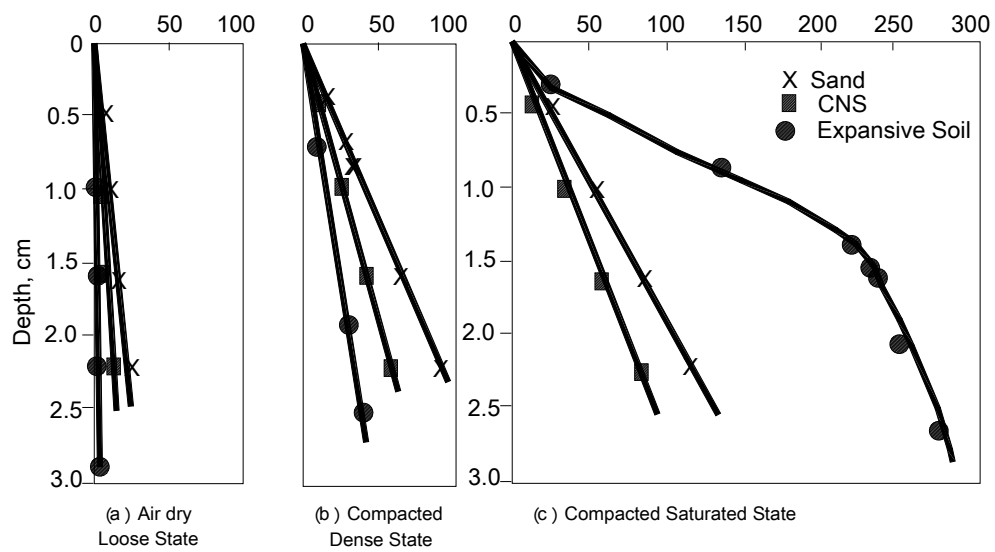


Figure 2. 63 Lateral Pressure Development versus Depth (a) Dry Loose State (b) Compacted State (c) Compacted Saturated State (After Katti et al., 1983)

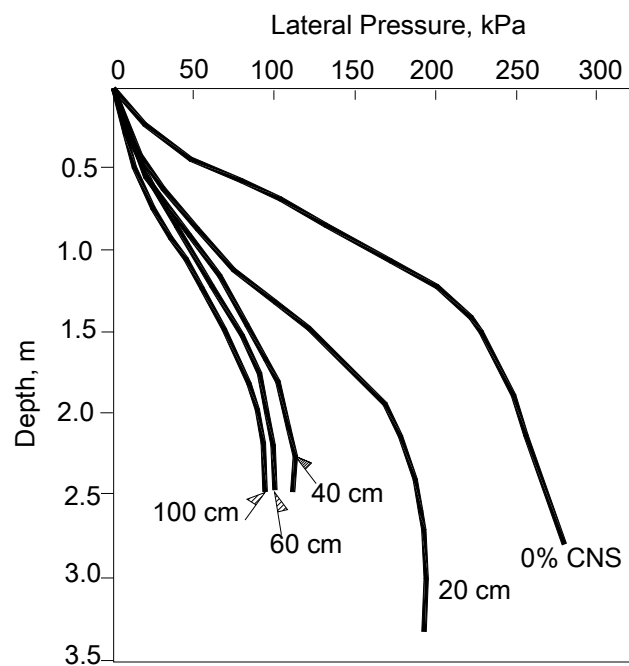


Figure 2. 64 Lateral Swell Pressure vs. Depth for Different Thicknesses of CNS (Katti et al., 1983)

Later, Joshi and Katti (1984) used the same set-up to examine the lateral swell pressures of expansive soils having different properties; although in this research, the dimensions of tank was reduced a little bit compared to the former one (Katti et al., 1983). The test set up had lateral pressure measuring units at various depths.

Joshi and Katti (1984) compacted the soil in 14 layers of 25.4 mm thickness at a void ratio of unity in the container tank and surcharge was applied. Then, the soil was saturated and the lateral pressure as well as the vertical movement was recorded at regular time intervals until the moisture level attained the equilibrium state. The experiments involved stepwise reduction of the surcharge and waiting for the system to reach to another state of equilibrium. In all phases, the lateral swelling pressure increased rapidly at the beginning of the saturation process, with the rate of increase slowing down in time up to the point where the lateral swelling pressure reached a peak value. With further increase in time, lateral swelling pressure decreased to some extent and then remained constant. This behaviour was similar to the behaviour observed from the previous investigations of different researchers. The lateral pressure versus time curve observed from this investigation is presented in Figure 2.65.

Evaluating the results obtained from these tests, Moza and Sudhindra (1987) developed an empirical relation for the lateral swell pressure at rest condition;

$$P = \frac{q_{sw} \cdot \frac{d}{d_0}}{\left( a + 0.6 \frac{d}{d_0} \right)} \dots\dots\dots (2.5)$$

where            P : Lateral Swell Pressure Corresponding to Depth d (kPa),  
                      d : Depth (cm),  
                      d<sub>0</sub> : Unit Depth (cm),  
                      q<sub>sw</sub> : Vertical Swell Pressure (kPa), and  
                      a : % Clay Content (<2µm)

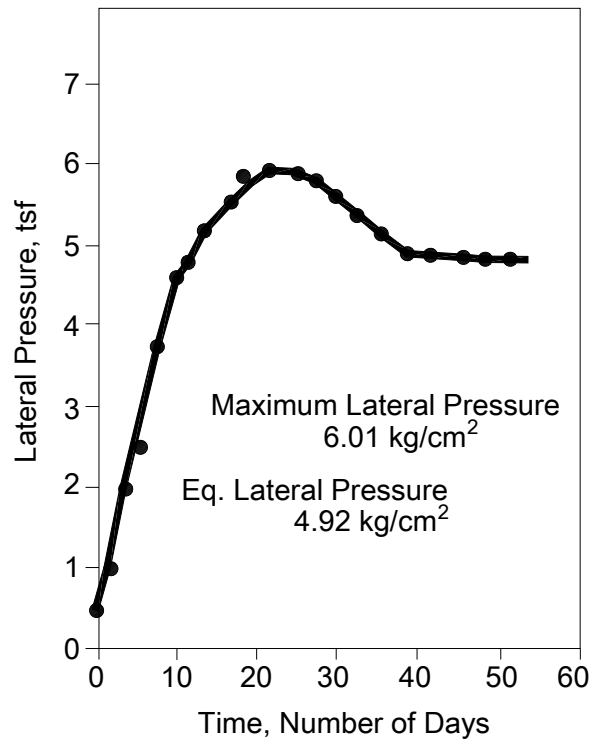


Figure 2. 65 Development of Lateral Pressure with Time (Joshi and Katti, 1984)

Aytekin et al. (1993) used the data from Katti et al. (1983) and performed a research to develop a finite element model to simulate the observed results. The named attempt used the soil parameters and suction relations that were previously proposed by McKeen (1977, 1980). The match between the obtained results with the ones shown in the original research was satisfactory. The authors noted that even very small lateral wall displacements resulted in a very large relief of lateral swelling pressure. They further emphasized the importance of the suction parameter in the numerical model, which was a function of the bulk clay content and mineralogy.

## 2.6 COMMONLY USED REHABILITATION METHODS

Expansive soils are a worldwide problem, particularly in arid and semi-arid regions, where evaporation rates are higher than the annual rainfall causing a moisture deficiency in the soil most of the time. Semi-arid regions are characterized by short periods of rainfall followed by long periods of draught, which in turn leads to volumetric changes in the soil, or namely cyclic swelling and shrinkage. It has been reported by Gourley et al. (1993) that the resulting ground movement gives rise to serious damage to civil engineering structures for which the cost of repair per annum is estimated as many billion dollars globally.

The hazards caused by expansive soils have been recorded in a diverse geography including countries like America, Australia, Canada, India, Israel, Iran, Mexico and South Africa (Chen, 1988). Hence, modern engineering practice is trying to offset the problems through innovative foundation techniques. Such techniques have been grouped into the following categories by various authors including but not limited to Satyanarayana (1966), Katti (1978), Chen (1988), Phanikumar and Sharma (2006), Rao and Rao (2008), Subbarao et al. (2011).

- **Deep Foundation Techniques:** The foundation is constructed to rest at a layer deeper than the active zone of the expansive clays to compensate volume changes due to seasonal moisture variations.
- **Under-Reamed Pile Foundations:** They are piles with bulbs provided in the inactive zone to achieve adequate anchorage.
- **Granular Pile Anchor Foundations (GPAF):** A steel rod is centrally placed in the granular pile, and is anchored to a mild steel anchor plate at the bottom to help the granular medium to resist the tensile uplift force during swelling. The frictional resistance at the soil-pile interface is found to be effective in counteracting the heave for a definite diameter around the pile.
- **Chemical Stabilization:** The theory of chemical stabilization is mainly built on alteration of the physical and chemical structure of the clay particles by the addition of chemicals such as lime or cement. Thus, the



water requirement of clay is decreased and water in and out of the system obscured.

- **Industrial Wastes Used as Additives:** There exists extensive research on the utilization of industrial wastes (e.g. fly-ash, rice husk ash, quarry dust, copper slag etc.) to overcome the swell-shrink behavior of expansive soils. The procedure also aims at the problematic disposal of such wastes.
- **Utilization of Fibers as Reinforcement:** Different fibers ranging from grated rubber tires to geogrids have been successfully used for stabilizing expansive soils.
- **Mechanical Alteration:** In places where the depth of the active zone, i.e. the depth to which seasonal moisture differences can reach, is feasibly shallow enough, the active zone is excavated to be replaced by a non-expansive layer. Most popular applications for mechanical alteration are the “sand cushion” technique and the “cohesive non-swelling soil” technique, although many variations have been developed to overcome the inadequacies implied by these methods.

Each of the methods listed above comes with a number of superiorities as well as limitations or shortcomings, when compared to the other processes. The following section summarizes previous research conducted on various stabilization techniques on expansive soils, concentrating on the advantages and disadvantages as defined by the researchers. Some of the investigation programs listed focuses on only one method, while others entail a combination, comparison or modification of various techniques.

### **2.6.1 Granular Pile Anchors**

Until the last two decades the use of granular piles, as an improvement technique for clays, have been restricted to non-swelling soft clay deposits as the tensile uplift force exerted by an expansive soil cannot be resisted by an ordinary

granular column, which is a particulate medium in nature. The theory behind the recently developed granular pile anchor foundation (GPAF) system, on the other hand, rests on the fact that the granular pile becomes tension resistant by the effect of the steel rod inside, anchored to the bottom of the pile, thus giving the pile ability to impede the upward heave.

Model studies on granular pile anchors conducted by Phanikumar et al. (2004) and re-summarized in Phanikumar and Sharma (2006) demonstrated the effectiveness of GPAF as a valuable method for the stabilization of expansive clays. In this laboratory program, totally 81 heave tests were conducted on the expansive clay bed reinforced with granular pile anchors in a specially designed experimental set-up (Figure 2.66). The test program involved the comparison of the rate and extent of heave of the original expansive clay sample having different initial dry unit weights ( $\gamma_d$ ), namely 13-14 and 15 kN/m<sup>3</sup>, with the results obtained for the clay bed reinforced with the granular piles. In addition, the effect of spacing of granular anchors was tested using two granular anchors at different spacing, and the resulting heave was compared with the test outcomes of single granular pile anchor. Furthermore, the effect of relative density of the granular material used in the pile anchor was investigated. Finally, the influence zone of the granular pile anchor in terms of radial distance from the center of the pile was also evaluated.

Main conclusions derived from the study are listed below and summarized in Table 2.16:

- Upon the installation of the GPAF system, the duration to attain the final heave decreased considerably – namely to one third, mainly due to the higher hydraulic conductivity of the granular material.
- Increasing the diameter of the granular pile ( $D_p$ ) for a given pile length ( $L_p$ ) or increasing the length of the pile for a given diameter resulted in a decrease in heave. This outcome can be accredited to the increased frictional resistance counteracting the uplift at the GPAF boundary. The

maximum reduction attained in the heave of the clay bed at the end of the test program was 96%.

- Another consequence that can be attributed to the effect of frictional resistance is that, an increase in the relative density of the granular material ( $d_r$ ) used for the pile system decreased the resulting heave.
- Percent heave increased with increasing radial distance from the center of a single pile, while for a given radial distance, it decreased with decreasing inter-pile spacing.

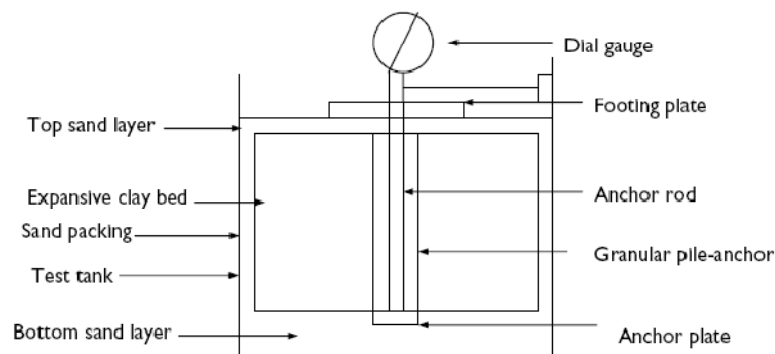


Figure 2. 66 Experimental Setup for GPAF System (Phanikumar et al., 2004)

Table 2. 16 % Heave of Expansive Clay Bed Reinforced by Granular Pile Anchors (Phanikumar et al., 2004)

$d_r$	0.50			0.60			0.70		
	$D_p(\text{mm})$			$D_p(\text{mm})$			$D_p(\text{mm})$		
	30	40	50	30	40	50	30	40	50
$L_p(\text{m})$	(a) %Heave for $\gamma_d = 13 \text{ kN/m}^3$ and $w_i = 14\%$ (Original % heave = 6 %)								
0.30	1.26	0.95	0.73	1.15	0.82	0.60	1.04	0.70	0.48
0.40	1.08	0.78	0.63	0.95	0.65	0.50	0.82	0.52	0.38
0.50	0.87	0.65	0.50	0.75	0.52	0.38	0.62	0.40	0.25
	(b) %Heave for $\gamma_d = 14 \text{ kN/m}^3$ and $w_i = 14\%$ (Original % heave = 9 %)								
0.30	1.75	1.25	0.92	1.60	1.15	0.87	1.44	1.04	0.80
0.40	1.52	1.12	0.86	1.41	1.04	0.80	1.30	0.96	0.72
0.50	1.35	1.00	0.81	1.24	0.94	0.76	1.14	0.82	0.62
	(c) %Heave for $\gamma_d = 15 \text{ kN/m}^3$ and $w_i = 14\%$ (Original % heave = 14 %)								
0.30	2.25	1.70	1.35	2.10	1.60	1.25	1.98	1.50	1.15
0.40	1.95	1.45	1.16	1.82	1.35	1.05	1.70	1.26	0.95
0.50	1.65	1.20	0.95	1.55	1.10	0.85	1.45	1.00	0.75

Similar innovative methods, mainly based on mobilizing a counteracting force against heave in the expansive soil bed, have been developed by Al-Omari and Hamodi (1991) in their study called “swelling resistant geogrid” – or simply “geopile”. This method was later matured by Sharma and Phanikumar (2005) who used different granular fill materials in the geopiles to achieve a relatively better resistance to heave than it can be accomplished via the geogrid apertures.

For their test program, Al-Omari and Hamodi (1991) used an enlarged oedometer apparatus with a mould 85 mm in height and 110 mm in diameter. As the reinforcement, a geogrid sheet was rolled to form a cylinder 75 mm in height and 70 mm in diameter, and placed inside the mould. To evaluate the effect of reinforcement on swelling potential, a kaolinite with plasticity index ( $I_p$ ) of 9 % and a bentonite with an  $I_p$  of 230% were mixed in various ratios to obtain soil samples with different plasticity indices. The stiffness of the reinforcing geogrid was another variable in the test schedule, as well as the amount of surcharge applied. Considerable reduction up to 51% that increased with increasing geogrid stiffness was obtained at the end of the experiments. Figure 2.67 gives a schematic representation of the utilization of geopiles in practice as proposed by Al-Omari and Hamodi (1991), whereas the results yielded by the test program are given in Table 2.17. The authors calculated the improvement factor (IF) as:

$$IF = \frac{W_{(u)} - W_r}{W_u} \dots\dots\dots(2.6)$$

where,

$W_{(u)}$  = final swell of unreinforced sample,

$W_{(r)}$  = final swell of the corresponding reinforced sample

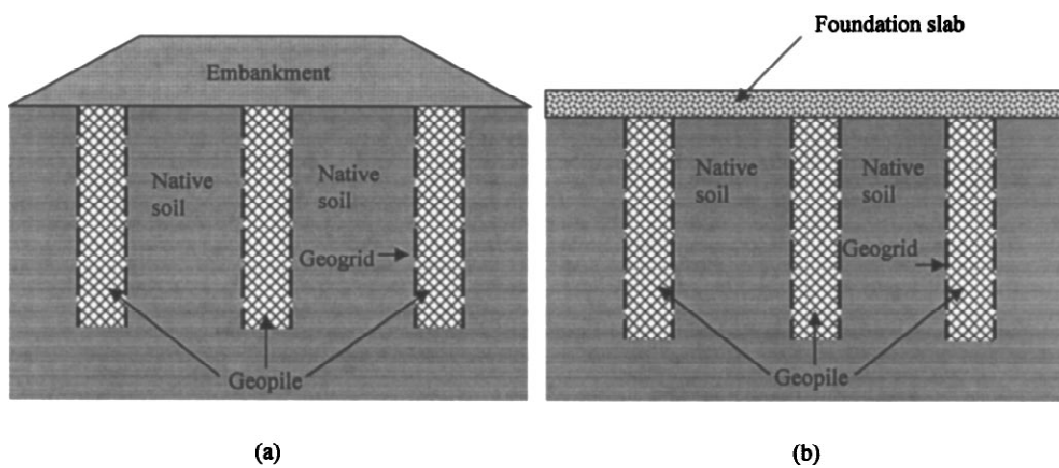


Figure 2. 67 Geopiles for Embankment and Building Foundations (Al-Omari and Hamodi, 1991)

Table 2. 17 Improvement Factors for Different Oedometer Tests (Al-Omari and Hamodi, 1991)

$I_p(\%)$	$\Upsilon_d (\text{kN/m}^3)$	Surcharge	Geogrid Stiffness ( $\text{kN/m}$ )	IF (%)
47	13	$50 \text{ kN/m}^2$	240	25
41	15	$7 \text{ kN/m}^2$	240	28
		$100 \text{ kN/m}^2$		32
		$50 \text{ kN/m}^2$		23
41	15	$50 \text{ kN/m}^2$	500	36
115	14	$7 \text{ kN/m}^2$	240	21
			500	39
			740	44
115	14	$50 \text{ kN/m}^2$	120	17
			240	22
			500	39
			740	42
115	14	$100 \text{ kN/m}^2$	240	23
115	14	$150 \text{ kN/m}^2$	240	34

According to Sharma and Phanikumar (2005), the presentations of Al-Omari and Hamodi (1991) involved some shortfalls, i.e;

- the study only focused on a single geopile, and did not mention any group effect mentioned,
- only a single length/diameter ratio was analyzed on the single geopile,
- the program did not consider the use of granular fill inside the geopiles, which would have certainly increase the skin friction to resist the heave, as well as increasing the hydraulic conductivity of the whole system, thus enhancing adaptation to moisture variations.

Sharma and Phanikumar (2005) conducted a total of 26 heave tests to compare the percent heave of a clay bed in unreinforced as well as in reinforced conditions, where the named reinforcement consists of geopiles of biaxial geogrids filled with different granular materials, such as fine sand, coarse sand and gravel. Tests were repeated for geopile with expansive clay fill also, to compare the results with the Al-Omari and Hamodi (1991) outcomes. In all of the tests, the depth of the clay bed as well as the length of the geopile was 100 mm; however, various diameters of geopiles , i.e. 40, 50 and 60 mm were utilized to visualize the effect of length to diameter ( $l/d$ ) ratio. The impact of geopile spacing on heave characteristics were displayed via pile group tests conducted on two and four geopiles. The experimental set-up used in the tests is presented in Figure 2.68.

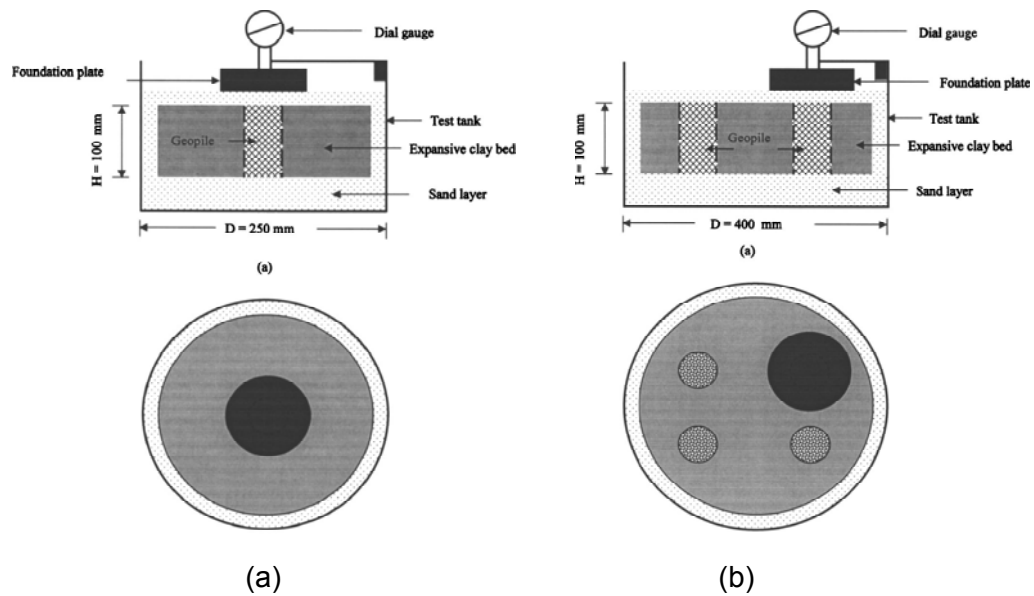


Figure 2. 68 Experimental Set-up for (a) Single and (b) Group Geopiles  
(Sharma and Phanikumar, 2005)

The effects of geopile diameter and fill material type are given in Table 2.18, whereas Table 2.19 lists the effect of spacing between two piles with respect to fill material type, where the pile diameter is fixed at 50 mm. The following conclusions can be made from the tabulated data:

- The results of tests conducted with geopiles only (expansive clay fill, no granular material) are consistent with the findings of Al-Omari and Hamodi (1991). For larger diameters of the geopile, lower values of heave were attained. Geopile reinforcement also increased the rate of heave
- The coarser the fill material was the more effective was the reinforcement in heave prevention.
- Amount of heave was found to be inversely related with the number of geopiles in the system. However, % heave increased by increasing the spacing between the piles, and for spacing exceeding 4 times the pile diameter ( $4d$ ), the effect from a second pile became negligible.

Table 2. 18 The Effect of Geopile Diameter and Fill Material Characteristics on % Heave (Sharma and Phanikumar, 2005)

Diameter (mm)	Clay		Fine Sand		Coarse Sand		Gravel	
	S' (%)	S <sub>R</sub> (%)	S' (%)	S <sub>R</sub> (%)	S' (%)	S <sub>R</sub> (%)	S' (%)	S <sub>R</sub> (%)
40	25.00	34	17.00	55	14.50	62	11.00	71
50	23.60	38	15.40	60	13.00	66	10.20	73
60	22.40	41	13.00	66	11.00	76	8.00	80

where;

S': Final heave

S<sub>R</sub>:Percent reduction in heave with respect to the original heave of untreated clay bed (S<sub>i</sub>=38%)

Table 2. 19 The Effect of Spacing between Two Piles with respect to Fill Material Type (d= 50 mm) (Sharma and Phanikumar, 2005)

Spacing s (mm)	Clay		Fine Sand		Coarse Sand		Gravel	
	S' (%)	S <sub>R</sub> (%)	S' (%)	S <sub>R</sub> (%)	S' (%)	S <sub>R</sub> (%)	S' (%)	S <sub>R</sub> (%)
100 (2d)	19.00	50	12.00	68	10.00	74	7.00	82
150 (3d)	21.40	44	14.50	62	12.00	68	9.00	76
200 (4d)	36.60	38	15.40	59	13.00	66	10.20	74

where;

S': Final heave

S<sub>R</sub>:Percent reduction in heave with respect to the original heave of untreated clay bed (S<sub>i</sub>=38%)

d: Geopile diameter (50 mm)

One major problem that is frequently encountered during the installation of granular pile anchors is defined as bulging, which is simply the loss of the granular material into the surrounding clay bed, especially in soils with  $c_u$  less than 10 kPa (Phanikumar and Rao, 2000). Jacketing the whole column with a



geosynthetic liner was a method proposed by Alamgir (1989) as well as Adayat and Hanna (1991), which proved to guarantee better functioning even in severe soil conditions.

A posterior investigation led by Phanikumar and Rao (2000), however, proposed the use of a bottom geotextile or geogrid above the anchor plate, to mobilize a supplementary frictional resistance. The experimental set-up used in this study is given in Figure 2.69. Tests were repeated for non-reinforced and reinforced granular pile anchors, where the two types of base geosynthetics (a nonwoven geotextile with a thickness of 0.5 mm and b. a polymer high-density (HD) geogrid with an aperture size of 6 mm x 6 mm), were used to evaluate the effect of stiffness of the base reinforcement material. The granular fill material for the piles consisted of 80% of coarse sand ( $2.4 \text{ mm} < d_{\text{sand}} < 4.8 \text{ mm}$ ) and 20% of metal chips ( $6 \text{ mm} < d_{\text{chips}} < 10 \text{ mm}$ ) compacted at a relative density of 0.60.

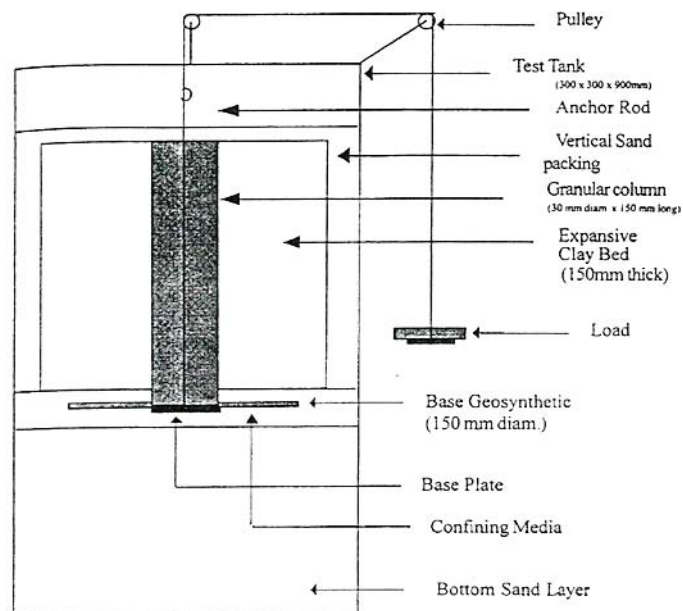


Figure 2. 69 Experimental Setup for GPAF System with Base Geosynthetics (Phanikumar and Rao, 2000)

The layer in which the geosynthetic is positioned (namely the “confining media” as given in Figure 2.69) were altered for the tests such that:

- |                       |  |
|-----------------------|--|
| Geotextile in between | (i) expansive clay and bottom sand layer,<br>(ii) fine sand ( $d_{\text{sand}} < 2.36 \text{ mm}$ ),<br>(iii) coarse sand ( $2.36 \text{ mm} < d_{\text{sand}} < 4.8 \text{ mm}$ ),<br>(iv) metal chips ( $6 \text{ mm} < d_{\text{chips}} < 10 \text{ mm}$ ), |
|-----------------------|--|

and,

- |                    |   |
|--------------------|---|
| Geogrid in between | (v) fine sand ( $d_{\text{sand}} < 2.36 \text{ mm}$ )<br>(vi) coarse sand ( $2.36 \text{ mm} < d_{\text{sand}} < 4.8 \text{ mm}$ )<br>(vii) metal chips ( $6 \text{ mm} < d_{\text{chips}} < 10 \text{ mm}$ ) |
|--------------------|---|

The uplift capacity of a single unreinforced granular pile at failure was defined to be around 45 N, and the interface friction angles for the combination of materials were determined through direct shear tests. The test results, showing the interface friction angles and the improvement of pile uplift capacity via the use of base geosynthetics are given in Table 2.19.

Table 2.20 yielded the following main conclusions:

- The application of base geosynthetics increases the pull-out resistance of granular pile anchors. The increase is more pronounced with the use of geogrids than geotextiles, therefore it can be concluded that the improvement is due to the friction between the geosynthetic and the confining medium.
- The greater the particle sizes of the confining medium, the higher the pull-out resistance.

Table 2. 20 Test Results – GPAF with Base Geosynthetics (Phanikumar and Rao, 2000)

Uplift Capacity of Granular Pile Anchor Alone (N)	Granular Pile Anchor with Base Geosynthetic			Increase in Uplift Capacity	
	Interface	Interface Friction Angle ( $^{\circ}$ )	Uplift Capacity (N)	N	%
45.45	Sand-geotextile-clay	18	109.09	63.64	140
45.45	Fine sand-geotextile-fine sand	22	144.54	99.09	218
45.45	Coarse sand-geotextile-coarse sand	35	166.44	120.99	266
45.45	Metal chips-geotextile-metal chips	40	162.06	116.61	257
45.45	Fine sand-geogrid-fine sand	26	212.00	166.55	366
45.45	Coarse sand-geogrid-coarse sand	44	245.00	199.84	438
45.45	Metal chips-geogrid-metal chips	46	267.20	221.75	488

### 2.6.2 Stabilization by Chemicals and Industrial Wastes

Chemical stabilization aims at the alteration of engineering properties of expansive soils by the utilization of additives. The most commonly used additives are Portland cement and lime and the benefits are well documented. Lime stabilization causes a reduction in plasticity index, the liquid limit, the swelling pressure, while enhancing strength and durability. Similar outcomes are offered via the addition of cement to expansive soils, in which the modification is a result of formation of cementitious bonds between calcium silicate, the aluminate hydration products and the soil particles (Nalbantoğlu, 2006; Stavridakis, 2006).

Other agents such as calcium chloride ( $\text{CaCl}_2$ ), gypsum, commercial acrylic resins, and industrial wastes with high pozzolanic value such as fly ash, rice husk ash, cereal fly ash, coal bottom ash, steel fly ash, aluminate filler and granulated blast furnace slag have also been tested and documented by various authors (Seco et al., 2011; Bhyravavajhala, 2000; Koteswara et al., 2011(a) and Koteswara et al. 2011(b); Anagnostopoulos, 2006; Muntohar, 2006; Turker et al., 2006 and Subbarao et al., 2011). Specifically, the utilization of industrial wastes

with cementitious worth for soil stabilization is beneficial from the viewpoints of environmental and economic consideration as they offer sustainability as well as cost effectiveness. However, there is evidence that in addition to the above mentioned materials, lime is still needed in the system as an accelerator for the Calcium-Silicate-Hydrate reactions to take place (Subbarao et al, 2011, Koteswara et al. 2011(a) and Seco et al., 2011).

The methods of in-situ lime stabilization of clayey soils are (i) shallow mixing and compacting and (ii) deep mixing. Shallow mixing falls short in meeting the stabilization requirements of thick layers of swelling soils, therefore, deep stabilization via lime columns, lime piles and lime slurry injections have frequently be used in practice.

As defined by Venkataswamy et al. (2003), lime columns with diameters up to 0.5 meters and lengths up to 10 meters are formed by mixing quick lime and clay in-situ to yield a material having enhanced shear strength parameters. In lime piles, however, the holes in ground are filled with lime. The lime piles maintain stabilization via clay dehydration and lime modification reactions. Finally, the lime slurry injections drive slurry into the soil texture by pressure. In deep mixing, lime migration is the main cause of stabilization. The mechanism involves the immigration of lime from the piles or columns to the surrounding soil, thus stabilizing the vicinity. However, the low permeability of clayey soils may somehow inhibit the effective distance of this migration process (Tonoz et al., 2006).

Venkataswamy et al. (2003) studied the effectiveness of lime migration on an in-situ set-up consisting on a borehole (diameter=150 mm) filled with a mixture of lime and sand. In contrary with the available literature which proposes the use of lime only, the authors preferred to use lime and sand in equal weight ratios to achieve better workability. Undisturbed samples were collected at varying depths and radial distances of the pile. The following outcomes were reached:

- Despite of using a half-and-half mixture of sand and lime instead of pure lime, the lime migration was observed up to a radial distance of 750 mm, although diffusion clearly decreased with increasing radial distance.
- Undisturbed samples are tested and an increase of unconfined compressive stress was observed, as well as a marked reduction in swelling pressure and plasticity index as a result of pozzolanic activity.
- The authors concluded that the radial diffusion was not a function of overburden pressure, as the improvement factors did not differ significantly for samples collected at depths of 3.5 m, 4.5 m and 5.5m.

The results of a more detailed study for lime columns in expansive clays were presented by Tono et al. (2003) and Tono et al. (2006). Laboratory tests were conducted on five sample blocks taken from a particular site, in which holes to form lime columns are drilled by hand augers. All necessary precautions were taken to mimic on-site lime column construction in laboratory conditions. Figure 2.70 shows the placement of group of 2 cm lime columns in sample blocks. Single columns of 4.8 cm diameter constituted another segment of the test program. At the end of the curing time necessary for development of mitigation, samples were extracted from the sample blocks at varying radial distances from the lime columns as given in Figure 2.71.

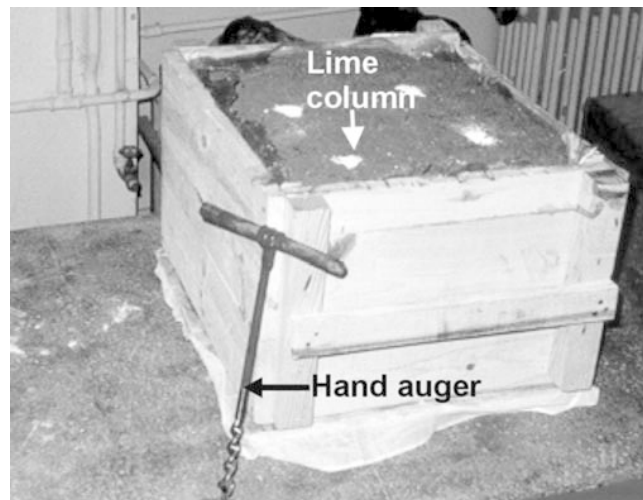


Figure 2. 70 Pattern of Lime Columns of 2 cm Diameter Constructed in the Block Clay Sample (Tonoz et al., 2003)

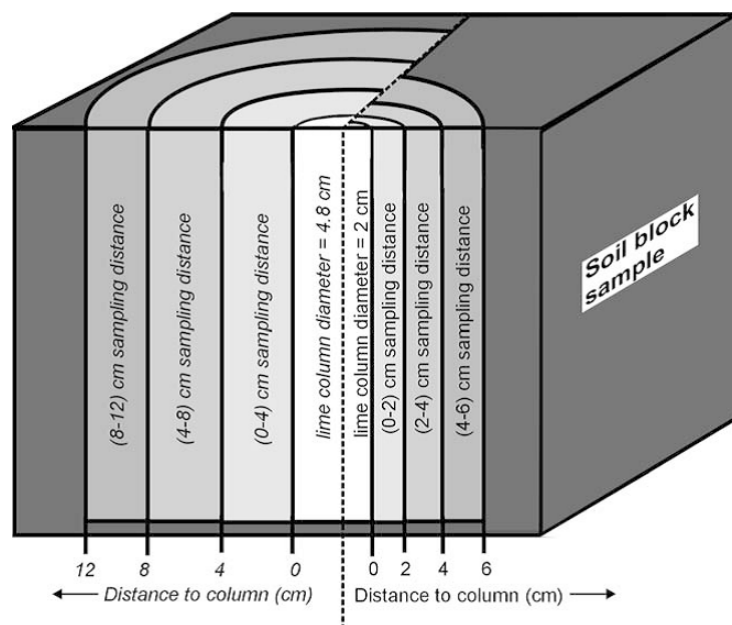


Figure 2. 71 Section from the Block Illustrating Sampling Distances from Lime Columns(Tonoz et al., 2003)

The lime columns led to a considerable reduction between 40-75% in swell pressure. The percentage variation in swelling pressure (VSP) of the soil was obtained using the following expression, where  $SP_T$  and  $SP_N$  consequently stand for “treated swell pressure” and “natural swell pressure”.

$$VSP(\%) = \frac{SP_T - SP_N}{SP_N} \times 100 \dots \dots \dots (2.7)$$

The swelling pressure values for the natural and corresponding treated samples are listed in Table 2.21. It is also noteworthy that the utmost reduction of swell pressure was observed at the point where the distance to the column was equal to the diameter of the column; whereas the swelling pressure had an increasing trend as the sampling distance was increased.

Table 2. 21 Values of Swelling Pressure in Terms of Distance to Column (Tono et al., 2003)

Lime column diameter : 2 cm					Lime column diameter : 4.8 cm				
Sample no.	Swelling Pressure (N/cm <sup>2</sup> )				Sample no.	Swelling Pressure (N/cm <sup>2</sup> )			
	Distance to Column					Distance to Column			
	Natural	0-2 cm	2-4 cm	4-6 cm		Natural	0-2 cm	2-4 cm	4-6 cm
S1	59.0	17.0	35.0	50.8	S2	25.0	14.0	15.2	23.0
S3	40.0	25.0	37.7	40.0	S5	26.0	20.0	23.3	25.2
S4	96.0	62.4	84.5	90.7					

### 2.6.3 Mechanical Alteration and the Cushion Technique

The very popular sand cushion technique involves the complete or partial replacement of the expansive soil stratum with a sand cushion, which is generally compacted to a low relative density to provide minimal volumetric change due to the wetting and drying cycles. However, as portrayed by Rao and Rao (2008),

the common procedure is to use an approximate thickness and density for the sand cushion. Therefore, the chances are high that the low relative density may result in bearing capacity problems, whereas the selected thickness - especially when inadequate - worsen the problem as the highly permeable sand allows surface run-off into the soil and facilitates the swelling process.

The test program conducted by Elhady (2007) intended to depict the effect of modifying the sand cushion to overcome its possible drawbacks and to compare the results with the ordinary chemical stabilization. The parameters tested were the effect of lime content and the particle size of the sand cushion as well as the lime percentage used for the chemical stabilization. The research was performed on an oedometer test apparatus and a large scale one dimensional test set-up. The test program is summarized in Table 2.22. The results of chemical stabilization are far beyond the scope of this study but the results of modified sand cushion test program are presented Table 2.23, from which the following conclusions may be reached (Elhady, 2007):

- Increasing the lime content yielded a more pronounced effect for medium sand than for the fine sand.
- For a lime content of 5%, the particle size of the sand cushion had no considerable impact on swelling potential.
- The minimum swelling potential was attained at a lime content of 5% for the oedometer test, and 20% for the large scale laboratory test.
- 5% of lime content decreased the swelling pressure of the fine sand cushion by 70% in the oedometer test apparatus.
- For 100% lime content, the swelling pressure for the large scale test decreased by 50%.



Table 2. 22 Test Program (adapted from Elhady, 2007)

Group No.	Study Factor	Test Type	Soil Type	Clay Content (%)	Sand Cushion Particle Size	Lime Content (%)
1	Untreated Expansive Soil	Oedometer	A	75	N/A	N/A
			B	44		
			C	50		
		Laboratory Model	A	75		
2	Treated Expansive Soil by Sand-Lime Cushion	Oedometer	A	75	Medium Sand	0,5,10,15, 25 and 100
			B	44		
			C	50		
		Laboratory Model	A	75		0,5,10,20 and 100
3	Treated Expansive Soil by Sand-Lime	Oedometer	A	75	Fine Sand	0,5,10,15 and 25
4	Treated Expansive Soil Lime Mix	Oedometer	A	75	N/A	5,10,15 and 20
			B	44		
			C	50		
		Laboratory Model	A	75		

Table 2. 23 Results for Sand-Lime Cushion (adapted from Elhady, 2007)

Property of Soil	Type of Test	Type of Soil	Sand Cushion	Lime Content of Sand Cushion (%)									
				0	0	5	10	15	20	25	100		
Swelling Potential (%)	Oedometer	A	Untreated	23.86									
			Medium Sand		15.86	12.86	12.86	13.73		15.35	14.02		
			Fine Sand		12.45	12.67	17.52	16.97		16.5			
		B	Untreated	23.24									
			Medium Sand		14.67	14.5	15.62	13.42		15.6	12.2		
			Untreated	19.13									
		C	Medium Sand		14.52	12.83	14.94	12.33		11.24	14.6		
			Laboratory Model	A	Untreated	24							
					Medium Sand		13.55	13.22	14.4		12		12.42
	Swelling Pressure (kg/cm <sup>2</sup> )	Oedometer	A	Untreated	13.5								
Medium Sand					10.9	9.7	7.65	9		7	9		
Fine Sand					7.3	4.2	12	10		11.5			
B			Untreated	20									
			Medium Sand		17	17	15	15.8		22.9	15		
			Untreated	15									
C			Medium Sand		12.6	8	15.8	8.4		8	9		
			Laboratory Model	A	Untreated	63.82							
					Medium Sand		49	44	54.8		53		30

Another popular cushioning technique, namely the cohesive non-swelling soil or CNS in short, has been explained in detail by Katti (1979). Based on vast experience from field practice supported by considerable laboratory data, the author recommended CNS specifications, which are summarized in Table 2.24.

The theory behind the CNS phenomenon was later on resummarized by Katti and Katti (2008). The authors reminded that highly swelling soils, with swell pressures around  $30 \text{ t/m}^2$  to  $150 \text{ t/m}^2$  and heave potential from 10 cm to more than 30 cm, surprisingly presented no volume change up to a depth of 1 to 1.5 m from the surface when exposed to water.

The ability of the expansive soils to demonstrate two very dissimilar characteristics i.e., (i) swelling and (ii) non-swelling zones within the same deposit, led the authors to assume that adequate Columbian (electrical) forces should also be present in the system to support the  $1.2 \text{ t/m}^2 - 2.5 \text{ t/m}^2$  Newtonian (gravitational) overburden load near to the surface of the expansive soil. It is known that, the three layer expanding lattice montmorillonite clay possess a high level of electrical charge deficiency, which can be observed in-between its layers, external surfaces and borders. This high ion exchange capacity is in turn responsible for the inter layer swelling character of the soil as well as the ability to develop external cohesive bonds to resist swelling at shallow overburden thicknesses. It has been determined that the internal and the external electrical fields are nearly of the same magnitude. According to Katti and Katti (2008), by keeping the same degree of the Newtonian (gravitational) and Coulombian (electrical) forces present in the system, a non-expanding material can be used to form a small thickness of a CNS layer to overcome heave. The authors also proposed the following methods for CNS layer creation:

- Chemical treatment of expansive soils
- Utilization of well graded silt material having fine capillarity of 2 to 5 microns
- Utilization of electrically charged coating films

Table 2. 24 Specifications for CNS Soil (Katti, 1979)

SI No	Properties	Specifications range
1	Grain size analysis Clay ( $<0.002$ mm) in % Silt (0.002–0.075 mm) in % Sand (0.075–4.75 mm) in % Gravel (4.75–80 mm) in %	15–25 30–45 30–40 10
2	Consistency Limits Liquid limit, % Plastic limit, % Plasticity Index, % Shrinkage limit, %	30–50 20–25 10–25 15 and above
3	(a) Swelling pressure when compacted to standard Proctor maximum dry density at no (b) Swelling Pressure when compacted to standard Proctor optimum conditions at no	Less than 10 Less than 5
4	Clay minerals	Preferably kaolinite and illite
5	Shear Strength of samples compacted to standard Proctor optimum conditions, after saturation (a) $1/2$ UCS (kPa) (b) Consolidated direct shear test @ 0.0125 $c_u$ (kPa) $\phi_u$ (deg)	15–35 10–30 8–15
6	Approximate thickness of CNS layer for swelling pressure (kPa) 100–150 200–300 350–500	Thickness in meter 0.75–0.85 0.90–1.00 1.05–1.15

As a matter of fact, it is possible to use pure clay consisting only from non-expanding clay minerals to form a CNS layer. However, in addition to adequate cohesion to maintain the Coulombian requirements and to keep the thickness of the CNS layer at a feasible level; a CNS layer must also hold optimal shear strength and bearing capacity properties. As the Coulombian requirements enforce the CNS layer to contain a significant amount of fine particles to provide

enough cohesion, it is natural that the bearing capacity of the no volume change zone is much higher than that of the CNS layer itself (Katti et al., 2002). Since saturated soils lose strength when wetted, the foundation sitting on the CNS layer may fail under progressive saturation. There is also evidence that the CNS cushion loses efficiency after the first cyclic swelling and shrinkage; and heave becomes inevitable. Hence, it was recommended by Katti and Katti (1996) to use a Mechanically Stabilized Mix (MSM) cushion in the foundation system, the details of which are given in Figure 2.72.

The MSM, which has a granular nature, is used as an intercepting cushion below the footing but above the CNS. Usually a mix design is prepared to decide on the thickness of the MSM and it is very common to make use of Fuller's curves to determine the required particle size ratios. According to past experience, the establishment of a MSM layer above the CNS is beneficial in bearing capacity improvement however the construction cost is increased in return (Rao et al., 2008).

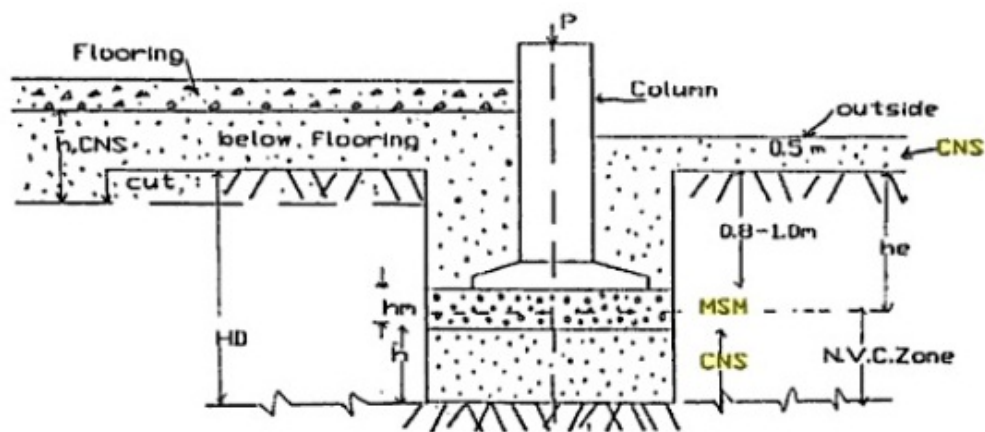


Figure 2. 72 Shallow Foundation with CNS and MSM Intercepting Layers (Katti et al., 2002)

## **CHAPTER III**

### **TEST APPARATUS**

#### **3.1 GENERAL**

While swell parameters can be estimated to some extent by using indirect methods including empirical correlations sensitive to site specific conditions, more rational values can be obtained by estimating them with laboratory and large scale tests developed for this particular purpose. The assessment of swell parameters reflecting the actual site conditions requires utilization of advanced stress and strain controlled testing techniques that properly fit the real behaviour that eliminates the effects of several constraints such as in-situ loading conditions. Compared to other test methods, hydraulic triaxial test apparatus is the most promising testing technique, despite its weaknesses in modeling the large scale in-situ behaviour which is in fact the major drawback for all laboratory test methods. On the other hand, unavailability of this apparatus in most of the laboratories due to the high investment cost and its time consuming nature, which needs almost a month for the execution of a single test, makes its use debatable in research activities which require sufficient number of data for the statistical reliability and the development of well-defined correlations.

Under the above mentioned circumstances, for the present investigation it was decided to use modified thin-wall oedometer tests, conventional oedometer tests and larger size laboratory scale tests on CBR moulds, to be performed both on untreated samples and on samples treated with central trenches filled with granular material. The trenches are modeled as a hole drilled at the center of the soil samples. The hole has a diameter that satisfies the predicted percent trench content and is then backfilled with granular material. Modified thin-wall oedometer

tests are performed with swell overburden technique to measure the vertical as well as lateral swell parameters of both untreated and treated samples, whereas the conventional oedometer tests and tests on samples placed in CBR moulds are performed to measure the vertical swell parameters of soils simultaneously. Tests are carried on artificially compacted samples to check out the behaviour both in the horizontal and vertical directions. The descriptions of each test apparatus used during the investigations, are presented in the following sections.

### **3.2 CONVENTIONAL OEDOMETER TESTS**

Oedometers available in the M.E.T.U. Soil Mechanics Laboratory are used for the swell tests. The inner diameter of the consolidation rings were 63.5mm, whereas the outer diameter was 83.4 mm.

### **3.3 THIN-WALL OEDOMETER RING**

In addition to the conventional oedometer tests, modified thin-wall oedometer rings are used to measure the lateral swell pressures. Two simultaneous test systems were prepared for this purpose. Due to their functioning mechanism and working principles, the conventional oedometers are known to be capable of simulating only at rest and/or nearly at rest conditions. However, with acceptable modifications performed on testing conditions of the apparatus, it turned out to be possible to model the behaviour in between active and at-rest conditions as well.

As it was thoroughly described in Chapter II, the modified thin-wall oedometer ring instrumented with an electrical strain loop surrounding the thin ring was first introduced by Komornik and Zeitlen (1965). This setup was further amended by Ofer (1980) who affixed the electrical strain gauges at the mid-height of the thin-wall and introduced pressurized air to the system.

Modified thin-wall oedometers developed and employed by Ertekin (1991) and Avşar (2007), Avşar et al. (2009) will be used for the present study. The two setups are similar with the exception that the diameter of the Avşar's ring is slightly smaller. Achieving the highest levels of lateral pressure to be exerted by the soil sample to the oedometer ring is very critical in lateral swell measurements. Due to their thin steel membrane structure, both rings have the capability to act as a lateral restraint and at the same time to apply back pressure to control strain levels. A cross sectional diagram of lateral swell pressure oedometer ring developed by Ertekin (1991) and its setup are shown in Figure 3.1 and Figure 3.2, whereas the ring manufactured by Avşar (2007) is presented in Figure 3.3. The top and bottom caps are used only during calibration.

### **3.3.1 Thin-Wall Swell Pressure Oedometer Ring Body**

For both rings, the main body is made of high quality alloy steel. The internal diameter of the ring developed by Ertekin (1991) is 63.5 mm, whereas the internal diameter of the Avşar (2007) ring is 54.5 mm. The wall thicknesses of both rings are 0.35 mm while the height of the ring of Ertekin (1991) is 78 mm and Avşar (2007) is 66 mm. The read-out unit connections of the cables and strain gauges on the thin-walled section are maintained through the four holes located at every 90° of the top collar for both of the oedometer rings. The additional three holes drilled at 120 degrees to each other are used as pivot bolt beds to keep the thin-wall of the oedometer shock resistant. Furthermore, the top cap is furnished with two screw-threaded outlets, one for fluid supply and the other for fluid release for calibration purposes.

The water and air tightness of the caps of the oedometers during calibration process is provided by the screw thread assembly at the outer ends of the ring bodies holding the caps, which are already machined to perfectly fit the ring, in place. In addition, the main ring is equipped with an o - ring groove to guarantee further sealing. The ring body is tempered to prevent any of the internal stresses due to machining and to avoid permanent deformations after release of the load

while testing. Protection against corrosion is maintained by galvanizing the metal parts of the setup.

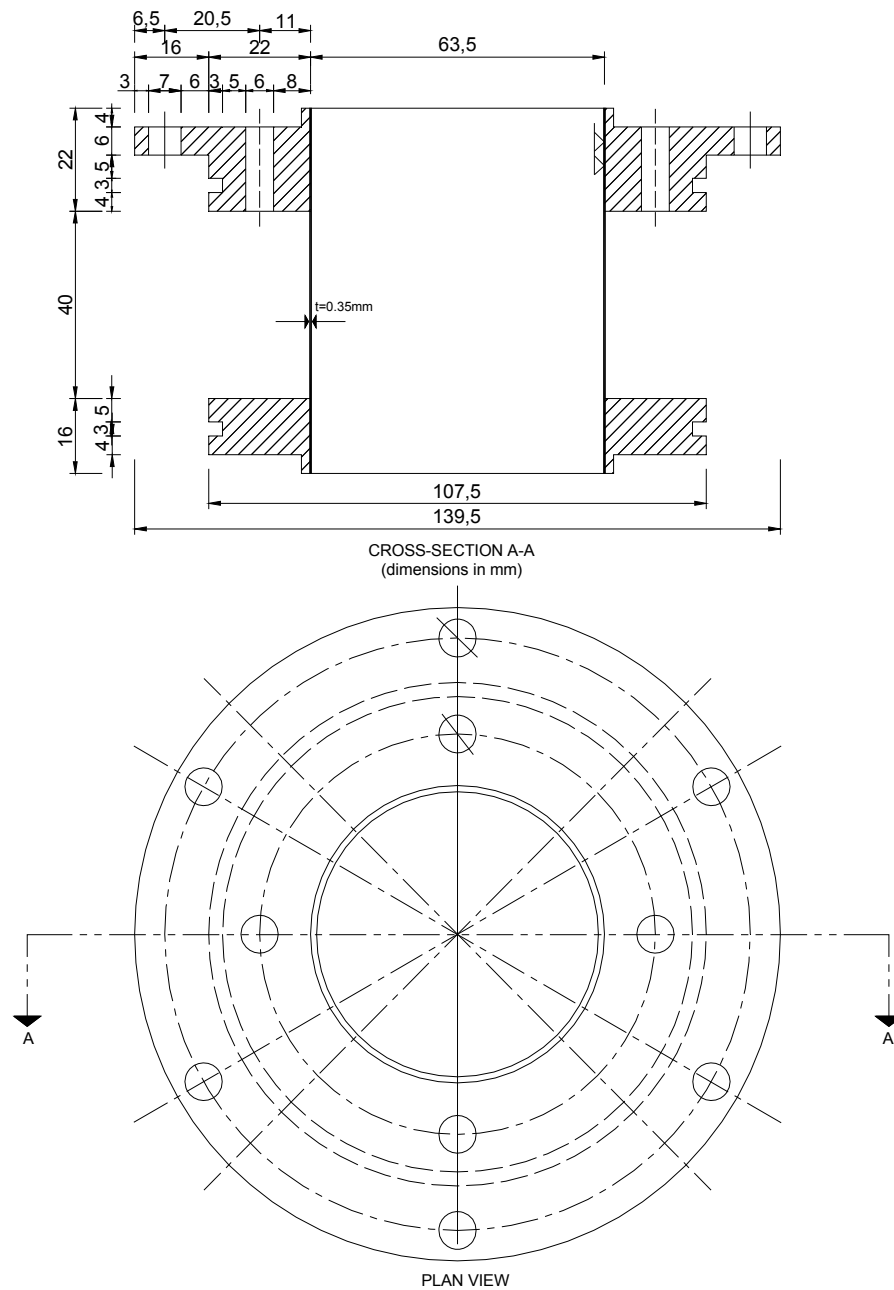


Figure 3. 1 Cross - Sectional and Plan View of Thin-Wall Oedometer Ring (Ertekin,1991)



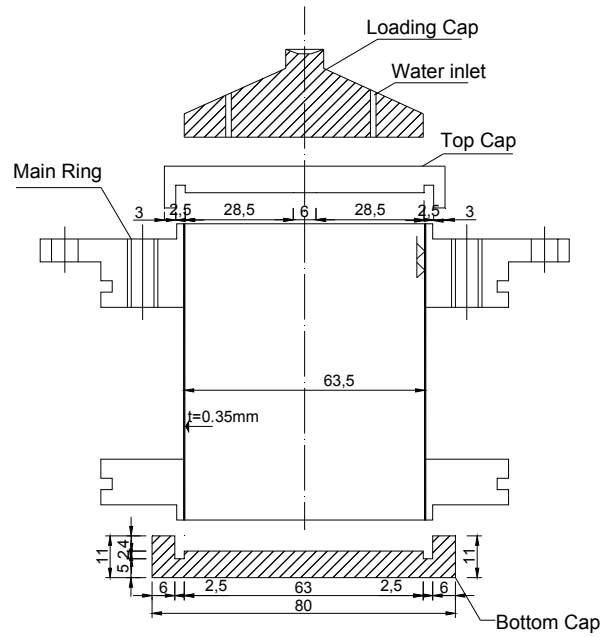


Figure 3. 2 Lateral Swell Pressure Test Set-Up Ready for Instrumentation (Ertekin, 1991)

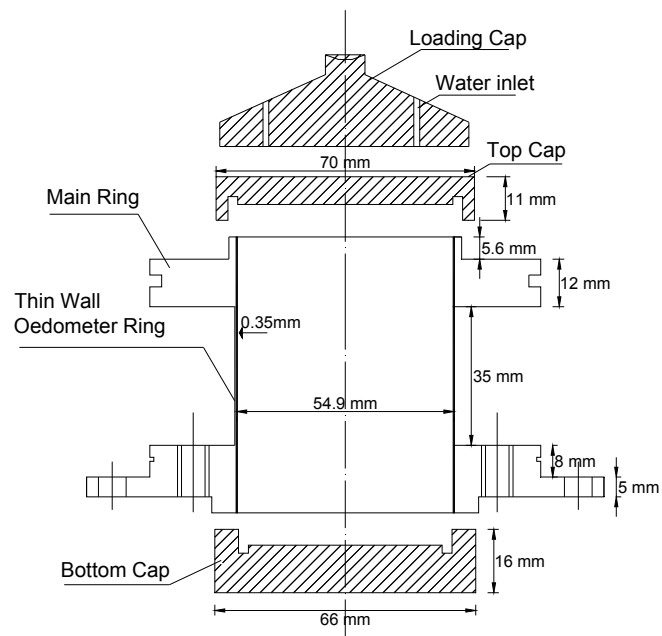


Figure 3. 3 Lateral Swell Pressure Test Set-Up Ready for Instrumentation (Avşar, 2007)

### 3.3.2 Instrumentation with Electrical Strain Gauges

As it is impossible to directly measure the stresses generated in any material, other measurable parameters such as strains are used to estimate the stresses under a predetermined loading condition. Among various methods available to measure strains, the use of electrical strain gauges is preferred for this particular investigation for the determination of lateral swelling pressures. These electrical strain gauges, which bear a critical function in the modified thin-wall oedometer test apparatus, are installed to the mid-height of the outer surface of the thin-wall of the oedometer ring. For the present study,  $4 \times 120\Omega$  electrical strain gauges are located at every 90 degrees along the circumference of the thin-wall. Figure 3.4 shows the installation of the strain gauges on the thin-wall surface. The catalogue values for the strain gauges as given by the manufacturer are listed in Table 3.1 and the strain gauge is schematically illustrated in Figure 3.5.

Table 3. 1 Catalogue Data for the Strain Gauges

General Specifications of the Strain Gauge	
Fatigue Life	$10^6$ loading – unloading cycles
Type of Sensor	Cu – Ni alloy foil in epoxy carrier
Operating Temperatures	-20 to +80°C
Gauge Factor	2.1

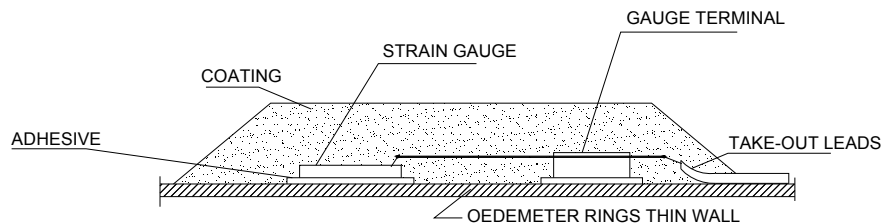


Figure 3. 4 Installation of the Strain Gauges (Ertekin, 1991)

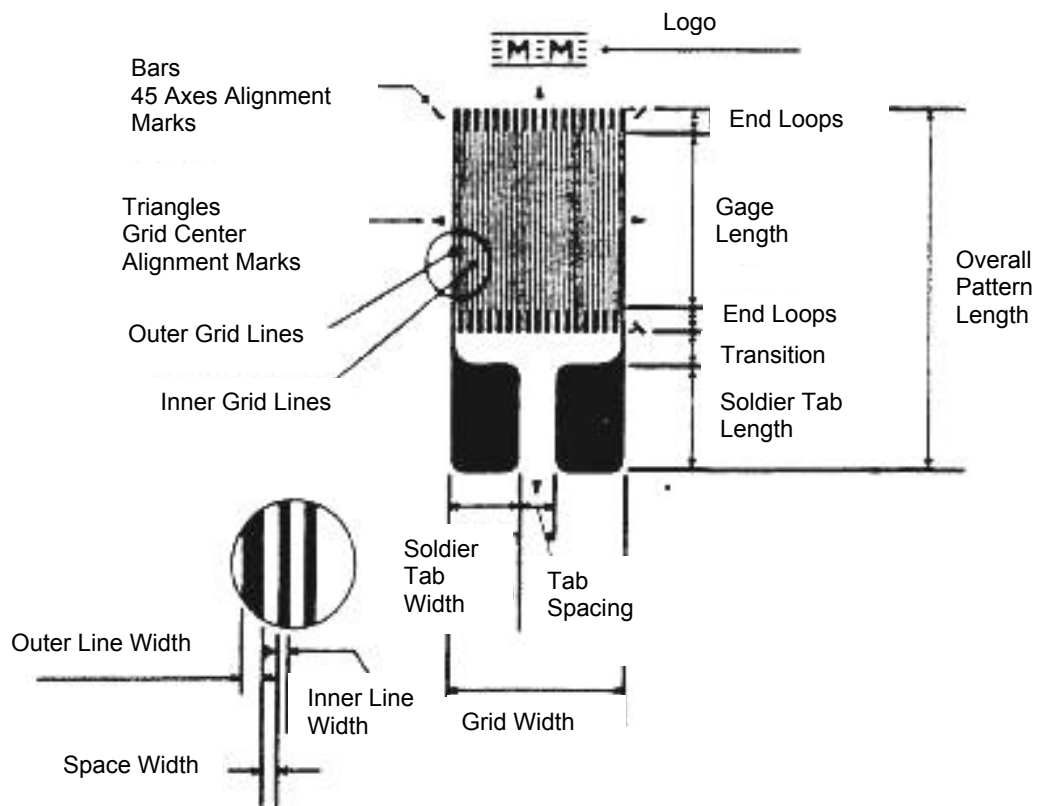


Figure 3. 5 Strain Gauge Nomenclature (Ertekin, 1991)

The strain gauges are installed to the outer wall of the thin-wall according to the Wheatston Bridge Configuration (Figure 3.6), which is simply an electrical circuit used to measure an unknown electrical resistance by balancing two legs of a bridge circuit, one leg being the unknown resistance. For this purpose, two of the gauges, namely the active gauges, are installed symmetrical to each other and parallel to the horizontal plane; while the other two, which are called the dummy strain gauges, are placed perpendicular to the base of the ring. A snapshot of one of the active strain gauges on the thin-wall surface is given in Figure 3.7.

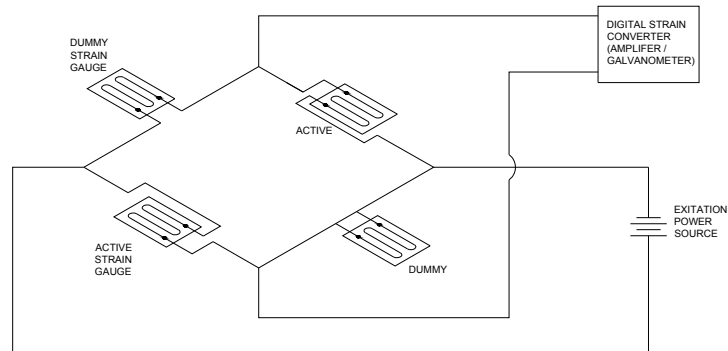


Figure 3. 6 Full Wheaston Bridge Configuration (Ertekin, 1991)



Figure 3. 7 An Active Strain Gauge on the Thin-Wall Ring (Ertekin, 1991)

### 3.3.3 Data Acquisition System

The data acquisition system used in this investigation is manufactured by a Turkish company; TDG Industrial Solutions Limited. The CODA AI8b portable unit is a multipurpose data acquisition unit capable of measuring several parameters such as current, stress, temperature, load or displacement by means of suitable sensors and transferring them to computer environment. The system is designed

to measure any of the parameters without a requirement of an additional electronic unit. The system is composed from CODA data acquisition software, CODA AI8b communicator unit and a data acquisition frame. There exist eight signal processing input channels on the frame communicating with the communicator unit that transfers the data to computer. Each channel can be adjusted to measure different parameters individually and simultaneously with proper sensor units attached to them. By means of high quality analog – digital circuit, the voltage change of up to 0.000305 V can be sensed in between  $\pm 10$  V measurement range. The sampling interval of each channel can be adjusted even up to 8 samples per second. The sensor feed voltage can be adjusted by either 5 or 10V by changing the position of the switch in each channel. It is possible to select up to eight gain factors for each channel. After the voltage is measured, processed and filtered, it is subjected to scaling process with either of the selected factors of 150, 247, 396, 494, 643,740 or 890. With the help of these special features of the system, the measurement accuracy is expected to be 0.1% of the full scale test. The system is not affected from noises generated by the power lines and the power supply units. Since it is fully compatible with bi-polar or uni-polar sensors, the sensors that can generate negative or positive voltages such as LVDT's, strain gauges and load cells can be used very effectively. TDG AI8b data acquisition unit is compatible to standard voltages of 220V and consumes a power of 5 Watt on average. The recommended working temperature of the system is in between +10 to +35<sup>0</sup>C and in case the working temperature is above or below these quantities, the repetition of calibration process is strongly recommended. TDG CODA software is compatible to Windows XP and Vista based operating systems. After the system is connected to the sensors and the software is started, the measurements are automatically recorded at selected time intervals to the computer. This feature serves for both night and day measurements regardless of the measurement interval and test duration. A snapshot of the data acquisition unit is presented in Figure 3.8.

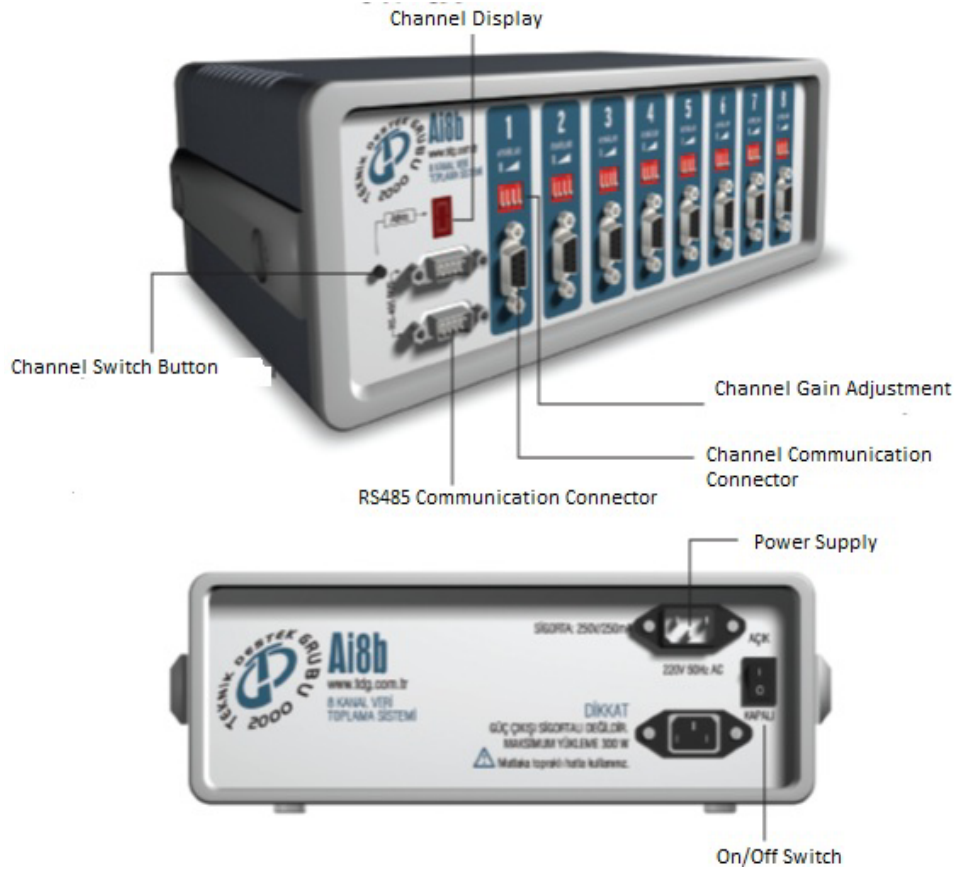


Figure 3. 8 Data Acquisition Unit

### 3.3.4 Calibration of the Swell Pressure Ring

The lateral swell pressure exerted on the thin-wall ring is planned to be measured by tracing the voltage changes on the strain gauges. For this reason, the amount of voltage difference (i.e. the strain generated on each gauge under an applied stress) for a particular lateral pressure change shall be defined. Based on the fact that strain is directly proportional to the material strength characteristics of the thin-wall steel ring, each of the rings were subjected to calibration process separately to define their behaviour under different applied pressures.

For calibration of each ring “Free Expansion Method” was used (Ertekin, 1991). In this method, a predetermined value of measurable fluid pressure is applied

inside the ring and the voltage change of the strain gauges are recorded simultaneously. Based on the fact that fluid applies a hydrostatic pressure inside the surfaces of the ring, the applied pressure can be treated as the lateral pressure exerted on the ring. By recording the voltages, i.e. strains, corresponding to each pressure level, a calibration curve that directly defines the amount of lateral pressure exerted on the ring by the expansive soil can be defined. Since the rings are expected to deform elastically under the probable ranges of lateral swell pressures anticipated throughout the investigations, the calibration curves are also presumed to be almost linear in nature. This cross-check is in fact an important part of the investigation due to the fact that there always exists a possibility that the ring may encounter plastic deformations resulting in serious errors in case the calibration curve observed is non-linear, This condition is also important to assure that deformations are negligible so that at rest condition during the tests is satisfied.

At the start of the calibration procedure, specially manufactured top and bottom caps were mounted on each ring (Figure 3.9). Water tightness is sustained via o-rings used on each cap and water inlet and outlet were achieved by two holes opened at the top cap.



Figure 3. 9 Bottom Cap (Left) and Top Cap (Right) with Supply (Center) Inlet and Release (Outlet) Points

Distilled water is used as fluid pressure during the calibration process. Initially water is allowed into the oedometer ring from the inlet hole on the top cap. After water seepage from the outlet hole is observed, which assures that the cell is completely full of water, the release valve is closed. Water pressure is applied to the system in increments up to 600 kPa ( $\approx 6 \text{ kg/cm}^2$ ) and the strain value corresponding to each pressure increment is recorded. Then, the load is gradually decreased recording the corresponding strains. The calibration cycle is repeated for at least four times to assure accurate results. The best fit of the calibration curves obtained from each ring is presented in Figure 3.10. It should be noted that calibration curves are observed to be almost linear meeting the aforementioned requirements.

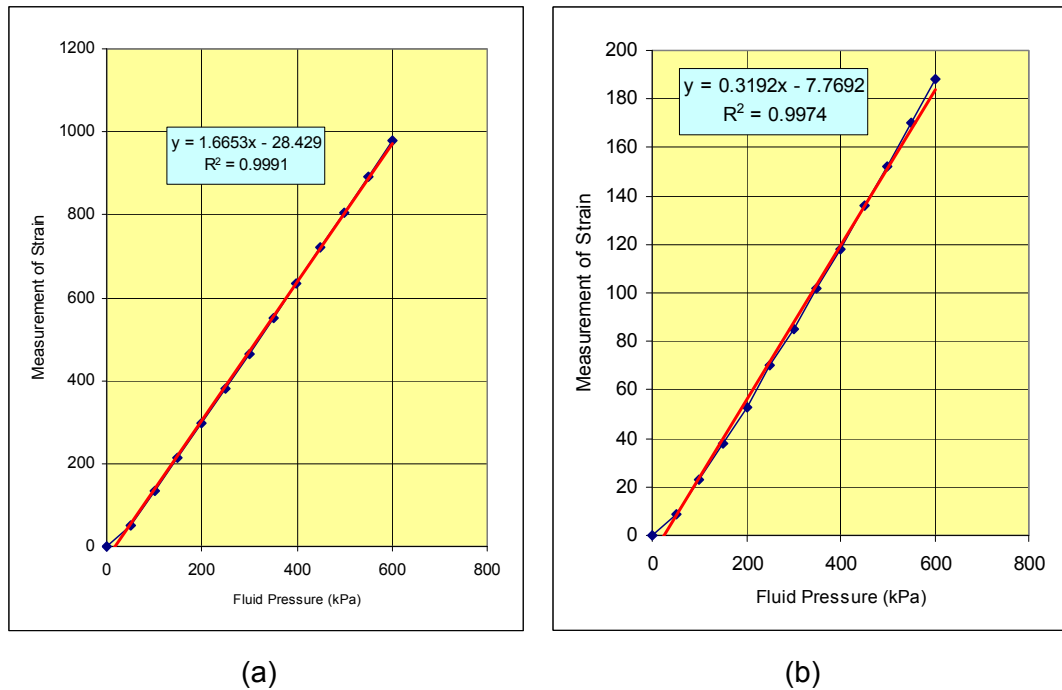


Figure 3. 10 Calibration Curve Obtained from the Thin-Wall Cell Developed by (a) Ertekin (1991), (b) Avşar (2007)



### 3.3.5 Verification of Swell Pressure Oedometer Ring

Based on its targeted operational properties, the thin-wall thickness should be thin enough so that the ring deformations are read by the strain gauges while at the same time sufficiently thick to fulfill the at rest pressure conditions, i.e., no lateral deformations. In order to assure these two contradictory requirements, the pressure ring is expected to deform in elastic phase and should not be subjected to plastic deformations under maximum operational testing pressure ranges. For all practical purposes, the above defined requirements can be checked by means of well-defined formulae presented in the elastic theory in combination with the principles of strength of materials. The terminology is therefore common and is also duplicated in Ertekin (1991) as it is listed below:

- $R$ : Internal Radius of the Ring
- $E$ : Modulus of Elasticity of the Ring Material
- $t$ : Thickness of the Ring Wall
- $P_i$ : Internal Pressure Acting on the Ring Wall
- $\sigma$ : Tensile Stress on the Ring Wall
- $\varepsilon$ : Strain on Outer Peripheral of the Ring Wall
- $dR$ : Enlargement of the Internal Radius
- $N$ : Total Normal Force Acting on Vertical Cross Sectional Area
- $A$ : Vertical Cross Sectional Area per Unit Height (For unit height,  $A = t$ )

The total normal force acting on the cross section is:

$$N = \int_0^{\pi/2} P_i \sin \theta ds \dots \dots \dots (3.1)$$

where,

$$ds = R. d\theta \dots \dots \dots (3.2)$$

By substituting equation (3.2) into (3.1);

$$N = \int_0^{\pi/2} P_i \cdot R \cdot \sin \theta \cdot d\theta \dots\dots\dots(3.3)$$

Knowing that;

$$\int_0^{\pi/2} \sin \theta \cdot d\theta = 1$$

The total normal force acting on the cross section can be rewritten as;

$$N = P_i \cdot R \dots\dots\dots(3.4)$$

and the tensile stress in the ring wall is;

$$\sigma = P_i \cdot (R/t) \dots\dots\dots(3.5)$$

From the above equation, the internal pressure acting on the ring wall can be defined as;

$$P_i = \sigma \cdot (t/R) \dots\dots\dots(3.6)$$

The tangential strain on the outer peripheral of the ring wall is;

$$\varepsilon = \frac{\sigma}{E} = \frac{P_i}{E \cdot t} \dots\dots\dots(3.7)$$

The enlargement of the internal radius of the ring under the applied pressure is;

$$\varepsilon = \frac{[(R+dR)2\pi - 2\pi R]}{2\pi R}$$

$$\frac{dR}{R} = \frac{P_i \cdot R}{E \cdot t}$$

$$dR = \frac{P_i R^2}{E.t} \dots\dots\dots(3.8)$$

The expected stress distribution inside the ring during the testing phase and corresponding hoop stresses are presented in Figure 3.11.

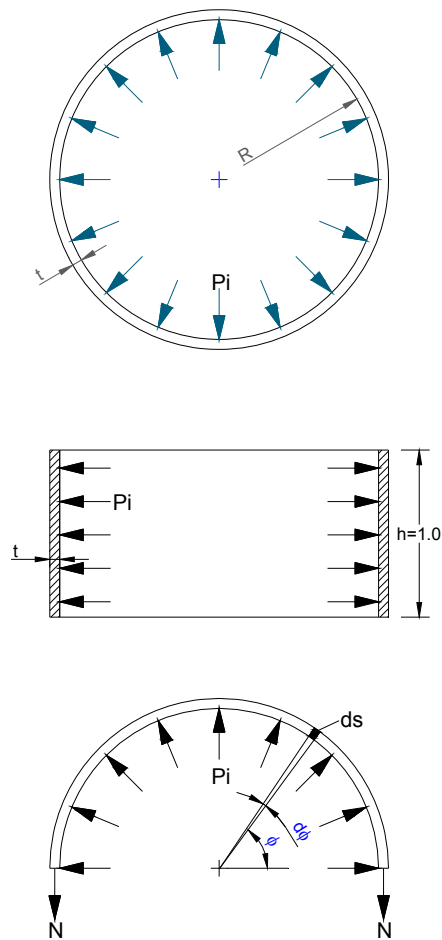


Figure 3. 11 Stress Distribution in the Thin-Wall Oedometer Ring Wall

The strength characteristics of the ring manufactured from high quality alloy steel with material code Ç4140 (equivalent to DIN42 Cr Mo 4) is given as:

- i. Design (Safe) Tensile Strength;  $\sigma_d = 550$  MPa
- ii. Modulus of Elasticity;  $E = 2.53 \times 10^5$  MPa

The maximum allowable inner pressure that can be applied on the ring without subjecting it to plastic deformations is calculated using Equation (3.6) such that;

a) for the Ertekin (1991) ring ( $t=0.35 \times 10^{-3}$  m;  $R=63.5 \times 10^{-3}/2 = 31.75 \times 10^{-3}$  m)

$$P_i = \sigma_d \cdot t / R = (550 \times 10^3 \times 0.35 \times 10^{-3}) / 31.75 \times 10^{-3} \approx 6000 \text{ kPa} (\approx 60 \text{ bars})$$

b) for the Avşar (2007) ring ( $t=0.35 \times 10^{-3}$  m;  $R=54.9 \times 10^{-3}/2 = 27.45 \times 10^{-3}$  m)

$$P_i = \sigma_d \cdot t / R = (550 \times 10^3 \times 0.35 \times 10^{-3}) / 27.45 \times 10^{-3} \approx 7000 \text{ kPa} (\approx 70 \text{ bars})$$

During the calibration procedure, the maximum pressure applied on the ring was 600 kPa which is almost 10 % of the allowable stress that can be applied on the ring safely; showing that the deflection of the ring will be expected within the elastic ranges during the tests.

From Equation (2.7), the tangential strain at the maximum calibration pressure of 600 kPa is calculated to be;

$$\varepsilon = (600 \times 27.45 \times 10^{-3}) / (2.53 \times 10^8 \times 0.35 \times 10^{-3}) = 186 \times 10^{-6} (186 \mu \text{ strain})$$

The above calculated strain value shows that the thin-wall ring is adequate for expected lateral swell pressure ranges of clayey soil.

### 3.4 MODIFIED CBR MOULD

CBR moulds as defined by ASTM-D 1883-05 were used to investigate the vertical swell parameters of larger soil samples, within the content of this research. Since the inner diameter of present CBR moulds at the laboratory are 15.2 cm, moulds and necessary attachments were modified to test a soil sample with a height of 4.55 cm that satisfies the aspect ratio of a standard oedometer test apparatus of  $H/D = 1.9/6.35 = 0.30$ . A perforated bottom plate and an inundation container are also manufactured and used during the tests. The vertical pressure was applied by means of a loading frame and dead weights placed on it, mounted on top of the loading cap. The general view of the modified CBR mould equipment is shown in Figure 3.12.



Figure 3. 12 Modified CBR Moulds with Inundation Containers

## **CHAPTER IV**

### **TEST PROGRAM**

#### **4.1 INTRODUCTION**

In this experimental study, a comprehensive laboratory test program including conventional oedometer tests, modified thin-wall oedometer tests and larger sized laboratory scale tests on modified CBR moulds were performed both on untreated samples and on samples treated with holes that are filled with granular materials. In a group of tests, the granular backfill material is interchanged with silt, which is also used as a blanket layer for CNS (Cohesive Non-Swelling Soil) effect in another set of experiments. The proposed treatment is represented by central holes drilled in clay samples such that the total hole diameter satisfies the predicted “trench to sample” ratio, which is in turn is indicated as the “area replacement ratio, ARR” in the rest of the text.

In this chapter, the properties of soils used in the experiments are explained. The results of the preliminary tests conducted on the test material involved in the program, i.e. the natural and artificial clays, the three types of granular materials and the coarse silt are enlisted. Next, the features of the test apparatus and the preparation of test samples are described in detail. Finally, a complete list of the test schedule is presented in tabular form.

#### **4.2 TEST MATERIAL**

Three artificially compacted and two natural clay samples were used in the experiments. The five samples were selected to bear different swelling potentials in order to investigate the probable effect of the replacement ratio and the soil

properties on swell. The artificial clays were prepared from a kaolinite readily available at the METU Soil Mechanics Laboratory and a commercially available bentonite at different blend ratios; whereas the natural clays were obtained from two distinct sites at different districts of Ankara. As the fill material, one type of sand, two types of gravel and one type of silt are utilized. The properties of the test material are given in detail in the following sections.

#### **4.2.1 Properties of Clays**

The three types of potentially expansive artificial soils were prepared by mixing 90% Kaolinite and 10% Na-Bentonite, 85% Kaolinite and 15% Na-Bentonite and 80% Kaolinite and 20% Na-Bentonite by dry mass for test purposes. The other two natural soil samples were obtained from the different parts of Ankara, namely from Gazi University Campus area in Beşevler District (Figure 4.1 and Figure 4.2) and from the vicinity of Esenboğa Airport in Çubuk District (Figure 4.3, Figure 4.4, Figure 4.5).



Figure 4. 1 Test Pit at Gazi University Campus Area



Figure 4. 2 Cracks Observed on building next to the test pit at Gazi University Campus Area



Figure 4. 3 Test Pit at Esenboğa





Figure 4. 4 A View from the Test Pit at Esenboğa



Figure 4. 5 Damaged Retaining Walls near Test Pit at Esenboğa

Some index properties of the samples are presented in Table 4.1. The grain size distributions of the expansive soil samples (Type 1 to Type 5) are presented in Figures 4.6, 4.7, 4.8, 4.9 and 4.10 respectively.

From the Unified Soil Classification Chart given in Figure 4.11, the artificial soil samples and Esenboğa Clay can be classified as highly plastic clay (CH), whereas Gazi Clay is classified as (CL).

Table 4. 1      Some Index Properties of Soils Used for Tests

	<b>Type-1</b> <b>(10% Bentonite)</b>	<b>Type-2</b> <b>(15% Bentonite)</b>	<b>Type-3</b> <b>(20% Bentonite)</b>	<b>Type-4</b> <b>(Gazi)</b>	<b>Type-5</b> <b>(Esenboğa)</b>
Liquid Limit, LL	67	86	100	43	127
Plastic Limit, PL	22	22	23	23	37
Plasticity Index, PI	45	64	77	20	90
Specific Gravity, G <sub>s</sub>	2.59	2.58	2.58	2.69	2.68
Percent Finer than #200 Sieve	97.60%	97.70%	97.80%	58.90%	99%
Clay Content, C (%)	38%	40%	42%	23%	62%
Activity, A = PI/C(%)	1.18	1.60	1.83	0.87	1.45
W <sub>opt</sub> (%)	20.07	20.85	22.1	18.8	34.89
Y <sub>d max</sub> (g/cm <sup>3</sup> )	1.61	1.59	1.55	1.69	1.23
USCS	CH (High Plasticity)	CH (Very High Plasticity)	CH (Extremely High Plasticity)	CL (Medium Plasticity)	CH (Extremely High Plasticity)

From the Activity Chart given in Figure 4.12 (Van der Merwe, 1975), the artificial soil samples, namely Type-1, Type-2 and Type-3, and Esenboğa Clay (Type-5) can be classified as highly expansive, whereas Gazi Clay (Type-4) can be classified as medium expansive.

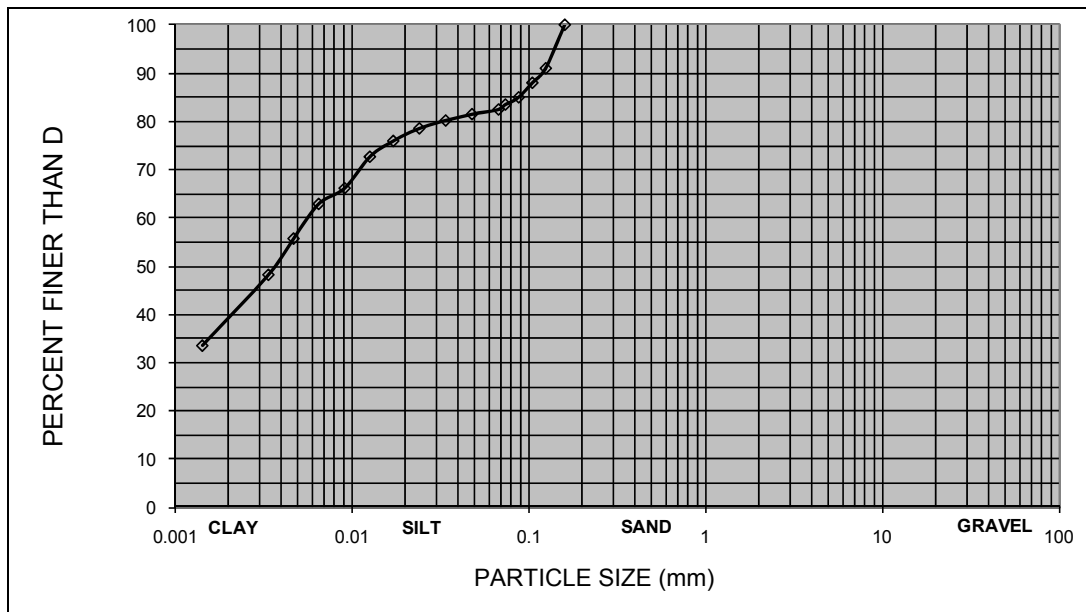


Figure 4. 6 Grain Size Distribution of the Sample Type-1

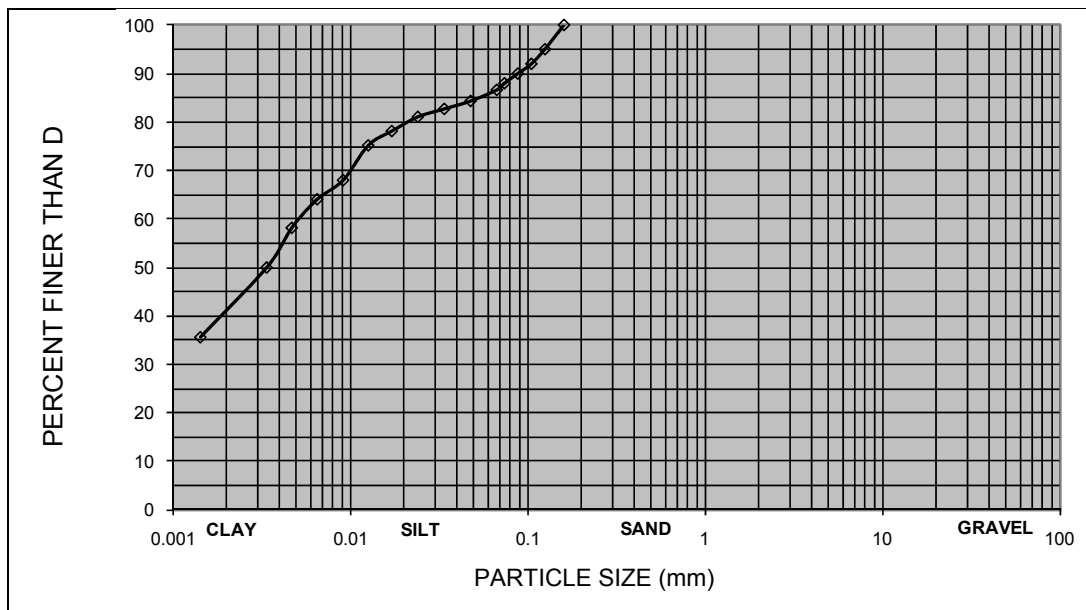


Figure 4. 7 Grain Size Distribution of the Sample Type-2

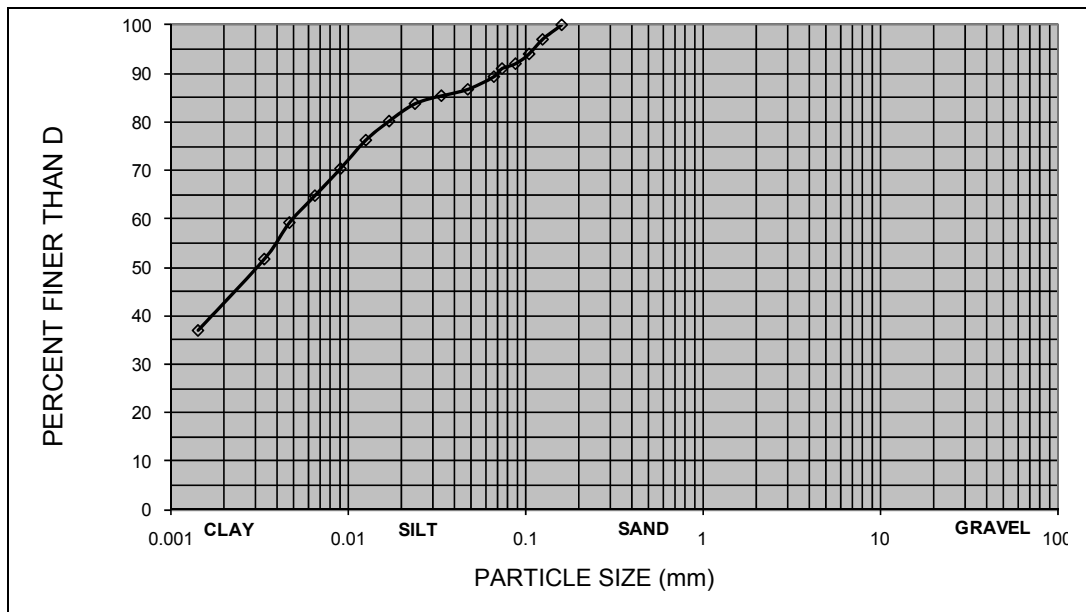


Figure 4. 8 Grain Size Distribution of the Sample Type-3

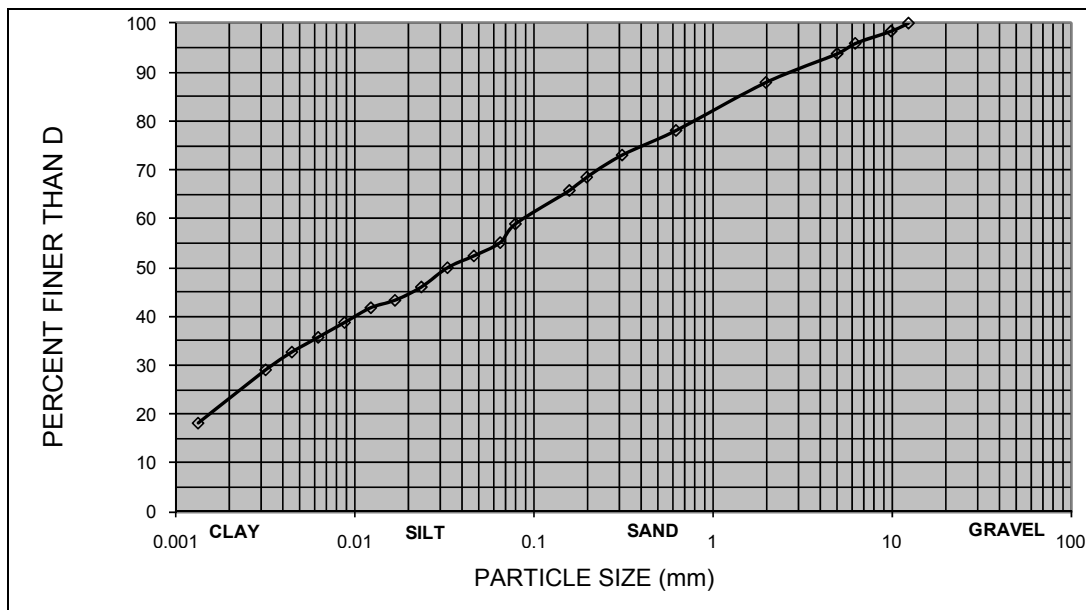


Figure 4. 9 Grain Size Distribution of the Sample Type-4

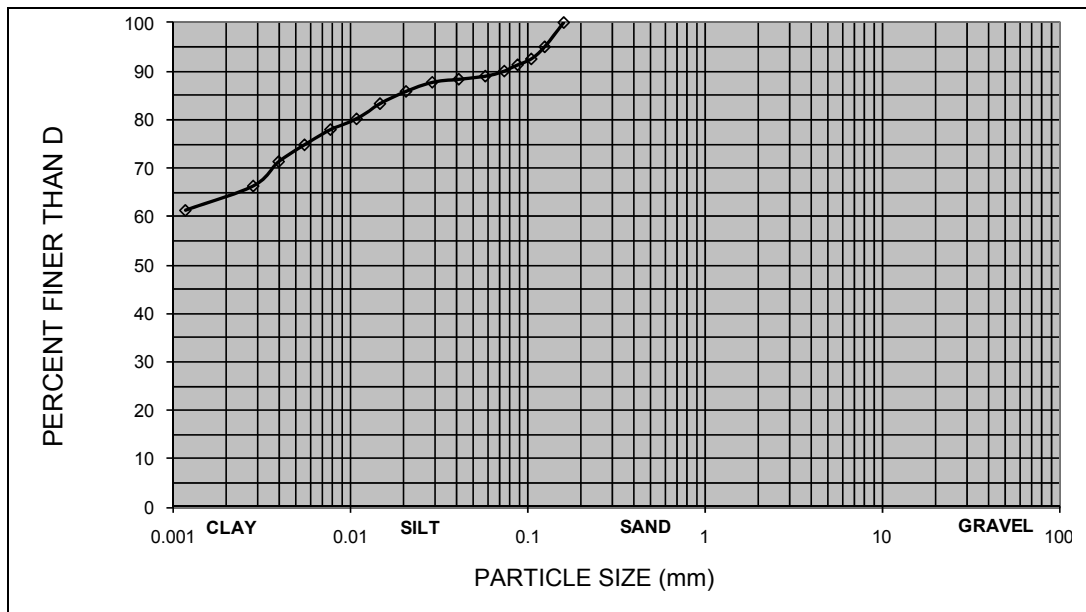


Figure 4. 10 Grain Size Distribution of the Sample Type-5

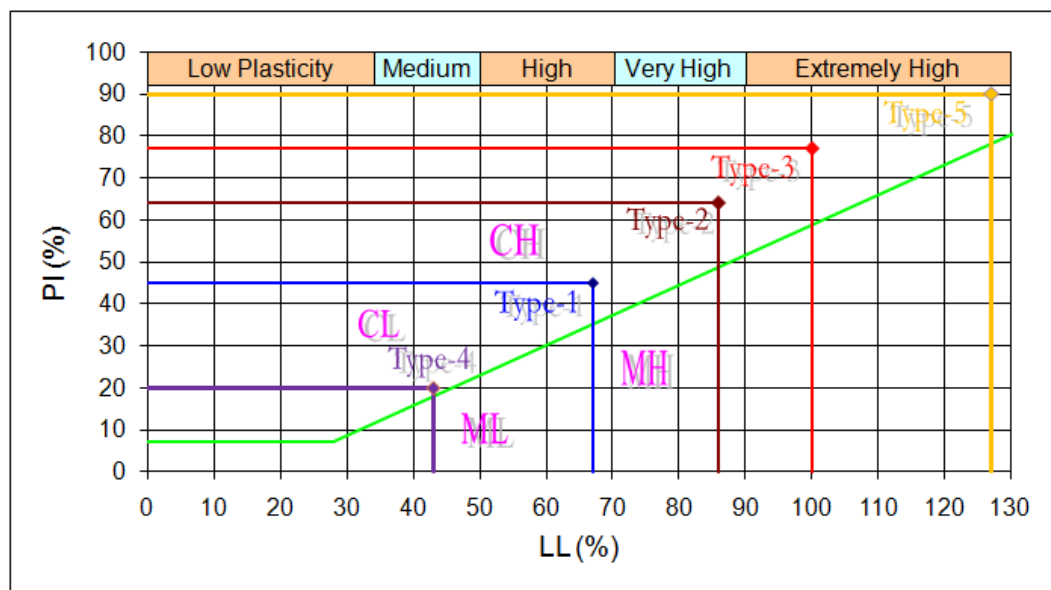


Figure 4. 11 USCS Chart and Classification of the Samples Used for Tests

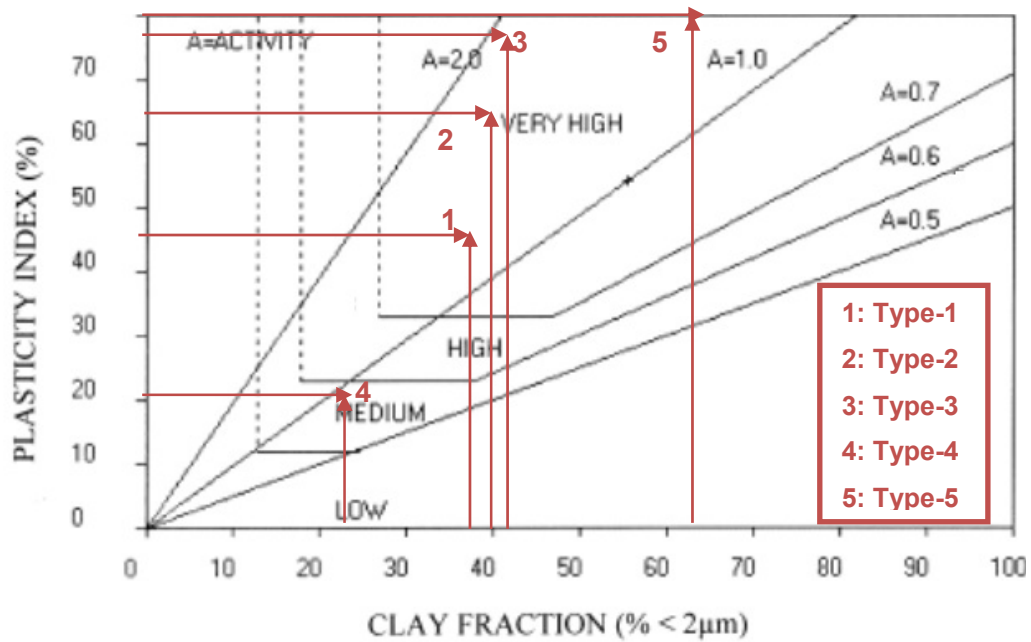


Figure 4. 12 Activity Chart for the Determination of Swell Potential of the Soil Samples Used in the Tests

Standard Proctor tests were carried out for all samples and the water contents and the dry unit weights for the test program were selected such that they are at their dry of optimum values. More specifically, tests on artificially prepared samples and Gazi Clay (Types 1 to 4) were performed on samples with initial moisture content of 15 % and dry density of  $1.5 \text{ g/cm}^3$  whereas Esenboğa sample was prepared with an initial moisture content of 15 % and a dry density of  $1.2 \text{ g/cm}^3$ .

On the other hand, samples of Gazi Clay (Type-4), similar to the one used for this investigation was tested previously by Özer et al. (2012) and Esenboğa Clay (Type-5) was also tested for this investigation at the Hacettepe University X-Ray Micro Analysis Laboratory to obtain its X-ray diffraction analyses and hence the mineralogical properties. Three forms of the same clay were prepared, which were namely (i) an untreated sample, (ii) a sample treated with ethyleneglycole, and (iii) an oriented sample that was heat treated for 2 hrs at  $500^\circ\text{C}$ . A

diffractometer having a goniometer speed of 2°/min was used, and the quantitative mineral estimations were based on the method which was previously suggested by Gündoğdu (1982). The typical results of the analyses as reported by the Hacettepe University are given in Tables 4.2 and 4.3 for the two different natural soil samples, whereas, the XRD patterns for the bulk sample clay and its clay fraction are given in Figures 4.13 to 4.16 for Gazi Clay and Esenboğa Clay, respectively.

Table 4. 2      Soil Mineralogy and Clay Mineralogy of Gazi Clay (Type-4 Sample) (Özer et al.,2012)

Clay and Non-Clay Minerals (%)				Clay Minerals (%)			
Calcite	Quartz	Feldspar	Clay	Smectite	Illite	Kaolinite	Chlorite
20	24	8	48	33	21	23	23

Table 4. 3      Soil Mineralogy and Clay Mineralogy of Esenboğa Clay (Type-5 Sample)

Clay and Non-Clay Minerals (%)						Clay Minerals (%)		
Calcite	Quartz	Mica	Dolomite	Feldspar	Clay	Smectite	Illite	Kaolinite
15	18	10	2	2	53	39	37	24

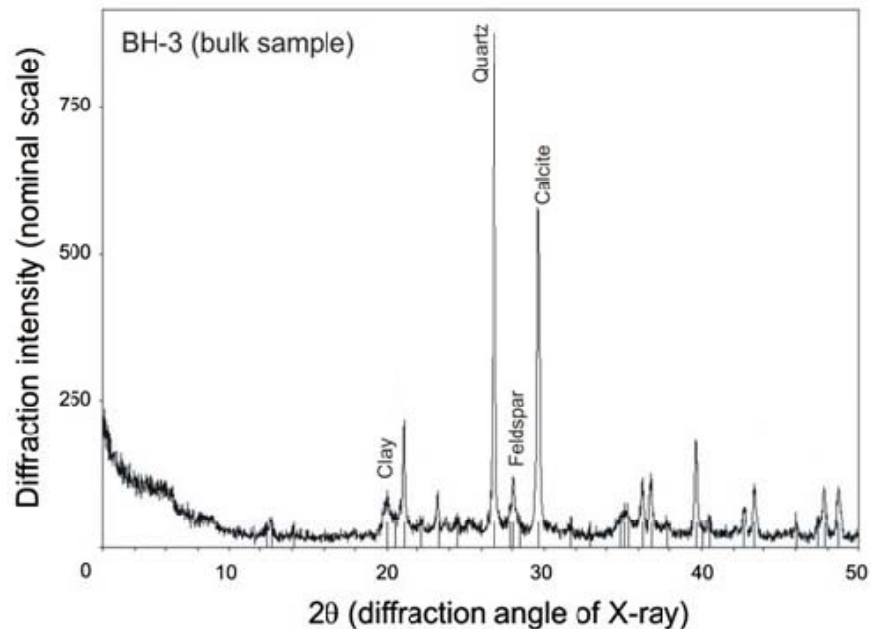


Figure 4. 13 X-Ray Diffractograms of Soil Type-4 for Bulk (Whole) Sample (Özer et al., 2012)

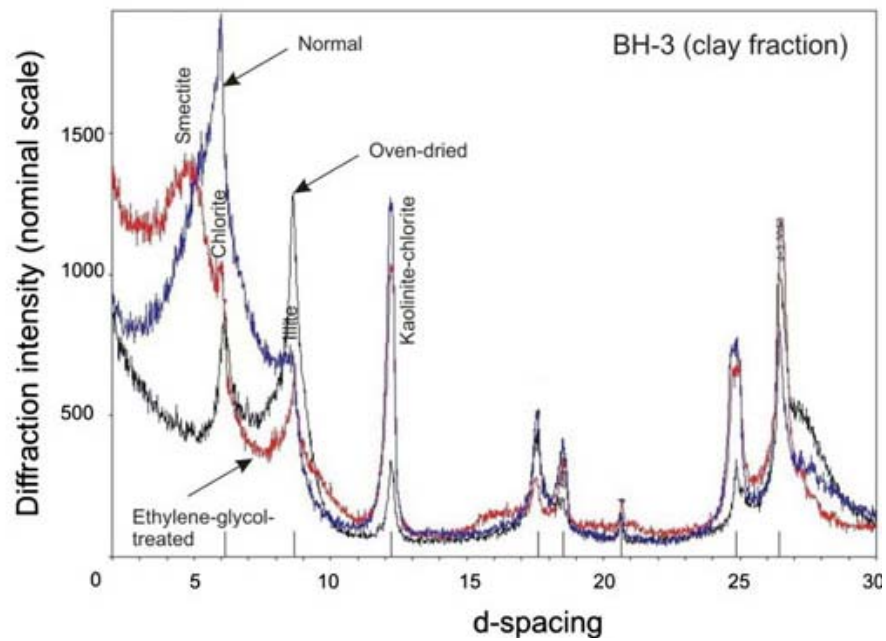


Figure 4. 14 XRD Pattern for Clay Fraction in Gazi Clay (Özer et al., 2012)



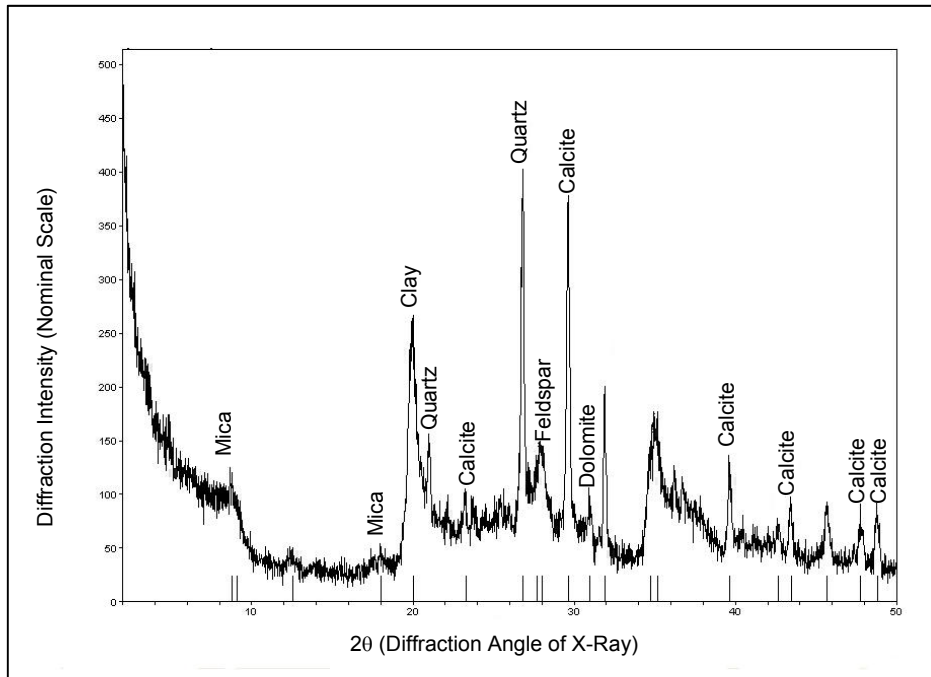


Figure 4. 15 X-Ray Diffractograms of Soil Type-5 for Bulk (Whole) Sample

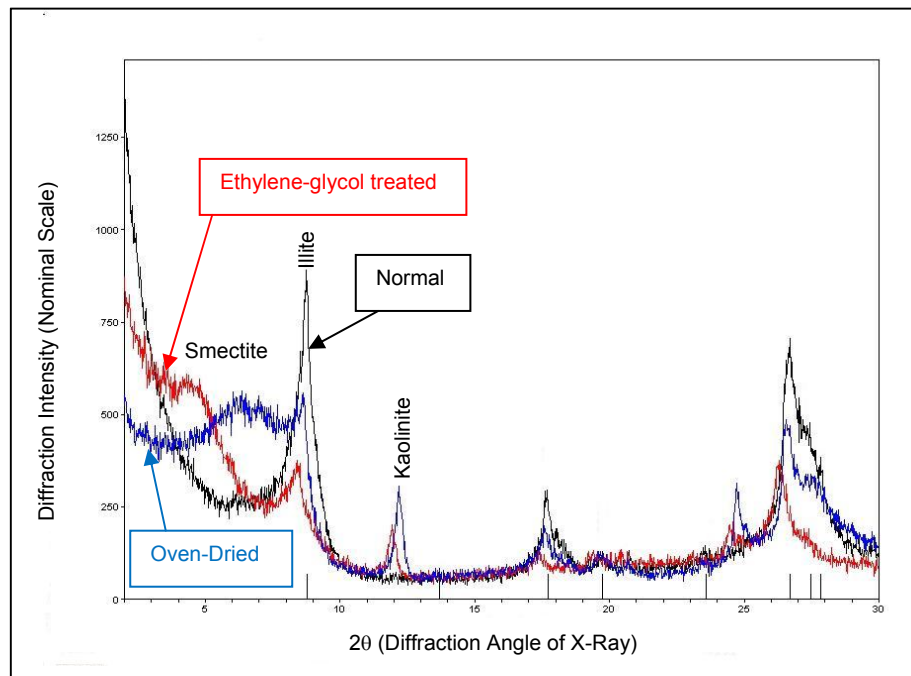


Figure 4. 16 XRD Pattern for Clay Fraction in Esenboğa Clay

#### 4.2.2 Properties of Granular Materials

As it was mentioned earlier, granular soils were placed into holes, opened in compacted clay samples, having a diameter that satisfies the predicted percent trench content. Since the grain size distribution and the physical properties of the granular soils have a major influence on the effectiveness of the treatment, two granular soils with different gradations were used for the conventional oedometer tests, whereas a third granular soil sample was prepared to be used in the modified CBR mould.

The first soil sample used was poorly graded sand which was originally prepared by Tekin (2005) to model the behaviour of granular columns under compression loading. The grain size distribution of sand used for the tests is presented in Figure 4.17, whereas the physical properties of sand are presented in Table 4.4.

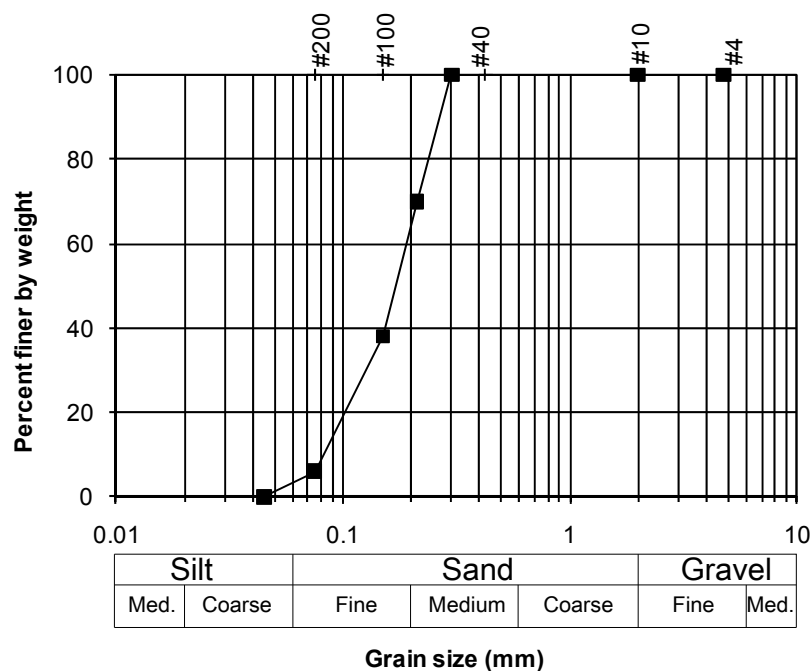


Figure 4. 17 Grain Size Distribution of the Sand Used in Oedometer Tests

Table 4. 4 Physical Properties of the Sand Used in the Preparation of Granular Columns for Conventional Oedometer Tests

USCS	D <sub>10</sub> (mm)	D <sub>30</sub> (mm)	D <sub>60</sub> (mm)	C <sub>u</sub>	C <sub>c</sub>	e <sub>max</sub>	e <sub>min</sub>	G <sub>s</sub>
SP	0.083	0.120	0.195	2.34	0.89	0.96	0.58	2.68

The second granular soil sample used during the conventional oedometer tests was fine gravel and its gradation was calculated based upon typical crushed stone particle sizes commonly used for constitution of stone bases and filling in bad mud conditions. The grain size distribution of fine gravel used during the tests is presented in Figure 4.18, whereas some physical properties are presented in Table 4.5.

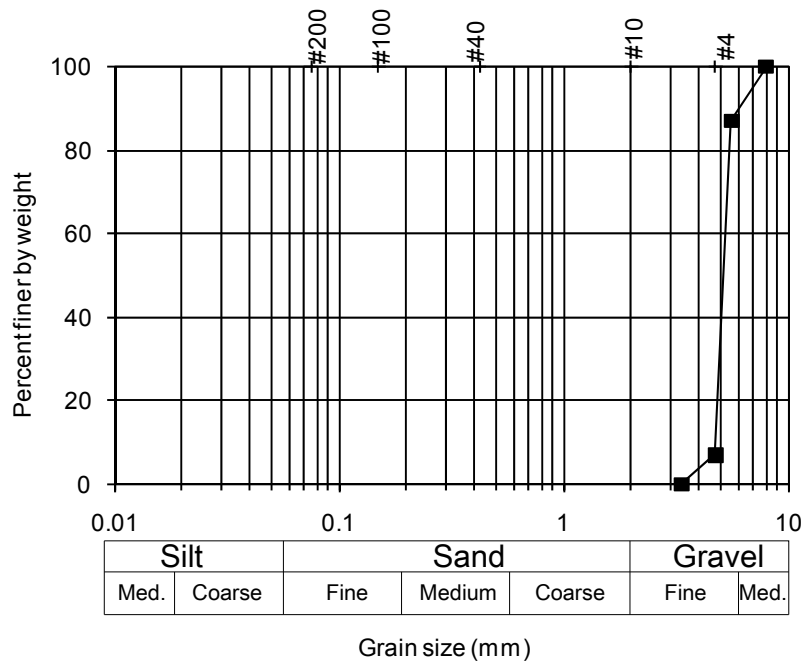


Figure 4. 18 Grain Size Distribution of Fine Gravel used in Oedometer Tests and Thin-Wall Tests

Table 4. 5      Some Physical Properties of Fine Gravel Used in the Preparation of Granular Columns for Conventional Oedometer Tests and Thin-Wall Oedometer Tests

USCS	D <sub>10</sub> (mm)	D <sub>30</sub> (mm)	D <sub>60</sub> (mm)	C <sub>u</sub>	C <sub>c</sub>	e <sub>max</sub>	e <sub>min</sub>	G <sub>s</sub>
GP	4.78	4.98	5.30	1.11	0.98	1.06	0.57	2.67

Based on the fact that modified CBR mould has greater diameter compared to conventional oedometer tests, a third granular soil sample was also used for this type of tests. The gradation of this material was also calculated based upon typical crushed stone particle sizes commonly used for constitution of stone bases and filling in bad mud conditions. The grain size distribution of this medium gravel used during the tests is presented in Figure 4.19, whereas some important physical properties are presented in Table 4.6.

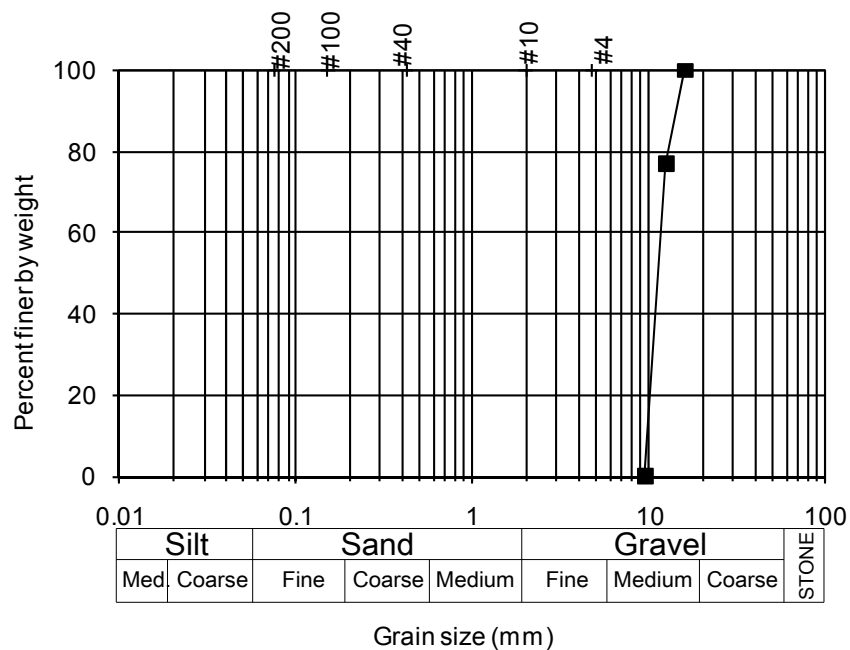


Figure 4. 19      Grain Size Distribution of Medium Gravel used in the Modified CBR Mould

Table 4. 6      Some Physical Properties of Medium Gravel Used in the Preparation of Granular Columns for Modified CBR Moulds

USCS	D <sub>10</sub> (mm)	D <sub>30</sub> (mm)	D <sub>60</sub> (mm)	C <sub>u</sub>	C <sub>c</sub>	e <sub>max</sub>	e <sub>min</sub>	G <sub>s</sub>
GP	9.85	10.57	11.77	1.20	0.97	0.99	0.66	2.71

#### 4.2.3 Properties of Silt

Silt is used not only as a fill material for the model trenches, but also as a CNS layer on top of the clay samples. The grain size distribution of the coarse silt is given in Figure 4.20, and some important physical properties are presented in Table 4.7.

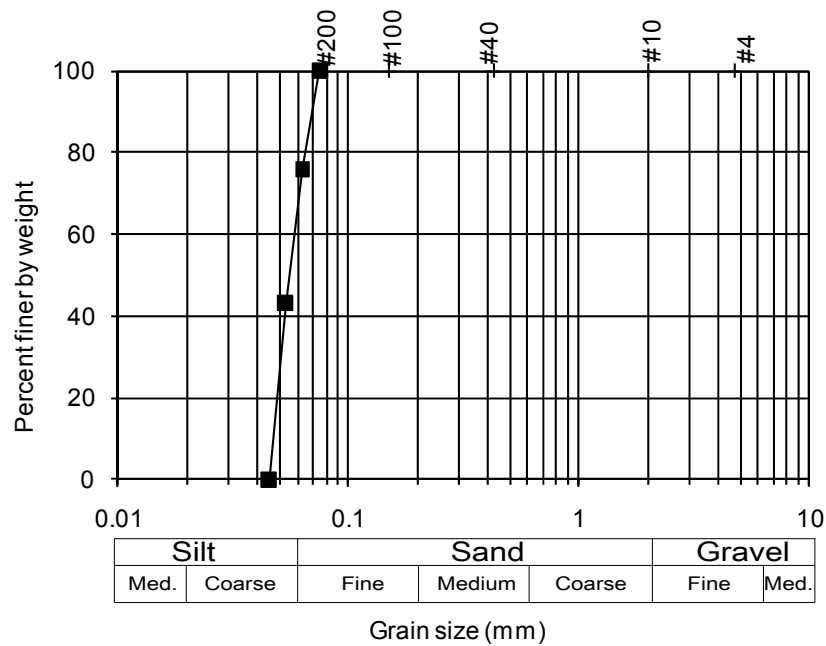


Figure 4. 20      Grain Size Distribution of Coarse Silt used in the Oedometer and Thin-Wall Tests

Table 4. 7      Some Physical Properties of Coarse Silt used in the Oedometer and Thin-Wall Tests

USCS	D <sub>10</sub> (mm)	D <sub>30</sub> (mm)	D <sub>60</sub> (mm)	C <sub>u</sub>	C <sub>c</sub>	e <sub>max</sub>	e <sub>min</sub>	G <sub>s</sub>
ML	0.047	0.050	0.058	1.23	0.94	1.29	0.91	2.72

### 4.3 PREPARATION OF TEST SAMPLES

The preparation phase of the samples to be tested in the conventional and thin-wall oedometer tests are more or less the same, with minor variations. Similarly, the preparation of the CBR samples is also alike, apart from the solution offered to overcome the difficulties imposed by the larger diameter of the hole to be drilled following the compaction. The methodologies followed for sample preparation are detailed in the following sections.

#### 4.3.1 Preparation of the Samples for the Conventional and Thin Wall Oedometer Tests

For the artificial samples, Na-Bentonite and Kaolinite was mixed using a trowel after weighing the constituents. Then the mixture was sieved together through No.30 (0.600 mm) sieve to obtain a more homogeneous blend. Obviously, the initial two steps are not performed for the natural soils. As mentioned in the previous sections, the swell tests were performed on soil samples having a predetermined initial moisture content and initial dry density. Therefore, after preparing the remolded soil samples to the required initial moisture content and dry density, the samples were wrapped into nylon bags and kept in desiccator for the provision of homogenous moisture distribution through the clay particles. The target initial density was achieved by compaction of the artificial as well as natural soil samples uniformly into the compaction mould in layers. The compaction mould and the soil sample were weighted to check if the desired amount of

density was reached. Then, by means of a hydraulic jack, sample was transferred into either the oedometer or the thin-wall ring (Figure 4.21). The height of the soil sample was selected to be 19 mm for conventional oedometer ring and 30 mm for thin-wall ring. For the thin-wall assembly, the necessary arrangements at the top and bottom were made to accord the midheight of the specimen with the strain gauges.

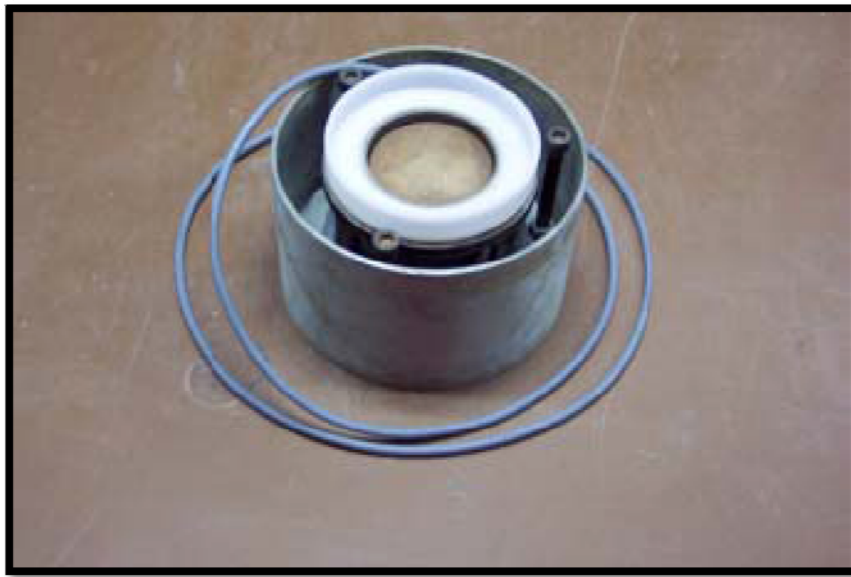


Figure 4. 21 Specimen Transferred into Thin-Wall Ring Ready to be Tested

Following this procedure ring was placed on the oedometer frame and connected with the data acquisition system for the untreated samples. For the treated samples however, a hole satisfying the replacement ratio is drilled at the centre of the sample by a hand auger (Figure 4.22) and the hole is then filled with granular material by hand as illustrated in Figures 4.23 and 4.24.



Figure 4. 22 Hole Opened inside Specimen to Construct Granular Column



Figure 4. 23 Placement of Granular Soil inside the Hole





Figure 4. 24 Hole Filled with Granular Soil

#### **4.3.2 Preparation of the Samples for Modified CBR Mould**

The clayey soil sample used inside the modified CBR mould was prepared by following the similar procedures performed for oedometer and thin-wall ring tests. Based on the fact that it is very hard to drill larger diameter holes inside the firmly compacted soil samples, cylindrical plugs were manufactured with diameters equal to that of holes beforehand. Clayey soil samples were placed around these cylindrical plugs and then compacted using a hydraulic jack system together with a special top cap manufactured for this purpose. Details of sample preparation for the Modified CBR moulds are given in Figures 4.25, 4.26 and 4.27.



Figure 4. 25 Placement of Sample inside Modified CBR Mould

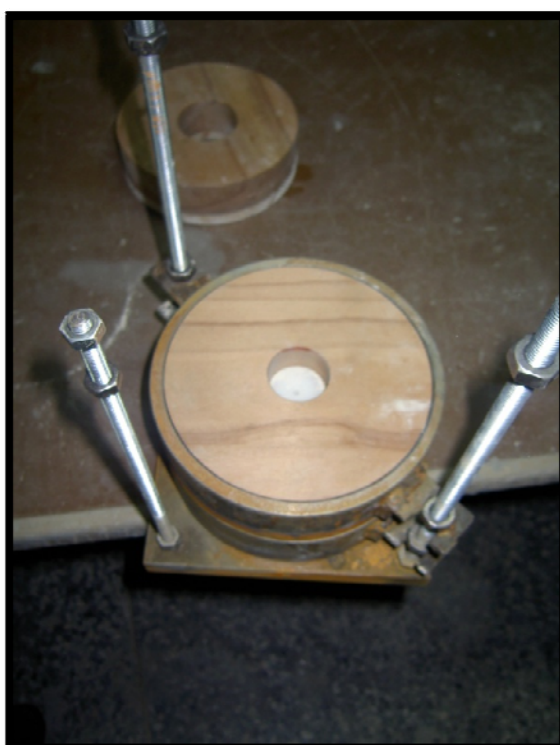


Figure 4. 26 Top Cap Placed inside CBR Mould for Compaction Purposes



Figure 4. 27 Sample Compacted inside CBR Mould

Following compaction of the specimen, the inner cylindrical plug was extracted from the sample with the help of a screw inserted inside the mould (Figure 4.28 and Figure 4.29). Similar to oedometer ring and thin-wall ring conducted with treated samples, the hole was manually filled with granular soil (Figure 4.30 and Figure 4.31). After this operation, a filter paper and top cap were placed on the mould (Figure 4.32) and test was started by inundating the specimen.



Figure 4. 28 Extraction of Cylindrical Mould from the Specimen



Figure 4. 29 Hole inside CBR Specimen





Figure 4. 30 Placement of Granular Material into Hole in CBR Sample



Figure 4. 31 Hole Filled with Granular Material in CBR Sample



Figure 4. 32 Top Cap Placed on CBR Specimen

#### **4.4 TEST SCHEDULE**

The possible positive effects of trenches and/or columns backfilled with granular material on the swelling potential of expansive soils is studied within the content of the extensive investigation program as presented below:

##### **Phase I:**

In this initial phase of the experiments, the efficiency of the proposed method as well as the effect of the particle size distribution of the granular fill material on the level of improvement was investigated. This phase involved a total of 65 conventional oedometer tests, for which the details are given in Table 4.8.

## **Phase II:**

The second phase of the test program was composed of modified CBR (48) tests) as well as conventional oedometer (43) tests, performed under different conditions listed in Table 4.8. The purpose of this phase was to investigate the effects of

- a) the seating pressure,
- b) the sample size (i.e. height and diameter) of the expansive soil
- c) the swell potential of expansive soil, and
- d) a light weight (1 to 2-storey) structure or a 1-meter surcharge layer

on the level of improvement attained by the proposed methodology.

## **Phase III:**

This phase of the test program was dedicated to the evaluation of silt as an alternative fill material for the trenches/columns, as well as a CNS (Cohesive Non-Swelling Soil) layer on top of the expansive soils. A total of 49 conventional oedometer tests were performed for this purpose, the details of which are given in Table 4.9.

## **Phase IV:**

This last phase of the experiments involved a total of 96 thin-wall oedometer tests performed on two different apparatus, namely the Ertekin's Ring (Ring-1) and the Avşar's Ring (Ring-2). The purpose of this phase was mainly to investigate

- a) the efficiency of the test apparatus mentioned above,
- b) the effect of granular material filled trenches or holes on level of improvement of lateral swell pressures,
- and
- c) the effect of a silt filled trench or hole on the level of improvement of lateral swell parameters.

The details of Phase IV experiments are given in Table 4.9, whereas the complete test program will be detailed in the next chapter with comprehensive explanations.

Table 4. 8 Test Schedule for Phase I and Phase II

INVESTIGATION DETAILS	PHASE 1	PHASE 2		
		Stage (a)	Stage (b)	Stage (c)
<b>Purpose</b>	Investigate the efficiency of the proposed method as well as the effect of granular particle size distribution on improvement level	(1) the effect of seating pressure (2) the effect of size of the expansive soil sample (3) the effect of swell potential of expansive soils involved (4) the effect of a light weight (1 to 2 storey) building or a 1-m surcharge layer on level of improvement	Investigate	
<b>Types of Soils Tested</b>	Type 2	Type 1 Type 2 Type 3	Type 1 Type 2 Type 3 Type 4 Type 5	Type 1 Type 2 Type 3 Type 4 Type 5
<b>Test Apparatus</b>	Conventional Oedometer	Modified CBR	Modified CBR Conventional Oedometer	Modified CBR Conventional Oedometer
<b>Granular Materials</b>	Sand and Fine Gravel	Medium Gravel	Medium Gravel (CBR) Fine Gravel (Conventional Oedometer)	Medium Gravel (CBR) Fine Gravel (Conventional Oedometer)
<b>Improvement Style</b>	Central Column	Central Column	Central Column	Central Column
<b>Test Types and No. of Tests</b>	Free Swell (16 tests) Swell Overburden (49 tests)	Free Swell (12 tests)	Free Swell - CBR (20 tests) Free Swell - Oedometer (25 tests)	Swell Overburden - CBR (15 tests) Swell Overburden - Oedometer (18 tests)
<b>Overburden Ranges</b>	7 kPa (Free Swell) 25-50-100-150 kPa (Swell Overburden)	1 kPa (as seating load)	7 kPa (as seating load)	25 kPa (as light weight building or 1 m fill)
<b>Area Replacement Ratio Range</b>	5%, 10%, 20%	10%, 20%, 30%	10%, 20%, 30%	10%, 20%, 30%



Table 4. 9 Test Schedule for Phase III and Phase IV

INVESTIGATION DETAILS	PHASE 3	PHASE 4			
		Stage (a)	Stage (b)	Stage (c)	Stage (d)
<b>Purpose</b>	Investigate the effect of a silt layer and/or a silt filled trench/hole on level of improvement	Investigate (1) the efficiency of the two thin wall oedometer test apparatus involved in the research program (2) the effect of granular material filled trenches on level of improvement of lateral swell pressures (3) the effect of a silt layer and/or a silt filled trench/hole on level of improvement			
<b>Types of Soils Tested</b>	Type 5	Type 3 Type 5 Thin Wall Ring	Type 3	Type 5	Type 5
<b>Test Apparatus</b>	Conventional Oedometer	Thin Wall Ring (for Type 3 - Ring-1 Ertekin Ring) (for Type 5- Ring-1 Ertekin & Ring-2 Avşar Rings)	Thin Walled Ring (Ring-1 Ertekin Ring)	Thin Wall Ring (Ring-1 Ertekin & Ring-2 Avşar Rings)	Thin Wall Ring (Ring-1 Ertekin & Ring-2 Avşar Rings)
<b>Granular Materials</b>	Silt	N/A	Fine Gravel	Fine Gravel	Silt
<b>Improvement Style</b>	Central Column and Overlay (CNS)	N/A	Central Column	Central Column	Central Column
<b>Test Types and No. of Tests</b>	Free Swell (26 tests) Swell Overburden (23 tests)	Free Swell (6 tests) Swell Overburden (22 tests)	Free Swell (6 tests) Swell Overburden (18 tests)	Free Swell (16 tests) Swell Overburden (16 tests)	Free Swell (16 tests)
<b>Overburden Ranges</b>	7 kPa (Free Swell) 25 kPa (Swell Overburden)	7 kPa (Free Swell) 25-50-100-150 kPa (Swell Overburden)	7 kPa (Free Swell) 25-50-100 kPa (Swell Overburden)	7 kPa (Free Swell) 25 kPa (Swell Overburden)	7 kPa
<b>Area Replacement Ratio Range</b>	10%, 20%, 30%	N/A	5%, 10%	10%, 20%, 30%	10%, 20%, 30%

## **CHAPTER V**

### **TEST RESULTS**

#### **5.1 GENERAL**

The effects of trenches and/or columns backfilled with granular material such as; crushed stone or rock, on the swelling potential of expansive soils, is studied in four phases. While each phase was aimed to reach a useful finding on its own section about the subject, they also enlightened the possible investigation subjects and main targets for the next phases. The results of each phase are presented in the next sections, whereas their findings and discussions are given in Chapter VI.

#### **5.2 EFFICIENCY OF THE METHOD AND EFFECT OF GRADATION ON PERFORMANCE (PHASE 1)**

In the first phase of the investigations, the efficiency of treatment of expansive soils by introducing a trench or hole and filling it with granular material was investigated. Conventional oedometer tests were performed on both untreated and treated samples of Type-2 clay (i.e. artificial sample composed from 15% bentonite and 85% kaolinite) for this purpose. Tests on samples were performed with an initial moisture content of 15 % and dry density of  $1.5 \text{ g/cm}^3$ . Based on the fact that the grain size distribution as well as the physical properties of the granular soils may have a major influence on the effectiveness of treatment, a poorly graded fine to medium coarse sand and poorly graded fine gravel were used as granular fill material during the first phase of investigations. The trenches were modeled by opening holes with diameters that satisfy area replacement ratios of 5%, 10% and 20%. Both sand and gravel were placed inside holes in a

loose to medium dense state with a relative density of 40%. Free Swell Tests with 7 kPa seating pressure and Swell Overburden Tests, with 25, 50, 100, and 150 kPa pressures, were conducted during the experiments.

### 5.2.1 Free Swell Tests

The results of the free swell tests performed with sand material and gravel material are presented in Table 5.1 and Table 5.2 whereas vertical swell percentage versus time relationships for the related tests are presented in Figure 5.1 for sand material and in Figure 5.2 for gravel material respectively.

After the primary swell was accomplished, the specimen were loaded in accordance with the pressure increments as performed in conventional oedometer tests until they were recompressed to their initial void ratio. The void ratio vs. logarithm of pressure graphs determined from the loading stage of free swell tests for the determination of swell pressures are presented in Figure 5.3 for sand material and Figure 5.4 for gravel material, respectively.

Table 5. 1 Results of Free Swell Tests Performed with Sand Material (Phase-1)

Test No	Area Replacement Ratio, ARR (%)	Final Water Content, $w_f$ (%)	Vertical Swell, $S_v$ (%)	Average Vertical Swell, $S_{v(av)}$ (%)
OE-FS-101	0	45.6	34.6	34.0
OE-FS-102	0	46.9	35.5	
OE-FS-103	0	44.8	32.1	
OE-FS-104	5	51.4	31.2	31.5
OE-FS-105	5	54.9	31.8	
OE-FS-106	10	54.8	29.1	29.2
OE-FS-107	10	53.1	29.3	
OE-FS-108	20	53.7	26.2	26.1
OE-FS-109	20	52.6	26.0	

Table 5. 2 Results of Free Swell Tests Performed with Gravel Material  
(Phase-1)

Test No	Area Replacement Ratio, ARR (%)	Final Water Content, $w_f$ (%)	Vertical Swell, $S_v$ (%)	Average Vertical Swell, $S_{v(av)}$ (%)
OE-FS-101	0	45.6	34.6	34.0
OE-FS-102	0	46.9	35.5	
OE-FS-103	0	44.8	32.1	
OE-FS-204	5	47.4	27.4	28.5
OE-FS-205	5	51.0	29.7	
OE-FS-206	10	47.7	29.2	25.9
OE-FS-207	10	48.8	22.9	
OE-FS-208	10	46.1	25.5	
OE-FS-209	20	49.9	17.4	18.1
OE-FS-210	20	51.4	18.8	

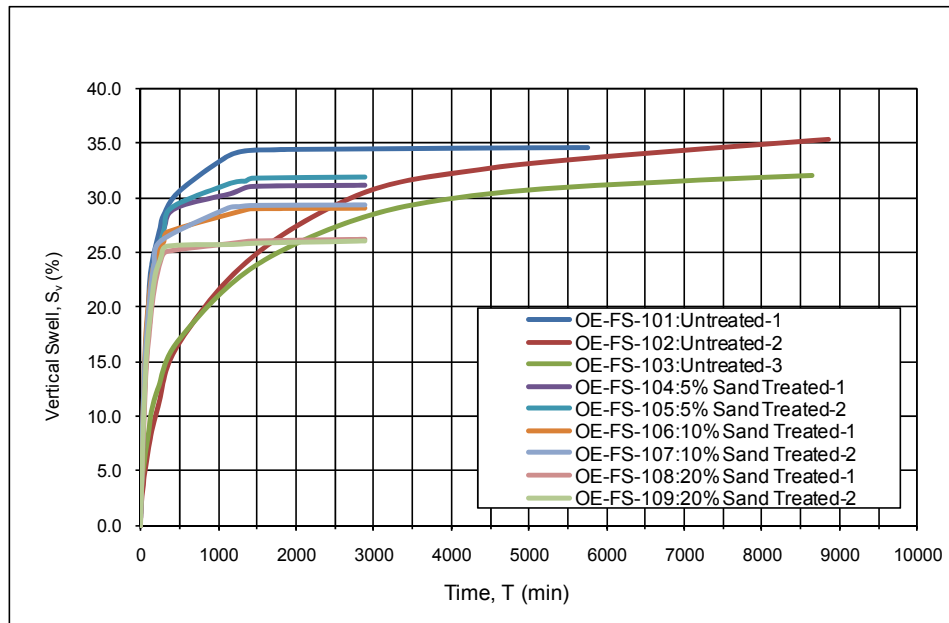


Figure 5. 1 Vertical Swell Percentage vs. Time Relationship for Oedometer Tests Performed with Free Swell Testing Technique on Type-2 Expansive Soil Samples Treated with Sand

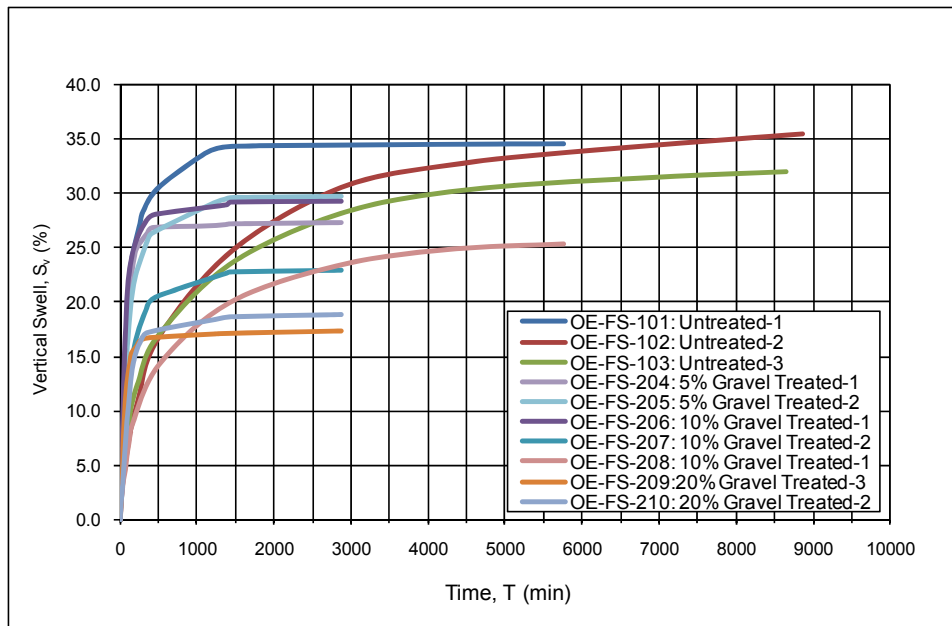


Figure 5.2 Vertical Swell Percentage vs. Time Relationship for Oedometer Tests Performed with Free Swell Testing Technique on Type-2 Expansive Soil Samples Treated with Gravel

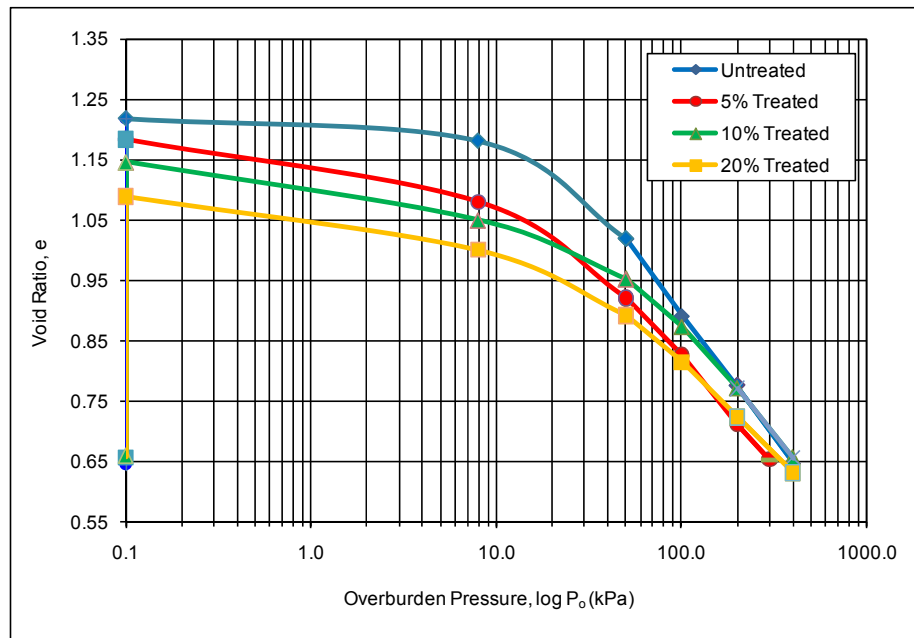


Figure 5.3 Void Ratio vs. Overburden Pressure Graphs Determined from the Loading Stage of Free Swell Tests Performed with Type-2 Soil Treated by Sand Material.

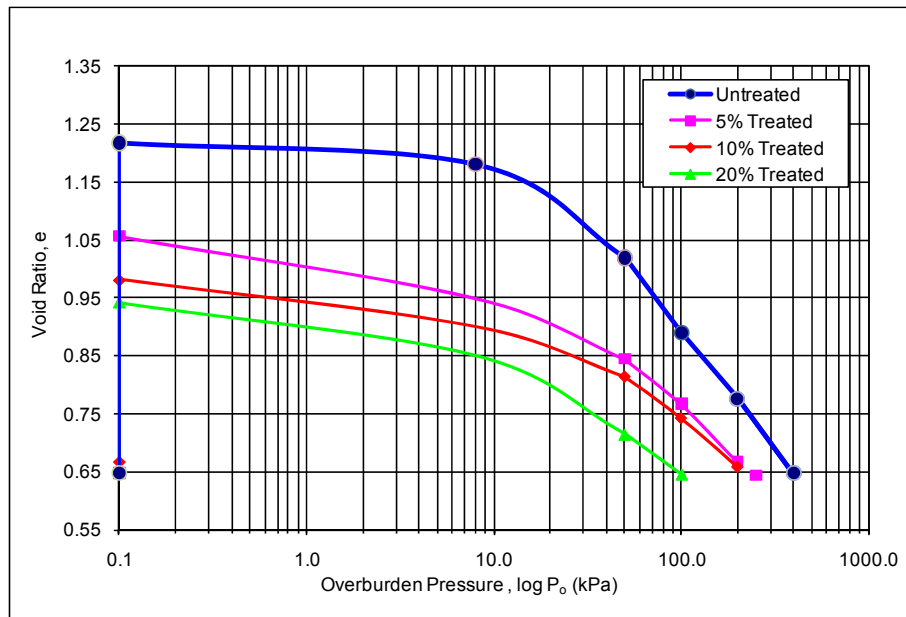


Figure 5. 4 Void Ratio vs. Overburden Pressure Graphs Determined from the Loading Stage of Free Swell Tests Performed with Type-2 Soil Treated by Gravel Material.

The vertical swell pressures calculated by means of Figure 5.3 and Figure 5.4 are presented in Table 5.3 for different area replacement ratios.

Table 5. 3 Vertical Swell Pressure,  $P_v$  (kPa) with respect to Material Type and Area Replacement Ratio Obtained from Free Swell Tests (Phase-1)

Material Type	Area Replacement Ratio, ARR (%)			
	0	5	10	20
Sand	400 kPa	300 kPa	390 kPa	325 kPa
Gravel		230 kPa	185 kPa	90 kPa

### 5.1.2 Swell Overburden Tests

The results and comparison of the swell overburden tests performed with sand material and gravel material are presented in Table 5.3 and Table 5.4 whereas

vertical swell percentage versus time relationships for the related tests are presented in Figures 5.5 to 5.8 for sand material and in Figures 5.9 to 5.12 for gravel material. The swell percentage vs. overburden pressure relationships for oedometer tests performed with swell overburden testing technique on Type-2 expansive soils are presented in Figure 5.13 and Figure 5.14 whereas the vertical swell pressures corresponding to each area replacement ratio calculated from swell overburden tests are presented in Table 5.6.

Table 5. 4 Results of Swell Overburden Tests Performed with Sand Material (Phase-1)

Test No	Overburden Pressure, $P_o$ (kPa)	Area Replacement Ratio, ARR (%)	Final Water Content, $w_f$ (%)	Vertical Swell, $S_v$ (%)	Average Vertical Swell, $S_{v(av)}$ (%)
OE-SO-101	25	0	37.4	12.3	13.7
OE-SO-102	25	0	42.9	15.0	
OE-SO-103	25	0	39.1	13.9	
OE-SO-104	25	5	45.1	13.5	12.8
OE-SO-105	25	5	43.9	12.1	
OE-SO-106	25	10	46.0	13.2	13.1
OE-SO-107	25	10	46.5	12.9	
OE-SO-108	25	20	49.4	10.1	9.9
OE-SO-109	25	20	49.6	9.6	
OE-SO-110	50	0	37.8	9.4	8.9
OE-SO-111	50	0	38.8	8.4	
OE-SO-112	50	5	40.3	8.8	8.0
OE-SO-113	50	5	39.7	7.1	
OE-SO-114	50	10	42.7	8.0	7.8
OE-SO-115	50	10	42.3	7.6	
OE-SO-116	50	20	46.2	7.2	7.2
OE-SO-117	50	20	46.0	7.2	
OE-SO-118	100	0	36.4	4.4	4.5
OE-SO-119	100	0	36.3	4.5	
OE-SO-120	100	5	37.6	4.4	4.0
OE-SO-121	100	5	37.5	3.5	
OE-SO-122	100	10	39.8	4.3	4.1
OE-SO-123	100	10	39.6	4.0	
OE-SO-124	100	20	41.9	3.6	3.3
OE-SO-125	100	20	42.8	3.0	
OE-SO-126	150	0	34.2	4.0	3.8
OE-SO-127	150	0	34.5	3.5	
OE-SO-128	150	5	36.2	3.0	3.2
OE-SO-129	150	5	36.0	3.3	
OE-SO-130	150	10	38.2	3.0	3.0
OE-SO-131	150	10	37.5	3.0	
OE-SO-132	150	20	41.6	1.3	1.6
OE-SO-133	150	20	41.6	1.9	

Table 5. 5 Results of Swell Overburden Tests Performed with Gravel Material (Phase-1)

Test No	Overburden Pressure, $P_o$ (kPa)	Area Replacement Ratio, ARR (%)	Final Water Content, $w_f$ (%)	Vertical Swell, $S_v$ (%)	Average Vertical Swell, $S_{v(av)}$ (%)
OE-SO-101	25	0	37.4	12.3	13.7
OE-SO-102	25	0	42.9	15.0	
OE-SO-103	25	0	39.1	13.9	
OE-SO-204	25	5	40.2	10.5	11.1
OE-SO-205	25	5	39.7	11.8	
OE-SO-206	25	10	40.3	9.3	9.7
OE-SO-207	25	10	41.0	10.1	
OE-SO-208	25	20	41.7	6.1	6.2
OE-SO-209	25	20	42.9	6.4	
OE-SO-110	50	0	37.8	9.4	8.9
OE-SO-111	50	0	38.8	8.4	
OE-SO-212	50	5	37.9	6.5	5.9
OE-SO-213	50	5	38.3	5.3	
OE-SO-214	50	10	38.2	5.6	5.7
OE-SO-215	50	10	39.8	5.8	
OE-SO-216	50	20	38.5	3.4	3.4
OE-SO-118	100	0	36.4	4.4	4.5
OE-SO-119	100	0	36.3	4.5	
OE-SO-220	100	5	35.2	3.1	3.1
OE-SO-222	100	10	36.1	2.2	2.2
OE-SO-224	100	20	37.1	0.9	0.9
OE-SO-126	150	0	34.2	4.0	3.8
OE-SO-127	150	0	34.5	3.5	
OE-SO-228	150	5	34.6	1.3	1.3
OE-SO-230	150	10	34.5	0.8	0.8

Table 5. 6 Vertical Swell Pressure,  $P_v$  (kPa) with respect to Material Type and Area Replacement Ratio Obtained from Swell Overburden Tests (Phase-1)

Material Type	Area Replacement Ratio, ARR (%)			
	0	5	10	20
Sand	251 kPa	233 kPa	226 kPa	210 kPa
Gravel		179 kPa	164 kPa	124 kPa



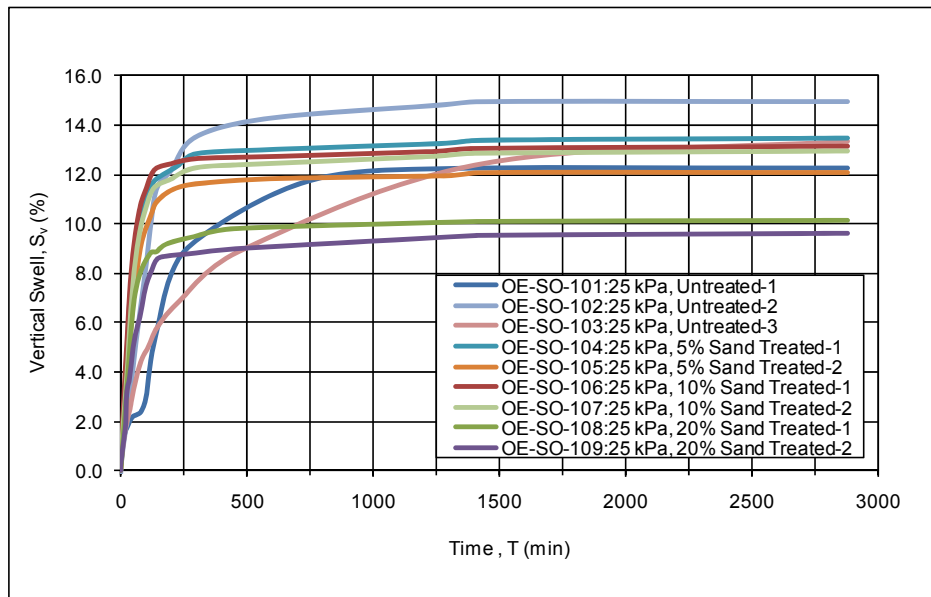


Figure 5.5 Vertical Swell Percentage vs. Time Relationship for Oedometer Tests Performed with Swell Overburden Testing Technique on Type-2 Expansive Soil Samples Treated with Sand ( $P_0=25$  kPa)

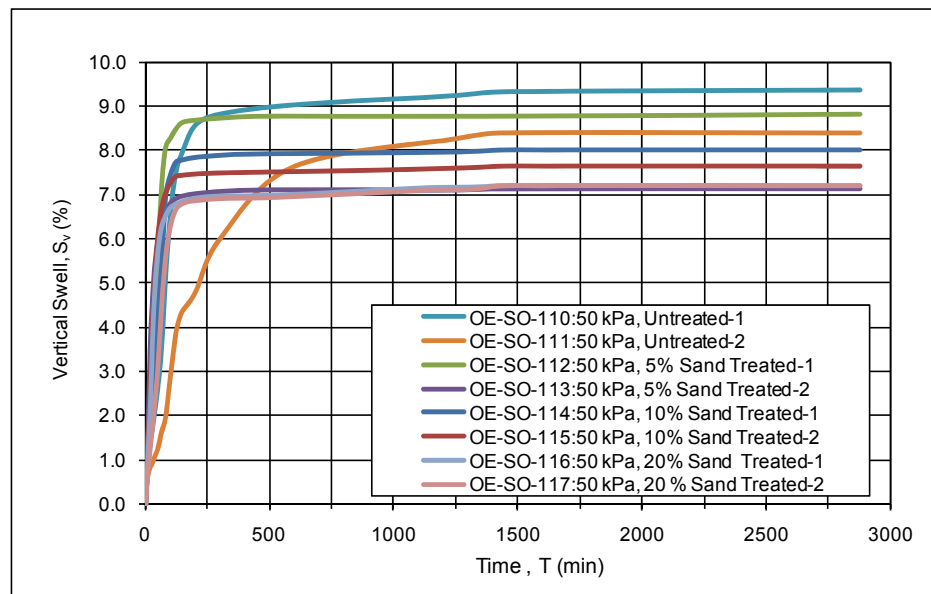


Figure 5.6 Vertical Swell Percentage vs. Time Relationship for Oedometer Tests Performed with Swell Overburden Testing Technique on Type-2 Expansive Soil Samples Treated with Sand ( $P_0 =50$  kPa)

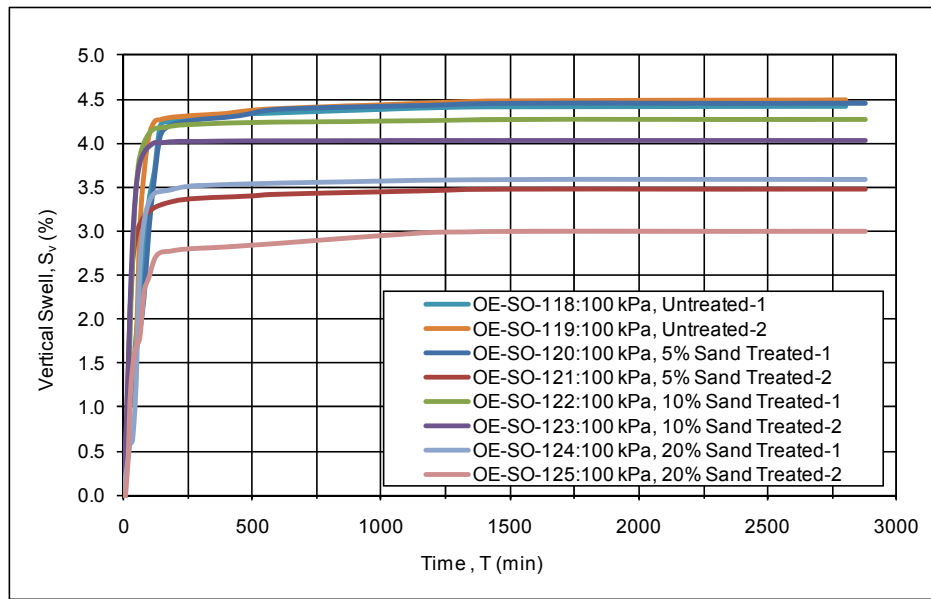


Figure 5. 7 Vertical Swell Percentage vs. Time Relationship for Oedometer Tests Performed with Swell Overburden Testing Technique on Type-2 Expansive Soil Samples Treated with Sand ( $P_o = 100$  kPa)

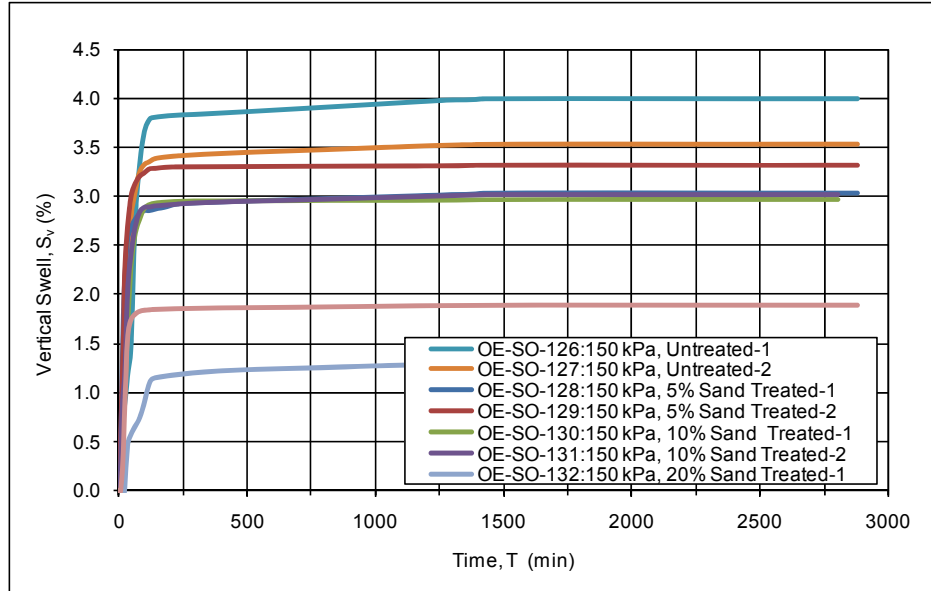


Figure 5. 8 Vertical Swell Percentage vs. Time Relationship for Oedometer Tests Performed with Swell Overburden Testing Technique on Type-2 Expansive Soil Samples Treated with Sand ( $P_o = 150$  kPa)

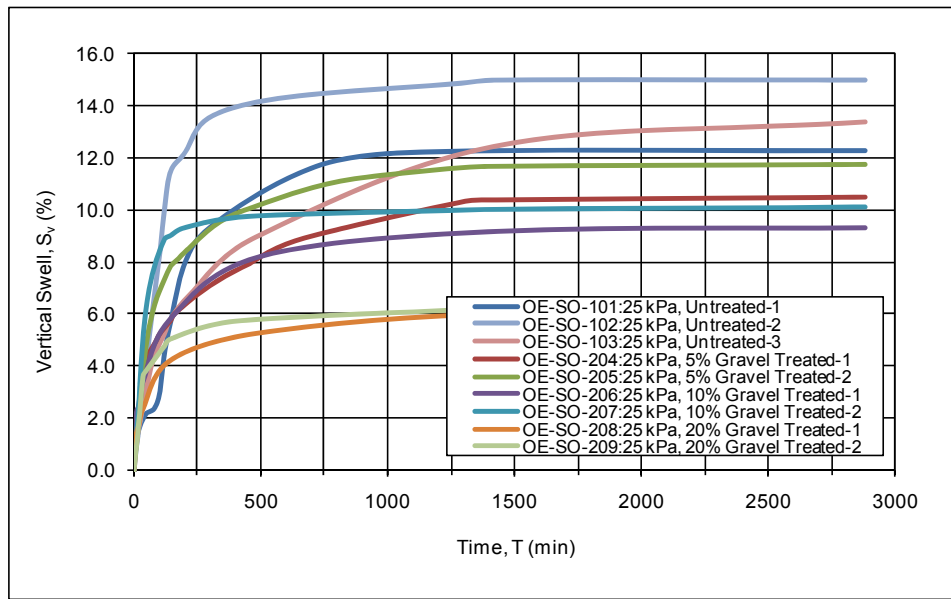


Figure 5. 9 Vertical Swell Percentage vs. Time Relationship for Oedometer Tests Performed with Swell Overburden Testing Technique on Type-2 Expansive Soil Samples Treated with Gravel ( $P_o = 25$  kPa)

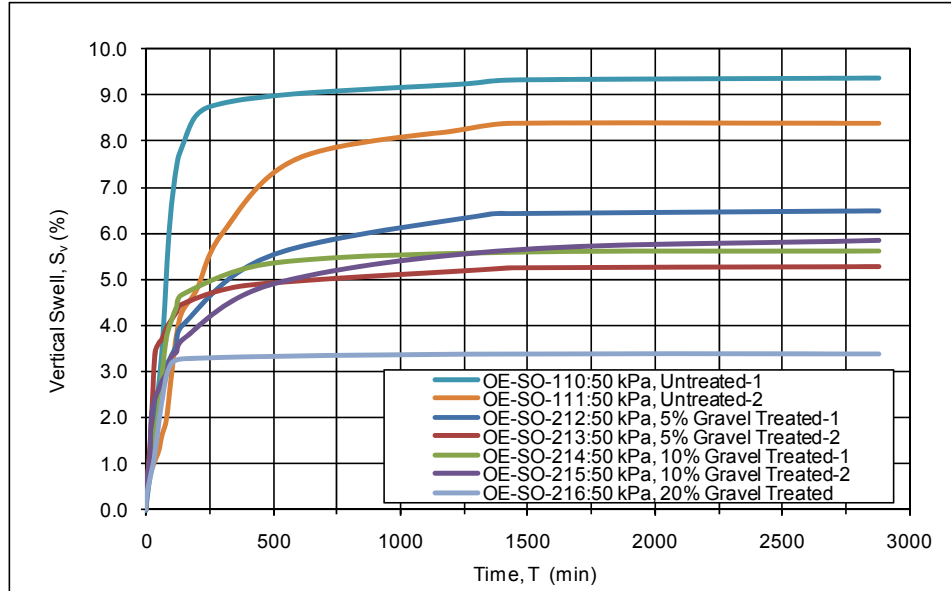


Figure 5. 10 Vertical Swell Percentage vs. Time Relationship for Oedometer Tests Performed with Swell Overburden Testing Technique on Type-2 Expansive Soil Samples Treated with Gravel ( $P_o = 50$  kPa)

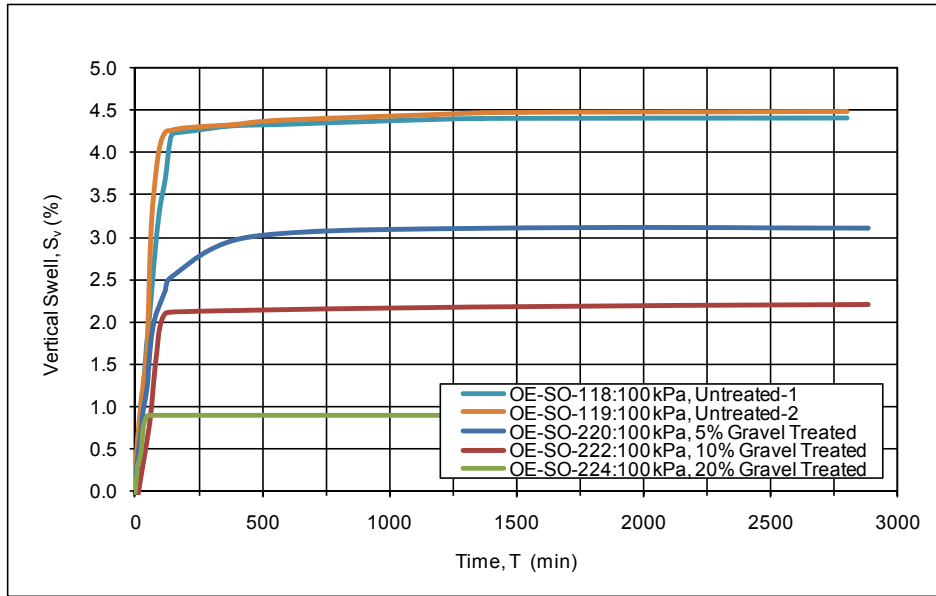


Figure 5. 11 Vertical Swell Percentage vs. Time Relationship for Oedometer Tests Performed with Swell Overburden Testing Technique on Type-2 Expansive Soil Samples Treated with Gravel ( $P_o = 100$  kPa)

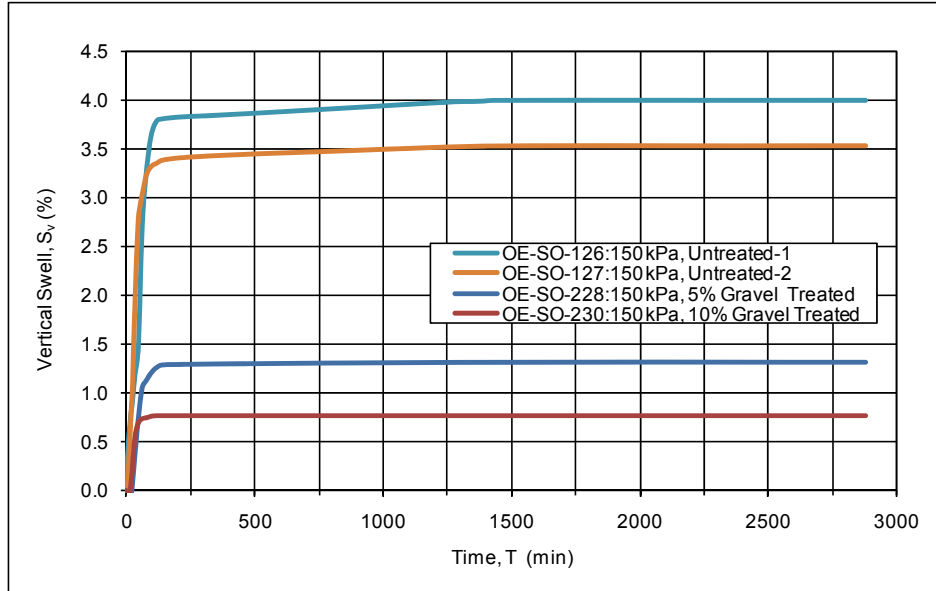


Figure 5. 12 Vertical Swell Percentage vs. Time Relationship for Oedometer Tests Performed with Swell Overburden Testing Technique on Type-2 Expansive Soil Samples Treated with Gravel ( $P_o = 150$  kPa)

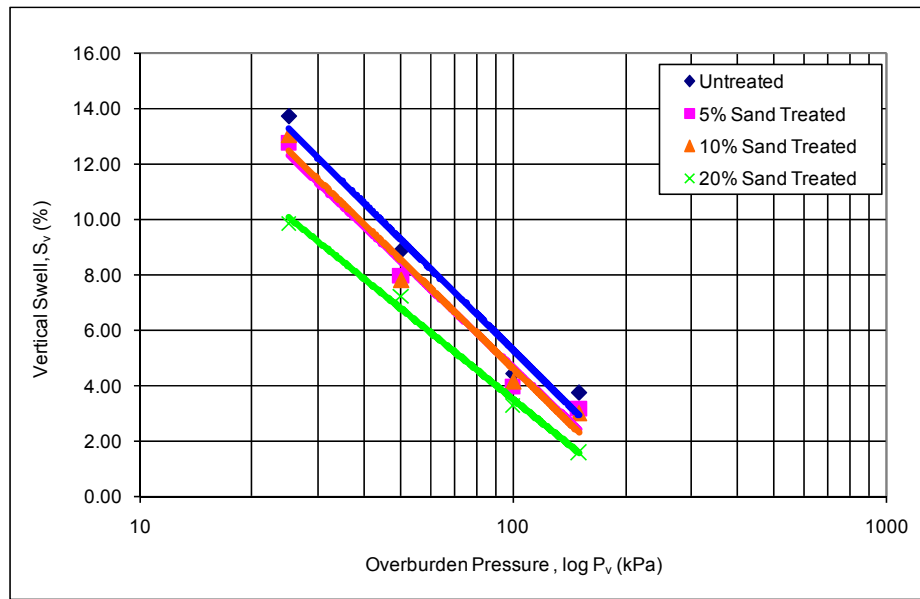


Figure 5. 13 Vertical Swell Percentage vs. Overburden Pressure for Oedometer Tests Performed with Swell Overburden Testing Technique on Type-2 Expansive Soil Samples Improved by Sand



Figure 5. 14 Vertical Swell Percentage vs. Overburden Pressure for Oedometer Tests Performed with Swell Overburden Testing Technique on Type-2 Expansive Soil Samples Improved by Gravel

## **5.2 EFFECT OF CLAY TYPE AND SAMPLE SIZE (PHASE.2)**

Since it was observed from the first phase of the investigations that treatment of expansive soils is possible via introducing a percent replacement of the soil by a granular fill, it was decided to enlarge the investigation by checking out the performance of treatment for different expansive soil types and dimensions. In addition, since the treatment with gravel, having a larger particle size compared to sand, gave more satisfactory treatment percentages in the first phase of the investigations, it was decided to use gravel as filling material for the next stages of the tests.

Based on the above facts, it is intended to evaluate the effect of sample size and the index properties of expansive soils on the level of improvement of expansive soils treated with granular trenches and/or columns in the second phase of the investigations. The effect of preferred seating pressure quantity as well as additional surcharge load on the improvement percentage was also decided to be investigated at this stage of the studies. Since this phase of the investigation involved several purposes, it was divided into subgroups and the results of each subgroup are presented in the subsections below.

### **5.2.1 Stage (a) Tests**

This stage of investigation was intended to study the suitability and efficiency of an apparatus designed to investigate the scale effects of soil samples. A modified CBR mould was used as an alternative to oedometer tests and three artificially prepared samples (i.e. Type-1, 2 and 3) were tested for this purpose. According to ASTM (ASTM D4546-08, 2008), a vertical seating pressure of at least 1 kPa shall be applied at the beginning of the free swell tests. Australian Standard (AS1289.7.1.1-2003, 2003) clearly defines it and suggests monitoring the swell amount after the specimen is loaded under a pressure of 25 kPa unless a larger overburden is present over the soil sample. Sridharan et al. (1986) on the other hand recommends a seating pressure of 1 psi ( $\approx 7$  kPa) for this purpose. In the

light of the knowledge that 1 kPa of pressure is generally satisfied by the weight of the loading cap and porous stone, no additional load was applied on samples at this stage of the tests, in order to compare with the results of tests performed at the next stages of the investigation with a seating pressure of 7 kPa.

A total of 12 tests were carried out with medium gravel material selected for modified CBR moulds with area replacement ratios of 10, 20 and 30%. Both three types of soils were prepared with an initial moisture content of 15 % and dry density of  $1.5 \text{ g/cm}^3$ . Similar to Phase 1 investigations, gravel was placed inside holes in a loose to medium dense state with a relative density of 40%. The results of the tests are presented in Table 5.7. Vertical swell versus time relationships for the tests performed at this stage of the investigations are presented in Figure 5.15, Figure 5.16 and Figure 5.17.

Table 5. 7 Modified CBR Mould Test Results with Seating Pressure of 1 kPa  
(Phase-2, Stage (a))

Test No	Soil Type	Area Replacement Ratio, ARR (%)	Final Water Content, $w_f$ (%)	Vertical Swell, $S_v$ (%)
CBR-F1-101	Type-1	0	66.0	42.5
CBR-F1-102	Type-1	10	64.0	35.2
CBR-F1-103	Type-1	20	65.4	26.4
CBR-F1-104	Type-1	30	66.6	19.1
CBR-F1-105	Type-2	0	67.3	62.3
CBR-F1-106	Type-2	10	63.3	53.2
CBR-F1-107	Type-2	20	64.6	41.4
CBR-F1-108	Type-2	30	63.1	34.2
CBR-F1-109	Type-3	0	73.3	72.9
CBR-F1-110	Type-3	10	77.5	61.9
CBR-F1-111	Type-3	20	81.8	51.0
CBR-F1-112	Type-3	30	83.3	41.4

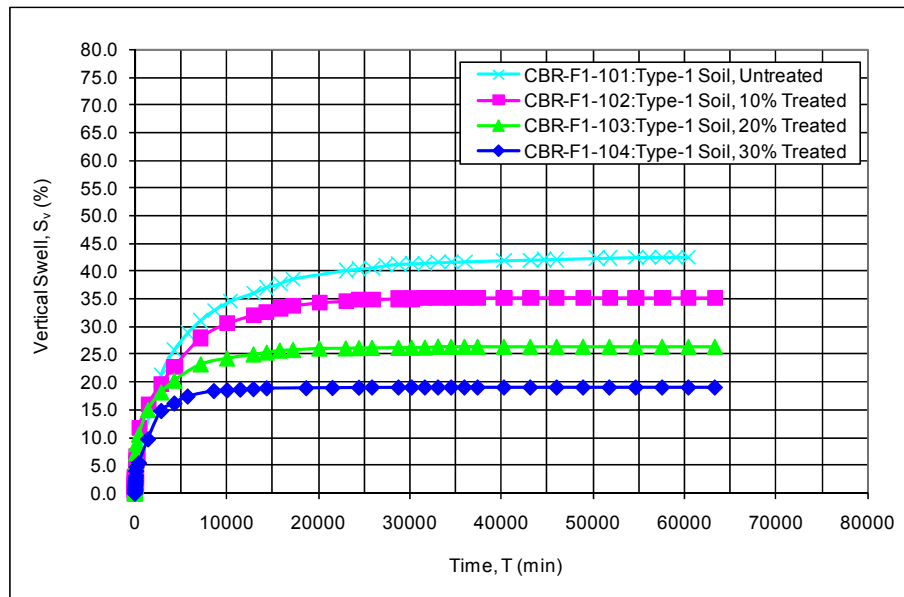


Figure 5. 15 Vertical Swell Percentage vs. Time Relationship for Modified CBR Mould Tests Performed with Free Swell Testing Technique ( $P_s=1$  kPa) on Type-1 Expansive Soil Samples Treated with Gravel

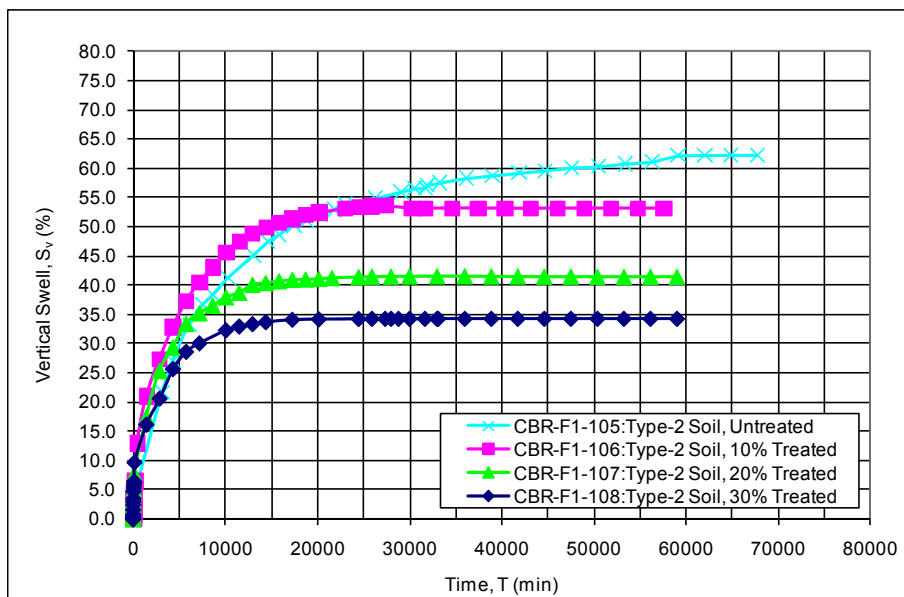


Figure 5. 16 Vertical Swell Percentage vs. Time Relationship for Modified CBR Mould Tests Performed with Free Swell Testing Technique ( $P_s=1$  kPa) on Type-2 Expansive Soil Samples Treated with Gravel



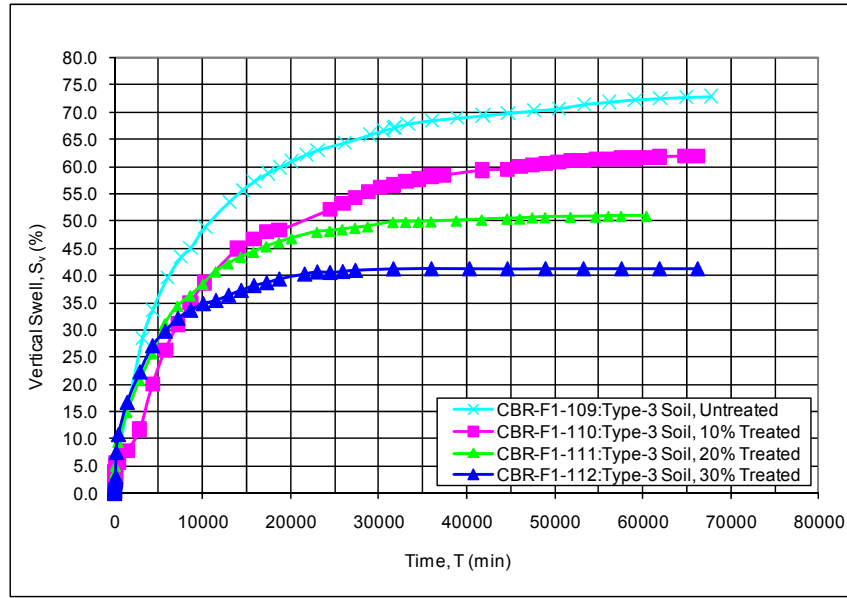


Figure 5. 17 Vertical Swell Percentage vs. Time Relationship for Modified CBR Mould Tests Performed with Free Swell Testing Technique ( $P_s=1$  kPa) on Type-3 Expansive Soil Samples Treated with Gravel

### 5.2.2 Stage (b) Tests

The second stage of Phase-2 investigations was dedicated to investigate the effect of soil properties as well as the area replacement ratio on the treatment percentage attained by opening trenches and backfilling them with granular material. Besides, the scale effect was also evaluated in this stage of the investigations.

Free swell tests with 7 kPa seating pressure were performed with modified CBR moulds and oedometer cells on five different soil samples treated with 10, 20 and 30% gravel. The relative density of the granular soil was once more selected as 40%. The granular soil sample used during the conventional oedometer tests was fine gravel, while coarse gravel was used for modified CBR mould tests. Tests on artificially prepared samples and Gazi Clay (Types 1 to 4) were performed on samples with initial moisture content of 15 % and dry density of  $1.5 \text{ g/cm}^3$

whereas Esenboğa sample was prepared with an initial moisture content of 15 % and a dry density of 1.2 g/cm<sup>3</sup>.

This stage involved a total number of 20 tests on CBR moulds and 25 tests on oedometer cells for which the details are presented in Table 5.8 for modified CBR moulds and in Table 5.9 for oedometer tests. Vertical swell versus time relationships for the mentioned tests are presented in Figures 5.18 to 5.27.

Table 5. 8 Modified CBR Mould Test Results Performed with Free Swell Testing Technique ( $P_s=7$  kPa) (Phase-2, Stage (b))

Test No	Soil Type	Area Replacement Ratio, ARR (%)	Final Water Content, $w_f$ (%)	Vertical Swell, $S_v$ (%)
CBR-FS-201	Type-1	0	36.9	19.0
CBR-FS-202	Type-1	10	39.3	14.3
CBR-FS-203	Type-1	20	42.2	10.3
CBR-FS-204	Type-1	30	45.4	5.3
CBR-FS-205	Type-2	0	39.2	28.0
CBR-FS-206	Type-2	10	39.7	22.6
CBR-FS-207	Type-2	20	44.6	17.0
CBR-FS-208	Type-2	30	46.1	11.9
CBR-FS-209	Type-3	0	49.8	35.4
CBR-FS-210	Type-3	10	52.9	28.4
CBR-FS-211	Type-3	20	59.8	21.1
CBR-FS-212	Type-3	30	65.1	14.9
CBR-FS-213	Type-4	0	31.2	4.5
CBR-FS-214	Type-4	10	34.1	3.5
CBR-FS-215	Type-4	20	35.2	2.9
CBR-FS-216	Type-4	30	36.3	2.0
CBR-FS-217	Type-5	0	73.1	37.2
CBR-FS-218	Type-5	10	77.4	30.8
CBR-FS-219	Type-5	20	83.6	23.4
CBR-FS-220	Type-5	30	86.9	18.2

Table 5.9 Oedometer Test Results Performed with Free Swell Testing Technique ( $P_s=7$  kPa) (Phase-2, Stage(b))

Soil Type	Test No	Reference Tests	Area Replacement Ratio, ARR (%)	Final Water Content, $w_f$ (%)	Vertical Swell, $S_v$ (%)
Type-1	OE-FS-301	-	0	42.1	23.2
	OE-FS-302	-	10	43.4	16.9
	OE-FS-303	-	20	40.4	11.2
	OE-FS-304	-	30	44.5	7.9
Type-2	OE-FS-305*	OE-FS-101	0	45.6	34.0
		OE-FS-102		46.9	
		OE-FS-103		44.8	
	OE-FS-306*	OE-FS-206	10	47.7	25.9
		OE-FS-207		48.8	
		OE-FS-208		46.1	
	OE-FS-307*	OE-FS-209	20	49.9	18.1
		OE-FS-210		51.4	
	OE-FS-308	-	30	51.0	13.1
	OE-FS-309	-	0	55.7	39.4
Type-3	OE-FS-310	-	10	56.1	31.0
	OE-FS-311	-	20	57.0	23.0
	OE-FS-312	-	30	58.1	18.0
	OE-FS-313	-	0	31.1	4.4
Type-4	OE-FS-314	-	10	31.4	3.9
	OE-FS-315	-	20	33.4	3.4
	OE-FS-316	-	30	37.7	3.0
	OE-FS-317	-	0	78.5	41.5
Type-5	OE-FS-318	-	0	82.0	
	OE-FS-319	-	0	78.7	
	OE-FS-320	-	0	75.6	
	OE-FS-321	-	0	78.0	
	OE-FS-322	-	0	76.2	
	OE-FS-323	-	0	80.9	
	OE-FS-324	-	10	82.2	31.5
	OE-FS-325	-	10	85.9	
	OE-FS-326	-	20	87.5	26.2
	OE-FS-327	-	20	91.5	
	OE-FS-328	-	30	96.2	20.7

\* These test results are the averages calculated from the values observed during the first phase of investigations. According to this, OE-FS-305 results are the averages of OE-FS-101, 102 and 103, OE-FS-306 results are the averages of OE-FS-206, 207 and 208, and OE-FS-307 results are the averages of OE-FS-209 and 210.

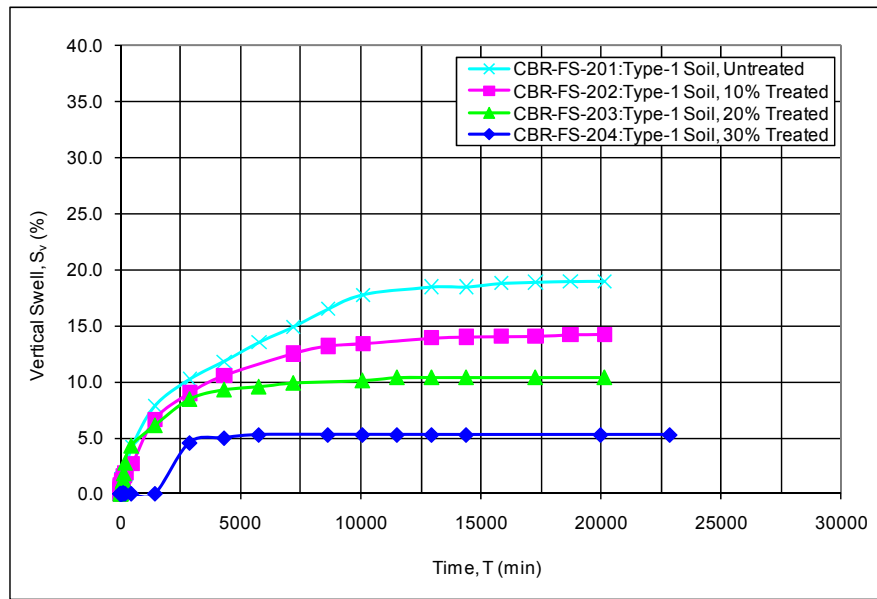


Figure 5. 18 Vertical Swell Percentage vs. Time Relationship for Modified CBR Mould Tests Performed with Free Swell Testing Technique ( $P_s=7$  kPa) on Type-1 Expansive Soil Samples Treated with Gravel

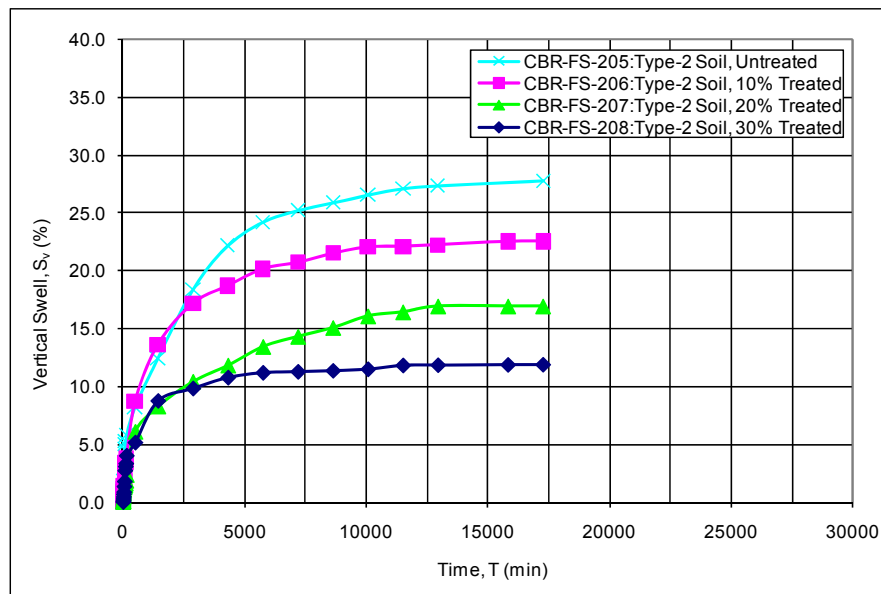


Figure 5. 19 Vertical Swell Percentage vs. Time Relationship for Modified CBR Mould Tests Performed with Free Swell Testing Technique ( $P_s=7$  kPa) on Type-2 Expansive Soil Samples Treated with Gravel

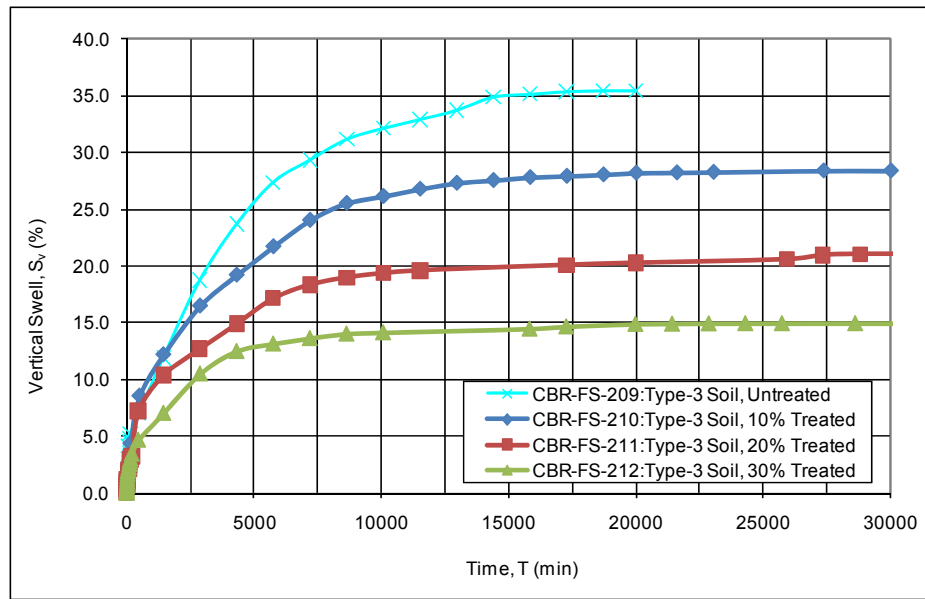


Figure 5. 20 Vertical Swell Percentage vs. Time Relationship for Modified CBR Mould Tests Performed with Free Swell Testing Technique ( $P_s=7$  kPa) on Type-3 Expansive Soil Samples Treated with Gravel

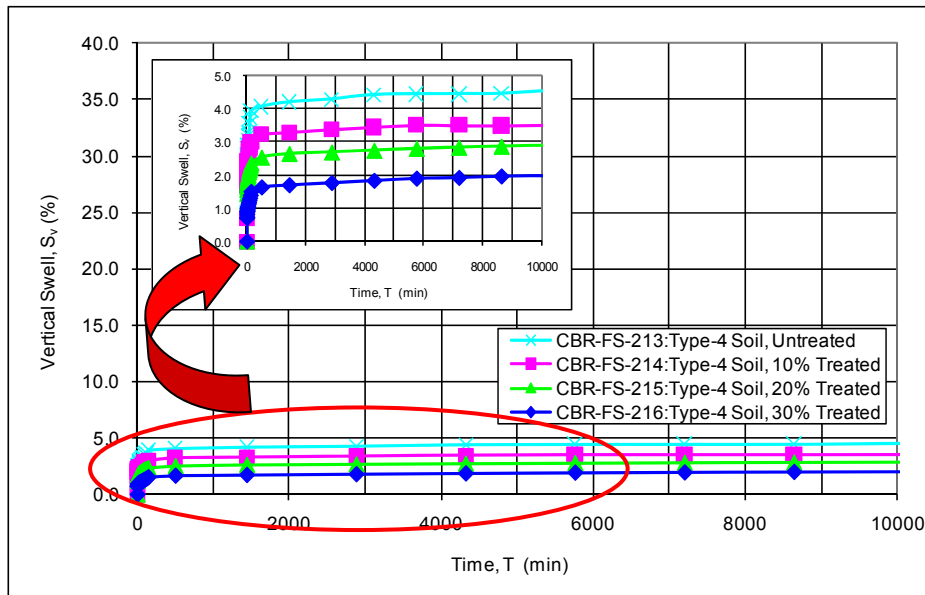


Figure 5. 21 Vertical Swell Percentage vs. Time Relationship for Modified CBR Mould Tests Performed with Free Swell Testing Technique ( $P_s=7$  kPa) on Type-4 Expansive Soil Samples Treated with Gravel

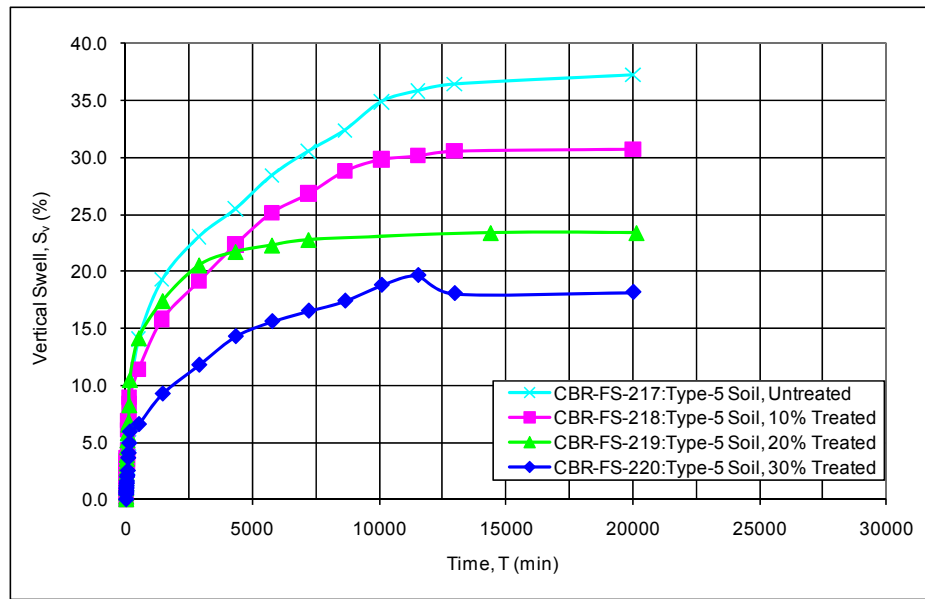


Figure 5.22 Vertical Swell Percentage vs. Time Relationship for Modified CBR Mould Tests Performed with Free Swell Testing Technique ( $P_s=7$  kPa) on Type-5 Expansive Soil Samples Treated with Gravel

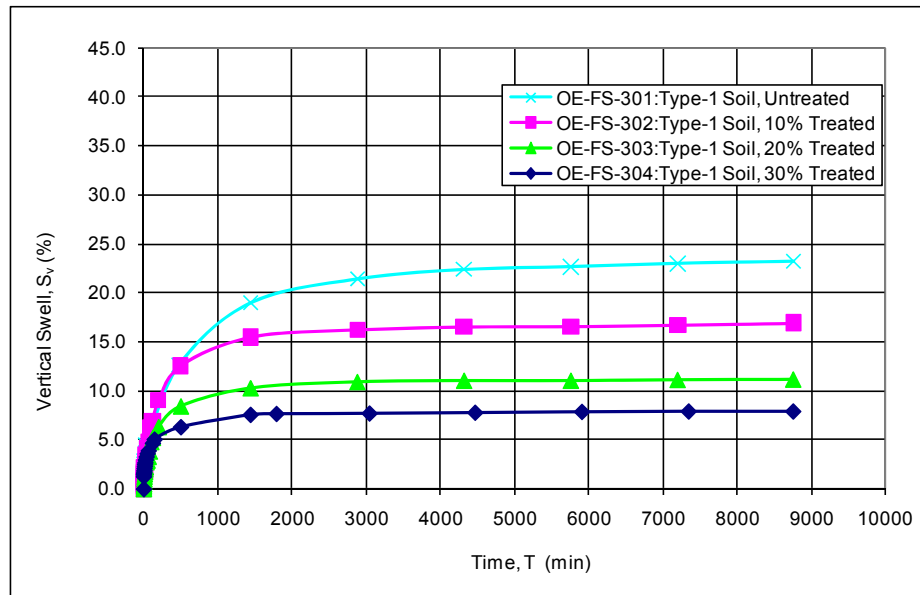


Figure 5.23 Vertical Swell Percentage vs. Time Relationship for Oedometer Tests Performed with Free Swell Testing Technique ( $P_s=7$  kPa) on Type-1 Expansive Soil Samples Treated with Gravel

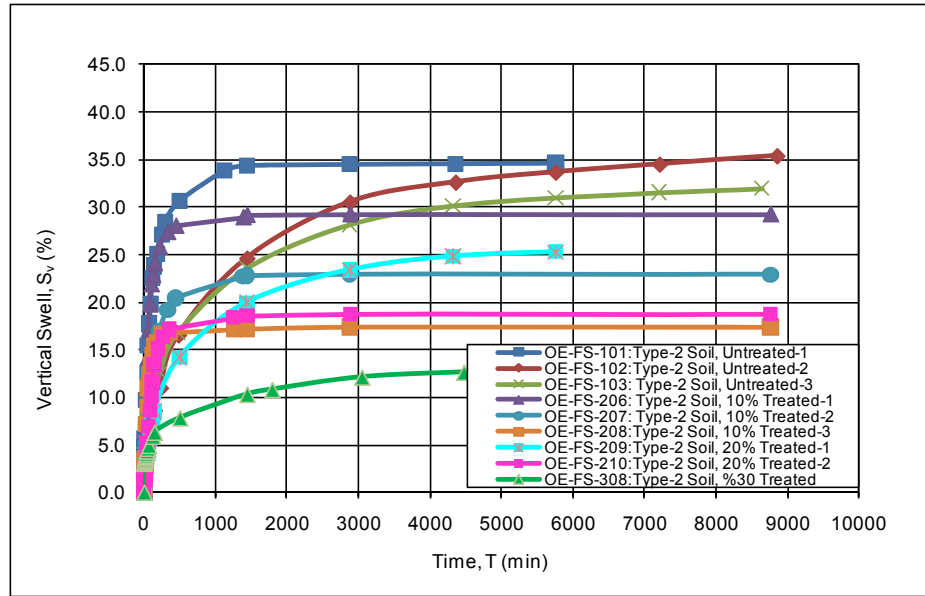


Figure 5. 24 Vertical Swell Percentage vs. Time Relationship for Oedometer Tests Performed with Free Swell Testing Technique ( $P_s=7$  kPa) on Type-2 Expansive Soil Samples Treated with Gravel

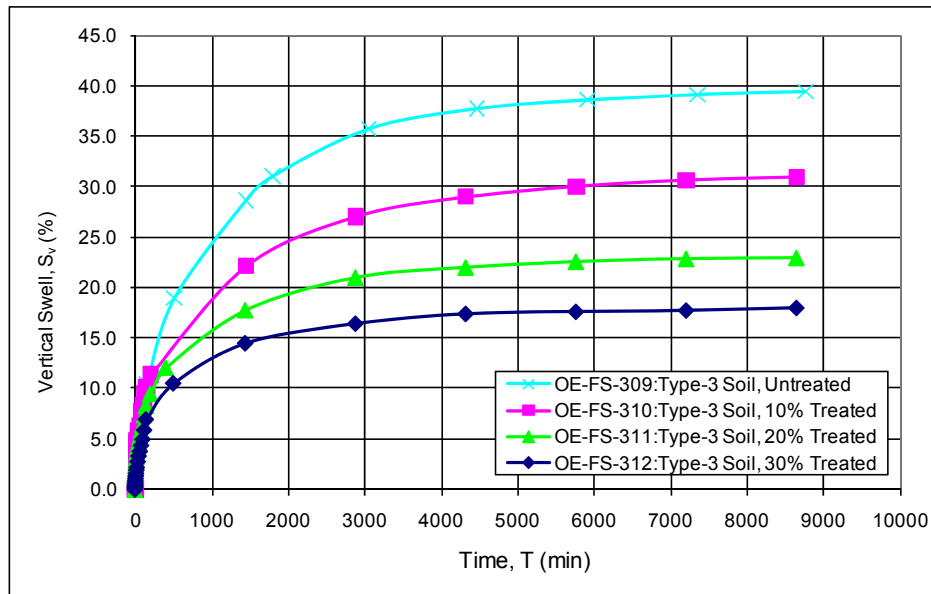


Figure 5. 25 Vertical Swell Percentage vs. Time Relationship for Oedometer Tests Performed with Free Swell Testing Technique ( $P_s=7$  kPa) on Type-3 Expansive Soil Samples Treated with Gravel

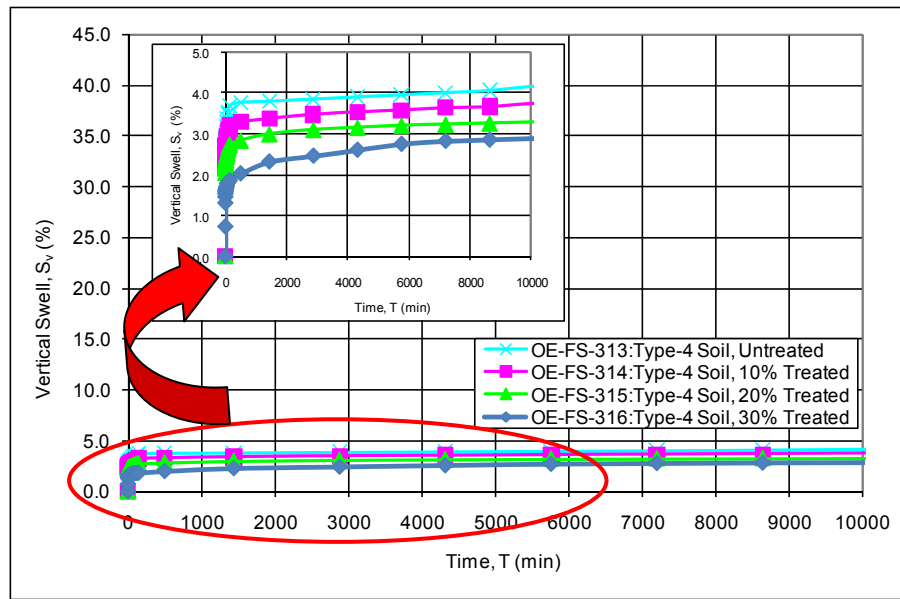


Figure 5. 26 Vertical Swell Percentage vs. Time Relationship for Oedometer Tests Performed with Free Swell Testing Technique ( $P_s=7$  kPa) on Type-4 Expansive Soil Samples Treated with Gravel

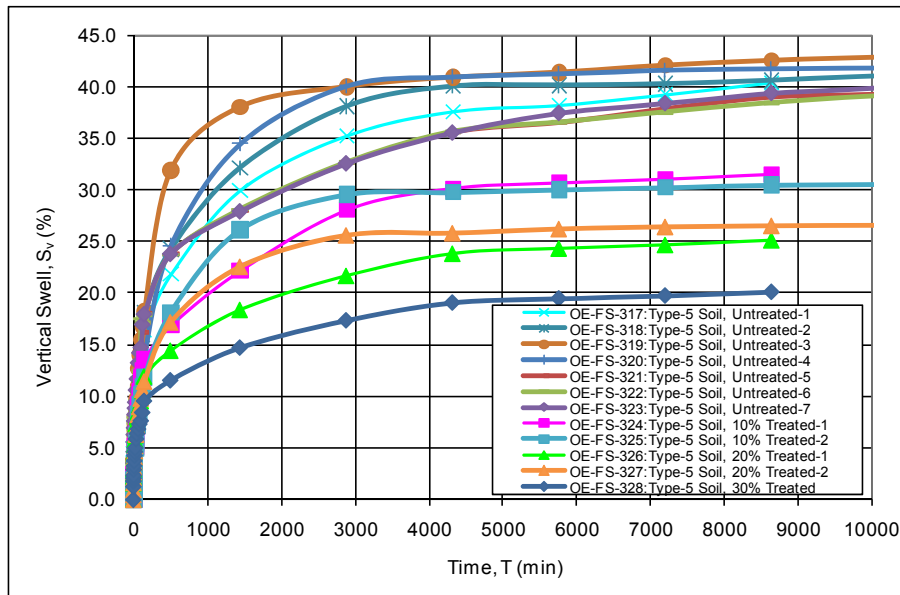


Figure 5. 27 Vertical Swell Percentage vs. Time Relationship for Oedometer Tests Performed with Free Swell Testing Technique ( $P_s=7$  kPa) on Type-5 Expansive Soil Samples Treated with Gravel



### 5.2.3 Stage (c) Tests

The third stage of Phase-2 investigations duplicates all the tests performed in Stage (b) except for the ones involving Type-4 Clay, this time however with an overburden pressure of 25 kPa instead of 7 kPa seating pressure, to simulate the effect of either a lightweight structure readily present or a manmade fill of 1 meter high constructed to fortify the treatment performance of trenches.

This stage involved a total number of 15 tests on CBR moulds and 18 tests on oedometer cells for which the details are presented in Table 5.10 for modified CBR moulds and in Table 5.11 for oedometer tests. Vertical swell versus time relationships for the mentioned tests are presented in Figures 5.28 to 5.35.

Table 5. 10 Modified CBR Mould Test Results Performed with Swell Overburden Testing Technique ( $P_o=25$  kPa) (Phase-2, Stage (c))

Test No	Soil Type	Area Replacement Ratio, ARR (%)	Final Water Content, $w_f$ (%)	Vertical Swell, $S_v$ (%)
CBR-SO-301	Type-1	0	35.9	5.0
CBR-SO-302	Type-1	10	37.1	3.9
CBR-SO-303	Type-1	20	40.2	2.3
CBR-SO-305	Type-2	0	38.4	9.4
CBR-SO-306	Type-2	10	40.4	5.9
CBR-SO-307	Type-2	20	41.6	2.4
CBR-SO-308	Type-2	30	44.3	0.6
CBR-SO-309	Type-3	0	41.6	14.7
CBR-SO-310	Type-3	10	43.7	12.1
CBR-SO-311	Type-3	20	44.5	8.3
CBR-SO-312	Type-3	30	47.2	4.5
CBR-SO-317	Type-5	0	64.3	21.9
CBR-SO-318	Type-5	10	64.7	17.4
CBR-SO-319	Type-5	20	69.5	14.4
CBR-SO-320	Type-5	30	74.6	10.8

Table 5. 11 Oedometer Test Results Performed with Swell Overburden Testing Technique ( $P_o=25$  kPa) (Phase-2, Stage (c))

Soil Type	Test No	Reference Tests	Area Replacement Ratio, ARR (%)	Final Water Content, $w_f$ (%)	Vertical Swell, $S_v$ (%)
Type-1	OE-SO-401	-	0	34.2	7.5
	OE-SO-402	-	10	37.8	6.1
	OE-SO-403	-	20	37.9	3.7
	OE-SO-404	-	30	44.9	0.0
Type-2	OE-SO-405*	OE-SO-101	0	37.4	13.7
		OE-SO-102		42.9	
		OE-SO-103		39.1	
	OE-SO-406*	OE-SO-206	10	40.3	9.7
		OE-SO-207		41.0	
	OE-SO-407*	OE-SO-208	20	41.7	6.2
		OE-SO-209		42.9	
	OE-SO-408	-	30	43.0	2.9
Type-3	OE-SO-409	-	0	42.0	12.6
	OE-SO-410	-	10	44.8	8.4
	OE-SO-411	-	20	45.7	2.5
	OE-SO-412	-	30	48.4	26.8
Type-5	OE-SO-413	-	0	68.5	26.8
	OE-SO-414		0	66.7	
	OE-SO-415		0	67.5	
	OE-SO-416		0	69.4	
	OE-SO-417		0	67.3	
	OE-SO-418		0	67.8	
	OE-SO-419	-	10	72.7	19.8
	OE-SO-420		10	75.1	
	OE-SO-421	-	20	74.1	17.7
	OE-SO-422		20	79.9	
	OE-SO-423	-	30	85.9	11.9

\* These test results are the averages calculated from the values observed during the first phase of investigations. According to this, OE-SO-405 results are the averages of OE-SO-101, 102 and 103, OE-SO-406 results are the averages of OE-SO-206 and 207, and OE-SO-407 results are the averages of OE-SO-208 and 209.

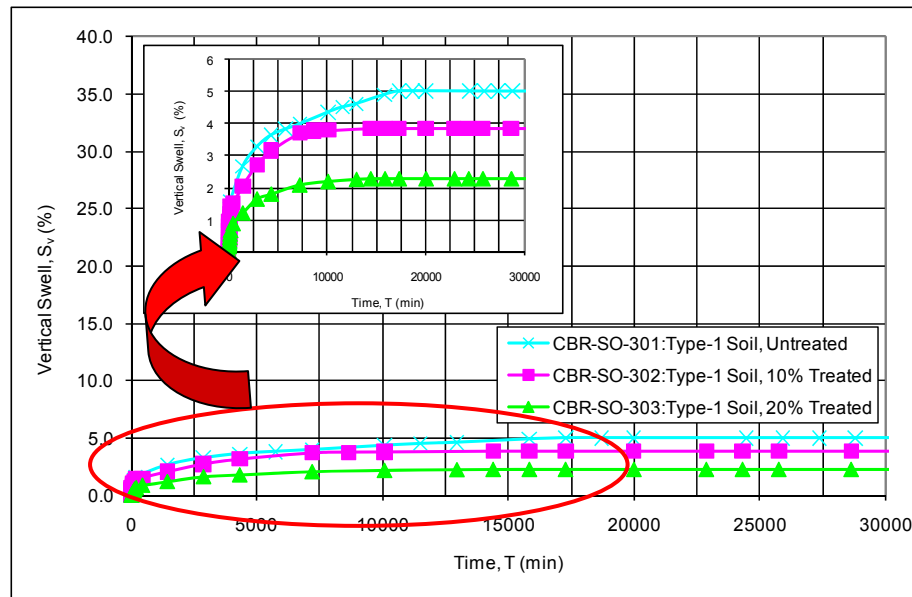


Figure 5. 28 Vertical Swell Percentage vs. Time Relationship for Modified CBR Mould Tests Performed with Swell Overburden Testing Technique ( $P_o=25$  kPa) on Type-1 Soil Samples Treated with Gravel

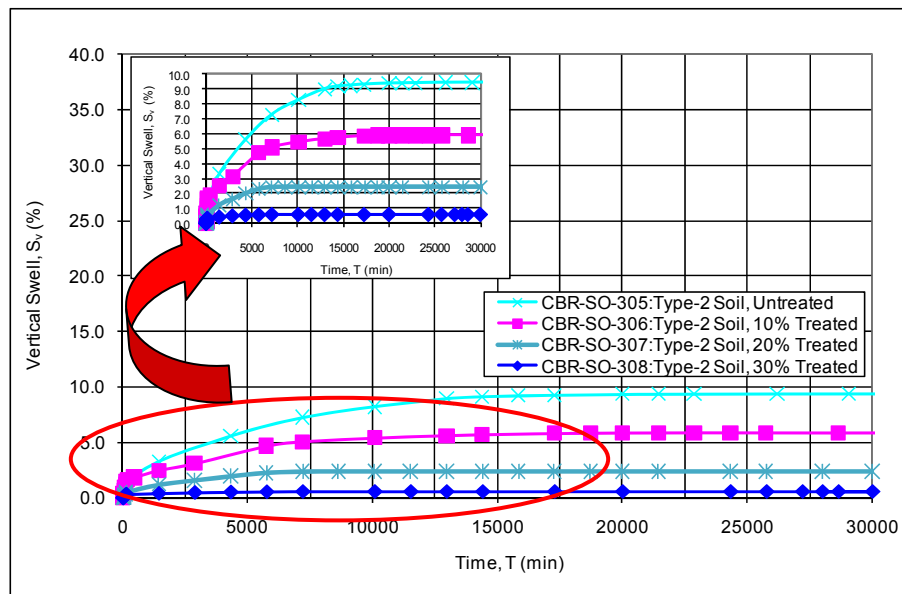


Figure 5. 29 Vertical Swell Percentage vs. Time Relationship for Modified CBR Mould Tests Performed with Swell Overburden Testing Technique ( $P_o=25$  kPa) on Type-2 Soil Samples Treated with Gravel

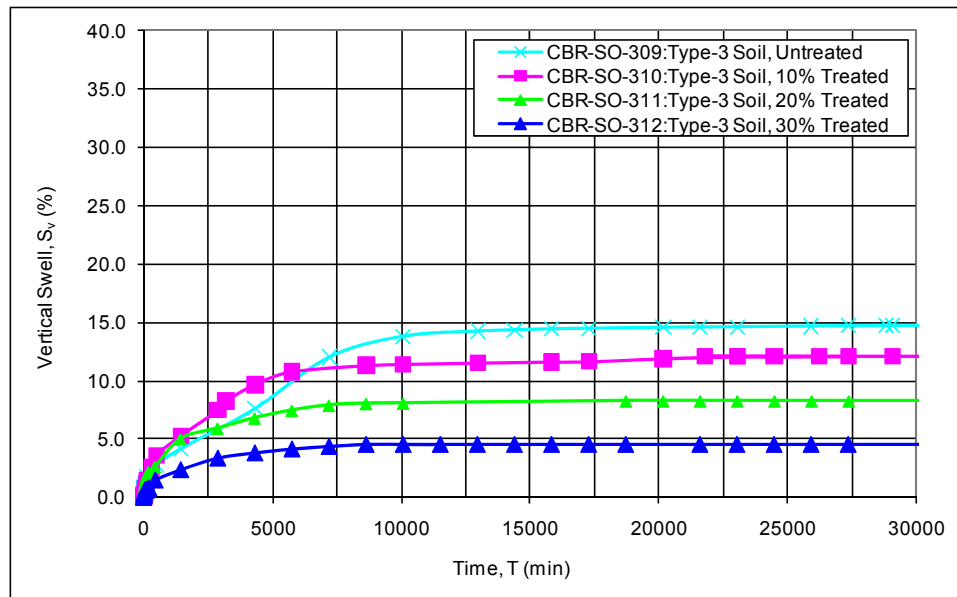


Figure 5. 30 Vertical Swell Percentage vs. Time Relationship for Modified CBR Mould Tests Performed with Swell Overburden Testing Technique ( $P_o=25$  kPa) on Type-3 Soil Samples Treated with Gravel

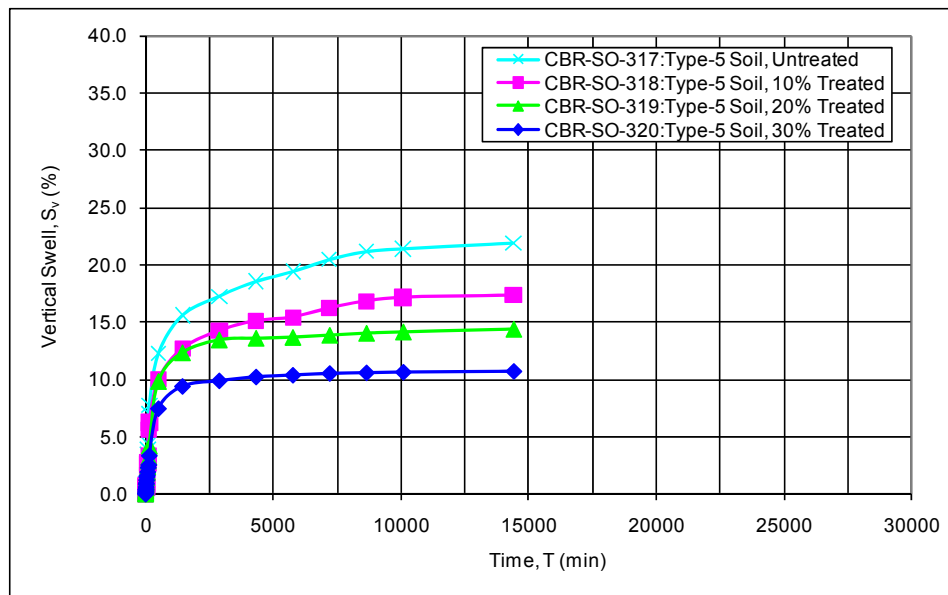


Figure 5. 31 Vertical Swell Percentage vs. Time Relationship for Modified CBR Mould Tests Performed with Swell Overburden Testing Technique ( $P_o=25$  kPa) on Type-5 Soil Samples Treated with Gravel

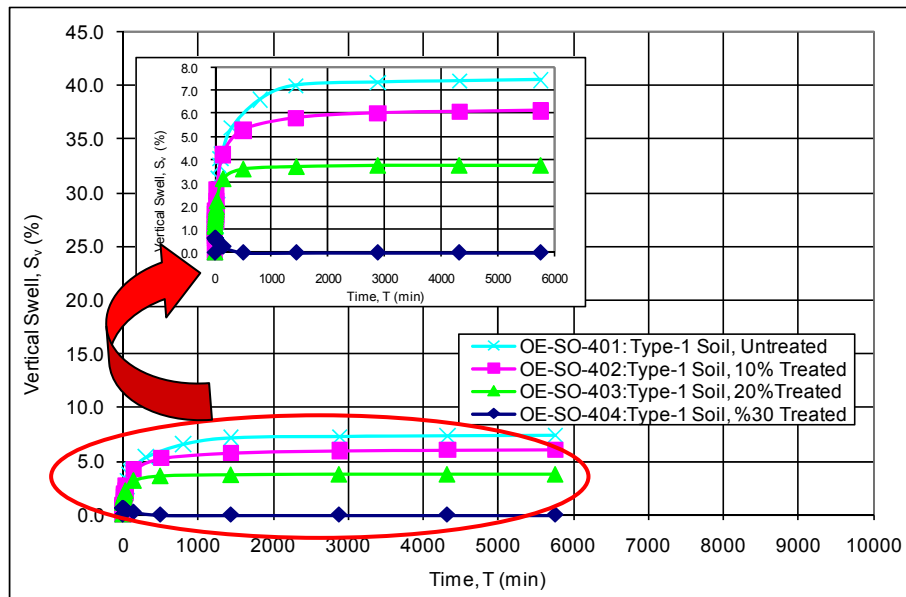


Figure 5.32 Vertical Swell Percentage vs. Time Relationship for Oedometer Tests Performed with Swell Overburden Testing Technique ( $P_o=25$  kPa) on Type-1 Expansive Soil Samples Treated with Gravel

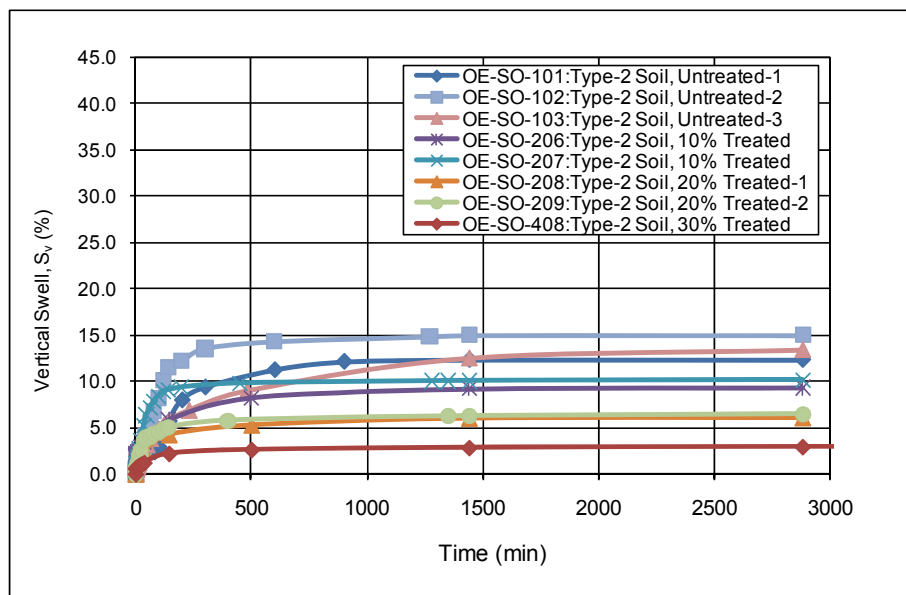


Figure 5.33 Vertical Swell Percentage vs. Time Relationship for Oedometer Tests Performed with Swell Overburden Testing Technique ( $P_o=25$  kPa) on Type-2 Expansive Soil Samples Treated with Gravel

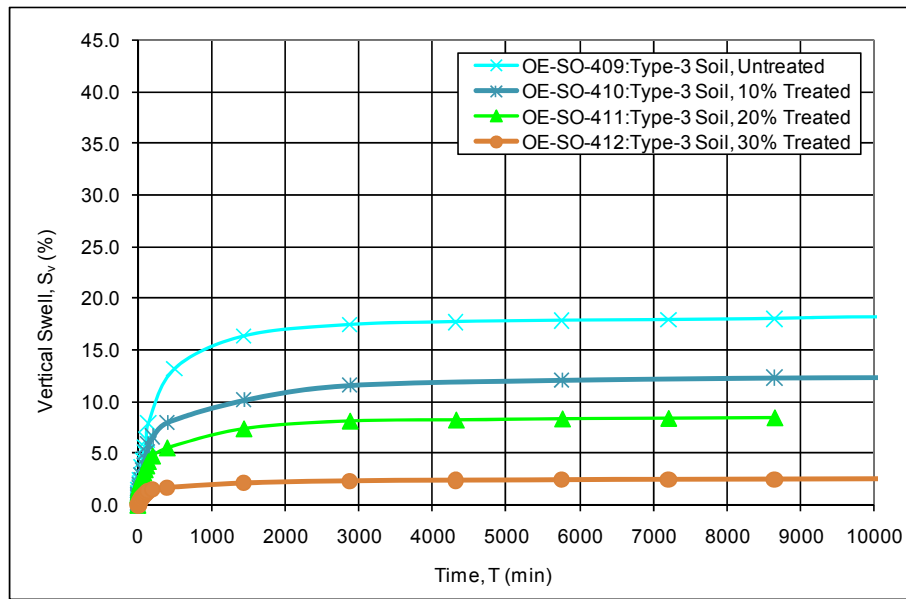


Figure 5. 34 Vertical Swell Percentage vs. Time Relationship for Oedometer Tests Performed with Swell Overburden Testing Technique ( $P_o=25$  kPa) on Type-3 Expansive Soil Samples Treated with Gravel

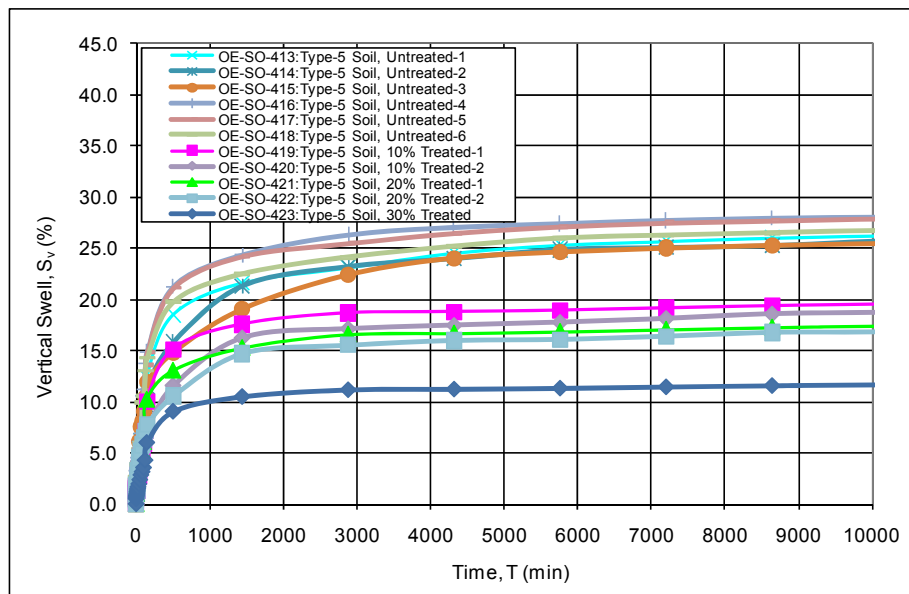


Figure 5. 35 Vertical Swell Percentage vs. Time Relationship for Oedometer Tests Performed with Swell Overburden Testing Technique ( $P_o=25$  kPa) on Type-5 Expansive Soil Samples Treated with Gravel

### **5.3 PERFORMANCE OF SILT AS TREATMENT MATERIAL (PHASE.3)**

In the third phase of the investigations, it was intended to evaluate the possible effects of silt material on the level of improvement of expansive soils. Silt was used as a trench filling material parallel to the general trend of the present investigation, as well as a superficial layer placed on the expansive clay samples with reference to Katti (1979).

Free swell tests with 7 kPa seating pressure and swell overburden tests under 25 kPa were performed with oedometer cells on Type-5 soil treated with 10, 20 and 30% silt. It was portrayed in Phase I of the test program that gravel as a granular fill performed better than sand which was placed at the same relative density, i.e. 40% for the present case. Based on this finding, it is expected that silt, having smaller particle size than sand and placed at a similar relative density, will yield comparatively lower treatment values, in case, the probable treatment factors in the system are primarily the filling of voids in the granular fill and possibly the friction generated on the expansive soil and the fill material interface. Therefore, in this phase of the study, it was anticipated to minimize the effects of above mentioned factors and hence to evaluate whether silt possesses any other significant power of treatment as proposed by Katti (1979). Consequently, silt was placed with a relative density greater than 90%, which in turn practically prevented the intrusion of clay into silt.

To inspect the validity and sensitivity of the experiments, additional tests were performed with empty holes. Since, it was anticipated from the results of investigations that the area replacement ratio plays a major role on the treatment level; it was also aimed to determine the best possible treatment that can be attained by testing the samples with empty holes. To evaluate the soundness of results, holes were filled with mercury both before and after the experiments, and difference in volume was recorded. An analogous procedure had been used for treatment with gravel, such that the mercury volume that could be carried by the voids in gravel was measured both before and after the experiments for similar purposes.

This phase involved a total number of 26 free swell tests and 23 swell overburden tests performed on oedometer cells for which the details are presented in Table 5.12 and Table 5.13 consecutively. Vertical swell versus time relationships for tests performed untreated and silt treated at different area replacement ratios are presented in Figures 5.36 to 5.41.

Table 5. 12 Oedometer Test Results Performed with Free Swell Testing Technique ( $P_s=7$  kPa) (Phase-3)

Soil Type	Test No	Treatment Type	% ARR	Average Water Content (wf, %)	Vertical Swell, (%)	Vertical Swell (Average), (%)
Type-5	OE-FS-317	-	0	78.5	41.55	41.48
	OE-FS-318	-	0	82.0	42.16	
	OE-FS-319	-	0	78.7	43.04	
	OE-FS-320	-	0	75.6	40.64	
	OE-FS-321	-	0	78.0	40.07	
	OE-FS-322	-	0	76.2	41.39	
	OE-FS-323	-	0	80.9	41.53	31.54
	OE-FS-324	Gravel Column	10	82.2	32.37	
	OE-FS-325	Gravel Column	10	85.9	30.71	26.22
	OE-FS-326	Gravel Column	20	87.5	25.85	
	OE-FS-327	Gravel Column	20	91.5	26.58	20.68
	OE-FS-328	Gravel Column	30	96.2	20.68	
	OE-FS-513	Silt Column	10	85.4	36.35	35.50
	OE-FS-514	Silt Column	10	87.3	35.61	
	OE-FS-515	Silt Column	10	89.3	35.24	
	OE-FS-516	Silt Column	10	88.6	34.79	
	OE-FS-517	Silt Layer	10	90.1	37.59	36.25
	OE-FS-518	Silt Layer	10	87.5	34.84	
	OE-FS-519	Silt Layer	10	88.8	36.45	
	OE-FS-520	Silt Layer	10	87.0	36.11	
	OE-FS-521	Empty Hole	10	86.8	28.60	28.60
	OE-FS-522	Silt Column	20	91.9	32.99	30.74
	OE-FS-523	Silt Column	20	92.8	29.22	
	OE-FS-524	Silt Column	20	97.8	34.07	
	OE-FS-525	Silt Column	20	91.6	29.42	
	OE-FS-526	Silt Column	20	94.9	29.47	
	OE-FS-527	Silt Column	20	93.3	29.26	
	OE-FS-528	Column+Layer	10+10	92.7	32.07	31.50
	OE-FS-529	Silt Layer	20	92.4	30.56	
	OE-FS-530	Silt Layer	20	91.2	33.41	
	OE-FS-531	Silt Layer	20	93.2	29.95	
	OE-FS-532	Empty Hole	20	93.5	20.40	20.40
	OE-FS-533	Silt Column	30	101.5	26.05	25.86
	OE-FS-534	Silt Column	30	99.0	23.84	
	OE-FS-535	Silt Column	30	105.4	27.67	
	OE-FS-536	Silt Layer	30	100.0	27.79	26.65
	OE-FS-537	Silt Layer	30	98.6	26.84	
	OE-FS-538	Silt Layer	30	96.3	25.32	



Table 5. 13 Oedometer Test Results Performed with Swell Overburden Testing Technique ( $P_o=25$  kPa) (Phase-3)

Soil Type	Test No	Treatment Type	% ARR	Average Water Content	Vertical Swell, (%)	Vertical Swell (Average),
Type-5	OE-SO-413	-	0	68.5	26.78	26.80
	OE-SO-414	-	0	66.7	25.88	
	OE-SO-415	-	0	67.5	25.48	
	OE-SO-416	-	0	69.4	28.05	
	OE-SO-417	-	0	67.3	27.95	
	OE-SO-418	-	0	67.8	26.68	
	OE-SO-419	Gravel Column	10	72.7	19.84	19.43
	OE-SO-420	Gravel Column	10	75.1	19.03	
	OE-SO-421	Gravel Column	20	74.1	17.68	17.39
	OE-SO-422	Gravel Column	20	79.9	17.09	
	OE-SO-423	Gravel Column	30	85.9	11.91	11.91
	OE-SO-612	Silt Column	10	73.9	22.63	21.42
	OE-SO-613	Silt Column	10	78.0	21.88	
	OE-SO-614	Silt Column	10	74.1	20.32	
	OE-SO-615	Silt Column	10	73.9	20.84	
	OE-SO-616	Silt Layer	10	74.5	24.32	23.65
	OE-SO-617	Silt Layer	10	73.1	23.21	
	OE-SO-618	Silt Layer	10	75.1	23.42	
	OE-SO-619	Empty Hole	10	79.2	17.63	17.63
	OE-SO-620	Silt Column	20	83.6	17.94	17.99
	OE-SO-621	Silt Column	20	81.3	21.24	
	OE-SO-622	Silt Column	20	84.4	16.07	
	OE-SO-623	Silt Column	20	81.2	17.26	
	OE-SO-624	Silt Column	20	80.8	17.45	
	OE-SO-625	Silt Layer	20	78.9	17.26	20.06
	OE-SO-626	Silt Layer	20	83.1	21.26	
	OE-SO-627	Silt Layer	20	79.7	21.66	
	OE-SO-628	Empty Hole	20	85.8	9.38	9.38
	OE-SO-629	Silt Column	30	91.2	16.04	15.40
	OE-SO-630	Silt Column	30	88.9	15.63	
	OE-SO-631	Silt Column	30	89.9	14.53	
	OE-SO-632	Silt Layer	30	90.7	16.11	16.56
	OE-SO-633	Silt Layer	30	88.6	16.89	
	OE-SO-634	Silt Layer	30	90.4	16.68	

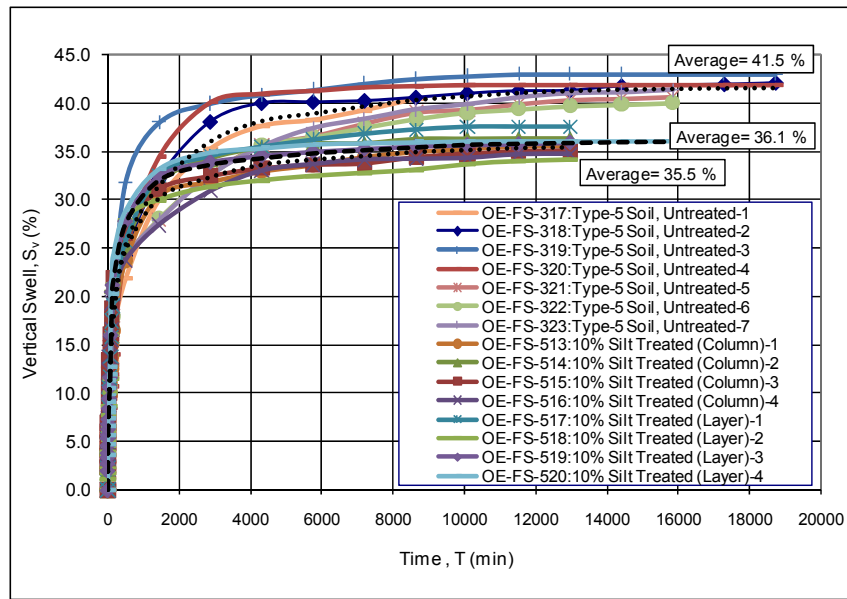


Figure 5.36 Vertical Swell Percentage vs. Time Relationship for Oedometer Tests Performed with Free Swell Testing Technique ( $P_s=7$  kPa) on Type-5 Expansive Soil Samples Treated with 10% Silt

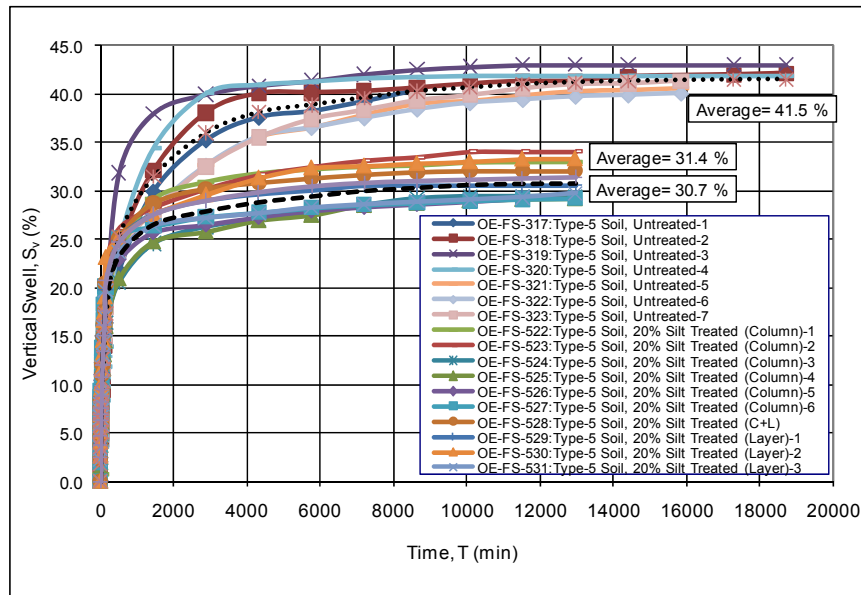


Figure 5.37 Vertical Swell Percentage vs. Time Relationship for Oedometer Tests Performed with Free Swell Testing Technique ( $P_s=7$  kPa) on Type-5 Expansive Soil Samples Treated with 20% Silt

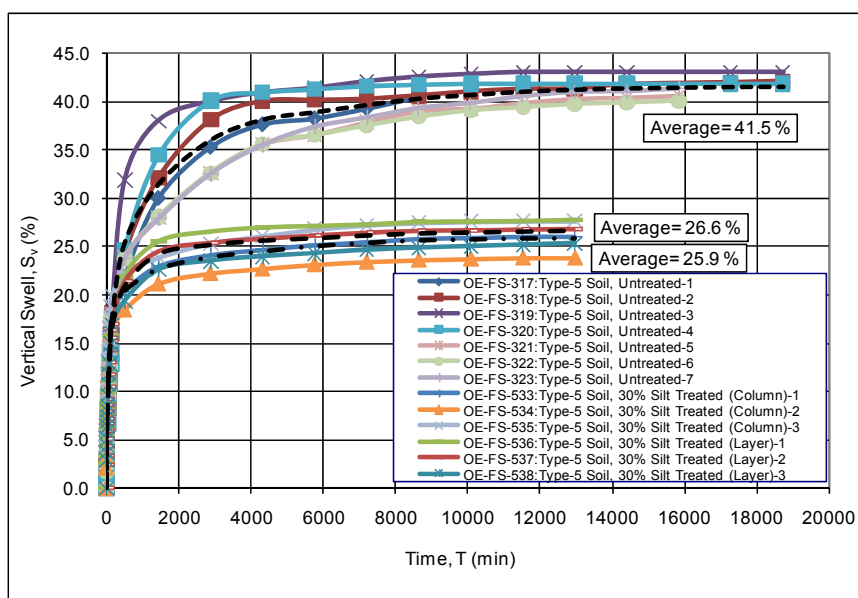


Figure 5.38 Vertical Swell Percentage vs. Time Relationship for Oedometer Tests Performed with Free Swell Testing Technique ( $P_s=7$  kPa) on Type-5 Expansive Soil Samples Treated with 30% Silt

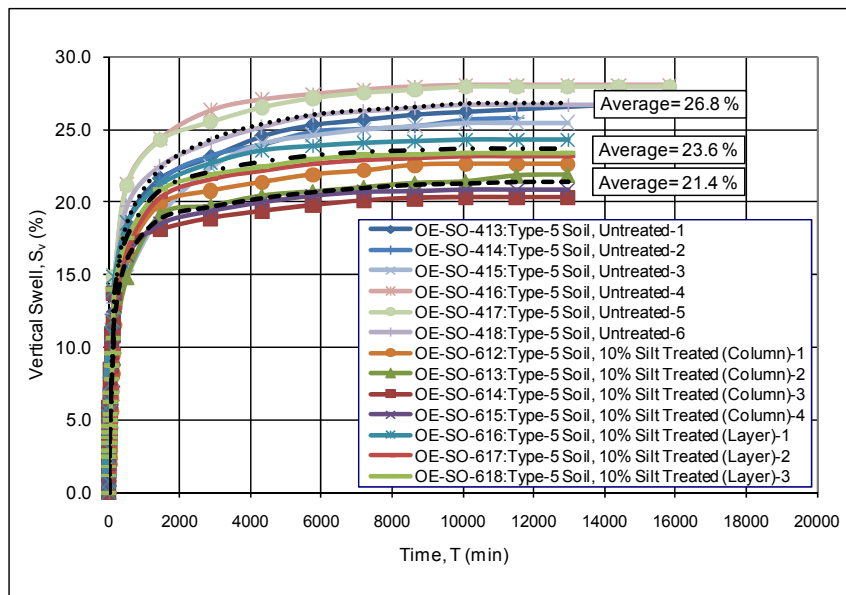


Figure 5.39 Vertical Swell Percentage vs. Time Relationship for Oedometer Tests Performed with Swell Overburden Testing Technique ( $P_o=25$  kPa) on Type-5 Expansive Soil Samples Treated with 10% Silt

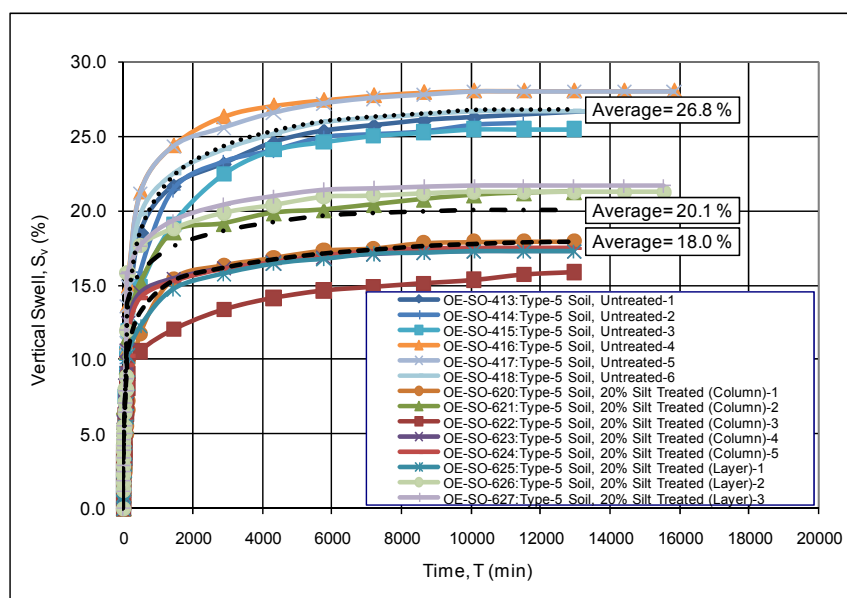


Figure 5. 40 Vertical Swell Percentage vs. Time Relationship for Oedometer Tests Performed with Swell Overburden Testing Technique ( $P_o=25$  kPa) on Type-5 Expansive Soil Samples Treated with 20% Silt

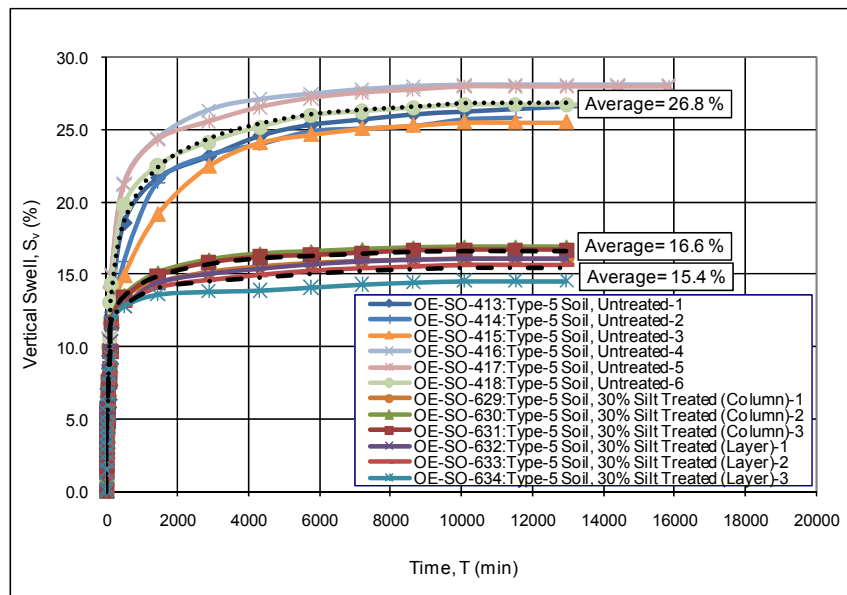


Figure 5. 41 Vertical Swell Percentage vs. Time Relationship for Oedometer Tests Performed with Swell Overburden Testing Technique ( $P_o=25$  kPa) on Type-5 Expansive Soil Samples Treated with 30% Silt

The averages of tests performed with silt treatment were compared with the results of empty hole and gravel treated samples are given in Figures 5.42 to 5.47. The vertical swell percentage corresponding to each time value on the expected curves in these figures are calculated from the following expressions:

- (i) For “Expected due to Replacement”:

$$S_v = S_{v(av)}(Untreated) \cdot (100 - ARR(\%)) \dots \dots \dots (5.1)$$

- (ii) For “Gravel Column (ARR,%) Expected” and “Hole (ARR,%) Expected” to be calculated for every area replacement ratio (ARR) separately:

$$S_v = S_{v(av)}(Untreated) \cdot \left\{ 1 - \left( \frac{V_{Hg(initial)} - V_{Hg(final)}}{V_{Hg(initial)}} \right) \right\} \dots \dots \dots (5.2)$$

where,  $S_v$ : Vertical Swell Percentage (%)

$S_{v(av)}(Untreated)$ : Average Vertical Swell Percentage for Untreated Soil Sample (%)

$V_{Hg(initial)}$ : Initial Volume of Mercury that Fills the Voids of Gravel or the Empty Hole prior to Swelling

$V_{Hg(final)}$ : Final Volume of Mercury that Fills the Voids of Gravel or the Empty Hole after Swelling

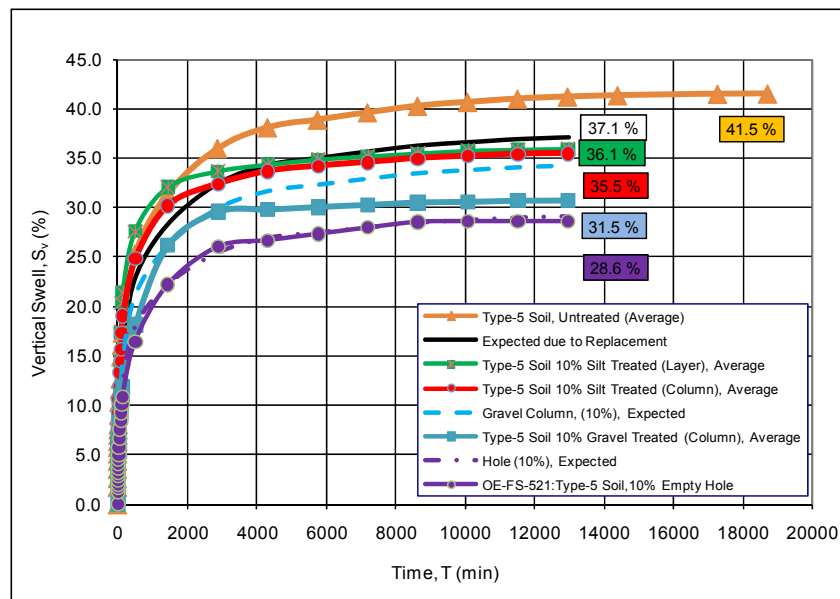


Figure 5.42 Vertical Swell Percentage vs. Time Relationship for Oedometer Tests Performed with Free Swell Testing Technique ( $P_s=7$  kPa) on Type-5 Expansive Soil for 10% ARR (Silt, Gravel and Empty Hole)

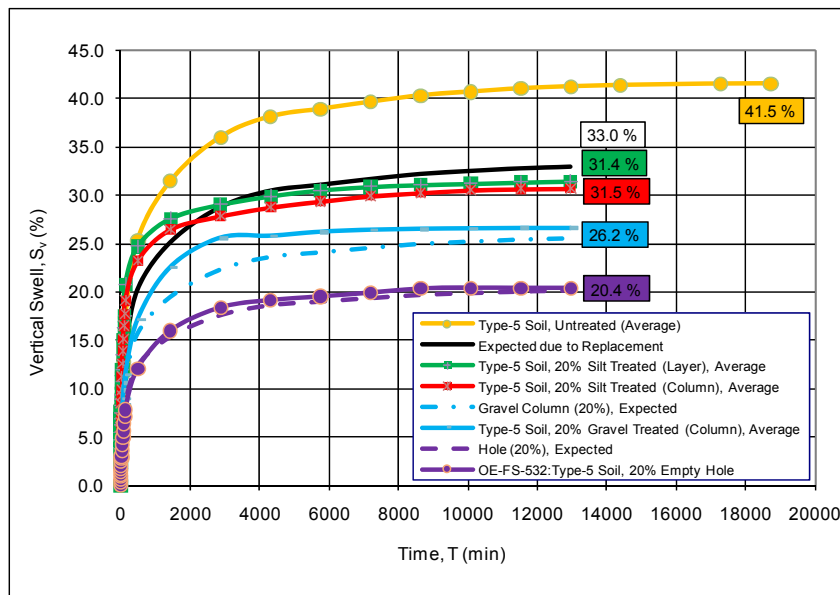


Figure 5.43 Vertical Swell Percentage vs. Time Relationship for Oedometer Tests Performed with Free Swell Testing Technique ( $P_s=7$  kPa) on Type-5 Expansive Soil for 20% ARR (Silt, Gravel and Empty Hole)

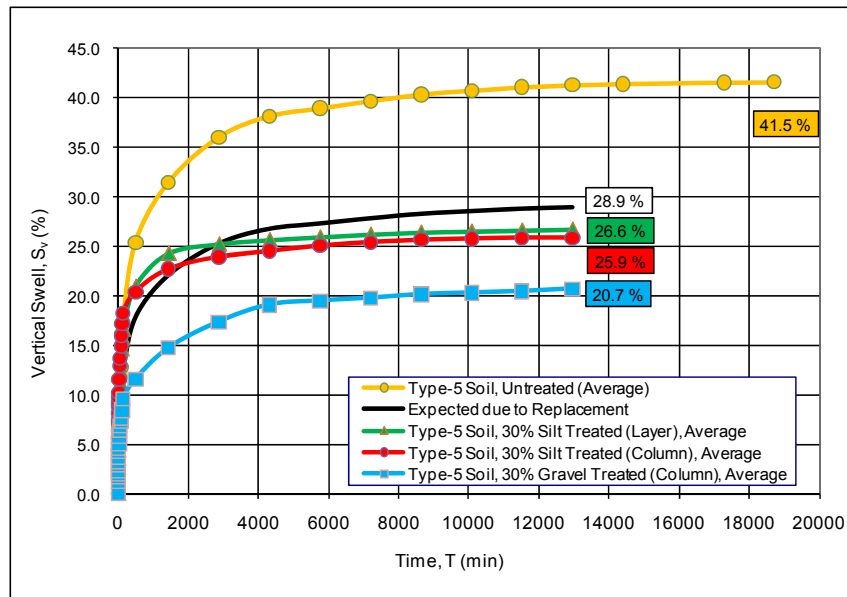


Figure 5.44 Vertical Swell Percentage vs. Time Relationship for Oedometer Tests Performed with Free Swell Testing Technique ( $P_s = 7$  kPa) on Type-5 Expansive Soil for 30% ARR (Silt, Gravel and Empty Hole)

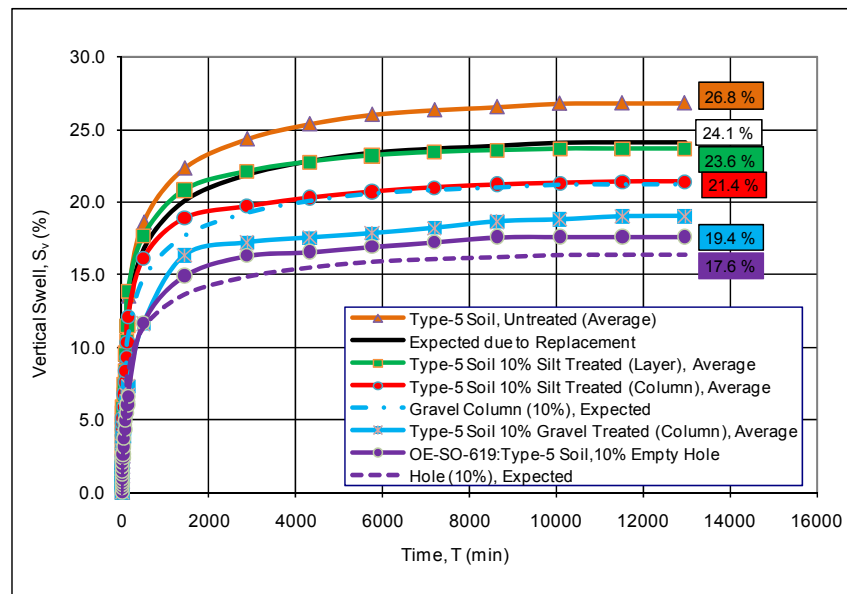


Figure 5.45 Vertical Swell Percentage vs. Time Relationship for Oedometer Tests Performed with Swell Overburden Tests ( $P_o = 25$  kPa) on Type-5 Expansive Soil for 10% ARR (Silt, Gravel and Empty Hole)

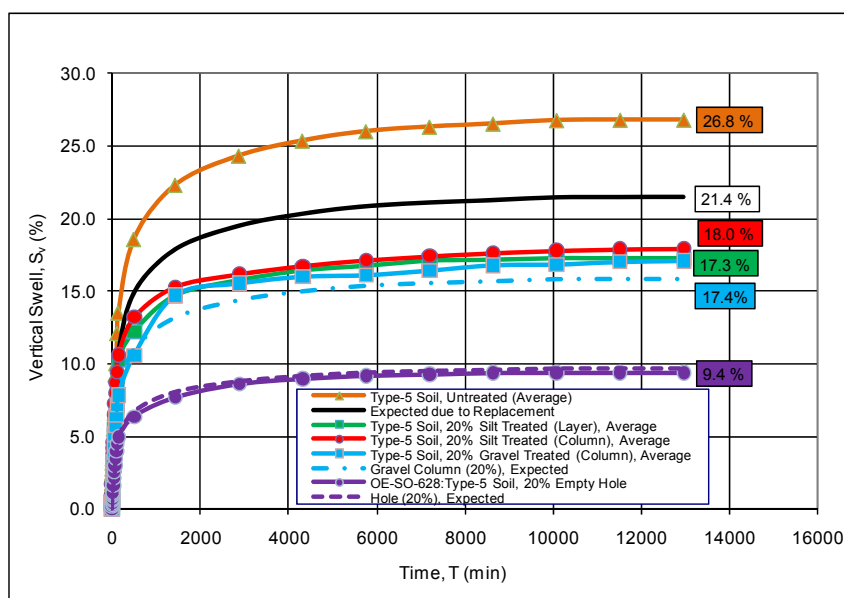


Figure 5. 46 Vertical Swell Percentage vs. Time Relationship for Oedometer Tests Performed with Swell Overburden Tests ( $P_0=25$  kPa) on Type-5 Expansive Soil for 20% ARR (Silt, Gravel and Empty Hole)

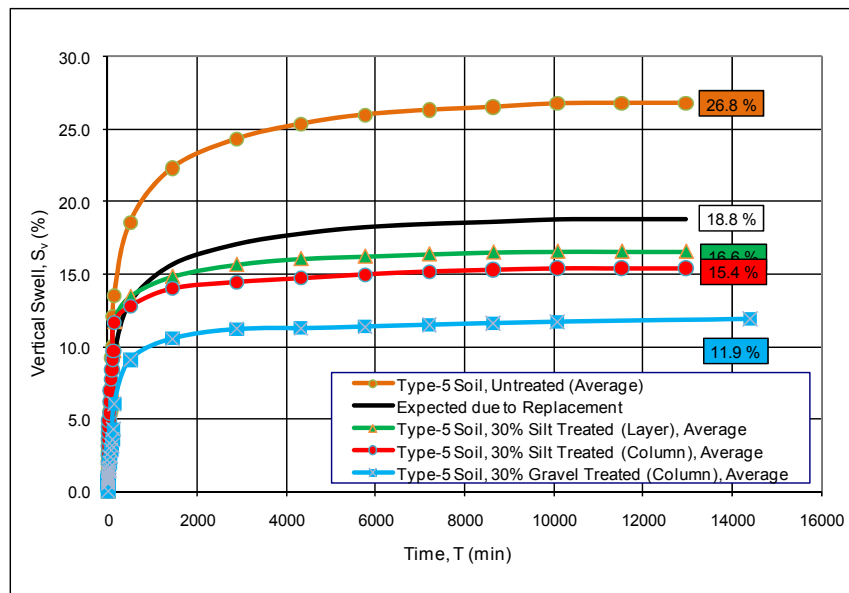


Figure 5. 47 Vertical Swell Percentage vs. Time Relationship for Oedometer Tests Performed with Swell Overburden Tests ( $P_0=25$  kPa) on Type-5 Expansive Soil for 30% ARR (Silt, Gravel and Empty Hole)



## **5.4 LATERAL SWELL PRESSURE MEASUREMENTS (PHASE.4)**

Parallel to the findings observed at the previous phases of the investigations, it was decided to extent the context of the study to include the probable positive effects of the subject method of treatment on the lateral swell parameters of expansive soils. For this purpose, thin-wall ring tests were incorporated into the test program the details of which are presented in the following subsections. During the tests two thin-wall rings with different diameters were used as it has already been discussed in Chapter III.

### **5.4.1 Stage (a) Tests**

This stage of investigation was intended to study the efficiency of the two thin-wall ring apparatus by conducting tests on one artificial (Type-3) and one natural (Type-5) untreated expansive soil samples. Total number of 28 tests were performed for this purpose. Ertekin's Ring (Ring-1) was used during the tests performed on soil Type-3, whereas both Ertekin's and Avşar's Rings (Ring-1 and Ring-2) were used for the tests performed on soil Type-5, which in turn led to the observation of a possible scale effect on measured parameters.

During the tests, the relative density of fine gravel was selected as 40%. Tests on artificially prepared samples (Types 3) were performed with initial moisture content of 15 % and dry density of  $1.5 \text{ g/cm}^3$  whereas Type-5 sample was prepared with an initial moisture content of 15 % and a dry density of  $1.2 \text{ g/cm}^3$ . Type-3 soils are tested under free swell and swell overburden test conditions with the application of vertical pressures of 25, 50 and 100 kPa, whereas Type-5 soils are tested with an additional pressure of 150 kPa in combination with the pressures exerted on Type-3 soils. The results of these tests are summarized in Table 5.14 and Table 5.15. The lateral swell pressure versus time relationships determined from the thin-wall ring tests performed on untreated soil Type-3 are presented in Figure.5 48. The lateral swell pressure versus time relationships constructed for Type-5 soil is presented in Figure 5.49 for Ring-1 and in Figure

5.50 for Ring-2. The vertical swell percentage versus time relationships determined from the thin-wall ring tests performed on untreated soil Type-3 and the lateral swell pressure vs. time relationships for each overburden pressure level are also presented in the Appendices.

Table 5. 14 Results of Thin-Wall Ring Tests (Ring-1) Performed on Untreated Soil Type-3 (Phase-4, Stage (a))

Test No	Overburden Pressure, $P_o$ (kPa)	Peak Lateral Pressure, $P_{hp}$ (kPa)	Ultimate Lateral Pressure, $P_{hu}$ (kPa)	Final Water Content, $w_f$ (%)	Vertical Swell, $S_v$ (%)
TW-01	7	258	209	32.6	17.13
TW-02	7	275	194	30.8	16.17
TW-07	25	205	170	30.9	7.73
TW-08	25	186	137	32.5	7.33
TW-13	50	189	170	32.5	4.35
TW-14	50	186	97	32.3	5.17
TW-19	100	230	185	31.4	1.41
TW-20	100	242	226	30.9	1.20

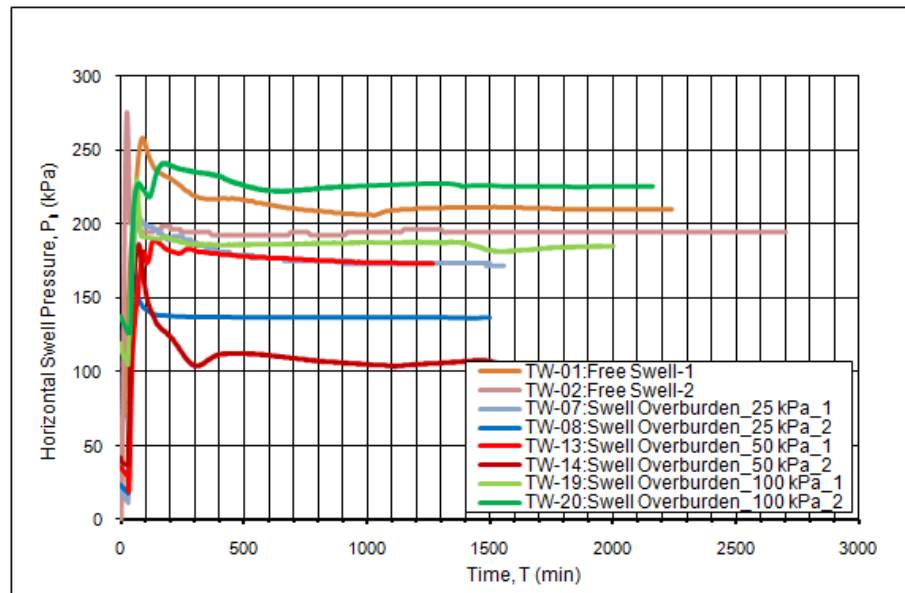


Figure 5. 48 Lateral Swell Pressure vs. Time Relationship for Thin-Wall Ring Tests (Ring-1) Performed on Type-3 Untreated Soil Samples

Table 5. 15 Results of Thin-Wall Ring Tests Performed on Untreated Soil Type-5 (Phase-4, Stage (a))

Test No	Ring #	Overburden Pressure, $P_o$ (kPa)	Peak Lateral Pressure, $P_{hp}$ (kPa)	Ultimate Lateral Pressure, $P_{hu}$ (kPa)	Final Water Content, $w_f$ (%)	Vertical Swell, $S_v$ (%)
TW-25	1	7	164	51	51.98	23.33
TW-26	1	7	183	56	53.31	21.07
TW-41	1	25	192	83	46.05	15.11
TW-42	1	25	179	68	48.44	17.53
TW-57	1	50	199	121	45.67	8.23
TW-58	1	50	217	92	47.03	10.47
TW-59	1	100	279	274	44.33	6.53
TW-60	1	100	327	271	47.47	6.70
TW-61	1	150	311	265	44.86	5.33
TW-62	1	150	364	234	44.58	5.03
TW-33	2	7	188	48	59.72	20.03
TW-34	2	7	208	20	58.83	23.50
TW-49	2	25	230	73	54.85	16.60
TW-50	2	25	212	67	48.87	14.60
TW-63	2	50	247	169	49.27	9.47
TW-64	2	50	214	110	52.07	10.13
TW-65	2	100	251	179	49.23	5.63
TW-66	2	100	332	244	53.91	5.37
TW-67	2	150	342	313	53.00	3.00
TW-68	2	150	372	342	50.04	2.40

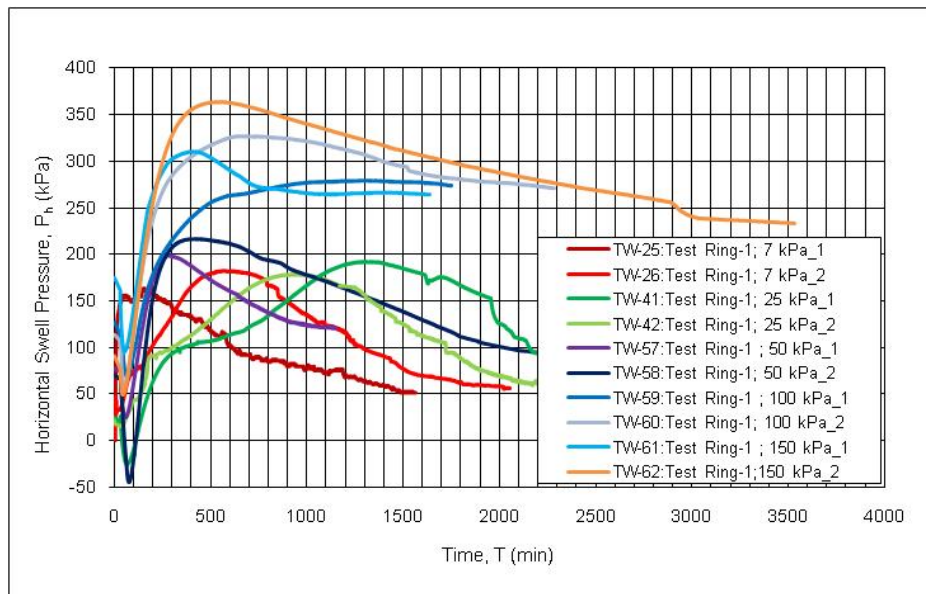


Figure 5. 49 Lateral Swell Pressure vs. Time Relationship for Thin-Wall Ring Tests (Ring-1) Performed on Type-5 Untreated Soil Samples

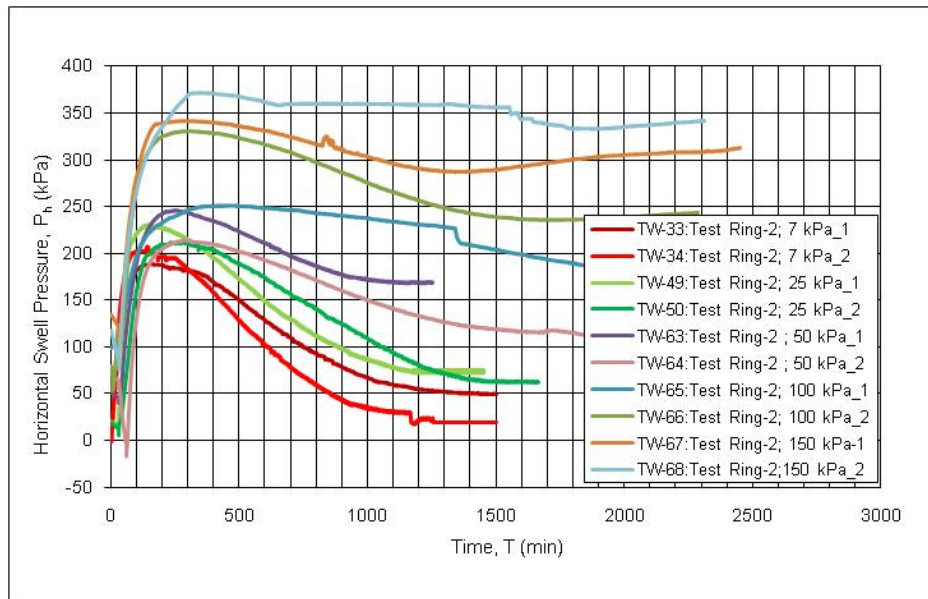


Figure 5.50 Lateral Swell Pressure vs. Time Relationship for Thin-Wall Ring Tests (Ring-2) Performed on Type-5 Untreated Soil Samples

#### 5.4.2 Stage (b) Tests

In the second stage of Phase-4 studies, the possible positive effects of columns and/or trenches, backfilled with granular material, on the improvement of lateral swell pressures of expansive soils, was investigated. The Ertekin Ring (Ring-1) was used during this stage. Type-3 expansive soils were tested under free swell (i.e. 7 kPa seating pressure) and vertical pressures of 25, 50 and 100 kPa and gravel material was used with 5 and 10% area replacement ratios for this purpose. Due to the fact that the lateral pressure treatment was observed to reach to 80% during the experiments, no additional tests were performed at larger area replacement ratios. On the other hand, it was concluded that the results of the tests performed under large vertical stresses are always open to question, based on the fact that some portion of the vertical stresses will be carried by the granular column, thus changing the lateral pressures generated on the walls of the ring.

Once again, the relative density of fine gravel was selected as 40%. Tests on artificially prepared samples (Types 3) were performed with initial moisture content of 15 % and dry density of 1.5 g/cm<sup>3</sup>. The results of total number of 24 tests performed on Type-3 soil including the untreated soil samples are presented in Table 5.16. The lateral swell pressure versus time relationships for free swell tests and tests performed with 25, 50 and 100 kPa overburden pressure are presented in Figures 5.51 to Figure 5.54. The lateral swell pressure vs. time relationships for each overburden pressure and area replacement ratio and the percent vertical swell versus time relationships of the relevant tests are also presented in the Appendices.

Table 5. 16 Results of Thin-Wall Ring Tests Performed on Soil Type-3 (Phase-4, Stage (b))

Test No	Overburden Pressure, $P_o$ (kPa)	Area Replacement Ratio, ARR (%)	Peak Lateral Pressure, $P_{hp}$ (kPa)	Ultimate Lateral Pressure, $P_{hu}$ (kPa)	Final Water Content, $w_f$ (%)	Vertical Swell, $S_v$ (%)
TW-01	7	0	258	209	32.6	17.13
TW-02	7	0	275	194	30.8	16.17
TW-03	7	5	78	46	43.3	17.37
TW-04	7	5	91	37	42.6	15.10
TW-05	7	10	68	14	46.0	13.07
TW-06	7	10	56	3	46.2	14.28
TW-07	25	0	205	170	30.9	7.73
TW-08	25	0	186	137	32.5	7.33
TW-09	25	5	118	105	39.8	7.01
TW-10	25	5	89	69	38.1	7.10
TW-11	25	10	95	88	42.0	5.33
TW-12	25	10	74	50	41.9	8.02
TW-13	50	0	189	170	32.5	4.35
TW-14	50	0	186	97	32.3	5.17
TW-15	50	5	140	129	36.7	3.26
TW-16	50	5	91	71	38.0	4.20
TW-17	50	10	103	99	34.1	1.50
TW-18	50	10	147	128	34.4	1.58
TW-19	100	0	230	185	31.4	1.41
TW-20	100	0	242	226	30.9	1.20
TW-21	100	5	225	218	32.7	1.47
TW-22	100	5	163	157	34.4	0.89
TW-23	100	10	150	119	34.0	0.45
TW-24	100	10	168	162	32.3	0.60

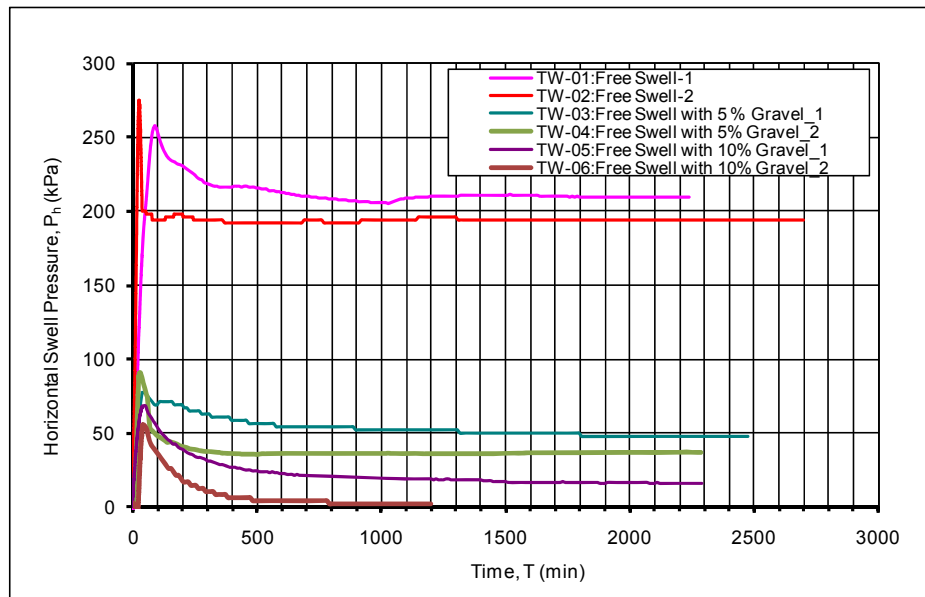


Figure 5. 51 Lateral Swell Pressure vs. Time Relationship for Thin-Wall Ring Tests (Ring-1) Performed on Type-3 Soil Samples for Different Treatment Percentages ( $P_s=7$  kPa)

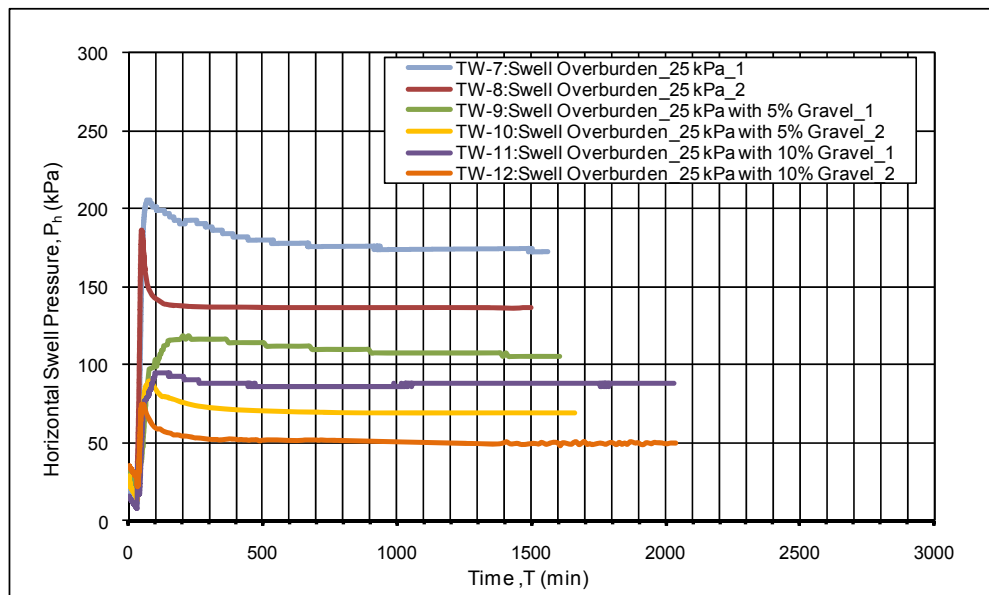


Figure 5. 52 Lateral Swell Pressure vs. Time Relationship for Thin-Wall Ring Tests (Ring-1) Performed on Type-3 Soil Samples for Different Treatment Percentages ( $P_o=25$  kPa)

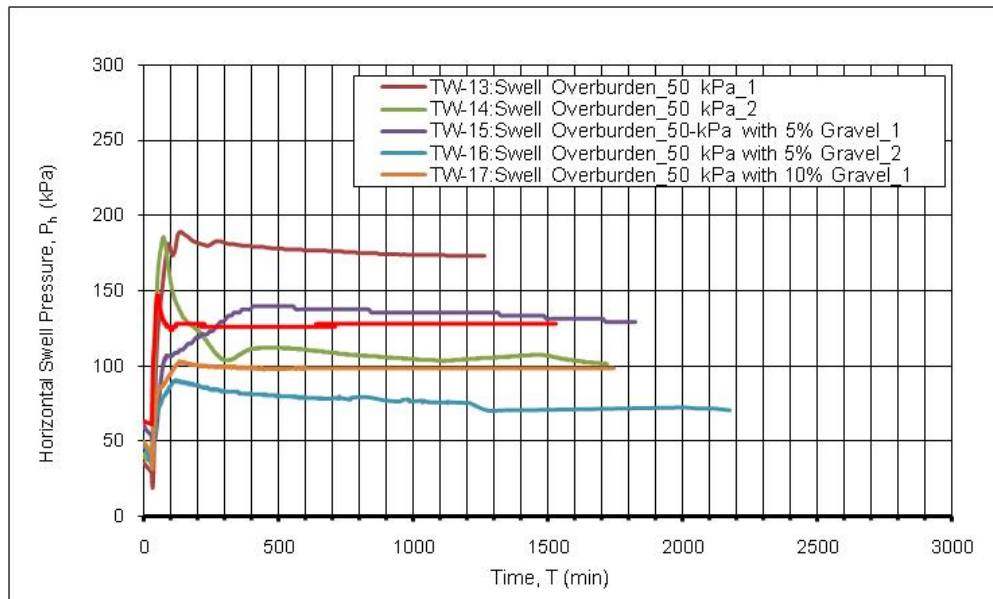


Figure 5. 53 Lateral Swell Pressure vs. Time Relationship for Thin-Wall Ring Tests (Ring-1) Performed on Type-3 Soil Samples for Different Treatment Percentages ( $P_o=50$  kPa)

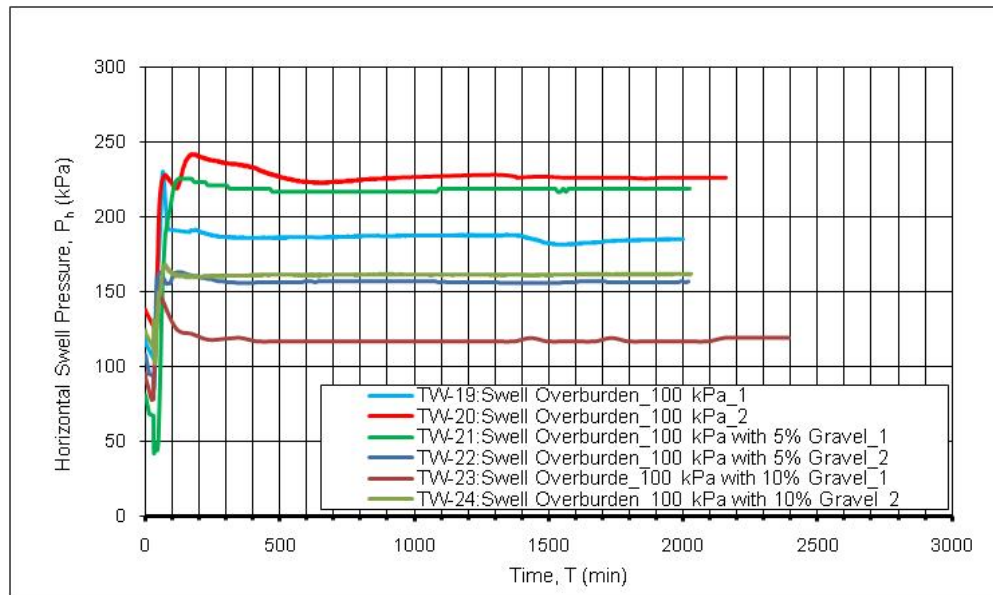


Figure 5. 54 Lateral Swell Pressure vs. Time Relationship for Thin-Wall Ring Tests (Ring-1) Performed on Type-3 Soil Samples for Different Treatment Percentages ( $P_o=100$  kPa)

### 5.4.3 Stage (c) Tests

In Stage (c) of Phase-4, the experiment program for Stage (b) was repeated for Type-5 soil. The possible positive effects of columns and/or trenches, backfilled with granular material, on the improvement of lateral swell pressures of expansive soils, was investigated by using both. The Ertekin Ring (Ring-1) and the Avşar Ring (Ring-2). Soil samples were tested under free swell (i.e. 7 kPa seating pressure) and vertical pressure of 25 kPa and different than Stage (b) tests, gravel material was used with 10%, 20% and 30% area replacement ratios. A total number of 32 tests were performed on Type-5 soils having an initial moisture content of 15 % and dry density of 1.2 g/cm<sup>3</sup>. The results of the tests are presented in Table 5.17. The lateral swell pressure versus time relationships for free swell tests and tests performed with 25 kPa overburden pressure are presented in Figure 5.51, 5.52, 5.53 and 5.54 for the two thin-wall rings respectively. The lateral swell pressure vs. time relationships for each overburden pressure and area replacement ratio of the relevant tests are also presented in the Appendices.

Table 5. 17 Results of Thin-Wall Ring Tests Performed on Soil Type-5 with  $P_s=7$  kPa (Phase-4, Stage (c))

Test No	Ring #	Area Replacement Ratio, ARR (%)	Peak Lateral Pressure, $P_{hp}$ (kPa)	Ultimate Lateral Pressure, $P_{hu}$ (kPa)	Final Water Content, $w_f$ (%)	Vertical Swell, $S_v$ (%)
TW-25	1	0	164	51	52.0	23.33
TW-26	1	0	183	56	53.3	21.07
TW-27	1	10	105	20	57.7	17.33
TW-28	1	10	130	45	58.9	18.78
TW-29	1	20	79	40	63.1	16.70
TW-30	1	20	75	54	61.1	15.67
TW-31	1	30	59	37	69.1	15.40
TW-32	1	30	50	45	71.7	15.63
TW-33	2	0	188	48	59.7	20.03
TW-34	2	0	208	20	58.8	23.50
TW-35	2	10	147	27	64.4	20.67
TW-36	2	10	161	55	62.1	19.20
TW-37	2	20	85	29	68.3	18.10
TW-38	2	20	110	47	76.6	21.66
TW-39	2	30	62	21	80.5	18.10
TW-40	2	30	58	45	75.1	17.73



Table 5. 18 Results of Thin-Wall Ring Tests Performed on Soil Type-5 with  $P_o=25$  kPa (Phase-4, Stage (c))

Test No	Ring #	Area Replacement Ratio, ARR (%)	Peak Lateral Pressure, $P_{hp}$ (kPa)	Ultimate Lateral Pressure, $P_{hu}$ (kPa)	Final Water Content, $w_f$ (%)	Vertical Swell, $S_v$ (%)
TW-41	1	0	192	83	46.05	15.11
TW-42	1	0	179	68	48.44	17.53
TW-43	1	10	131	82	56.93	13.67
TW-44	1	10	144	68	54.77	14.57
TW-45	1	20	105	100	60.09	12.42
TW-46	1	20	88	87	60.04	11.83
TW-47	1	30	81	72	61.44	8.83
TW-48	1	30	89	86	60.81	8.07
TW-49	2	0	230	73	54.85	16.60
TW-50	2	0	212	67	48.87	14.60
TW-51	2	10	169	99	59.17	12.27
TW-52	2	10	158	83	63.19	11.67
TW-53	2	20	104	68	60.41	13.00
TW-54	2	20	136	94	66.37	10.33
TW-55	2	30	89	65	66.87	6.67
TW-56	2	30	103	86	66.07	7.40

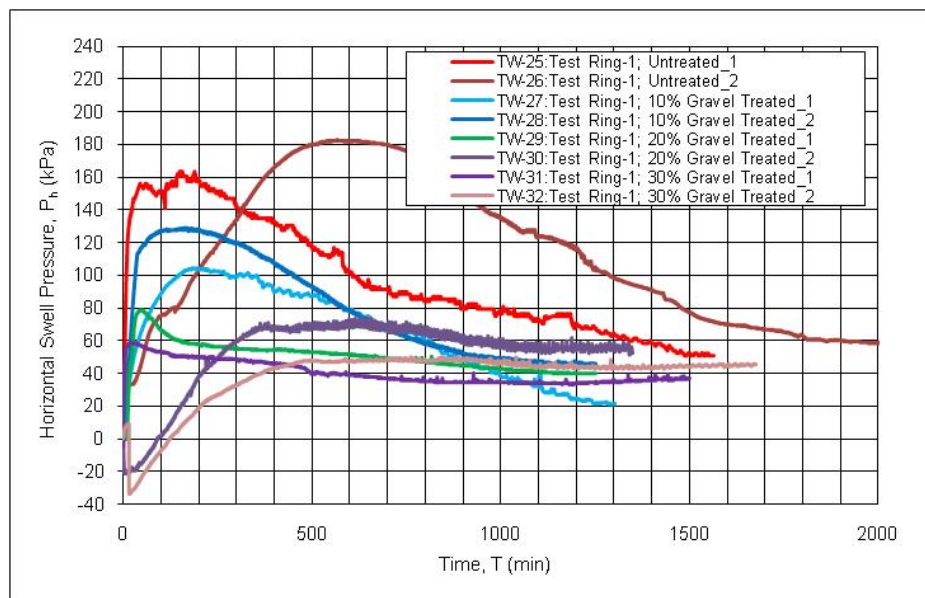


Figure 5. 55 Lateral Swell Pressure vs. Time Relationship for Thin-Wall Ring Tests (Ring-1) Performed on Type-5 Soil Samples for Different Treatment Percentages ( $P_s=7$  kPa)

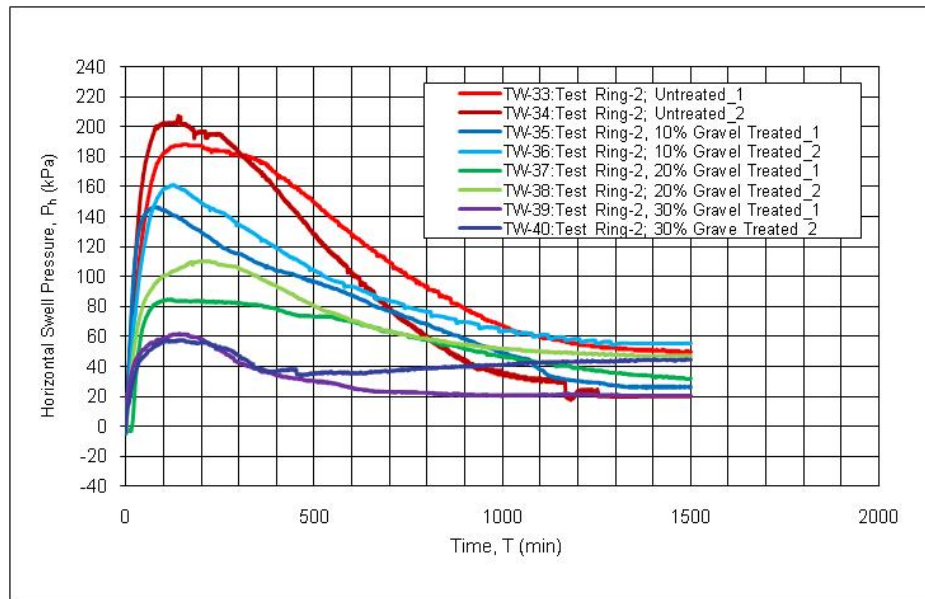


Figure 5. 56 Lateral Swell Pressure vs. Time Relationship for Thin-Wall Ring Tests (Ring-2) Performed on Type-5 Soil Samples for Different Treatment Percentages ( $P_s=7$  kPa)

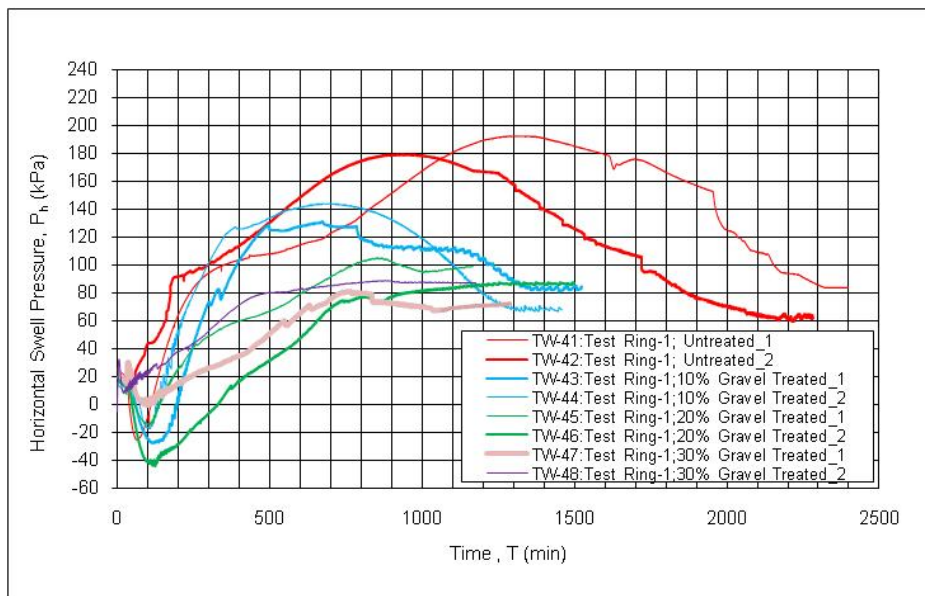


Figure 5. 57 Lateral Swell Pressure vs. Time Relationship for Thin-Wall Ring Tests (Ring-1) Performed on Type-5 Soil Samples for Different Treatment Percentages ( $P_o=25$  kPa)

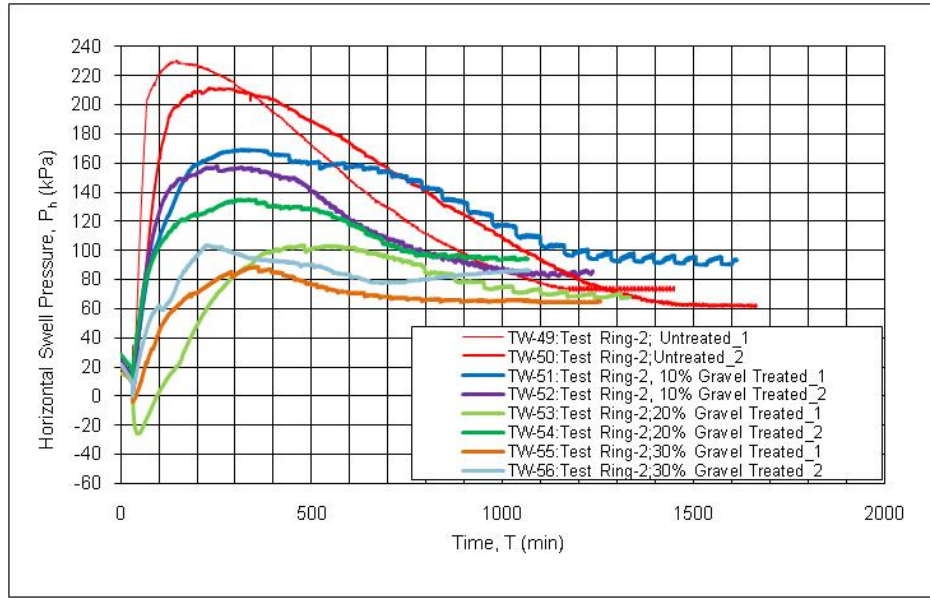


Figure 5. 58 Lateral Swell Pressure vs. Time Relationship for Thin-Wall Ring Tests (Ring-2) Performed on Type-5 Soil Samples for Different Treatment Percentages ( $P_o=25$  kPa)

#### 5.4.4 Stage (d) Tests

In the last phase of the investigations, the effect of silt on the improvement of lateral swell pressure of expansive soils was also investigated. For similar reasons explained in the results of Phase III investigations, silt was placed with a relative density greater than 90%, which in turn practically prevented the intrusion of clay into silt. The Ertekin's Ring (Ring-1) and the Avşar's Ring (Ring-2) were used simultaneously during the studies. Free swell tests with 7 kPa seating pressure were performed on Type-5 soil treated with 10, 20 and 30% area replacement ratio by silt. A total number of 32 tests were performed on Type-5 soils having an initial moisture content of 15 % and dry density of  $1.2 \text{ g/cm}^3$ .

The results of total number of 16 tests are presented in Table 5.19. The lateral swell pressure versus time relationship for free swell tests treated by silt with different area replacement ratios are presented in Figure 5.59 for Ring-1 and in Figure 5.60 for Ring-2, respectively. The lateral swell pressure vs. time

relationships for each area replacement ratio are also presented in the Appendices.

Table 5. 19 Results of Thin-Wall Ring Tests Performed on Silt Treated Soil Type-5 with  $P_s=7$  kPa (Phase-4, Stage (d))

Test No	Ring #	Area Replacement Ratio, ARR (%)	Peak Lateral Pressure, $P_{hp}$ (kPa)	Ultimate Lateral Pressure, $P_{hu}$ (kPa)	Final Water Content, $w_r$ (%)	Vertical Swell, $S_v$ (%)
TW-41	1	0	164	51	46.05	15.11
TW-42	1	0	183	56	48.44	17.53
TW-69	1	10	149	55	63.84	20.77
TW-70	1	10	145	35	70.42	14.67
TW-71	1	20	126	124	74.97	18.33
TW-72	1	20	150	143	68.55	12.53
TW-73	1	30	150	148	79.57	16.13
TW-74	1	30	128	86	77.72	15.37
TW-49	2	0	188	48	54.85	16.60
TW-50	2	0	208	20	48.87	14.60
TW-75	2	10	207	47	69.21	21.07
TW-76	2	10	164	123	61.61	15.13
TW-77	2	20	150	143	80.71	17.67
TW-78	2	20	163	112	68.86	10.00
TW-79	2	30	153	135	79.37	16.43
TW-80	2	30	125	120	80.94	15.57

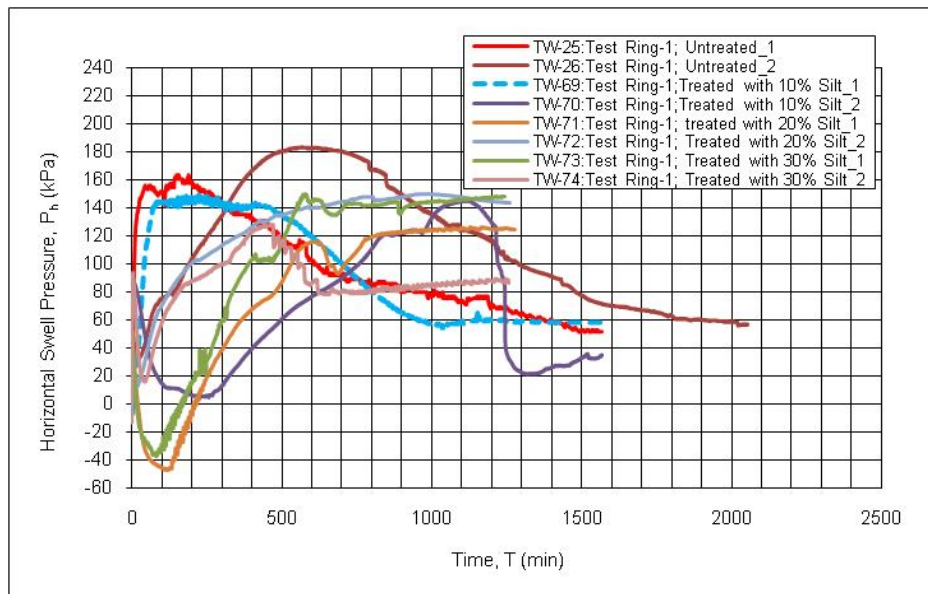


Figure 5. 59 Lateral Swell Pressure vs. Time Relationship for Thin-Wall Ring Tests (Ring-1) Performed on Type-5 Soil Samples for Different Treatment Percentages with Silt ( $P_s=7$  kPa)

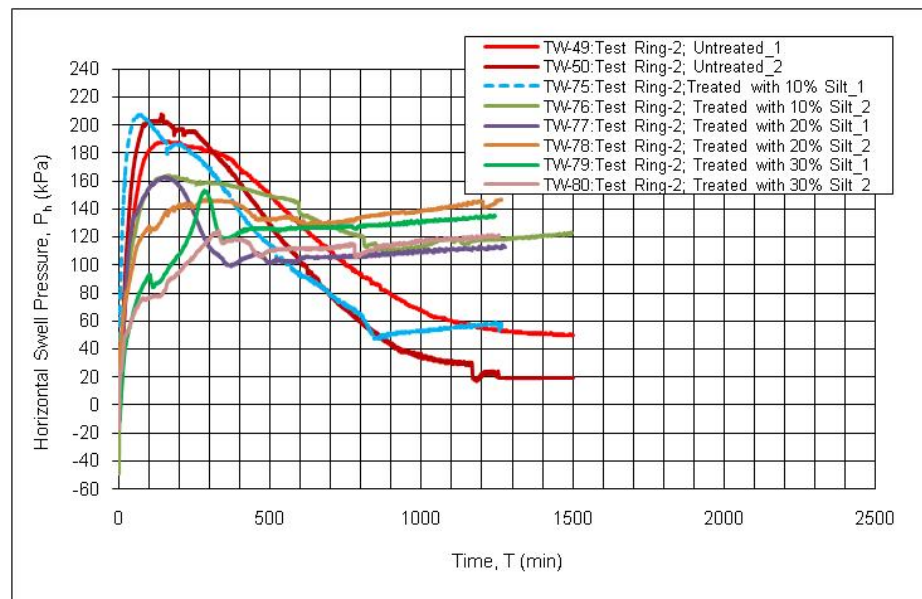


Figure 5. 60 Lateral Swell Pressure vs. Time Relationship for Thin-Wall Ring Tests (Ring-2) Performed on Type-5 Soil Samples for Different Treatment Percentages with Silt ( $P_s=7$  kPa)

## **CHAPTER VI**

### **DISCUSSION OF RESULTS**

#### **6.1 GENERAL**

The idea behind the present investigation is to study the possible positive effects of trenches and/or columns backfilled with granular material such as; crushed stone or rock, on the swelling potential of expansive soils. The research program is performed in four phases to investigate the efficiency of the proposed method as well as various factors that may influence its performance. The results of the tests performed within the content of the above mentioned study have been presented in Chapter V whereas the outcomes and their discussions are presented in the next subsections.

#### **6.2 INVESTIGATION PHASE 1**

The first phase of the investigations was dedicated to study the efficiency of the subject treatment methodology of expansive soils. Conventional oedometer tests were performed by introducing two types of granular soils with different gradations as well as three different treatment percentages, i.e. area replacement ratios, into the system, for this purpose.

The results and comparison of the free swell tests performed with sand and gravel are presented in Table 6.1 and Table 6.2. For different area replacement ratios, the treatment percentage in vertical swell is calculated from Equation 6.1 where Equation 6.2 gives the treatment percentage in vertical swell pressure.

Table 6. 1 Vertical Swell,  $S_v$  (%) and Treatment,  $TS_v$  (%) with respect to Material and Area Replacement Ratio Obtained from Free Swell Tests (Phase-1)

Area Replacement Ratio, ARR (%)	Average Vertical Swell, $S_{v(av)}$ (%)		Treatment, $TS_{(v)}$ (%)	
	Sand	Gravel	Sand	Gravel
0	34.0		-	
5	31.5	28.5	7.4	16.2
10	29.2	25.9	14.2	24.0
20	26.1	18.1	23.4	46.8

Table 6. 2 Vertical Swell Pressure,  $P_v$  (kPa) and Treatment,  $TP_v$  (%) with respect to Material and Area Replacement Ratio Obtained from Free Swell Tests (Phase-1)

Area Replacement Ratio, ARR (%)	Vertical Swell Pressure, $P_v$ (kPa)		Treatment, $TP_{(v)}$ (%)	
	Sand	Gravel	Sand	Gravel
0	400.0		-	
5	300	230	25.0	42.5
10	390	185	2.5	53.8
20	325	90	18.8	77.5

$$TS_{(v)}(\%) = \left( \frac{S_{v(av)}(Untreated) - S_{v(av)}(Treated)}{S_{v(av)}(Untreated)} \right) \cdot 100 \dots \dots \dots (6.1)$$

where :  $TS_{(v)}$ : The treatment percentage in vertical swell

$S_{v(av)}(Untreated)$ : Average Vertical Swell Percentage for Untreated Soil Sample (%)

$S_{v(av)}(Treated)$ : Average Vertical Swell Percentage for Treated Soil Sample (%)

$$TP_{(v)}(\%) = \left( \frac{P_{v(av)}(Untreated) - P_{v(av)}(Treated)}{P_{v(av)}(Untreated)} \right) \cdot 100 \dots\dots (6.2)$$

where :  $TP_{(v)}$ : The treatment percentage in vertical swell pressure

$P_{v(av)}(Untreated)$ : Average Vertical Swell Pressure for Untreated Soil Sample (%)

$P_{v(av)}(Treated)$ : Average Vertical Swell Pressure for Treated Soil Sample (%)

The treatment percentage in vertical swell and swell pressure versus area replacement ratio relationships are presented in Figure 6.1 and Figure 6.2, respectively.

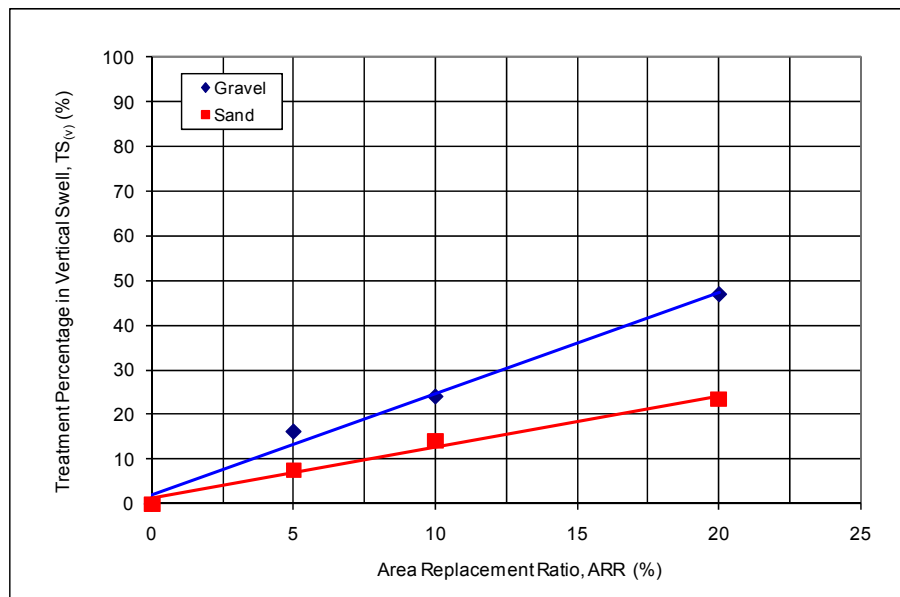


Figure 6. 1 Treatment Percentage in Vertical Swell vs. Area Replacement Ratio for Free Swell Oedometer Tests Performed on Type-2 Soil Samples



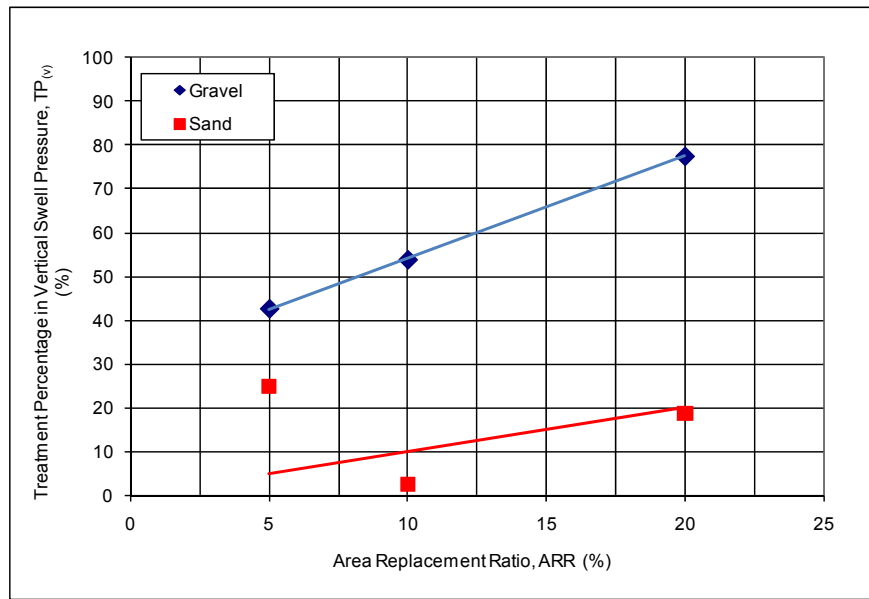


Figure 6. 2 Treatment Percentage in Vertical Swell Pressure vs. Area Replacement Ratio for Free Swell Oedometer Tests Performed on Type-2 Soil Samples

Table 6.3 and Table 6.4 summarize the results and comparison of the swell overburden tests performed with sand and gravel under 25, 50, 100 and 150 kPa overburden pressures.

The treatment percentage in vertical swell versus area replacement ratio for sand and gravel are presented in Figure 6.3 and Figure 6.4, respectively. The treatment in vertical swell pressure with respect to different area replacement ratios for sand and gravel are illustrated in Figure 6.5.

Table 6. 3 Vertical Swell,  $S_v$  (%) and Treatment,  $TS_v$  (%) with respect to Material and Area Replacement Ratio Obtained from Swell Overburden Tests (Phase-1)

Overburden Pressure, $P_o$ (kPa)	Area Replacement Ratio, ARR (%)	Average Vertical Swell, $S_{v(av)}$ (%)		Treatment, $TS_{(v)}$ (%)	
		Sand	Gravel	Sand	Gravel
25	0	13.7		-	
	5	12.8	11.1	6.9	19.0
	10	13.1	9.7	4.9	29.2
	20	9.9	6.2	28.0	54.5
50	0	8.9		-	
	5	8.0	5.9	10.4	33.9
	10	7.8	5.7	12.0	35.4
	20	7.2	3.4	18.8	62.1
100	0	4.5		-	
	5	4.0	3.1	11.1	30.3
	10	4.1	2.2	6.9	50.4
	20	3.3	0.9	26.1	79.9
150	0	3.8		-	
	5	3.2	1.3	15.6	65.1
	10	3.0	0.8	20.4	79.6
	20	1.6	0.0	57.4	-

Table 6. 4 Vertical Swell Pressure,  $P_v$  (kPa) and Treatment,  $TP_v$  (%) with respect to Material and Area Replacement Ratio Obtained from Swell Overburden Tests (Phase-1)

Area Replacement Ratio, ARR (%)	Vertical Swell Pressure, $P_v$ (kPa)		Treatment, $TP_v$ (%)	
	Sand	Gravel	Sand	Gravel
0	251		-	
5	233	179	7.0	28.7
10	226	164	9.7	34.6
20	210	124	16.2	50.6

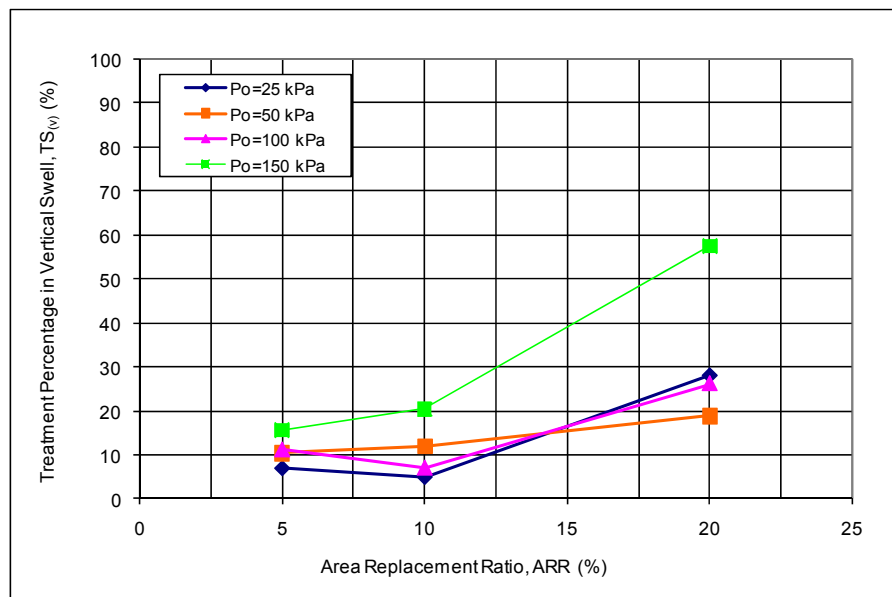


Figure 6. 3 Treatment Percentage in Vertical Swell vs. Area Replacement Ratio for Swell Overburden Oedometer Tests Performed on Type-2 Soil (Sand Treated)

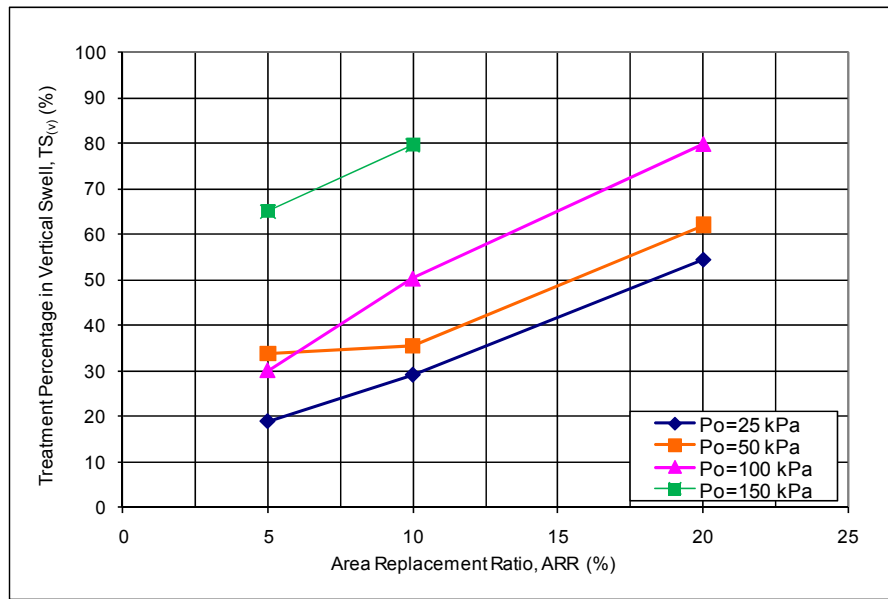


Figure 6. 4 Treatment Percentage in Vertical Swell vs. Area Replacement Ratio for Swell Overburden Oedometer Tests Performed on Type-2 Soil (Gravel Treated)

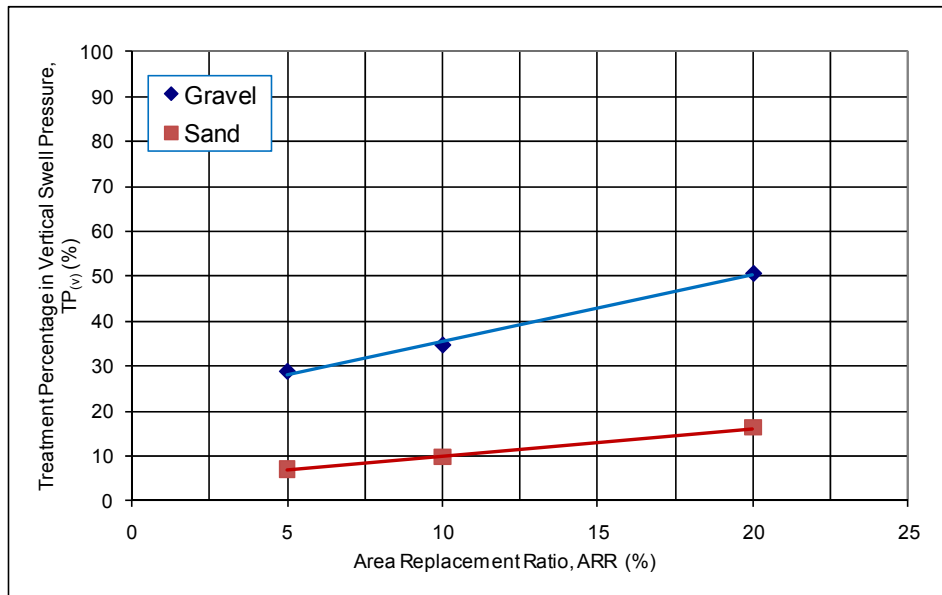


Figure 6. 5 Treatment Percentage in Vertical Swell Pressure vs. Area Replacement Ratio for Swell Overburden Oedometer Tests Performed on Type-2 Soil

Both free swell and swell overburden test data reveal that treatment of expansive soils is possible via introducing a percent replacement of the soil by a granular fill. For free swell tests the treatment percentage ranges were observed to change between 7 to 23% for sand whereas for gravel the treatment ranged between 16 to 47%, the treatment amount being increased with increasing area replacement ratios. For swell overburden tests on the other hand, the treatment percentage in vertical swell for sand is observed to be between 7 and 57% while gravel performed better yielding treatment percentages between 19 to 100%.

From the above observations, it can be depicted that the treatment with gravel, having a larger particle size compared to sand, gives more satisfactory treatment percentages. This result can be explained by the larger void spaces which allow the volumetric expansion and intrusion of the expansive soil into the granular soil. This foresight is also realized from the cross-sectional views of the treated samples, prepared after the tests have been finished. As can be seen from Figure 6.6 and Figure 6.7, expansive soil sample shows a tendency to expand volumetrically through the voids of the granular material.

The treated samples are observed to reach to their peak swell percentages more rapidly when compared to untreated expansive clay samples. Time to reach the ultimate swell amounts for untreated samples were recorded to be more than 8000 minutes, whereas this duration decreased to around 1500 minutes for samples treated with different percentages of granular materials. This outcome is attributed to the behaviour of the granular soils acting as a vertical drainage channel, hence facilitating intrusion of water into central parts of the soil sample.

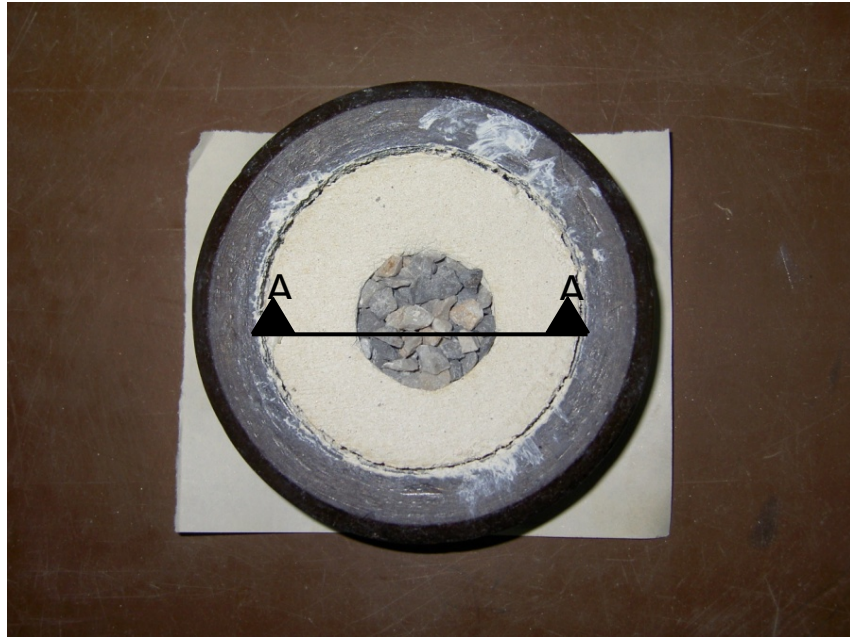


Figure 6. 6 Plan View of Soil Sample Intruded into Granular Material after Expanding

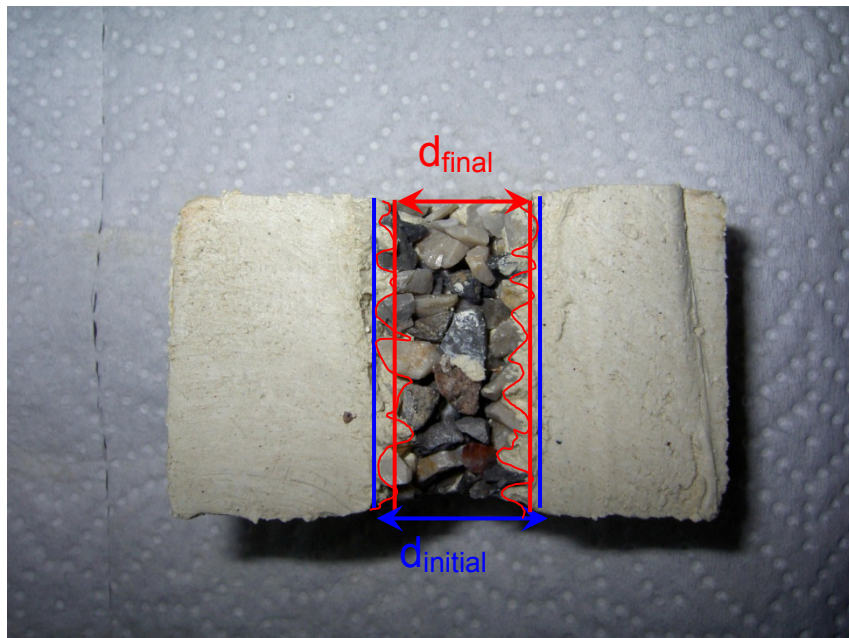


Figure 6. 7 A-A Cross Sectional View of Soil Sample Intruded into Granular Material after Expanding

The treatment percentages in vertical swell pressures with respect to different area replacement ratios have been presented in Figure 6.2 for swell tests and in Figure 6.5 for swell overburden tests. As can be seen from the results, for samples treated by gravel, the treatment in swell pressures is observed between 43 and 78% for free swell tests and between 29 to 51% for swell overburden tests. However for both types of tests performed on sand, the treatment could not reach above 25%. Although this finding seems to support the outcome that gravel treatment performs better compared to sand, it should always be kept in mind that there is a possibility that the granular material may act as a rigid member during the application of vertical pressures, thus affecting the magnitude of swell pressure measured during the loading stages of tests. Therefore, the swell pressures, calculated during the loading stages of expansive soils treated with granular material, shall be evaluated with utmost caution.

When the results of Phase-1 tests are summarized, the following points are noteworthy;

- The treatment of expansive soils is possible via introducing a percent replacement of the soil by a granular fill.
- The treatment with gravel, having a larger particle size compared to sand, gives more satisfactory treatment percentages.
- The treatment amount is increased with increasing area replacement ratio.
- The treated samples are observed to reach to their peak swell percentages more rapidly when compared to untreated expansive clay sample which is attributed to the behaviour of the granular soils acting as a vertical drainage channel, hence facilitating intrusion of water into central parts of the soil sample.

Although the principle behind the treatment mechanism is fundamentally different from the present study, the results of the investigations performed by Al-Omari and Hamodi (1991), Phanikumar and Rao (2000), Phanikumar et al. (2004), and Sharma and Phanikumar (2005) are compatible with the points mentioned above.

Different from the scope of this study, which emphasizes the possible positive effects of trenches backfilled with crushed stone or rock on the swell parameters of expansive soils, the above mentioned research mainly focused on rehabilitation of expansive clays with granular columns reinforced with different types of anchorages, i.e. base geosynthetics, anchor plate and central rod or peripheral geosynthetics such as geotextile or geogrid.

As described in detail in Chapter II, Phanikumar and Rao (2000) and Sharma and Phanikumar (2005) concluded that heave protection became more effective as the particle size of the granular fill is increased, this result being attributed to the frictional resistance mobilized between the granular column and the surrounding medium. Although the end result is consistent, it differs from the present study in which the major anticipated mechanism is the filling of voids of the granular material inside trenches.

Similarly it was shown by Phanikumar and Rao (2000), Phanikumar et. al. (2004), and Sharma and Phanikumar (2005) that the amount of heave decreased as the diameter of granular column was increased, which, in turn, was explained by the frictional effects. In the present study, however, the reduction in heave as the area replacement ratio is increased, is dedicated to the increase in volume of voids introduced by granular material.

The results of Phanikumar et. al. (2004), and Sharma and Phanikumar (2005) revealed that the duration to reach the final heave decreased considerably upon the introduction of granular material into the expansive soil which is in fact a natural outcome due to the hydraulic conductivity of the granular media. This is also consistent with the present study.

Figure 6.8 and Figure 6.9 show the change of final water content with increasing overburden pressure while average final water content values plotted against area replacement ratio under different overburden pressures for sand and gravel treated soil samples are illustrated in Figure 6.10 and Figure 6.11, respectively.



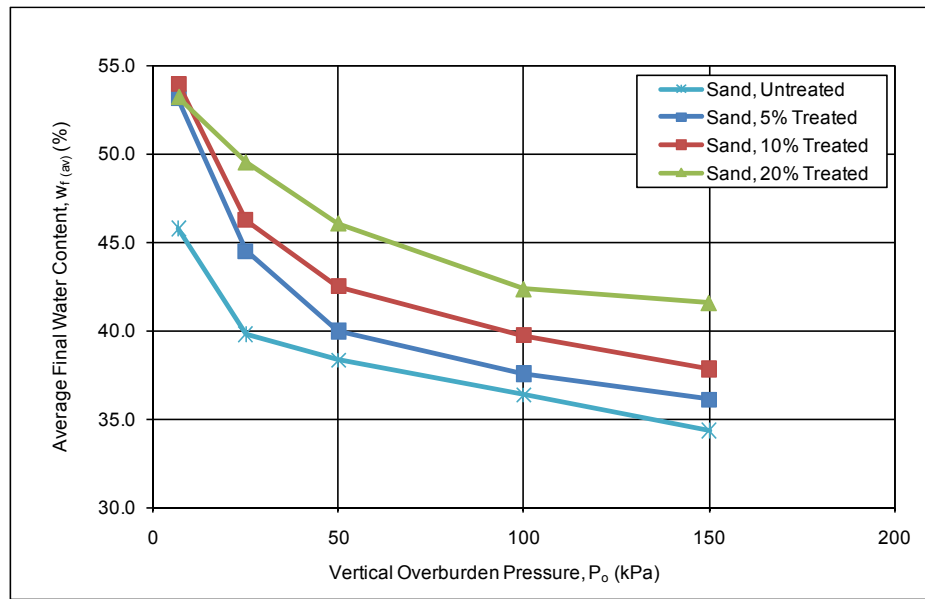


Figure 6. 8 Average Final Water Content vs. Vertical Overburden Pressure for Oedometer Tests Performed on Type-2 Soil Treated with Sand

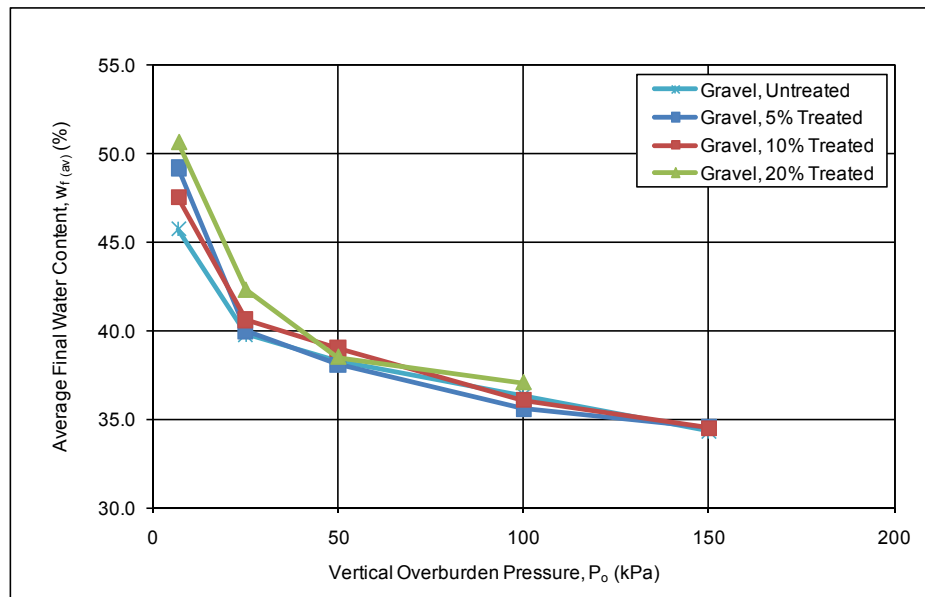


Figure 6. 9 Average Final Water Content vs. Vertical Overburden Pressure for Oedometer Tests Performed on Type-2 Soil Treated with Gravel

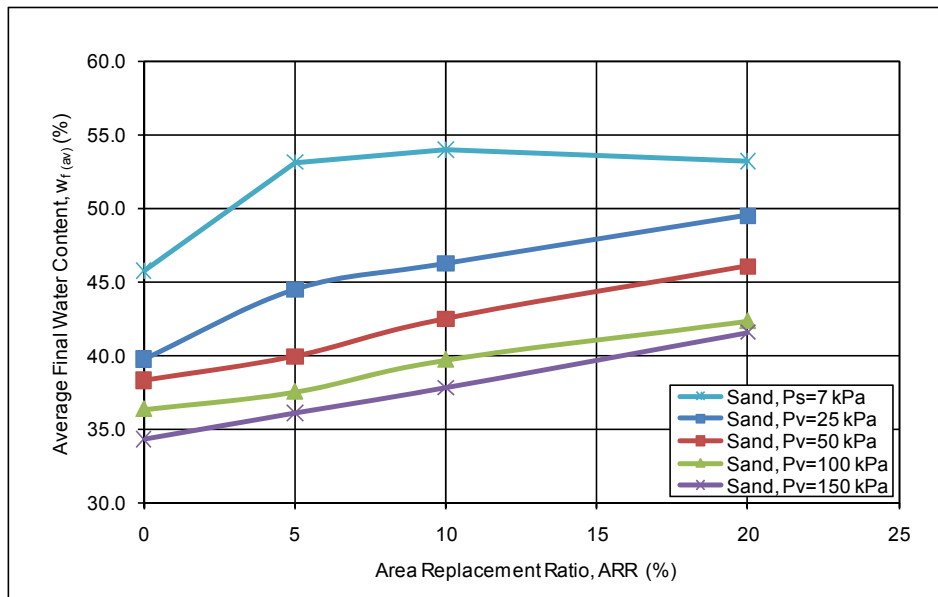


Figure 6. 10 Average Final Water Content vs. Area Replacement Ratio for Oedometer Tests Performed on Type-2 Soil Treated with Sand

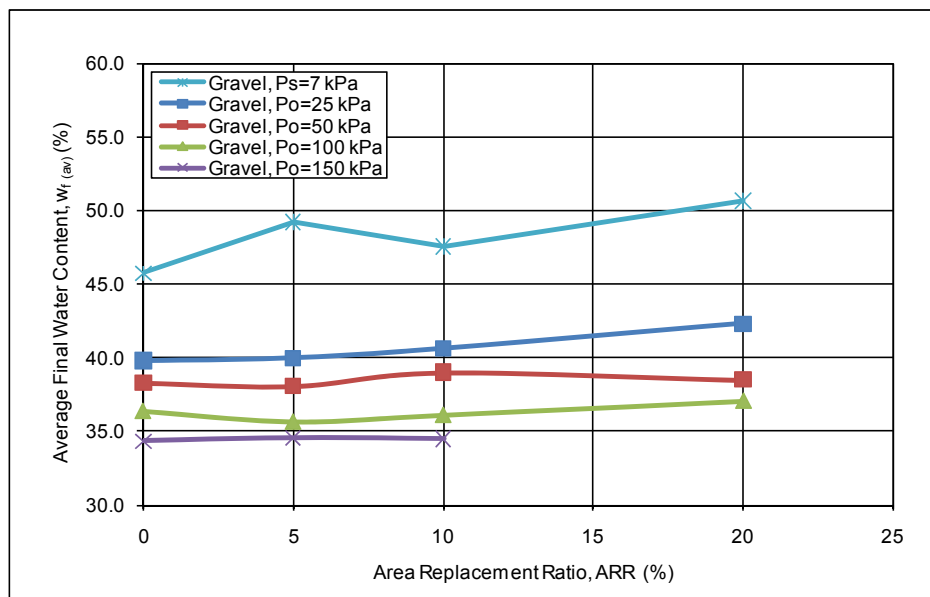


Figure 6. 11 Average Final Water Content vs. Area Replacement Ratio for Oedometer Tests Performed on Type-2 Soil Treated with Gravel

As it can be seen from the figures, the final water content values are observed to decrease with increasing overburden pressures for both untreated as well as sand and gravel treated samples. This finding is parallel to observations presented by Al-Shamrani and Al-Mhaidib (2000). On the other hand, the effect of area replacement ratio was observed to be more emphasized in the case of sand compared to gravel treatment. As explained previously, gravel performed better than sand as treatment material under similar testing conditions. Therefore, it is expected that soil treated with sand will have a higher affinity to imbibe water thus giving higher final water contents compared to gravel.

### **6.3 INVESTIGATION PHASE 2**

In the second phase of the investigations, the effect of sample size as well as the index properties of expansive soils on the level of improvement of expansive soils treated with granular trenches and/or columns were evaluated. The effect of seating pressure and additional surcharge load on the improvement percentage were also investigated at this phase.

As a starting point, modified CBR mould tests were performed under a minimal seating pressure of 1 kPa on Type-1, Type-2 and Type-3 artificially prepared expansive soil samples. Following this stage, the test program was continued by the initial step of the second stage comprised of modified CBR mould tests performed under a seating pressure of 7 kPa on all of the five clay samples. For the two mentioned test groups, the corresponding sets with respect to soil type are compared for 1 kPa and 7 kPa seating pressures in Table 6.5. The vertical swell and treatment in vertical swell versus area replacement ratio plots are illustrated in Figures 6.12 and 6.13.

Table 6. 5 Average Vertical Swell,  $S_{v(av)}$  (%) and Treatment,  $TS_v$  (%) with respect to Area Replacement Ratio and Seating Pressure Obtained from Modified CBR Mould Tests (Phase-2, Stage(a))

Soil Type	Area Replacement Ratio, ARR (%)	Average Vertical Swell, $S_{v(av)}$ (%)		Treatment, $TS_v$ (%)	
		1 kPa	7 kPa	1 kPa	7 kPa
Type-1	0	42.5	19.0	-	-
	10	35.2	14.3	17.2	25.0
	20	26.4	10.3	38.0	45.6
	30	19.1	5.3	55.2	72.3
Type-2	0	62.3	28.0	-	-
	10	53.2	22.6	14.6	19.5
	20	41.4	17.0	33.5	39.4
	30	34.2	11.9	45.1	57.5
Type-3	0	72.9	35.4	-	-
	10	61.9	28.4	15.1	20.0
	20	51.0	21.1	30.1	40.5
	30	41.4	14.9	43.3	57.9

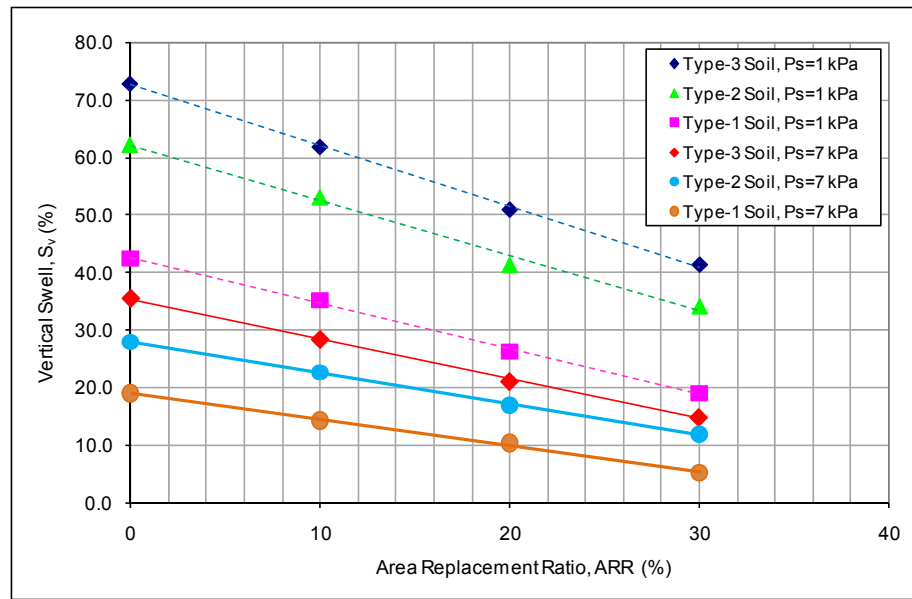


Figure 6. 12 Vertical Swell vs. Area Replacement Ratio for Modified CBR Mould Tests Performed with 1 kPa and 7 kPa Seating Pressures (Phase-2, Stage(a))

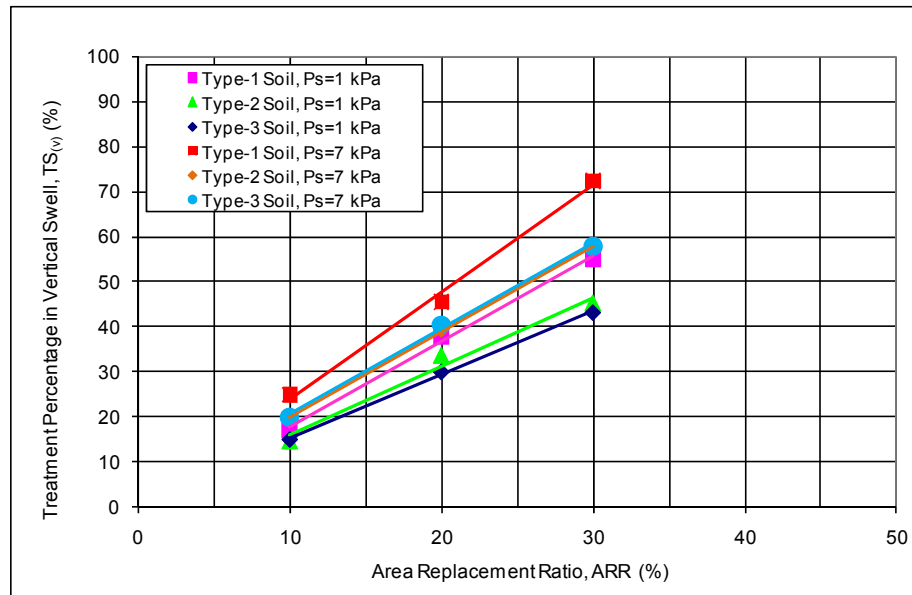


Figure 6. 13 Treatment Percentage in Vertical Swell vs. Area Replacement Ratio for Modified CBR Mould Tests Performed with 1 kPa and 7 kPa Seating Pressures (Phase-2, Stage(a))

The results of the first stage investigation of Phase-2 once more confirmed that expansive soils could be treated by introducing a percent replacement of the soil by a granular fill. Besides, modified CBR moulds were observed to work well thus they can be accepted as a suitable alternative to oedometer tests for the next stages of investigations. Applying a seating pressure of 1 psi ( $\approx 7$  kPa) instead of a negligible pressure of 1 kPa, which in turn is the minimum pressure recommended by ASTM (ASTM D 4546 – 08, 2008) resulted in a great reduction in swell percentages. This result is consistent with that of the first phase of the investigations showing that a small increase in overburden pressure resulted in a large reduction in the final water content under lower overburden pressures with the rate of reduction being dissipated as the overburden pressure is increased. Moreover, the treatment percentages were also observed to increase under 7 kPa pressure. The results of the first stage tests showed that the selected seating pressure during the tests played an important role on the final swell and treatment percentages in free swell tests, therefore its influence shall be taken into account when evaluating these parameters

In the second stage of the investigations on Phase-2, the effect of expansive soil properties on the treatment methodology was investigated. Scale effects were also examined by performing the tests both with modified CBR moulds and oedometer cells. Free swell tests were performed on five different samples with 7 kPa seating pressure. The results of these tests are compared in Table 6.6. The vertical swell percentage versus time relationship for oedometer and modified CBR mould tests performed on Type-5 soil are presented in Figure 6.14 for illustrative purposes while the relevant plots for the other four types of soils are presented in the Appendices.

Table 6. 6 Average Vertical Swell,  $S_{v(av)}$  (%) and Treatment,  $TS_v$  (%) with respect to Area Replacement Ratio for Free Swell CBR Mould and Oedometer Tests under  $P_s=7$  kPa Pressure (Phase-2, Stage(b))

Soil Type	Area Replacement Ratio, ARR (%)	Average Vertical Swell, $S_{v(av)}$ (%)		Treatment, $TS_v$ (%)	
		Oedo	CBR	Oedo	CBR
Type-1	0	23.2	19.0	-	-
	10	16.9	14.3	27.1	25.0
	20	11.2	10.3	51.9	45.6
	30	7.9	5.3	65.9	72.3
Type-2	0	34.0	28.0	-	-
	10	25.9	22.6	24.0	19.5
	20	18.1	17.0	46.8	39.4
	30	13.1	11.9	61.4	57.5
Type-3	0	39.4	35.4	-	-
	10	31.0	28.4	21.3	20.0
	20	23.0	21.1	41.7	40.5
	30	18.0	14.9	54.4	57.9
Type-4	0	4.4	4.5	-	-
	10	3.9	3.5	12.4	21.8
	20	3.4	2.9	23.8	36.2
	30	3.0	2.0	32.9	55.8
Type-5	0	41.5	37.2	-	-
	10	31.5	30.8	24.1	17.3
	20	26.2	23.4	36.9	37.1
	30	20.7	18.2	50.2	51.2

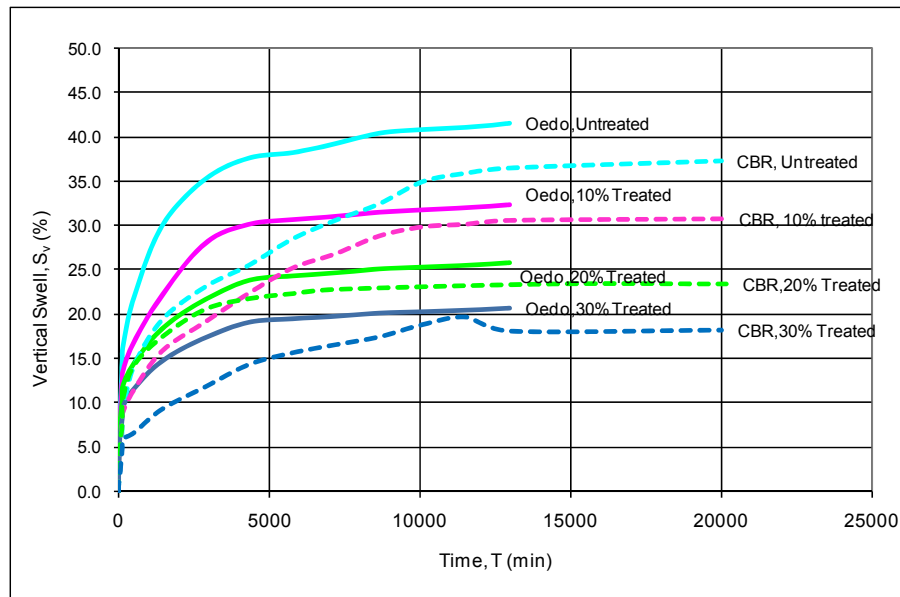


Figure 6. 14 Vertical Swell Percentage vs. Time Relationship for Oedometer Tests and Modified CBR Mould Tests on Type-5 Soil Samples ( $P_s=7$  kPa)

Table 6.6 and the vertical swell pressure versus time relationships depict that excluding Type-4 soil with less swell potential, oedometer tests gave higher expansion values compared to modified CBR mould test results. Swell values measured from oedometer tests were observed to be 6 to 34% higher with an average value of 15% compared to modified CBR mould tests. A similar outcome was presented by Azam (2006) who tested undisturbed clay samples on conventional circular as well as large scale circular and square oedometer tests defining a reduction of 40% in final vertical swell percentage when sample section change from conventional circular oedometer to large scale circular oedometer. Azam (2006) explained this issue by the effect of the high wall contact areas of the large scale samples. However, the aspect ratio (Length/Diameter) of both the oedometer and modified CBR samples were selected to be equal for the present investigation thus yielding identical circumferential resistance. Therefore, the effect of side friction is decided to be invalid for this study. As a result, the variance between vertical swell percentages of the two specimens was attributed to specimen preparation and testing



conditions. On the other hand, as it can be seen from the results, oedometer showed 6 to 28% higher treatment for 10% area replacement ratio and 3 to 16% higher treatment for 20% area replacement ratio with an average value of 7%, whereas the treatment percentages for 30% replacement are almost comparable for both types of tests. As both test types gave almost comparable results in terms of total treatment percentages regardless of their dimensions, it can be concluded that both tests can be used to estimate the treatment percentages of soils improved by granular soils.

The vertical swell versus area replacement ratio for modified CBR tests and oedometer tests performed under a seating pressure of 7 kPa are presented in Figure 6.15 and Figure 6.16, whereas the combined plots of these two test types are given in Figure 6.17. The treatment percentage in vertical swell versus area replacement ratio plots observed from the experiments, are presented in Figure 6.18.

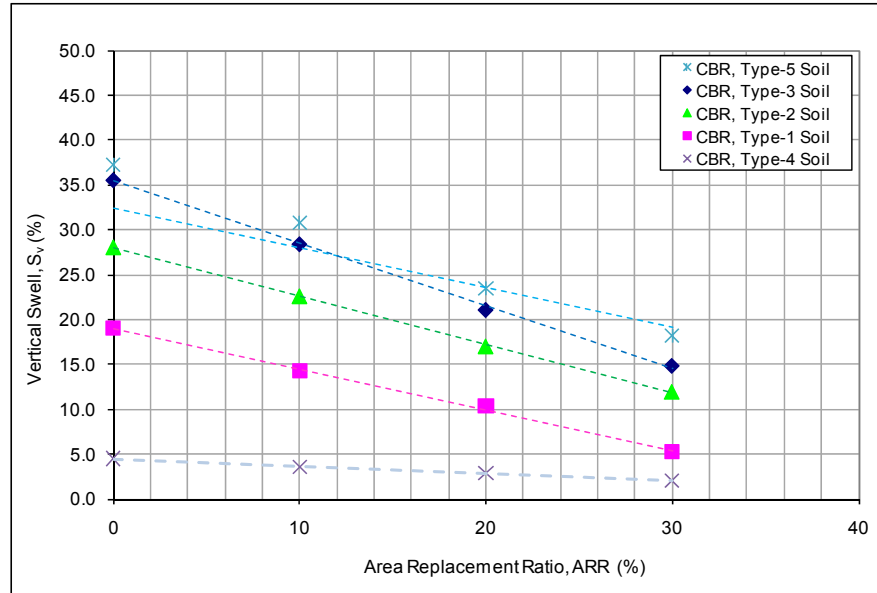


Figure 6. 15 Vertical Swell vs. Area Replacement Ratio for Modified CBR Mould Tests Performed with 7 kPa Seating Pressure (Phase-2, Stage(b))

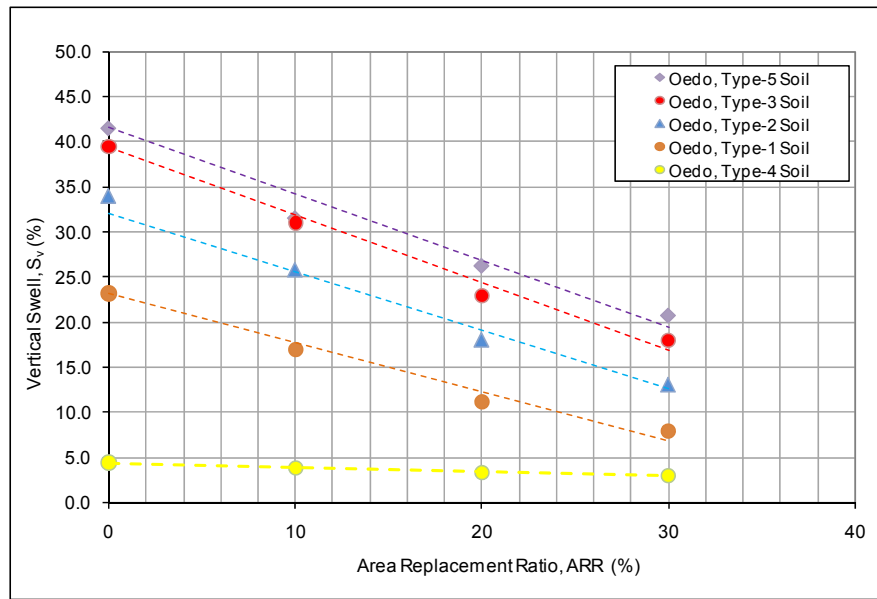


Figure 6. 16 Vertical Swell vs. Area Replacement Ratio for Oedometer Tests Performed with 7 kPa Seating Pressure (Phase-2, Stage(b))

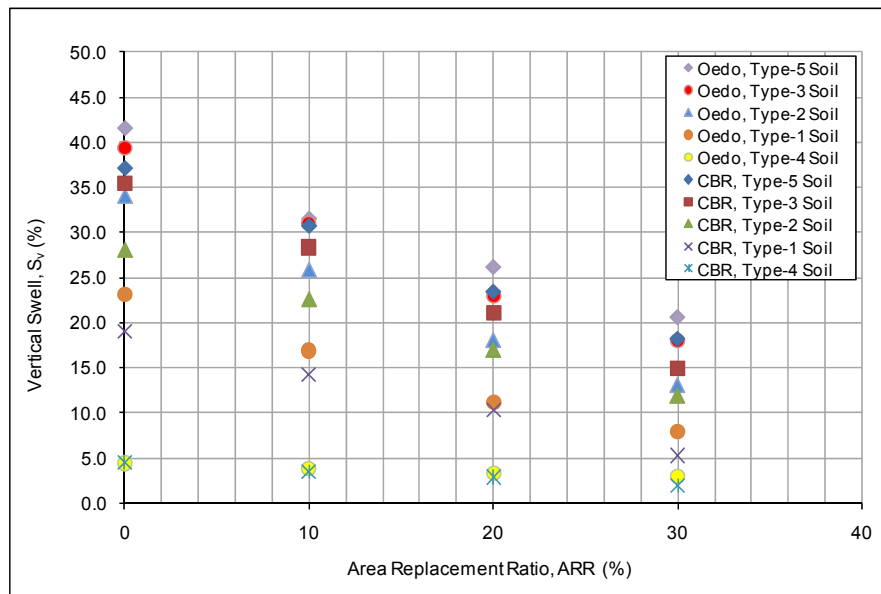


Figure 6. 17 Vertical Swell vs. Area Replacement Ratio for Modified CBR Mould and Oedometer Tests Performed with 7 kPa Seating Pressure (Phase-2, Stage(b))

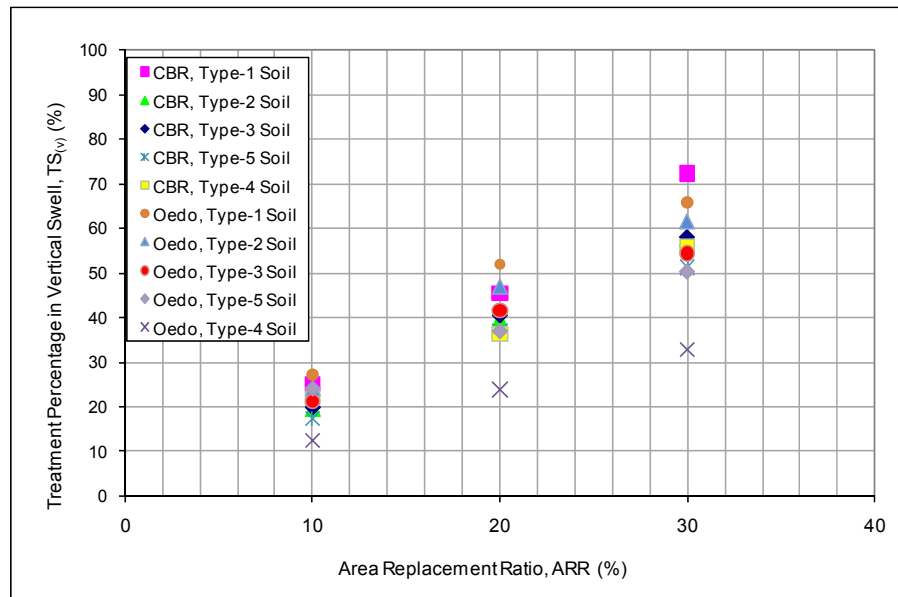


Figure 6. 18 Treatment Percentage in Vertical Swell vs. Area Replacement Ratio for Modified CBR Mould and Oedometer Tests Performed with 7 kPa Seating Pressure (Phase-2, Stage(b))

Table 6.6 in combination with the above mentioned figures show that excluding the results of Type-4 soil, which has a low swell potential compared to four other types of soil samples, the treatment percentages in vertical swell range in between 17 to 27% for an area replacement ratio of 10%, 37 to 52% for an area replacement ratio of 20% and 51 to 72% for an area replacement ratio of 30%, with smaller values corresponding to soils having higher swelling potential. Although the resultant treatment is observed to be less efficient for soils with higher swell potential, the results indicate that, even Type-5 soil, which has the highest potential to swell, showed a treatment up to 51%, proving the effectiveness of the methodology. As a result, it can be concluded that opening a trench inside soil and backfilling it with a granular soil, effectively improves the expansive behaviour where the attained values are considerably higher than the replacement ratios.

A multiple regression analysis for the vertical swell percentage versus area replacement ratio data for different soil types presented in Figure 6.17 is carried out with the statistical analysis software package SPSS and the following empirical equation, that is statistically significant at  $p=0.05$  level based on F-test statistics with a coefficient of determination of  $R^2=0.85$ , has been developed, under a seating pressure of  $P_s=7$  kPa:

$$\log(1 + S_v) = 0.588 + 0.014PI - 0.581 \log(1 + ARR) \dots \dots \dots (6.1)$$

where,  $S_v$ : Vertical Swell Percentage (%)

PI: Plasticity Index

ARR: Area Replacement Ratio (%)

The relationship between the measured values of percent vertical swell and the predicted values is presented in Figure 6.19. The relationship is observed to best fit within the range of the experimental data limits used during regression analysis. However, after a vertical swell percentage of 42%, which is the maximum value reached during this investigation, error in swell prediction tends to increase. It is a well known fact that, swell behaviour is highly dependent upon the initial water content and the dry unit weight of the soil prior to expansion (El Sohby and Rabba, 1981 and Erol,1987). Therefore, it should be noted that Equation 6.1 is valid for the particular values of initial water content ( $w_i$ , %) and initial dry unit weight ( $\gamma_d$ ) of the expansive soil and relative density ( $D_r$ , %) of the granular material selected for the experimental program and the accuracy of the equation shall be assessed in case different parameters are used.

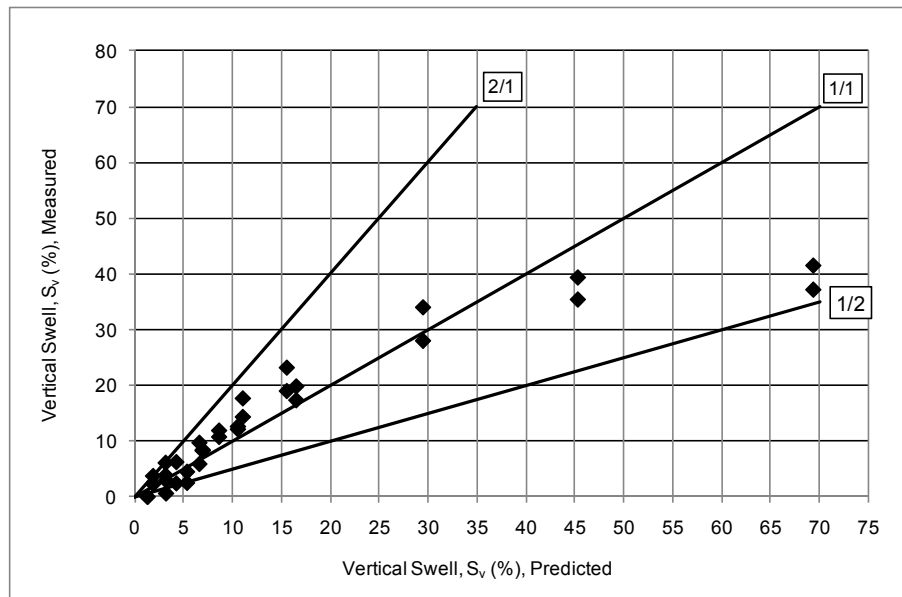


Figure 6. 19 Scatter of the Predicted versus Measured Vertical Swell Percentages for Oedometer Tests and Modified CBR Mould Tests on Type-5 Soil Samples ( $P_s=7$  kPa)

In the third stage, Stage (b) tests excluding Type-4 Soil, were repeated with an overburden pressure of 25 kPa representing the effect of a lightweight structure or an artificial fill of 1 meter high constructed to improve the treatment performance of trenches. The results of these tests are compared in Table 6.7. The vertical swell percentage versus time relationship for oedometer and modified CBR mould tests performed on Type-5 soil are presented in Figure 6.20 for illustrative purposes while the relevant plots for the other four types of soils are presented in the Appendices.

Table 6. 7      Average Vertical Swell,  $S_{v(av)}$  (%) and Treatment,  $TS_v$  (%) with respect to Area Replacement Ratio for Swell Overburden CBR Mould and Oedometer Tests under  $P_o=25$  kPa Pressure (Phase-2, Stage(c))

Soil Type	Area Replacement Ratio, ARR (%)	Average Vertical Swell, $S_{v(av)}$ (%)		Treatment, $TS_v$ (%)	
		Oedo	CBR	Oedo	CBR
Type-1	0	7.5	5.0	-	-
	10	6.1	3.9	18.3	22.8
	20	3.7	2.3	50.0	54.4
	30	0.0	0.0	100.0	100.0
Type-2	0	13.7	9.4	-	-
	10	9.7	5.9	29.2	37.4
	20	6.2	2.4	54.5	74.4
	30	2.9	0.6	78.5	93.5
Type-3	0	18.2	14.7	-	-
	10	12.6	12.1	30.4	17.7
	20	8.4	8.3	53.6	43.9
	30	2.5	4.5	86.2	69.5
Type-5	0	26.8	21.9	-	-
	10	19.8	17.4	25.9	20.8
	20	17.7	14.4	34.0	34.5
	30	11.9	10.8	55.5	50.9

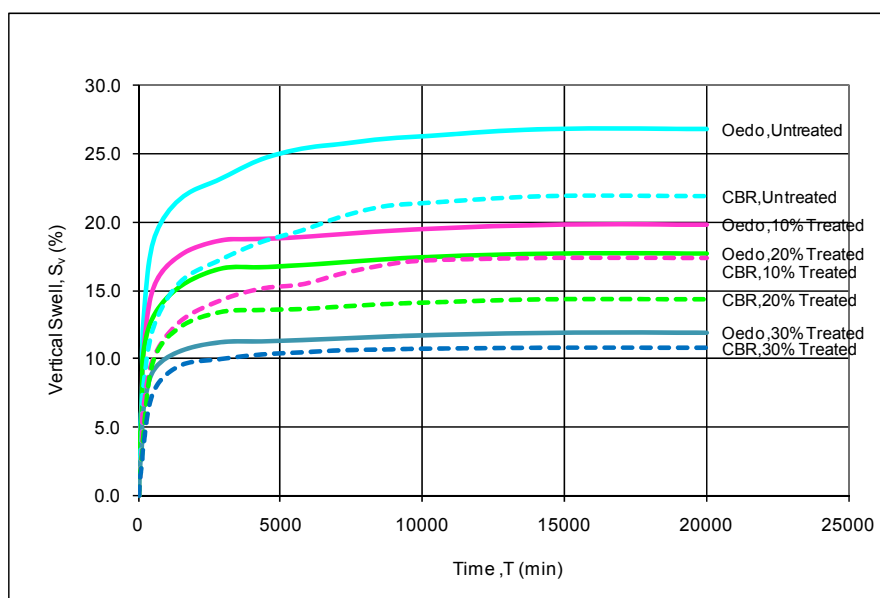


Figure 6. 20 Vertical Swell Percentage vs. Time Relationship for Oedometer Tests and Modified CBR Mould Tests on Type-5 Soil Samples ( $P_o=25$  kPa)

Similar to free swell tests performed at the previous investigation stage, swell values measured from swell overburden oedometer tests were observed to be higher compared to modified CBR tests, the average difference between the results of the two test types being 26%. Recalling that swell percentages are low due to presence of overburden, both oedometer and modified CBR mould results are found to be comparable i.e. if Type-3 and Type-5 soils with higher swell potential are compared, the difference is calculated to be 12% on average.

The vertical swell versus area replacement ratio for modified CBR tests and oedometer tests performed under an overburden pressure of 25 kPa are presented in Figure 6.21 and Figure 6.22 whereas the combined plots of these two test types are given in Figure 6.23. The treatment percentage in vertical swell versus area replacement ratio plots observed from the experiments, are presented in Figure 6.24.

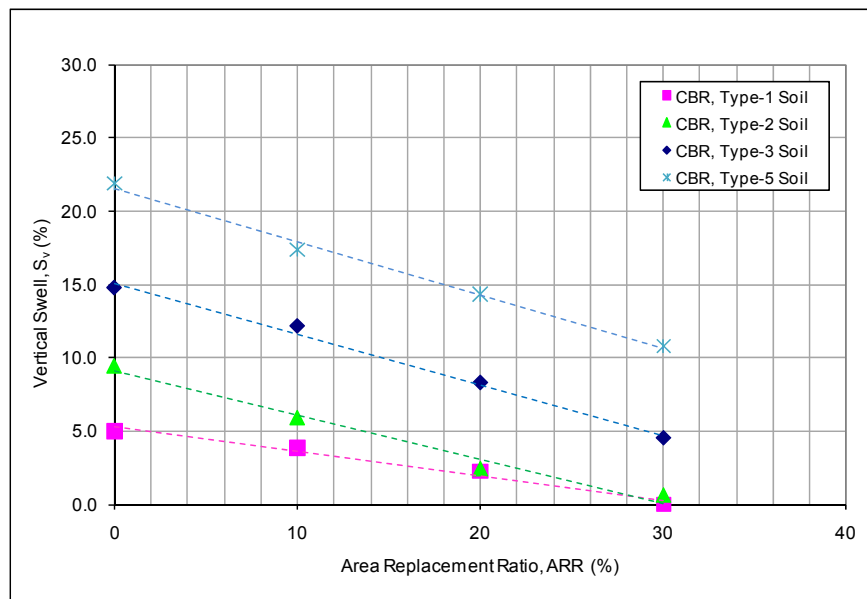


Figure 6. 21 Vertical Swell vs. Area Replacement Ratio for Modified CBR Mould Tests Performed with 25 kPa Overburden Pressure (Phase-2, Stage(c))

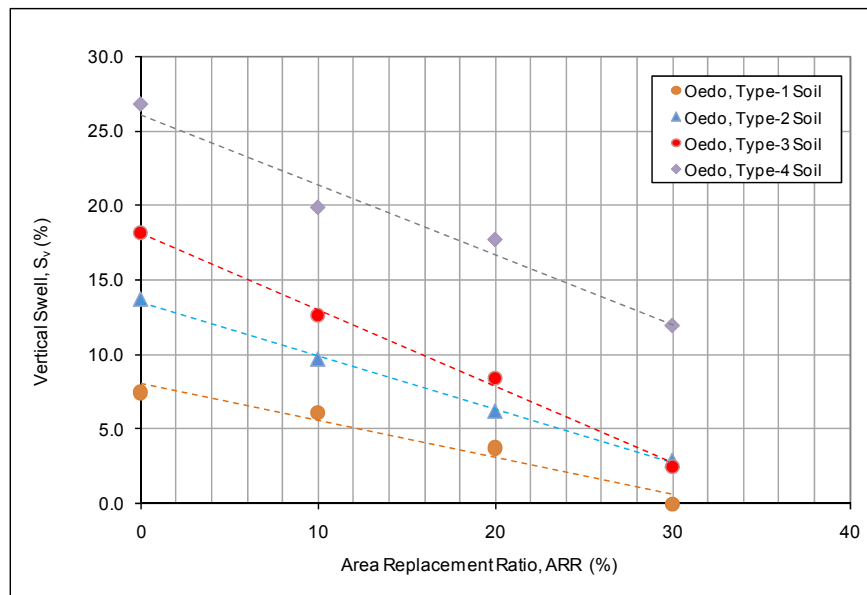


Figure 6. 22 Vertical Swell vs. Area Replacement Ratio for Oedometer Tests Performed with 25 kPa Overburden Pressure (Phase-2, Stage(c))



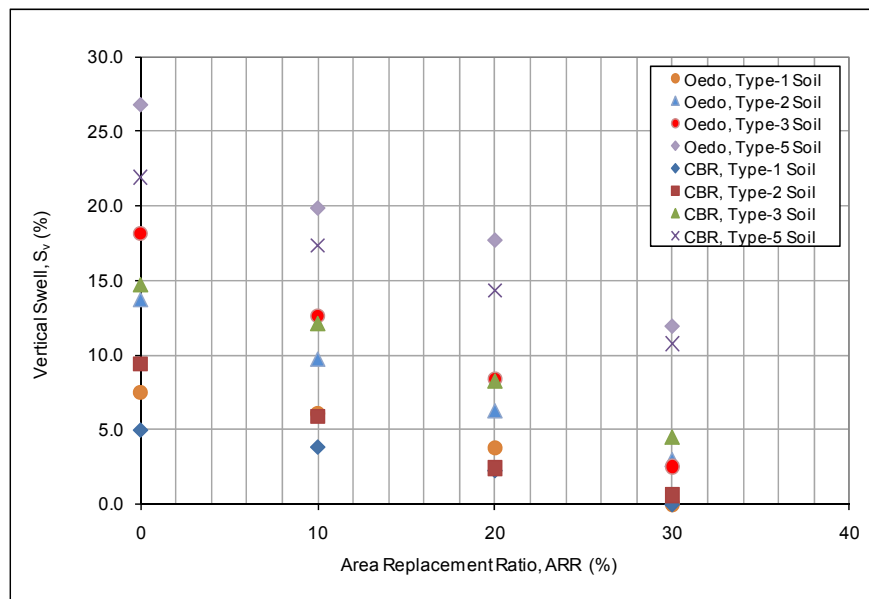


Figure 6. 23 Vertical Swell vs. Area Replacement Ratio for Modified CBR Mould and Oedometer Tests Performed with 25 kPa Overburden Pressure (Phase-2, Stage(c))

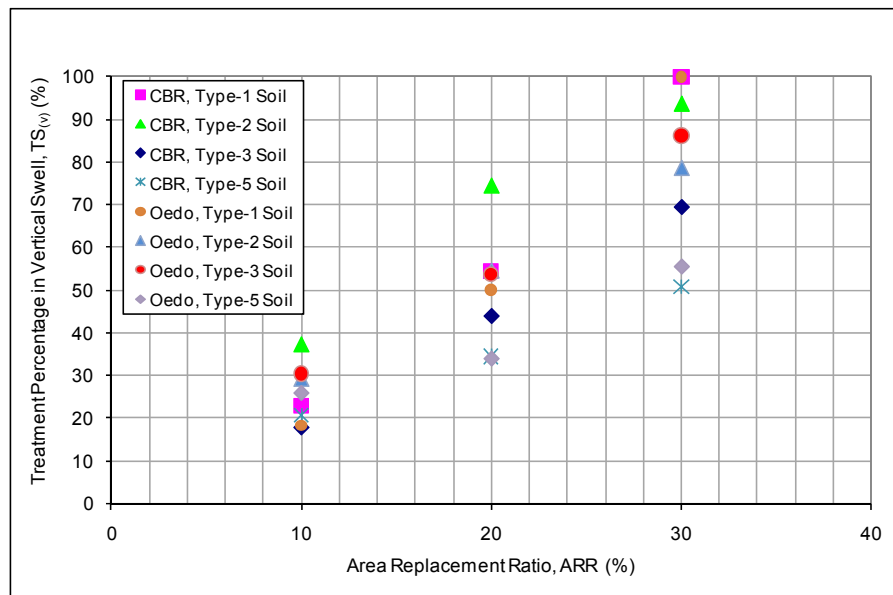


Figure 6. 24 Treatment Percentage in Vertical Swell vs. Area Replacement Ratio for Modified CBR Mould and Oedometer Tests Performed with 25 kPa Overburden Pressure (Phase-2, Stage(c))

The treatment percentages in vertical swell during the swell overburden tests on oedometer cells and CBR moulds change in between 18 to 37% for an area replacement of 10%, 34 to 74% for an area replacement of 20% and 51 to 100% for an area replacement of 30%, with smaller values mostly corresponding to soils with higher swelling potential. As a result, the subject methodology proves to be efficient under an overburden pressure of 25 kPa.

The outcome of the multiple regression analysis, performed on the vertical swell percentage versus area replacement ratio data for different soil types given in Figure 6.23, is presented in Equation 6.2. The equation, which is statistically significant at  $p=0.05$  level based on F-test statistics with a coefficient of determination of  $R^2=0.86$ , has been developed, under an overburden pressure of  $P_o=25$  kPa:

$$\log(1 + S_v) = 0.136 + 0.015PI - 0.02ARR \dots\dots\dots(6.2)$$

where,  $S_v$ : Vertical Swell Percentage (%)

PI: Plasticity Index

ARR: Area Replacement Ratio (%)

The relationship between the measured values of percent vertical swell and the predicted values is presented in Figure 6.25. It should be once more noted that similar to Equation 6.1, Equation 6.2 is also valid for the particular values of initial water content ( $w_i$ , %) and initial dry unit weight ( $\gamma_d$ ) of the expansive soil and relative density ( $D_r$ , %) of the granular material selected for the experimental program and the accuracy of the equation shall be assessed in case different parameters are used.

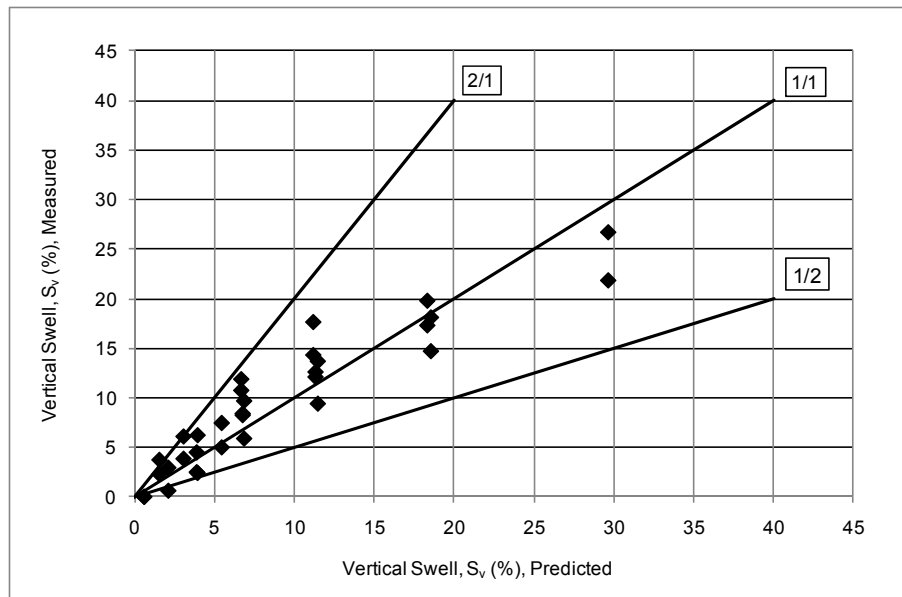


Figure 6. 25 Scatter of the Predicted versus Measured Vertical Swell Percentages for Oedometer Tests and Modified CBR Mould Tests on Type-5 Soil Samples ( $P_o=25$  kPa)

Table 6.8 summarizes the effect of granular material filled trenches in combination with a lightweight structure or a manmade fill of 1 meter high as defined by the untreated free swell tests of Stage (b) and the treated swell overburden tests of Stage (c) of Phase-2.

Table 6. 8 Average Vertical Swell,  $S_{v(av)}$  (%) and Treatment,  $TS_v$  (%) for Swell Overburden CBR Mould and Oedometer Tests Describing the Combined Effect of Trench and Surcharge (Phase-2, Stage(c))

Soil Type	Overburden Pressure, $P_o$ (kPa)	Area Replacement Ratio, ARR (%)	Average Vertical Swell, $S_{v(av)}$ (%)		Treatment, $TS_v$ (%)	
			Oedo	CBR	Oedo	CBR
Type-1	7	0	23.2	19.0	-	-
	25	10	6.1	3.9	73.7	79.7
	25	20	3.7	2.3	83.9	88.0
	25	30	0.0	0.0	100.0	100.0
Type-2	7	0	34.0	28.0	-	-
	25	10	9.7	5.9	71.5	79.0
	25	20	6.2	2.4	81.7	91.4
	25	30	2.9	0.6	91.3	97.8
Type-3	7	0	39.4	35.4	-	-
	25	10	12.6	12.1	67.9	65.8
	25	20	8.4	8.3	78.6	76.7
	25	30	2.5	4.5	93.7	87.3
Type-5	7	0	41.5	37.2	-	-
	25	10	19.8	17.4	52.2	53.4
	25	20	17.7	14.4	57.4	61.4
	25	30	11.9	10.8	71.3	71.1

The treatment percentages in vertical swell under the presence of both trenches and overburden are observed to be around 52 to 80% for 10% area replacement ratio, 57 to 91% for 20% area replacement ratio and 71 to 100% for 30% area replacement ratio. The treatment percentage is observed to decrease as the swell potential of the expansive soil increases. However, with respect to the increasing area replacement ratio, the final treatment attained at Type-1, Type-2 and Type-3 soils with lower swell potential compared to Type-5 soil, was determined to reach 70 to 100%

The final water content values plotted against area replacement ratio for modified CBR mould tests and oedometer tests under 7 kPa and 25 kPa pressures are presented in Figure 6.26, Figure 6.27, Figure 6.28 and Figure 6.29, respectively. For both test types it was observed that the final water contents attained at 25 kPa pressure were less than the values reached under 7 kPa pressure. This finding is consistent with the observation demonstrated in Figure 6.8 and Figure 6.9. The final water content values calculated from the oedometer tests are found to be higher when compared to values from the modified CBR mould tests, confirming that oedometer samples absorb water more thus giving higher swell percentages. As expected, the final water content values tend to increase with increasing swelling potential of the samples. In addition, it was observed that the final water content tend to increase as area replacement ratio increased with the rate of change being more pronounced in the soil samples with higher swelling potential. To give a better understanding of the findings presented above, the final water content versus area replacement ratio plots for each soil type are also presented individually through Figure 6.30 to Figure 6.33.

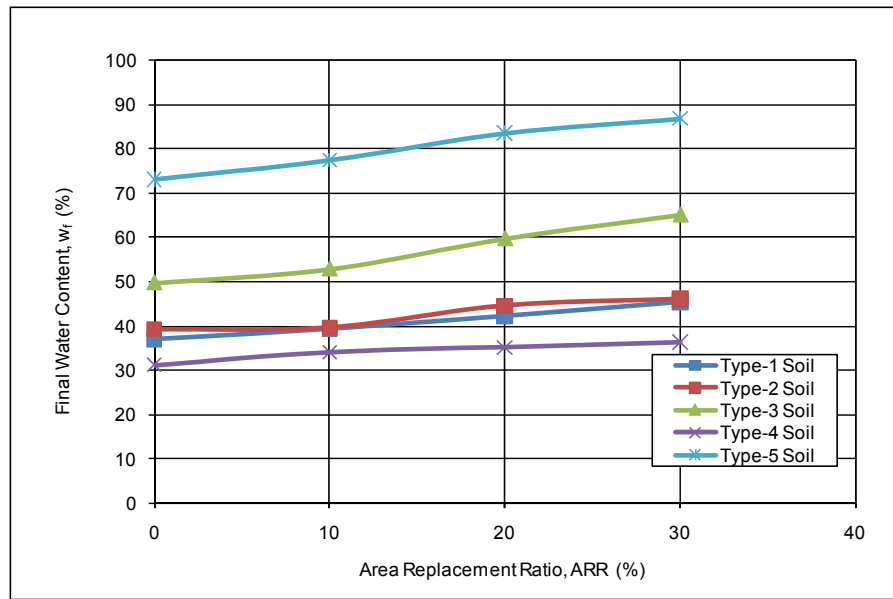


Figure 6. 26 Final Water Content vs. Area Replacement Ratio for Modified CBR Mould Tests Performed with 7 kPa Seating Pressure

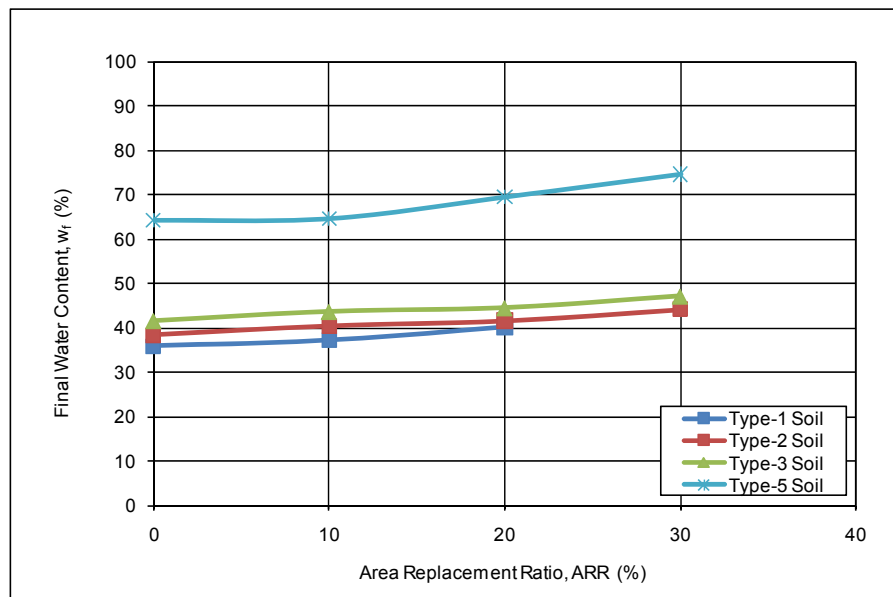


Figure 6. 27 Final Water Content vs. Area Replacement Ratio for Modified CBR Mould Tests Performed with 25 kPa Overburden Pressure

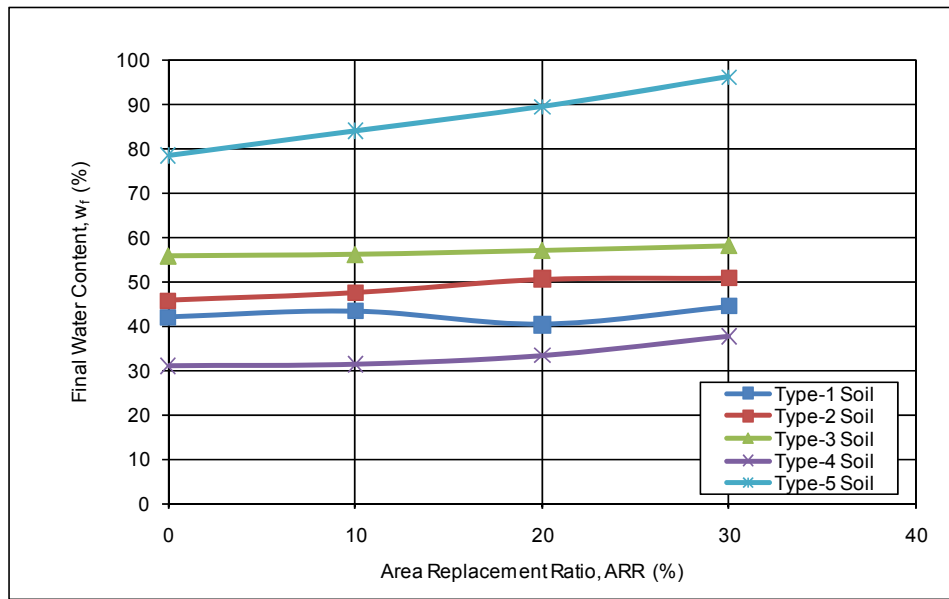


Figure 6. 28 Final Water Content vs. Area Replacement Ratio for Oedometer Tests Performed with 7 kPa Seating Pressure

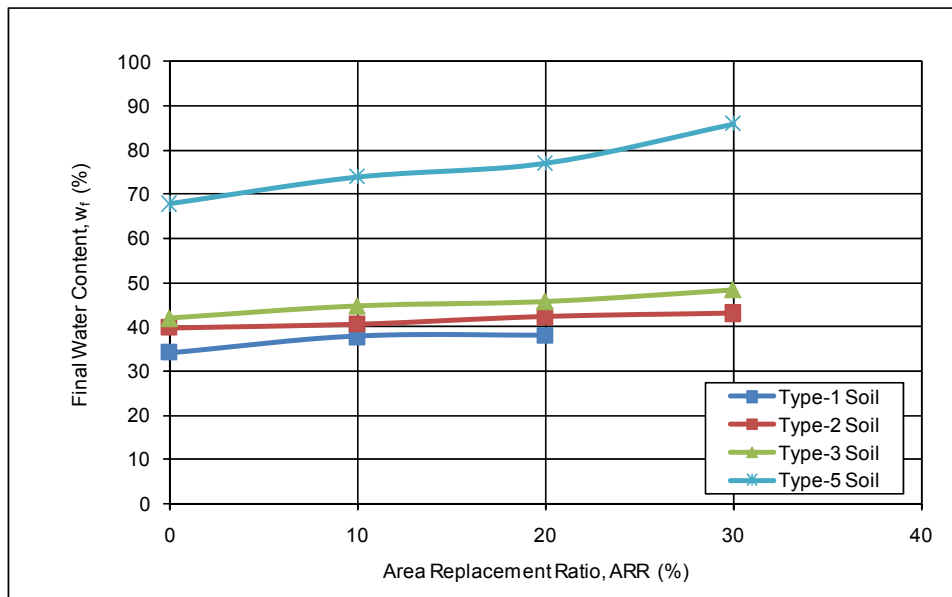


Figure 6. 29 Final Water Content vs. Area Replacement Ratio for Oedometer Tests Performed with 25 kPa Overburden Pressure

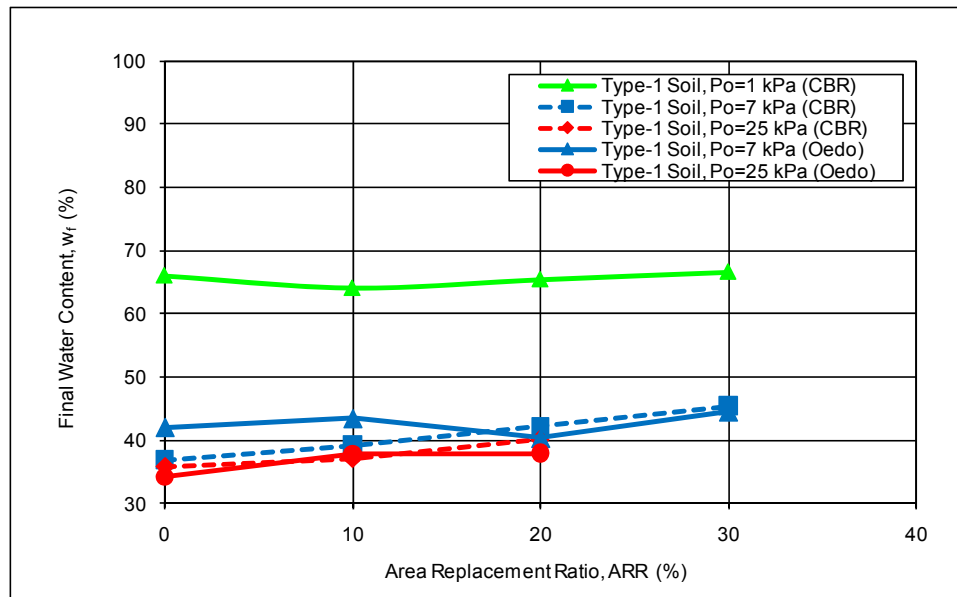


Figure 6. 30 Final Water Content vs. Area Replacement Ratio (Type-1 Soil)

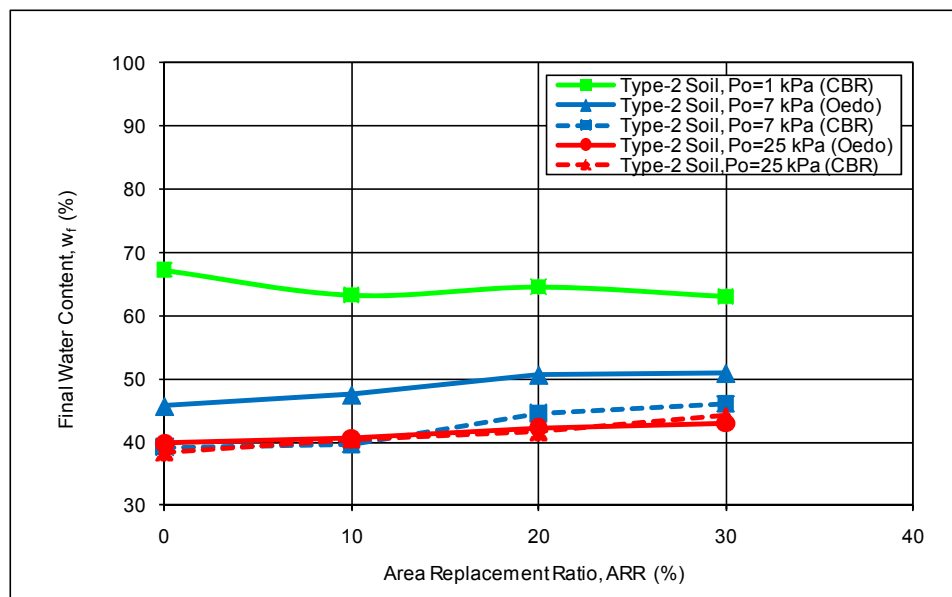


Figure 6. 31 Final Water Content vs. Area Replacement Ratio (Type-2 Soil)



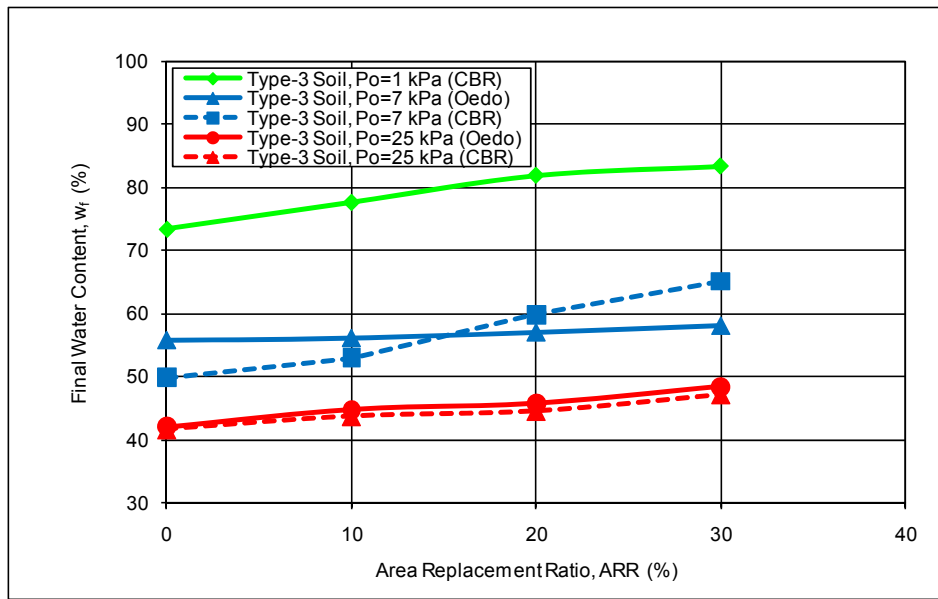


Figure 6. 32 Final Water Content vs. Area Replacement Ratio (Type-3 Soil)

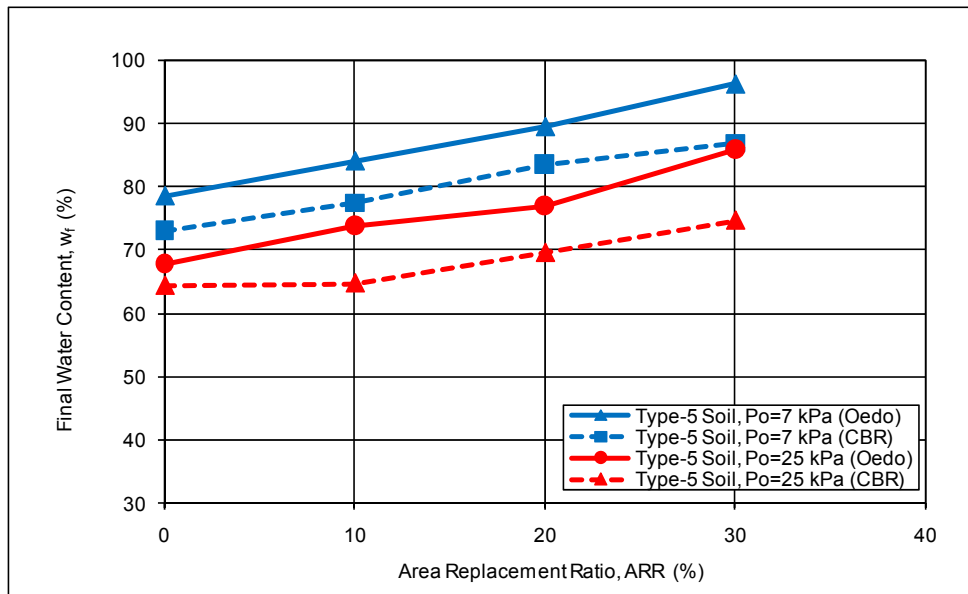


Figure 6. 33 Final Water Content vs. Area Replacement Ratio (Type-5 Soil)

#### 6.4 INVESTIGATION PHASE 3

The third phase of the investigation was dedicated to evaluate the silt material as a trench backfill in place of granular material used in the previous investigation phases. Silt was placed with a relative density of more than 90% to minimize the intrusion of swelling clay so that any possible additional benefit as proposed by Katti (1979) could be observed.

The average vertical swell and treatment percentages observed from the tests performed with 7 kPa and 25 kPa vertical pressure on gravel and silt as column and layer for treatment purposes as well as empty hole tests are presented in Table 6.9. The relevant graphs plotted in the light of the values given in Table 6.9 are given in Figure 6.34 to 6.37.

Table 6. 9 Average Vertical Swell,  $S_{v(av)}$  (%) and Treatment,  $TS_v$  (%) for Free Swell and Swell Overburden Oedometer Tests Performed on Gravel, Silt (As Layer), Silt (As Column) and Hole (Phase-3)

Applied Pressure, (kPa)	Area Replacement Ratio, ARR (%)	Vertical Swell Percentage, $P_s$ (%)				Treatment, $TS_v$ (%)			
		Gravel	Silt (As column)	Silt (As Layer)	Empty Hole	Gravel	Silt (As column)	Silt (As Layer)	Empty Hole
7 kPa	0	41.5				-			
	10	31.5	35.5	36.2	28.6	24.1	14.4	12.6	31.1
	20	26.2	30.7	31.5	20.4	36.9	25.9	24.1	50.8
	30	20.7	25.9	26.6	-	50.2	37.7	35.8	-
25 kPa	0	26.8				-			
	10	19.8	21.4	23.6	17.6	25.9	20.1	11.8	34.2
	20	17.7	18.0	20.1	9.4	34.0	32.9	25.2	65.0
	30	11.9	15.4	16.6	-	55.5	42.5	38.2	-

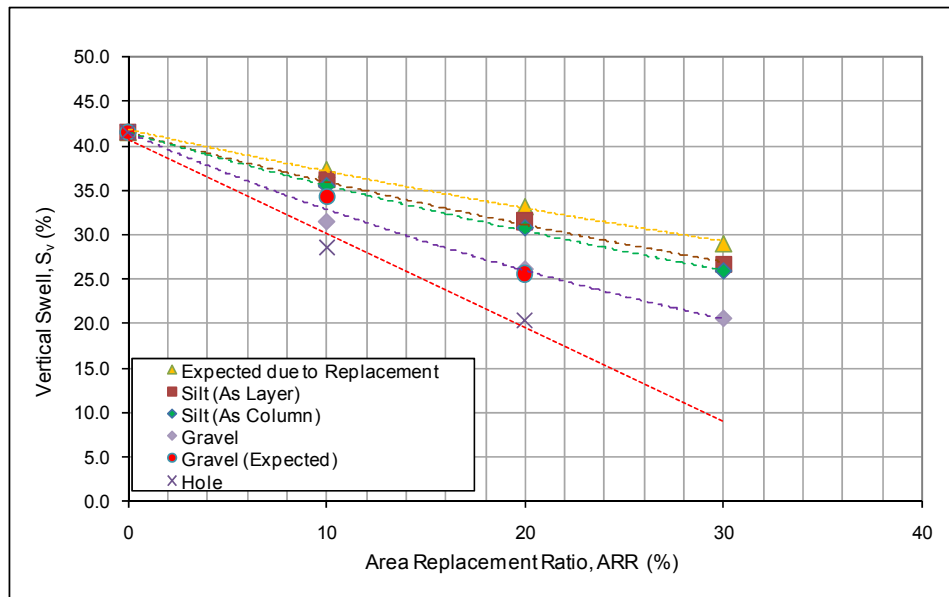


Figure 6. 34 Vertical Swell vs. Area Replacement Ratio for Oedometer Tests Performed on Type -5 Soil, Treated with Gravel, Silt Layer and Silt Column with 7 kPa Seating Pressure (Phase-3)

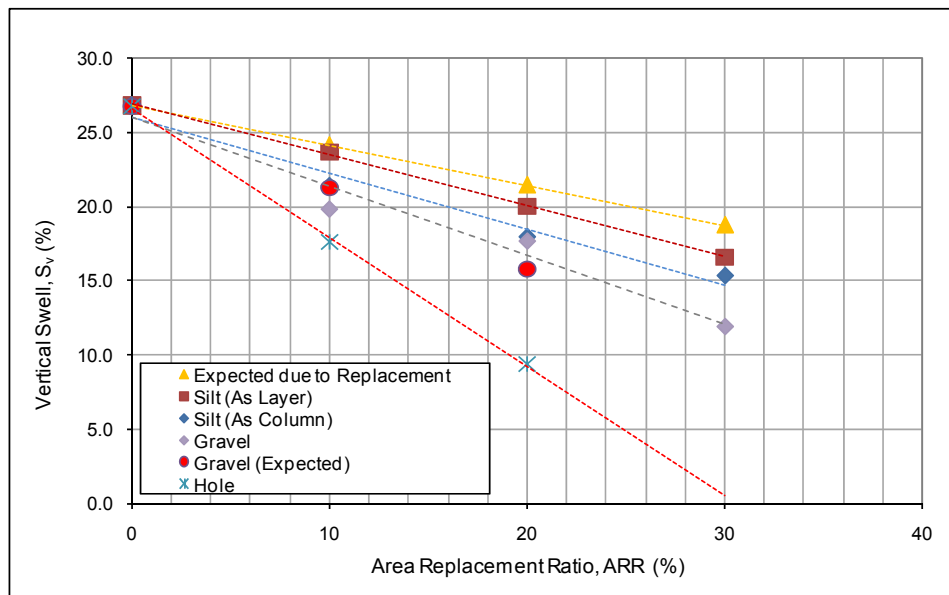


Figure 6. 35 Vertical Swell vs. Area Replacement Ratio for Oedometer Tests Performed on Type -5 Soil, Treated with Gravel, Silt Layer and Silt Column with 25 kPa Overburden Pressure (Phase-3)

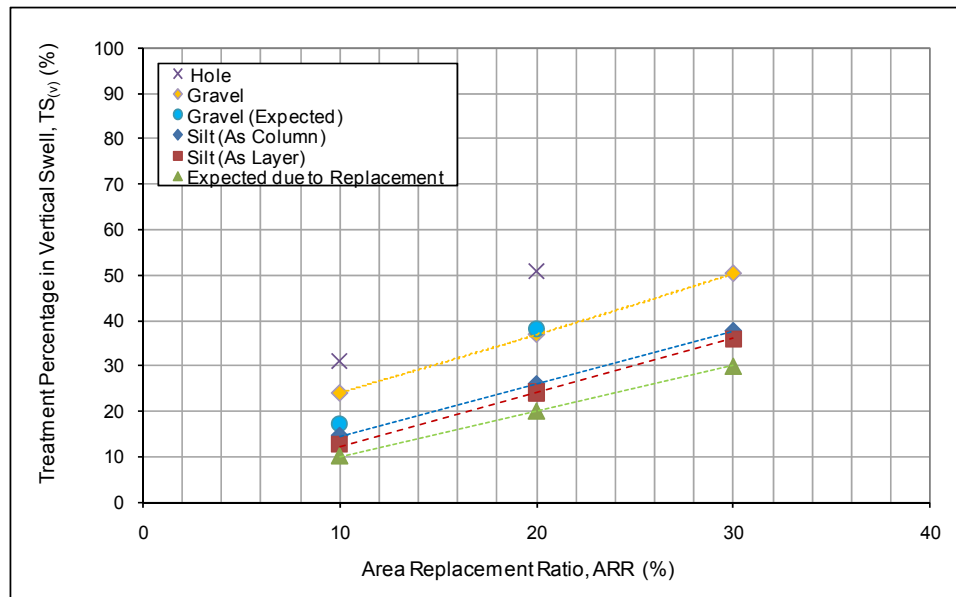


Figure 6. 36 Treatment Percentage in Vertical Swell vs. Area Replacement Ratio for Oedometer Tests Performed on Type -5 Soil, Treated with Gravel, Silt Layer and Silt Column with 7 kPa Seating Pressure (Phase-3)

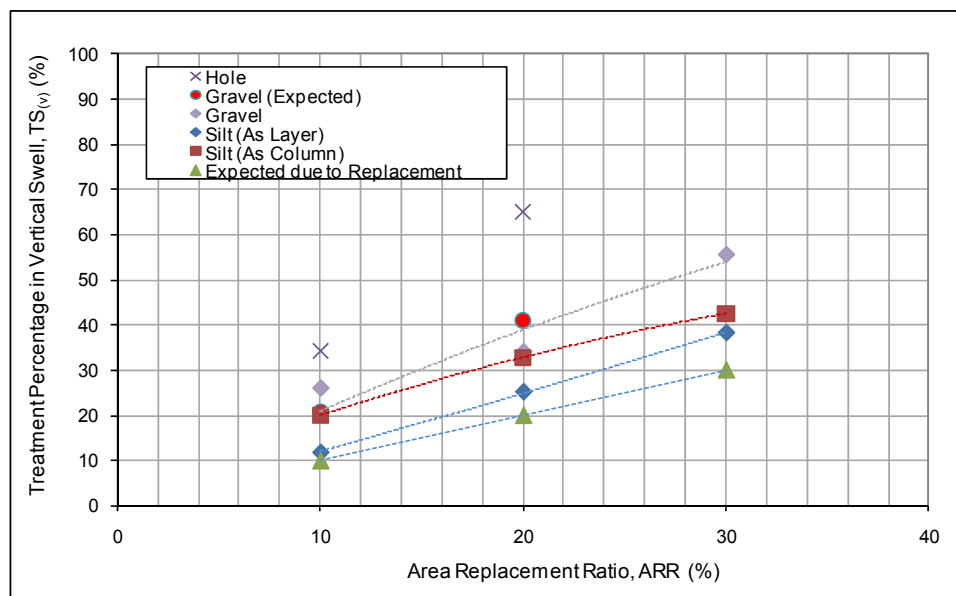


Figure 6. 37 Treatment Percentage in Vertical Swell vs. Area Replacement Ratio for Oedometer Tests Performed on Type -5 Soil, Treated with Gravel, Silt Layer and Silt Column with 25 kPa Seating Pressure (Phase-3)

Figure 6.34 and Figure 6.35 showed that samples treated by silt as a column or as a layer yielded almost equal swell percentages both at 7 kPa and 25 kPa vertical pressures. In addition, the final swell percentages are observed to be close to expected values calculated for that replacement ratio. Therefore, it was concluded that silt as a trench filling material or as a superficial layer on expansive soil showed no additional distinct treatment ability. The small difference between the expected values for replacement and the measured swell percentages for tests performed with silt can be attributed to the testing conditions, disturbances made during drilling the holes and the relatively low friction that generates between the clay and the circumferential surface of the silt column. Figure 6.34 and 6.35 in combination with the treatment percentage in vertical swell with respect to area replacement ratio graphs presented in Figure 6.36 and 6.37 showed that, samples treated with gravel performed approximately in the midway between the expected replacement and hole limits, showing that treatment of expansive soil by means of granular columns may be an effective way of onsite treatment of similar types of soils.

As it has been defined in Chapter V, empty hole tests were performed by the measurement of change in mercury volume filling the void spaces both before and after the experiments. The results of the tests revealed that the measured volume difference between the initial and final state is similar to the decrease in the vertical swell percentages observed from the tests. From the analogous procedure used for the tests involving gravel treatment, it was pointed out that the difference in mercury volume that filled the voids in gravel before and after the swell was observed to be close to the decrease in vertical swell. This outcome in combination with the results reached during the tests involving silt treatment showed that the mechanism governing the proposed treatment methodology is mainly dependent on filling of voids of the fill material selected to be used in the trenches. However, it is also anticipated that the friction between the soil and the trench filling material as well as the probable disturbance during opening of trenches may also effect the treatment performance but with a lower impact compared to filling of void spaces.

The final water content values plotted against area replacement ratio under 7 kPa and 25 kPa pressure for gravel, silt as column and layer and empty hole tests are presented in Figure 6.38. Parallel to the previous observations, the final water content values measured at 25 kPa pressure were lower compared to values observed under 7 kPa. For both overburden pressures, the highest final water content was recorded for empty hole tests whereas gravel tests yielded the lowest values. In addition, it was observed that the final water content tend to increase as area replacement ratio increased for all cases. When this trend is evaluated together with the vertical swell percentage versus area replacement ratio plots presented in Figure 6.34 and 6.35, it can be interpreted that the increase in water content for silt tests results in final swell that is close to expected value for replacement, defining that the predicted mechanism of filling of voids could not be achieved; whereas in gravel tests the swelling soil travels into void spaces thus decreasing the swell percentage well beyond the expected values for replacement.

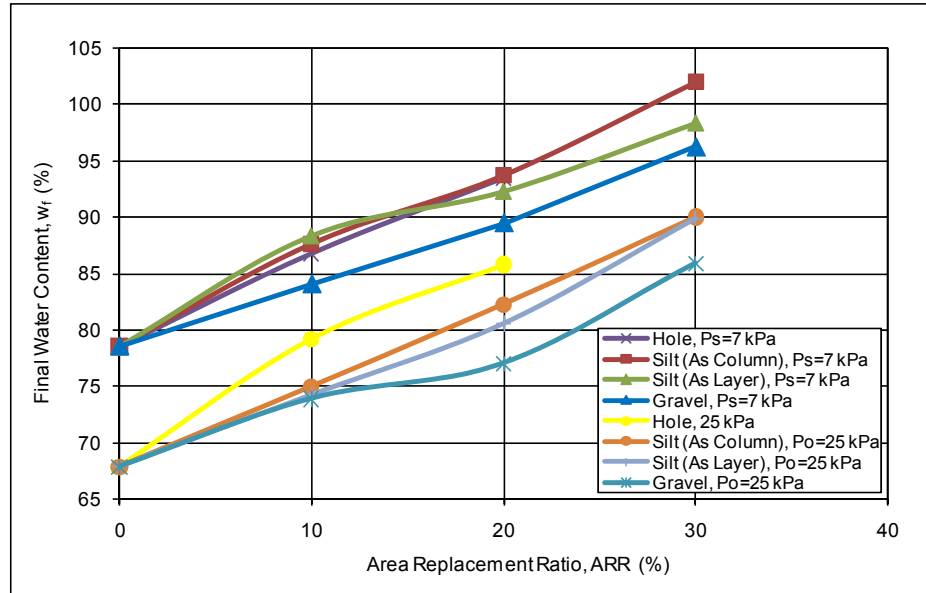


Figure 6. 38 Final Water Content vs. Area Replacement Ratio for Type-5 Soil under Overburden Pressures of 7 kPa and 25 kPa (Phase-3)

## 6.5 INVESTIGATION PHASE 4

In the fourth phase of the investigation, thin-wall ring apparatus was incorporated to the test schedule particularly to study the possible positive effects of granular material filled trenches on the level lateral swell parameters. Before starting to investigate the treatment capability of granular material in the lateral direction, two test rings were evaluated in terms of their efficiencies by conducting tests on untreated Type-3 and Type-5 expansive soil samples with different overburden pressures.

The percent vertical swell versus overburden pressure plots for untreated Type-3 and Type-5 soil samples are presented in Figure 6.39 whereas a comparison of vertical swell percentages under 7 kPa and 25 kPa pressure for oedometer tests and thin-wall ring tests performed on Type-3 and Type-5 samples are tabulated in Table 6.10. As can be seen from Figure 6.39, there exists a linear relationship between the vertical swell percentage and logarithm of overburden pressure as it was previously defined by Brackley (1975), Yanıkömeroğlu (1990) and Ertekin (1991).

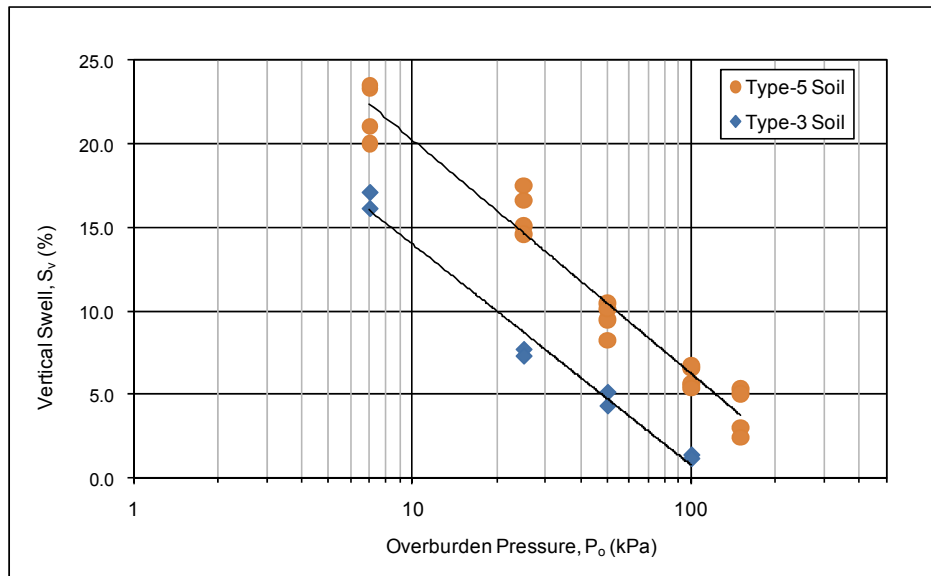


Figure 6. 39 Vertical Swell Percentage vs. Overburden Pressure for Thin-Wall Ring Tests (Phase-4, Stage (a))

Table 6. 10 Comparison of Average Vertical Swell,  $S_{v(av)}$  (%) for Free Swell and Swell Overburden Oedometer and Thin-Wall Ring Tests (Phase-4, Stage (a))

Overburden Pressure, $P_o$ (kPa)	Average Vertical Swell Percentage, $S_{v(av)}$ (%)					
	Oedometer Tests, $S_{v(oedo)}$		Thin Wall Ring, $S_{v(tw)}$		$S_{v(tw)}/S_{v(oedo)}$	
	Type-3	Type-5	Type-3	Type-5	Type-3	Type-5
7	39.4	41.5	16.65	22.0	0.42	0.53
25	18.2	26.8	7.53	16.0	0.41	0.60

The vertical swell percentages obtained from thin-wall ring tests are observed to be approximately 42% of oedometer tests for soil Type-3 and 56% for soil Type-5. This difference is mainly attributed to the lateral strain differences between the rigid wall of the oedometer ring and the flexible thin-wall ring and partly due to the higher aspect ratio of thin-wall ring samples that result in larger wall contact areas, thus reducing swell percentages compared to oedometer tests. In addition, the final water contents measured from the oedometer tests were observed to be higher than those in the thin-wall ring tests, similar to the observations of Al-Shamrani and Al-Mhaidib (2000). This finding shows that the affinity to absorb water is higher in oedometer samples with respect to thin-wall ring specimens mainly due to lateral confinement effect and this factor should be taken into account when oedometer test results are used in predicting heave as suggested by Erol et al. (1987).

The ratio of peak and ultimate lateral swell pressures observed from this study and the study performed by Ertekin (1991) at different overburden pressures, are summarized in Table 6.11. Ertekin (1991) used a highly plastic gray clay with the following properties: LL=146%, PL=30%, PI=116%, SL=16%,  $G_s=2.741$ , Percent finer than No.200 sieve= 99%, Percent finer than 2micron= 70%, Group Symbol = CH,  $w_n=16\%$ ,  $\gamma_d = 15\text{kN/m}^3$  (Intact A),  $\gamma_d = 14.3\text{kN/m}^3$  (Intact B). It is noted that the ratio of peak and ultimate lateral swell pressure is strongly dependent on the surcharge pressure for both peak and ultimate conditions. Lateral swell pressures



(i.e.  $P_h/P_o$  ratio) decrease sharply with increasing overburden stresses as shown in Figure 6.40. Test results of Ertekin (1991), Joshi and Katti (1984), Windal and Shahrour (2002) and Özalp (2010) are also given in Figure 6.41 for comparison.

Table 6. 11 Thin-Wall Ring Test Results (Phase-4, Stage (a))

Soil Sample	Overburden Pressure, $P_o$ (kPa)	Peak Lateral Pressure, $P_{hp}$ (kPa)	Ultimate Lateral Pressure, $P_{hu}$ (kPa)	$P_{hp}/P_o$	$P_{hu}/P_o$
This Study, Type-3	7	258	209	36.9	29.8
	7	275	194	39.3	27.7
	25	205	170	8.2	6.8
	25	186	137	7.4	5.5
	50	189	170	3.8	3.4
	50	186	97	3.7	1.9
	100	230	185	2.3	1.9
	100	242	226	2.4	2.3
This Study, Type-5	7	164	51	23.4	7.3
	7	183	56	26.2	8.1
	7	188	48	26.9	6.8
	7	208	20	29.7	2.8
	25	192	83	7.7	3.3
	25	179	68	7.2	2.7
	25	230	73	9.2	2.9
	25	212	67	8.5	2.7
	50	199	121	4.0	2.4
	50	217	92	4.3	1.8
	50	247	169	4.9	3.4
	50	214	110	4.3	2.2
	100	279	274	2.8	2.7
	100	327	271	3.3	2.7
	100	251	179	2.5	1.8
	100	332	244	3.3	2.4
	150	311	265	2.1	1.8
	150	364	234	2.4	1.6
	150	342	313	2.3	2.1
	150	372	342	2.5	2.3
Ertekin,(1991) Intact A	50	520	292	10.4	5.8
	200	574	410	2.9	2.1
Ertekin,(1991) Intact B	25	160	105	6.4	4.2
	50	241	133	4.8	2.7
	100	280	260	2.8	2.6

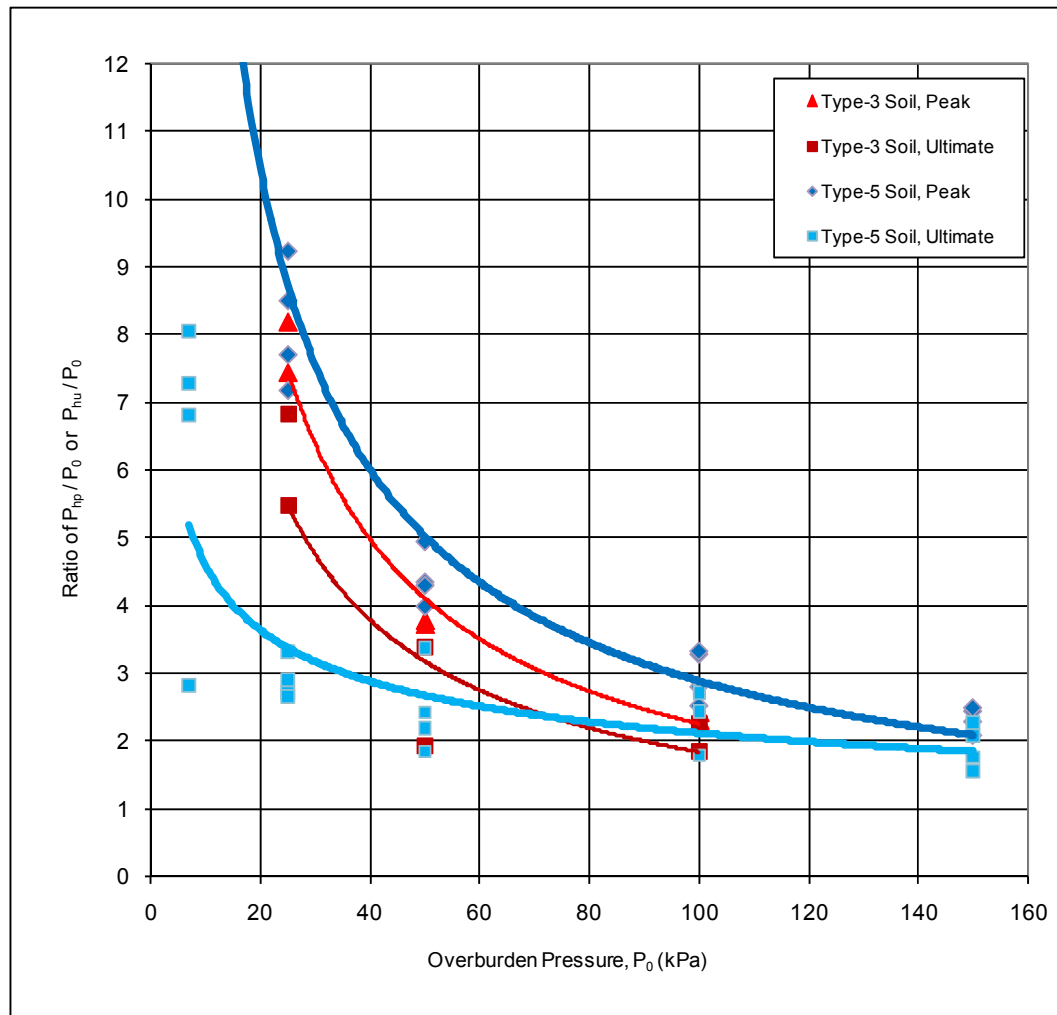


Figure 6. 40 Effect of Overburden Pressure on Lateral Swell Pressure (Present Study)

Joshi and Katti (1984) investigated the lateral swell pressures of Black Cotton soil of India ( $w_i=20-24\%$ ) by designing a special large scale model. Windal and Shahrour (2002) performed thin-wall ring tests on Bavent Clay ( $w_i=11.5-14\%$ ) by using thin-wall rings with different thicknesses to investigate the rigidity of the oedometer ring on the swelling behaviour of soil. Özalp (2010) has also used a thin-wall ring similar to Ertekin (1991) and investigated the lateral swell pressures of Çatalca clay ( $w_i=18\%$ ).

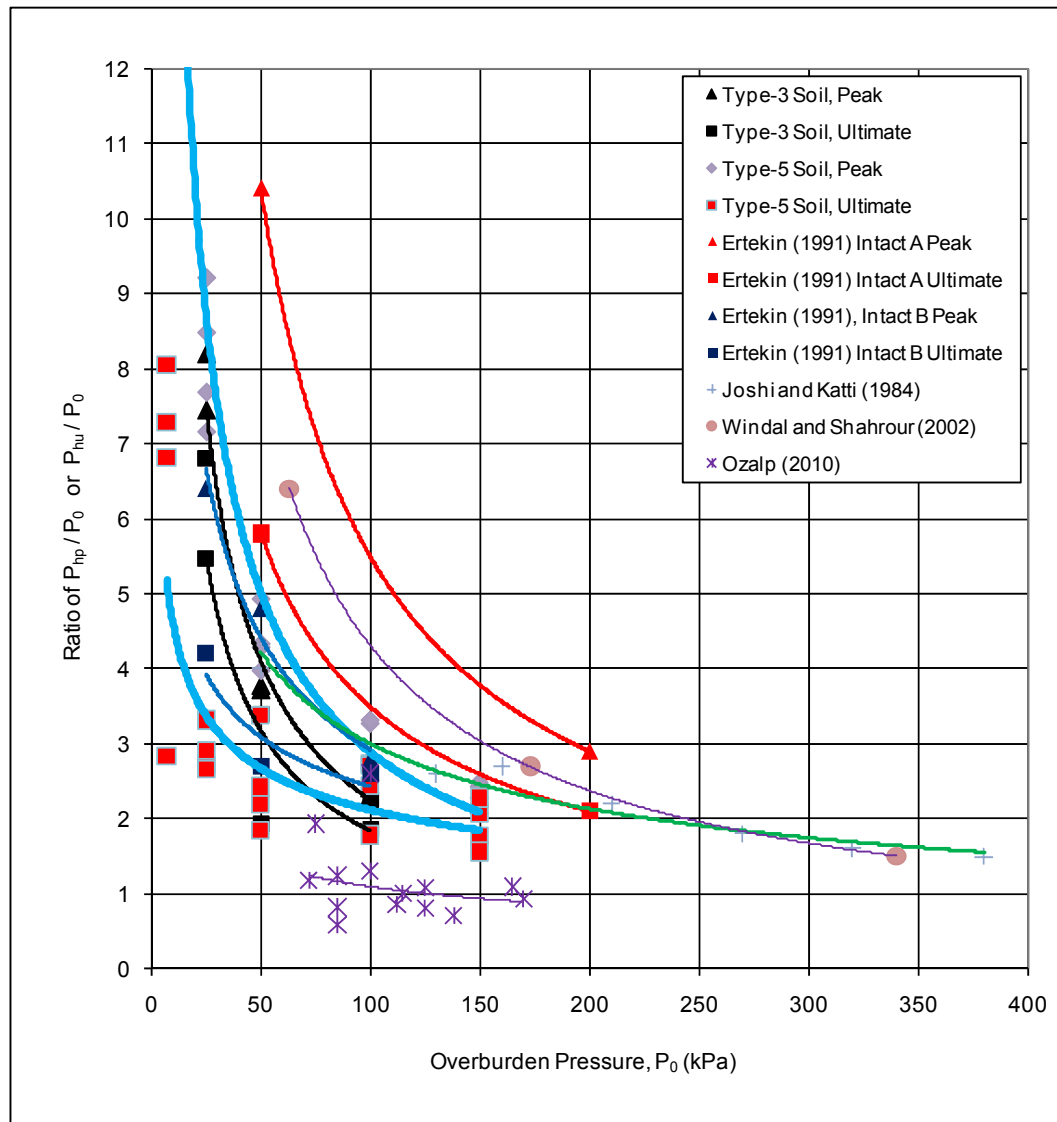


Figure 6.41 Effect of Overburden Pressure on Lateral Swell Pressure (Comparison with Previous Research)

As it can be seen from Table.6.11, the lateral swell pressure reaches to a peak value and then decreases to an ultimate value. This result is similar to the findings of Joshi and Katti (1980), based on the results of the large scale model tests under constant overburden stress. From the results of these tests, it has been observed that the lateral swell pressure has reached to a peak and then decreased to an ultimate value which remained constant afterwards. One way of

explaining this mechanism is through the clay mineralogy. Most of expansive mineral crystals have sheet or plate arrangements with flocculated or dispersed structure (Lambe and Whitman, 1969). Flocculated clay generally exhibits isotropic expansion whereas the parallel particle arrangement of dispersed clay causes it to expand anisotropically. It has been outlined by Chen and Huang (1997) that the swell pressure perpendicular to the particle orientation is higher than the swell pressure in parallel orientation. Since, in this study, the static compaction was applied to the soil samples, at the beginning of test flocculated soil structure may be assumed.

Therefore, the swell is expected to be isotropic resulting in almost equal vertical and horizontal swell pressures. The lateral and vertical swell pressures increase as the water content of the sample increases. After the lateral swell pressure attains a peak value, a gradual reorientation of particles from initially flocculated state to more dispersed state is observed. Based on the fact that, the highest swell pressure is expected in direction perpendicular to the preferred particle orientation, reorientation towards dispersed state may cause an increase in vertical swell pressures and reduction in lateral swell pressures.

One alternative way of explaining the above phenomenon may be the passive failure of expansive soil (Blight, 1971; Ertekin, 1991; Hatipoğlu, 1993; Erol & Ergun, 1994). For the test types with constant vertical stress (ISO and SO tests), as the sample swells, the lateral swell pressure reaches to a peak, consecutively becoming the major principal stress which may cause a passive failure of the sample.

The second and the third stages of investigation Phase-4 intended to study the effect of subject treatment methodology on lateral swell parameters. For this purpose, the most expansive ones among the artificial and natural soil samples, namely Type-3 and Type-5 clays, were selected to be used for the tests. The tests performed on Type-3 clay were terminated at the area replacement ratio of 10% as the lateral treatment percentages under free swell testing conditions

reached 80%. However, the tests on Type-5 clay were performed to involve the area replacement ratios of up to 30%.

The results of the thin-wall ring tests performed on Type-3 soil with Ring-1 are presented in Table 6.12.

Table 6. 12 Thin-Wall Ring Test Results (Phase-4, Stage (b))

Overburden Pressure, $P_o$ (kPa)	Area Replacement Ratio, ARR (%)	Average Lateral Swell Pressure, $P_{h(av)}$ (kPa)		Treatment, $TP_{(h)}$ (%)	
		Peak	Ultimate	Peak	Ultimate
7	0	267	201	-	-
7	5	84	41	68.3	79.5
7	10	62	8	76.8	95.8
25	0	196	153	-	-
25	5	104	87	47.0	43.3
25	10	85	69	56.8	55.1
50	0	188	133	-	-
50	5	115	100	38.5	25.0
50	10	125	113	33.3	15.1
100	0	236	205	-	-
100	5	194	188	17.7	8.7
100	10	159	140	32.6	31.7

The treatment percentage values given in the table are calculated from,

$$TP_{(h)}(\%) = \left( \frac{P_{h(av)}(Untreated) - P_{h(av)}(Treated)}{P_{h(av)}(Untreated)} \right) \cdot 100 \dots\dots (6.3)$$

where :  $TP_{(h)}$ : The treatment percentage in lateral swell pressure

$P_{h(av)}(Untreated)$ : Average Lateral Swell Pressure for Untreated Soil Sample (%)

$P_{h(av)}(Treated)$ : Average Lateral Swell Pressure for Treated Soil Sample (%)

The lateral swell pressure versus area replacement ratio relationships under each overburden pressure of 7 kPa, 25 kPa, 50 kPa and 100 kPa are presented in Figure 6.42 to Figure 6.45.

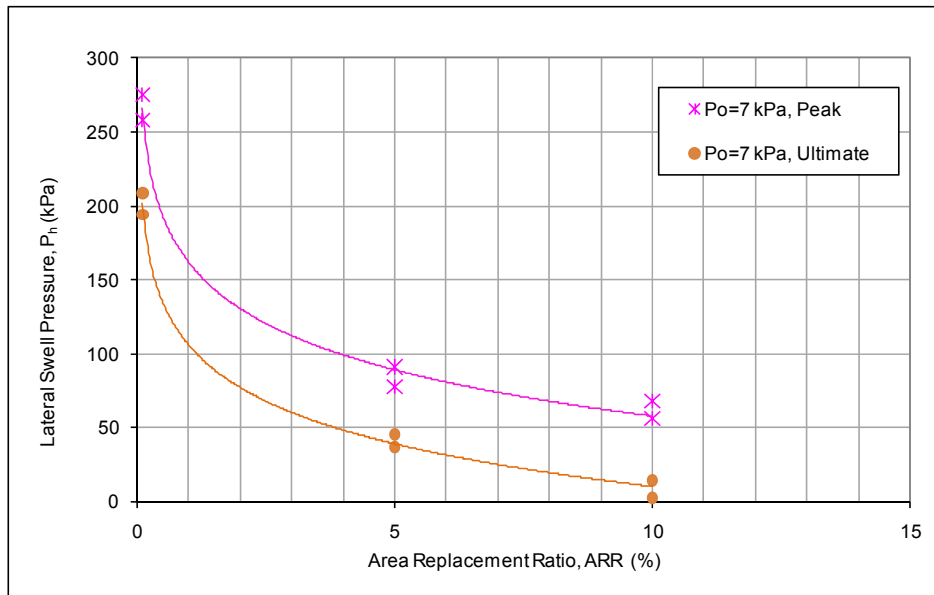


Figure 6. 42 The Lateral Swell Pressure vs. Area Replacement Ratio Relationships for Type-3 Soil ( $P_s=7$  kPa)

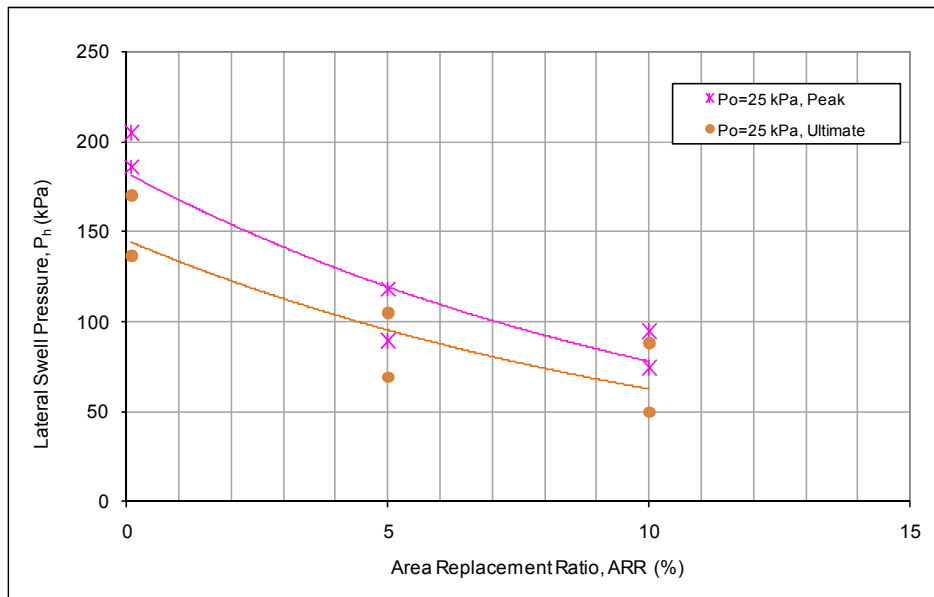


Figure 6. 43 The Lateral Swell Pressure vs. Area Replacement Ratio Relationships for Type-3 Soil ( $P_o=25$  kPa)

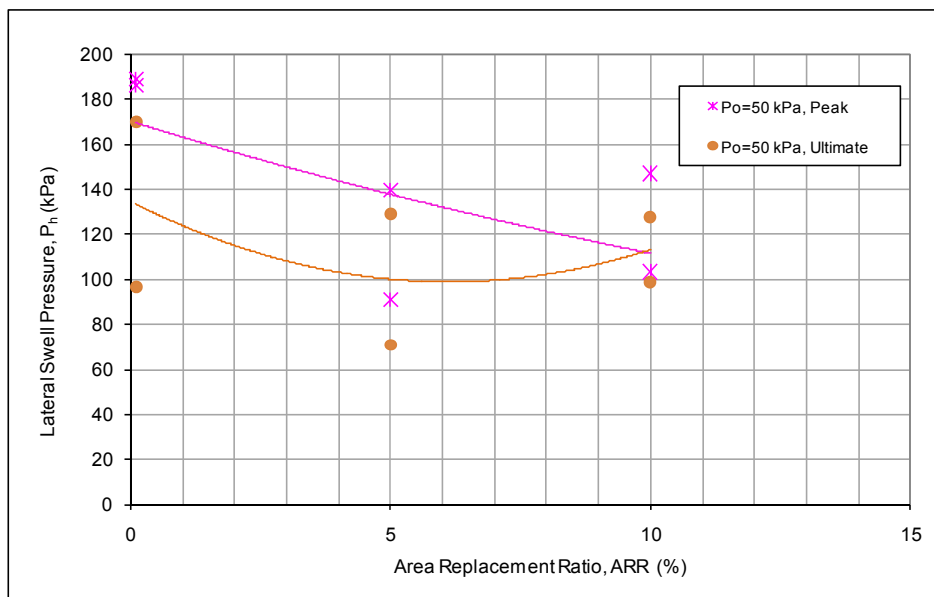


Figure 6. 44 The Lateral Swell Pressure vs. Area Replacement Ratio Relationships for Type-3 Soil ( $P_o=50$  kPa)

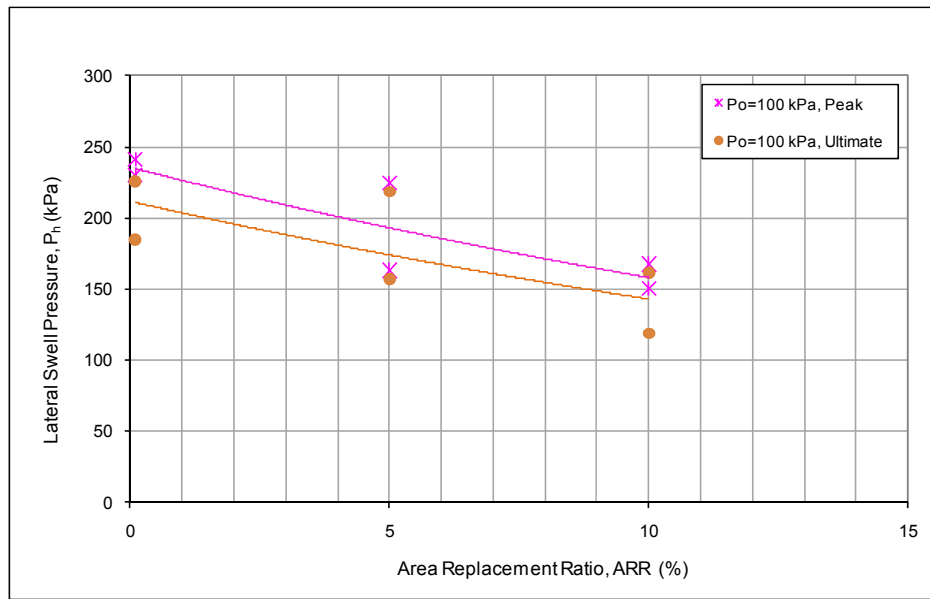


Figure 6. 45 The Lateral Swell Pressure vs. Area Replacement Ratio Relationships for Type-3 Soil ( $P_o=100$  kPa)

Similar to the results of the tests performed at the first stage, the results of second stage tests showed that the lateral swell pressure tend to reach to a peak value and then decreased to ultimate. It can be depicted from the above figures that both the peak and ultimate lateral swell pressures decrease with the increase in area replacement ratio, the decrease being more accentuated under smaller vertical pressures. As this issue directly influences the treatment percentage in lateral swell pressures, the highest treatment is observed at the lowest vertical pressure level and tends to decrease as the vertical pressure is increased as illustrated in Figure 6.46. This behaviour can be attributed to the contribution of vertical pressure in the lateral direction.

As far as the vertical swell percentages are concerned, it can be seen from Figure 6.47 that there exists a linear relationship between the vertical swell percentage and logarithm of overburden pressure both for the untreated and the treated samples. The vertical swell percentage decreases with increasing overburden for all cases and the treated samples swell less compared to the untreated sample.



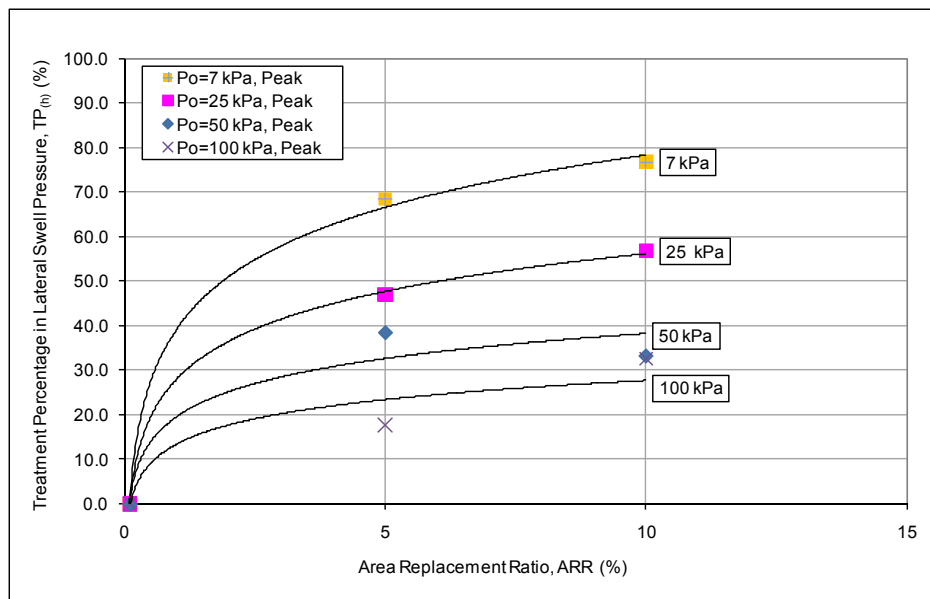


Figure 6. 46 The Treatment in Lateral Swell Pressure vs. Area Replacement Ratio Relationships for Type-3 Soil

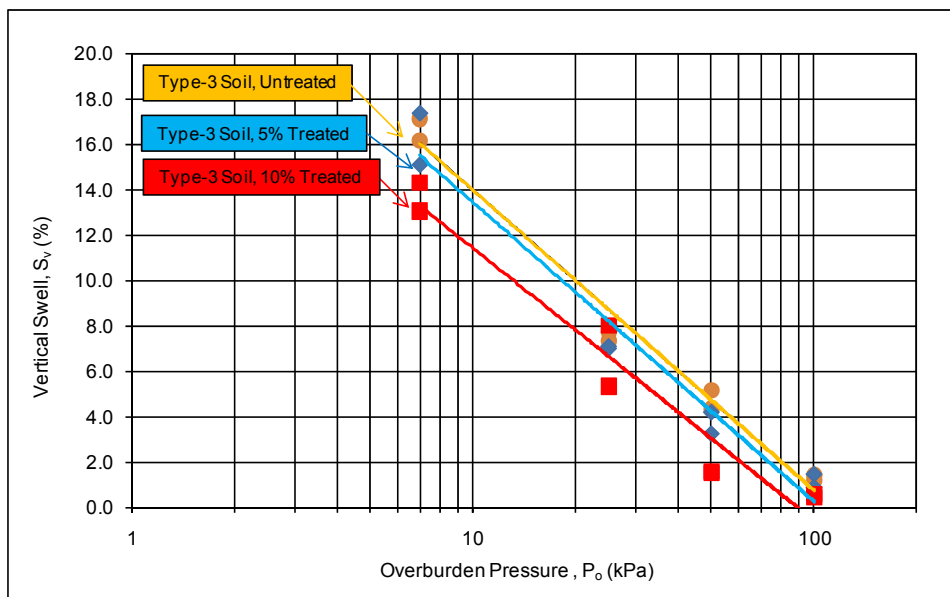


Figure 6. 47 Vertical Swell Percentage vs. Overburden Pressure for Different Area Replacement Ratios for Type-3 Soil

Similar to the vertical swell percentages obtained from thin-wall ring tests for untreated samples in the first stage, the vertical swell percentages for treated samples were obtained to be approximately 44% for free swell tests and 53% for 10% treated samples (Table 6.13). As discussed before, this difference is once more attributed to the lateral strain differences between the rigid wall of the oedometer ring and the flexible thin-wall ring as well as the higher aspect ratio of thin-wall ring samples.

Table 6. 13 Comparison of Average Vertical Swell,  $S_{v(av)}$  (%) for Free Swell and Swell Overburden Oedometer and Thin-Wall Ring Tests for Type-3 Soil (Phase-4, Stage (b))

Overburden Pressure, $P_o$ (kPa)	Average Vertical Swell Percentage, $S_{v(av)}$ (%)					
	Oedometer Tests, $S_{v(oedo)}$		Thin Wall Ring Tests, $S_{v(tw)}$		$S_{v(tw)} / S_{v(oedo)}$	
	Untreated	10% Treated	Untreated	10% Treated	Untreated	10% Treated
7	39.4	31.0	16.7	13.7	0.42	0.44
25	18.2	12.6	7.5	6.7	0.41	0.53

The average final water content values plotted against area replacement ratio for thin-wall ring tests under different overburden pressures are presented in Figure 6.48. It was observed that as the overburden pressure is increased, the final water content decreased for the untreated and treated samples. On the other hand, the average final water content tends to increase as the area replacement ratio is increased.

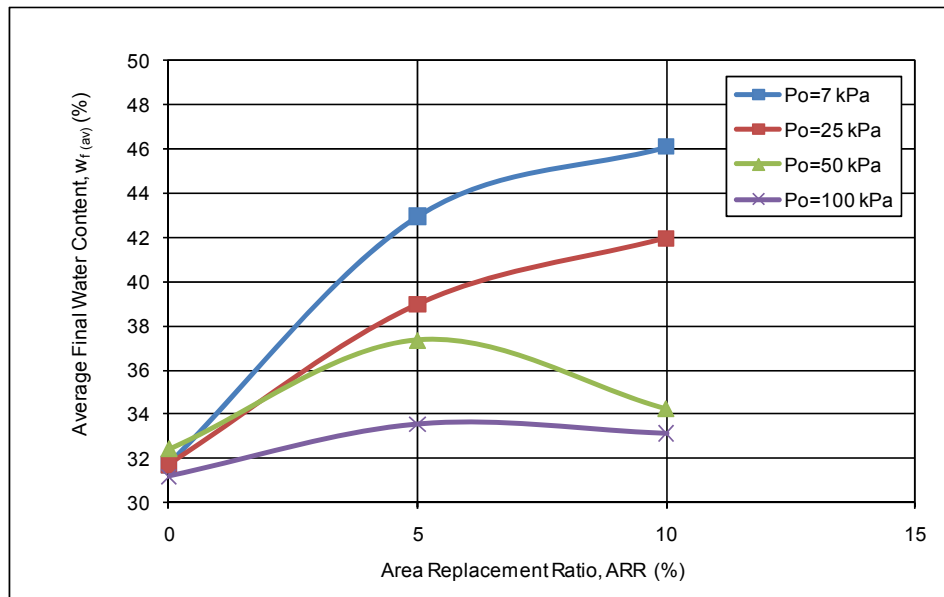


Figure 6. 48 Final Water Content vs. Area Replacement Ratio for Type-3 Soil under Different Overburden Pressures (Phase-4, Stage (b))

In Stage (c) of Phase-4, Type-5 soil was tested in Ring-1 and Ring-2 under vertical pressures of 7 kPa and 25 kPa. The results of the thin-wall ring tests performed on Type-5 soil are presented in Table 6.14. The treatment percentage values given in the table are calculated using Equation 6.3.

The lateral swell pressure versus area replacement ratio relationships under overburden pressures of 7 kPa and 25 kPa for each thin-wall ring are presented in Figure 6.49 to Figure 6.52. As it can be seen from these figures, there exists a linear relationship between the peak lateral swell pressure and the area replacement ratio, whereas the ultimate swell pressure is observed to be almost constant at least for the area replacement ratio ranges evaluated during this study. The combined plots for the data presented in the above figures are once more illustrated in Figure 6.53 for comparison.

Table 6. 14 Thin-Wall Ring Test Results (Phase-4, Stage (c))

Overburden Pressure, $P_o$ (kPa)	Area Replacement Ratio, ARR (%)	Average Lateral Swell Pressure, $P_{h(av)}$ (kPa)				Treatment, $TP_{(h)}$ (%)			
		Ring-1		Ring-2		Ring-1		Ring-2	
		Peak	Ultimate	Peak	Ultimate	Peak	Ultimate	Peak	Ultimate
7	0	173	54	198	34	-	-	-	-
7	10	117	33	154	41	32.4	39.5	22.1	-21.8
7	20	77	47	97	38	55.7	12.7	50.8	-13.4
7	30	54	41	60	33	68.7	23.6	69.7	3.7
25	0	186	75	221	70	-	-	-	-
25	10	137	75	163	91	26.0	0.8	26.1	-30.6
25	20	96	94	120	81	48.1	-24.4	45.9	-15.9
25	30	85	79	96	76	54.3	-4.7	56.5	-8.4

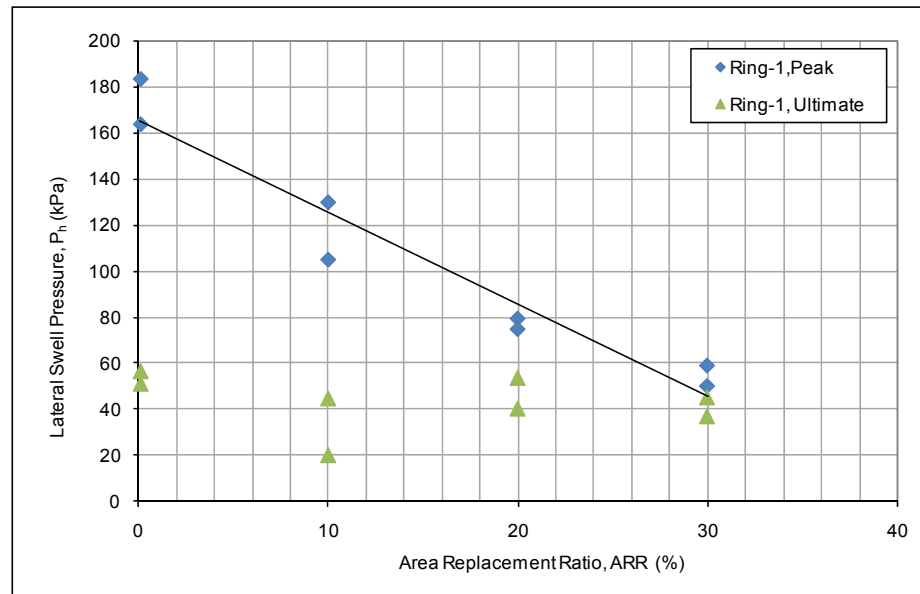


Figure 6. 49 The Lateral Swell Pressure vs. Area Replacement Ratio Relationships for Type-5 Soil and Ring-1 ( $P_s=7$  kPa)

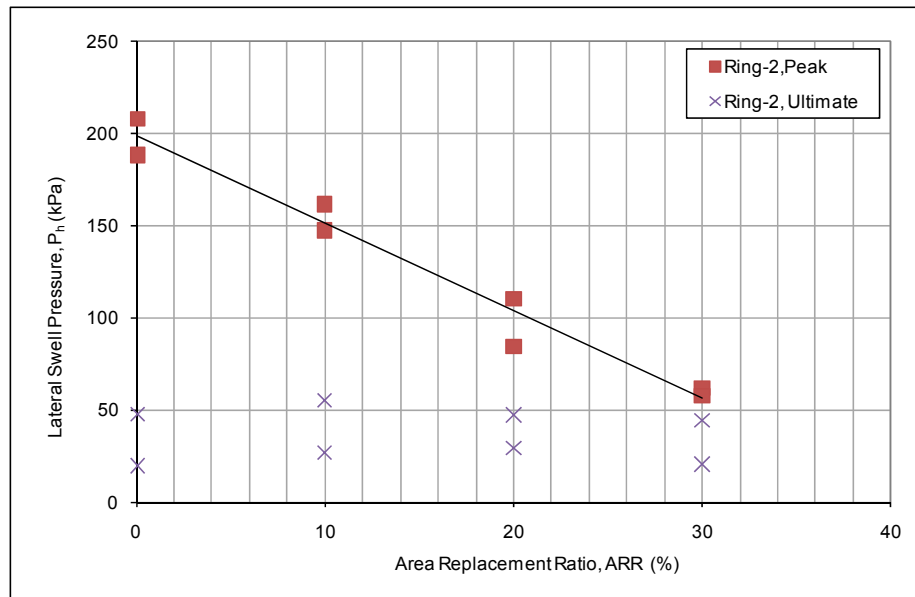


Figure 6. 50 The Lateral Swell Pressure vs. Area Replacement Ratio Relationships for Type-5 Soil and Ring-2 ( $P_s=7$  kPa)

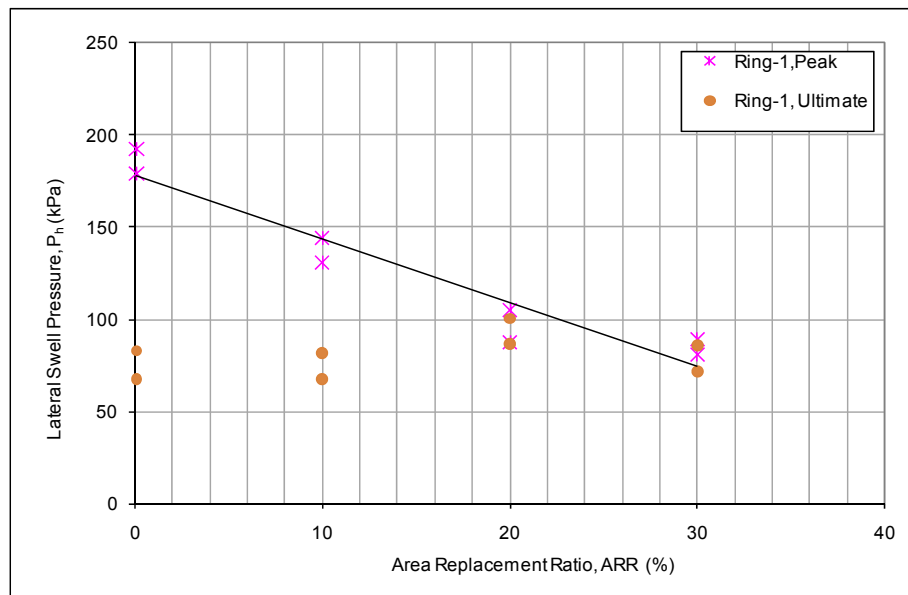


Figure 6. 51 The Lateral Swell Pressure vs. Area Replacement Ratio Relationships for Type-5 Soil and Ring-1 ( $P_o=25$  kPa)

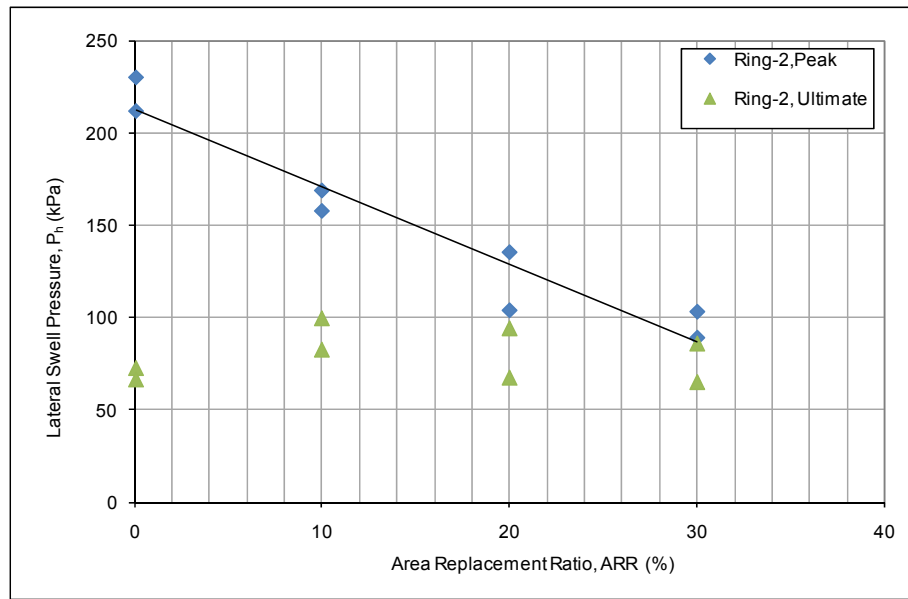


Figure 6. 52 The Lateral Swell Pressure vs. Area Replacement Ratio Relationships for Type-5 Soil and Ring-2 ( $P_o=25$  kPa)

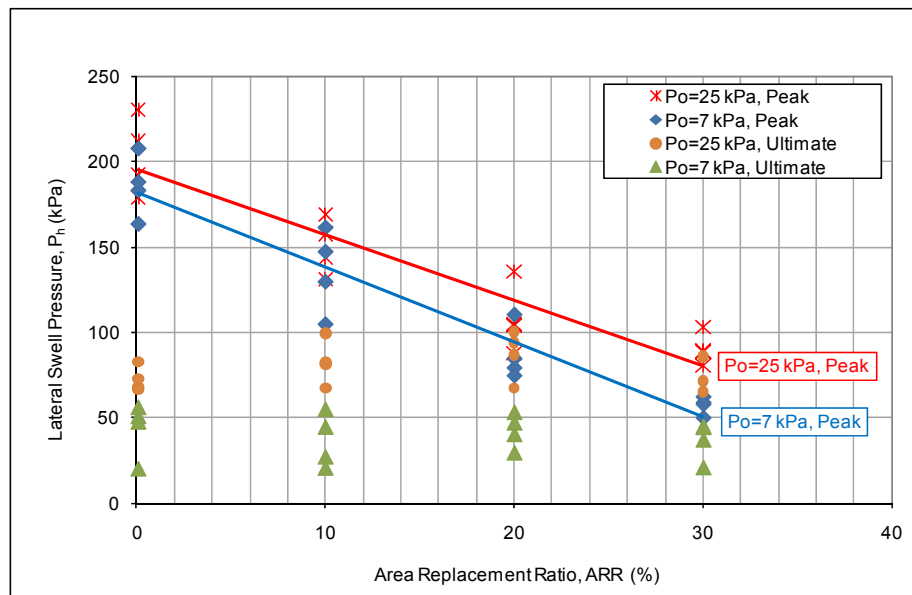


Figure 6. 53 The Lateral Swell Pressure vs. Area Replacement Ratio Relationships for Type-5 Soil

Parallel to the results of the previous stages, the lateral swell pressure is observed to reach to a peak value and then decreased to ultimate. However, in this stage, under 7 kPa and 25 kPa vertical pressures, it was seen that while the peak lateral swell pressures decrease with the increase in area replacement ratio, the variation in the ultimate is of less significance when compared to peak values (Figure 6.54)

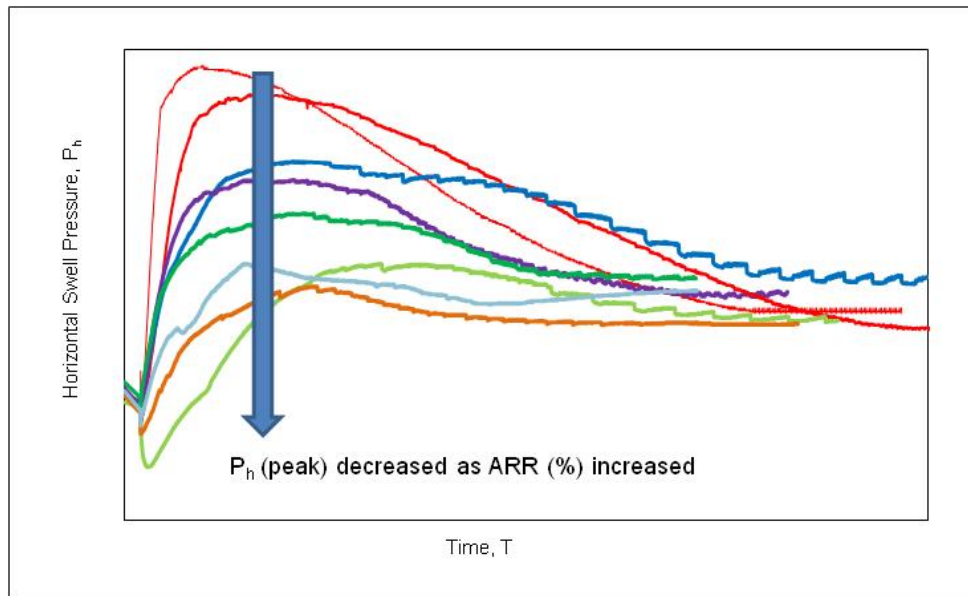


Figure 6. 54 Schematic Description of the Decrease in Peak Horizontal Swell Pressure as Area Replacement Ratio is Increased

The behaviour observed in Figure 6.54 supports the assessment defined in the previous stages of the investigation. The flocculated structure generated at the beginning of the test forces expansion to be isotropic resulting in almost equal horizontal and vertical pressures. The void spaces formed by opening trenches and filling them back by granular material yields movement of clay into these voids in the early stages of expansion. As the water content is increased, clay particles tend to expand and rearrange themselves into a more dispersed configuration. The movement of clay into these voids results in a reduced peak

swell pressure thus dispersed structure is attained with less swell pressure and more expansion through the voids in the lateral direction. Consequently, as the volume of void spaces is increased, the peak swell pressure is expected to decrease. Following the reorientation of clay towards dispersed state, the peak swell pressure is expected to decrease to an ultimate pressure value which is almost constant to some extent. Further increase in void spaces is expected to decrease both peak and ultimate lateral swell pressures accordingly.

Alternatively, the reason for the reduction in peak lateral pressure, as the void spaces are increased, can be explained as the increased lateral strain ability of soil, thus the passive failure condition can be reached at lower peak swell pressures.

The treatment percentage versus area replacement ratio relationships under the overburden pressures of 7 kPa and 25 kPa are presented in Figure 6.55. There exists a linear relationship between the treatment in peak lateral swell pressure and the area replacement ratio. As it can be seen from Figure 6.55 as well as Table 6.14, the level of improvement attained in peak lateral swell pressures for Type-5 soil are observed to be between 22% to 70% under 7 kPa and between 26% to 57% under 25 kPa of overburden pressure for the area replacement ratios of 10% to 30% range. These percentages are comparatively lower than those obtained for Type-3 soil for which the treatments reached almost up to 80% at an area replacement ratio of 10%. The differences may be attributed to lower swelling potential of soil Type-3, which results in drastic decreases in lateral swell pressures with the introduction of free space provided by the granular trenches. However, this proposal shall be verified by further testing of different soil samples with varying swell potentials. The change in treatment of the ultimate pressure, on the other hand, is around  $\pm 20\%$  and can be accepted as ineffective for the ranges of area replacement ratios used in this investigation.



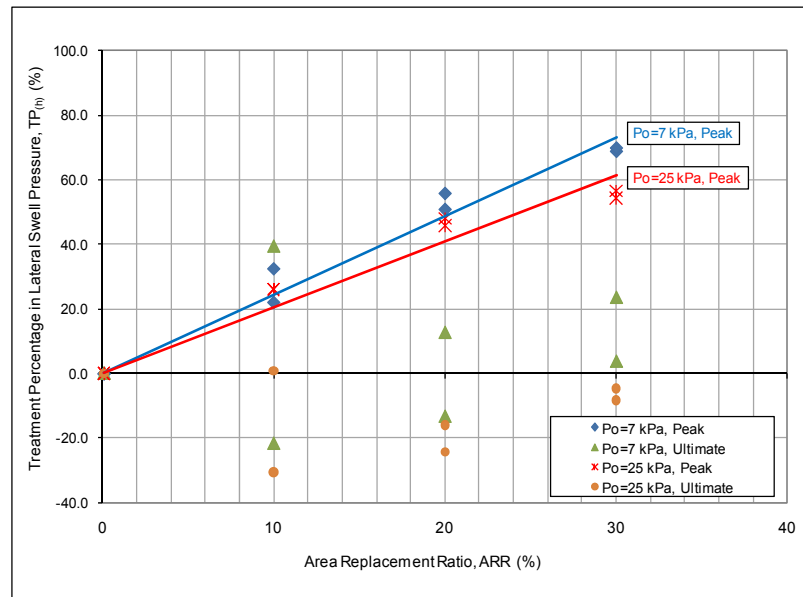


Figure 6. 55 The Treatment Percentage vs. Area Replacement Ratio Relationships for Type-5 Soil

The test results show that for Type-3 and Type-5 soils, the treatment in lateral swell pressure is more effective compared to treatment levels in vertical swell evaluated in the previous phases of the investigation.

The vertical swell percentages obtained from the two thin-wall ring apparatus performed on Type-5 soil as well as the results of oedometer tests are compared in Table 6.15. Similar relationships are also illustrated in Figures 6.56 and 6.57. As it can be seen from the above mentioned figures and table, the vertical swell percentage is observed to decrease with increasing area replacement ratio for all cases. The lateral swell pressure values measured from Ring-2 tests are observed to be 20% higher compared to that of Ring-1 tests. This difference is mainly attributed to the higher aspect ratio of Ring-2. The vertical swell percentages for the two rings, on the other hand, are calculated to be comparable and almost equal in average.

Table 6. 15 Comparison of Average Vertical Swell,  $S_{v(av)}$  (%) for Free Swell and Swell Overburden Oedometer and Thin-Wall Ring Tests for Type-5 Soil (Phase-4, Stage (c))

Overburden Pressure, $P_o$ (kPa)	Area Replacement Ratio, ARR (%)	Average Vertical Swell Percentage, $S_{v(av)}$ (%)				
		Oedometer Tests, $S_{v(oedo)}$	Thin Wall Ring Tests, $S_{v(tw)}$		$S_{v(tw)} / S_{v(oedo)}$	
			Ring-1	Ring-2		
7	0	41.5	22.2	21.8	0.53	0.52
	10	31.5	18.1	19.9	0.57	0.63
	20	26.2	16.2	19.9	0.62	0.76
	30	20.7	15.5	17.9	0.75	0.87
25	0	26.8	16.3	15.6	0.61	0.58
	10	19.8	14.1	13.4	0.71	0.68
	20	17.7	12.1	11.7	0.69	0.66
	30	11.9	8.5	7.0	0.71	0.59

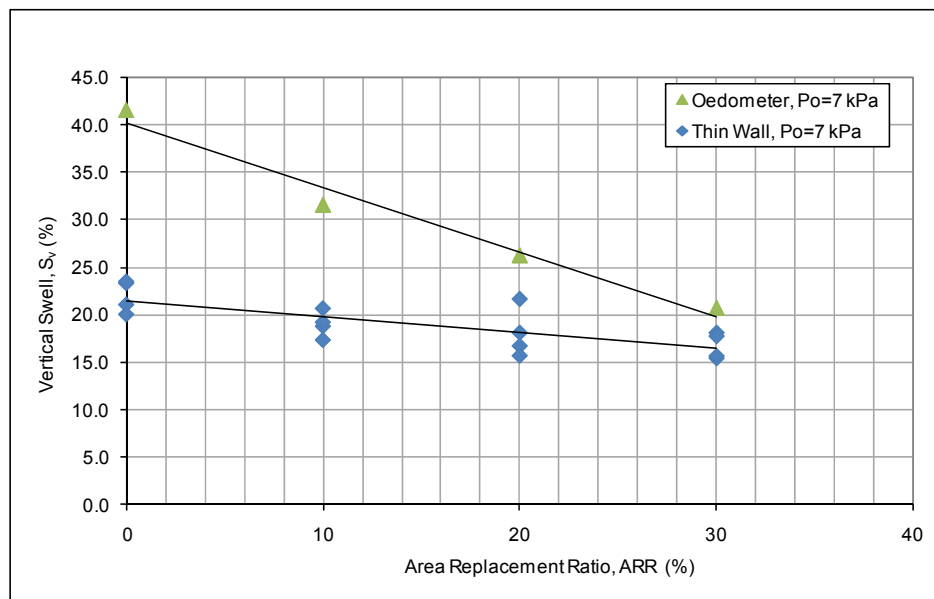


Figure 6. 56 Vertical Swell Percentage vs. Area Replacement Ratios for Type-5 Soil under Vertical Pressure of 7 kPa

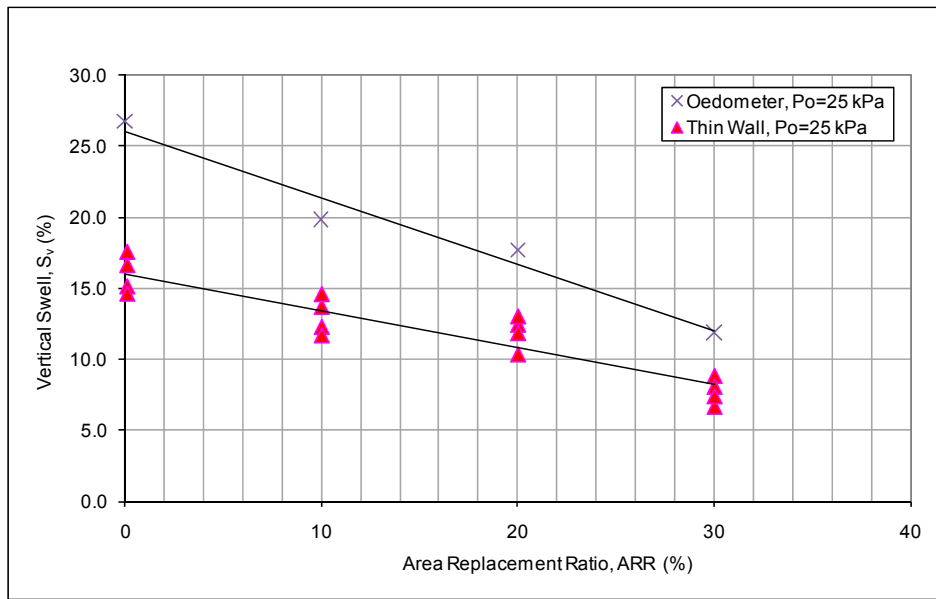


Figure 6. 57 Vertical Swell Percentage vs. Area Replacement Ratios for Type-5 Soil under Vertical Pressure of 25 kPa

Comparison of the results obtained from oedometer tests at Phase-2 and the thin-wall ring tests at this stage shows that the vertical swell percentages obtained from thin-wall ring tests are approximately 52% to 87% for different area replacement ratios. Once more, this difference is attributed to the lateral strain differences between the rigid wall of the oedometer ring and the flexible thin-wall ring as well as the higher aspect ratio of thin-wall ring samples. In addition, as the area replacement ratio is increased, the differences between the vertical swell percentages of thin-wall ring and oedometer samples are observed to reduce.

The average final water content versus area replacement ratio for thin-wall ring tests under different overburden pressures are presented in Figure 6.58 and Figure 6.59. Oedometer test results observed from Phase-2 are also presented for comparison. For both test types, it was observed once more that as the overburden pressure is increased, the final water content decreased for the untreated and treated samples. Besides, the average final water content tends to increase as the area replacement ratio is increased. Similar to the findings observed at Stage (a) and Stage (b) of Phase-4, the final water contents measured from the oedometer tests were observed to be higher than the thin-wall ring tests showing that the affinity to absorb water is higher in oedometer samples with respect to thin-wall ring specimens mainly due to lateral confinement effect.

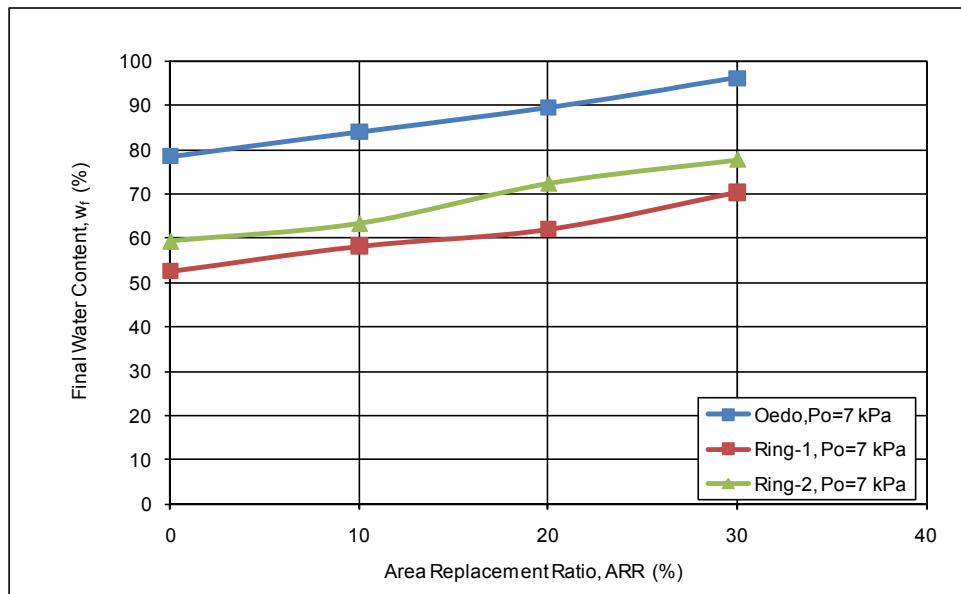


Figure 6. 58 Final Water Content vs. Area Replacement Ratio for Type-5 Soil under Vertical Pressure of 7 kPa (Phase-4, Stage (c))

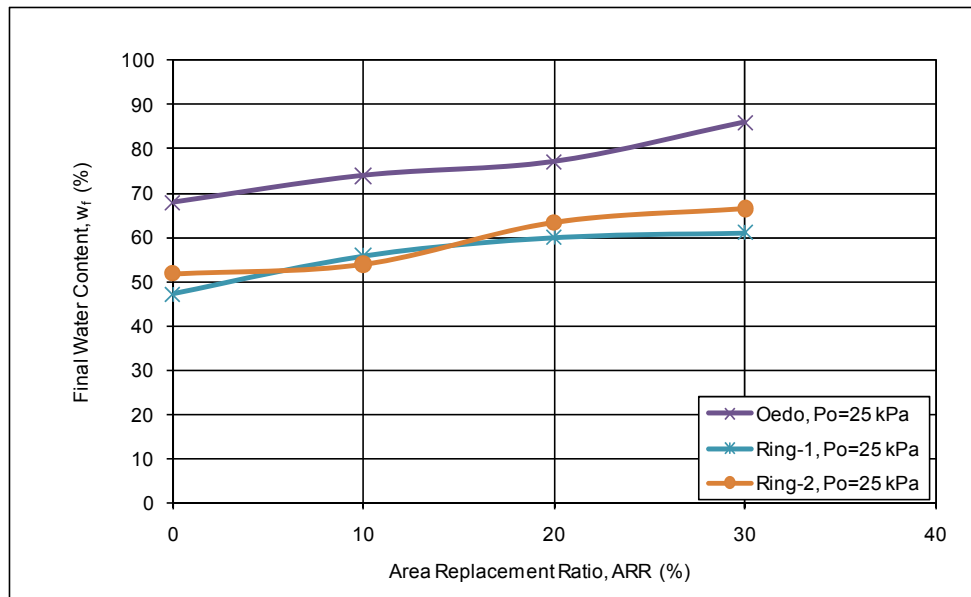


Figure 6. 59 Final Water Content vs. Area Replacement Ratio for Type-5 Soil under Vertical Pressure of 7 kPa (Phase-4, Stage (c))

The effect of silt on the improvement of lateral swell pressure of expansive soils was evaluated at the fourth stage of the investigation Phase-4. Similar to the investigation Phase-3, silt was placed with a relative density of more than 90% to minimize the intrusion of swelling clay so that any possible additional benefit could be observed.

The average lateral swell pressure and treatment percentages observed from the free swell thin-wall ring tests performed on silt as well as gravel for comparison are presented in Table 6.16. The peak and ultimate lateral swell pressure versus area replacement ratio graph is given Figure 6.60.

Table 6. 16 Comparison of Average Lateral Swell Pressure,  $P_{h(av)}$  (kPa) for Free Swell Oedometer and Thin-Wall Ring Tests for Type-5 Soil Treated with Gravel and Silt (Phase-4, Stage (d))

Treatment Material	Dr (%)	Area Replacement Ratio, ARR (%)	Average Lateral Swell Pressure, $P_{h(av)}$ (kPa)				Treatment, $TP_{(h)}$ (%)	
			Ring-1		Ring-2		Ring-1	Ring-2
			Peak	Ultimate	Peak	Ultimate	Peak	Peak
Untreated	-	0	173	54	198	34	-	-
Fine Gravel	40	10	117	33	154	41	32.4	22.1
		20	77	47	97	38	55.7	50.8
		30	54	41	60	33	68.7	69.7
Silt	>90	10	147	45	186	85	15.1	6.2
		20	138	134	156	128	20.4	21.1
		30	139	117	139	128	20.0	29.8

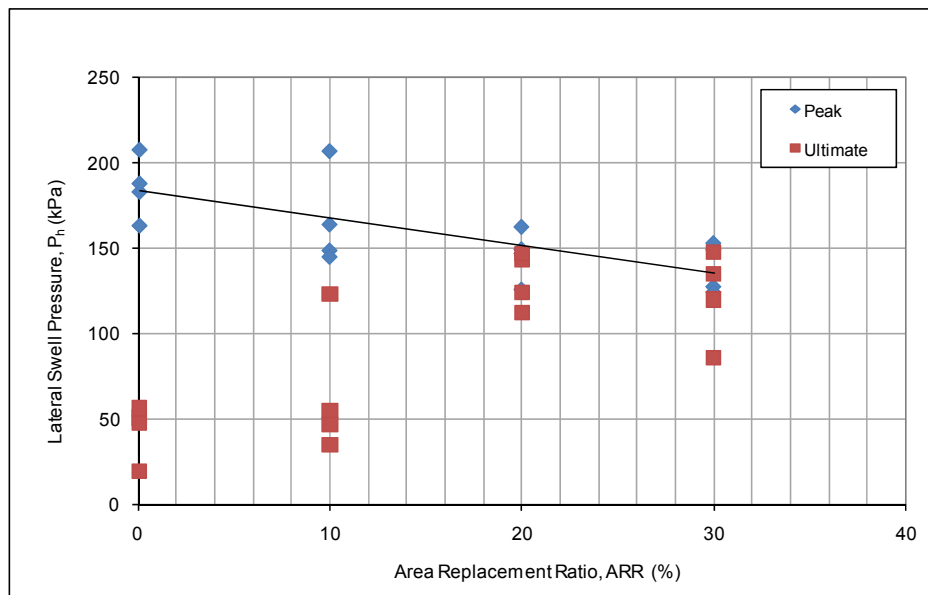


Figure 6. 60 The Lateral Swell Pressure vs. Area Replacement Ratio Relationships for Thin-Wall Ring Tests Performed on Type-5 Soil under Vertical Pressure of 7 kPa (Phase-4, Stage (d))

Figure 6.60 in combination with Table 6.16 showed that, as the area replacement ratio increased, the lateral swell pressures decreased to some extent, but the reduction in peak was not greater than the area replacement ratio applied at that level. This result supports the finding defined in Phase-3 of the investigation and it was once more concluded that silt as a trench filling material showed no additional distinct treatment ability. In addition, although the lateral swell pressure is observed to decrease after reaching a peak, the ultimate values for the treated samples in most of the cases are measured to be larger than to that of untreated soil sample. It can be concluded that the passive failure condition could not be reached, i.e. the reorientation of particles from flocculated to dispersed structure could not be finalized.

The vertical swell percentages obtained from the two thin-wall ring apparatus performed on Type-5 soil treated with either silt or gravel and the results of oedometer tests performed under the similar conditions are presented in Table 6.17. Similar relationship is presented in Figure 6.61. From the above mentioned data, the vertical swell percentages for the two rings are calculated to be comparable. Evaluation of the oedometer tests performed at Phase-2 and Phase-3 and the thin-wall ring tests of this stage shows that the vertical swell percentages obtained from thin-wall ring tests are approximately 45% to 62% for different area replacement ratios. The difference is again defined by the lateral strain differences between the rigid wall of the oedometer ring and the flexible thin-wall ring. On the other hand, the vertical swell percentages attained from the thin-wall ring tests performed with silt and gravel treatment were observed to be close to each other.

Table 6. 17 Comparison of Average Vertical Swell,  $S_{v(av)}$  (%) for Free Swell Oedometer and Thin-Wall Ring Tests for Type-5 Soil Treated with Gravel and Silt (Phase-4, Stage (d))

Treatment Material	Area Replacement Ratio, ARR (%)	Average Vertical Swell Percentage, $S_{v(av)}$ (%)			
		Oedometer Tests, $S_{v(oedo)}$	Thin Wall Ring Tests, $S_{v(tw)}$		$S_{v(tw)} / S_{v(oedo)}$
			Ring-1	Ring-2	
Untreated	0	41.5	22.2	21.8	0.53
Gravel	10	31.5	18.1	19.9	0.57
	20	26.2	16.2	19.9	0.62
	30	20.7	15.5	17.9	0.75
Silt	10	35.5	17.7	18.1	0.50
	20	30.7	15.4	13.8	0.50
	30	25.9	15.8	16.0	0.61

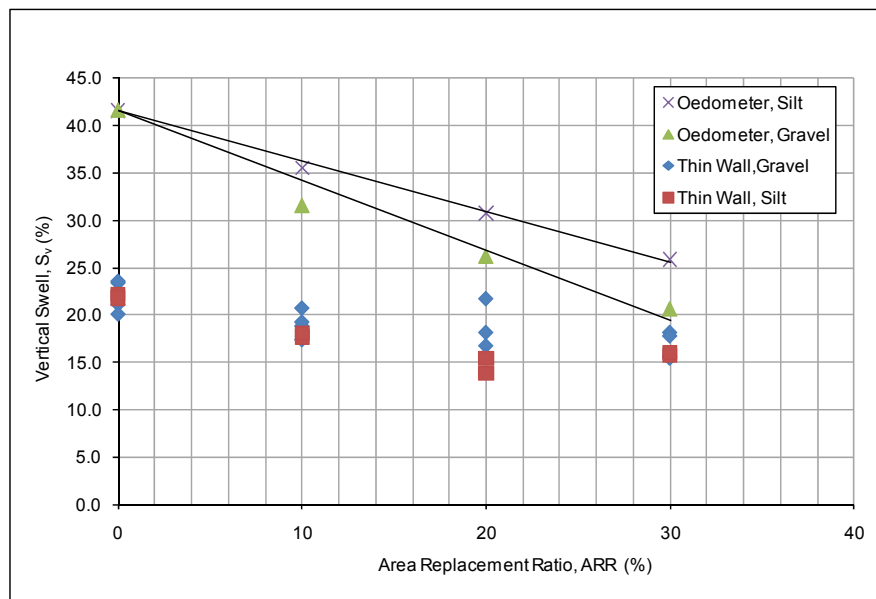


Figure 6. 61 Vertical Swell Percentage vs. Area Replacement Ratios for Type-5 Soil under Vertical Pressure of 7 kPa for Gravel and Silt Treatment (Phase-4, Stage (d))

The final water content values plotted against area replacement ratio under 7 kPa pressure for gravel, silt tests performed on thin-wall rings and oedometer are presented in Figure 6.62. Parallel to the previous observations, oedometer tests yielded higher final water content values compared to those obtained from the



thin-wall ring tests for all area replacement ratios. In addition, the tests involving silt treatment showed higher final water content values to that of tests performed with gravel. Finally, the water content values attained at the end of thin-wall tests for both rings are comparable.

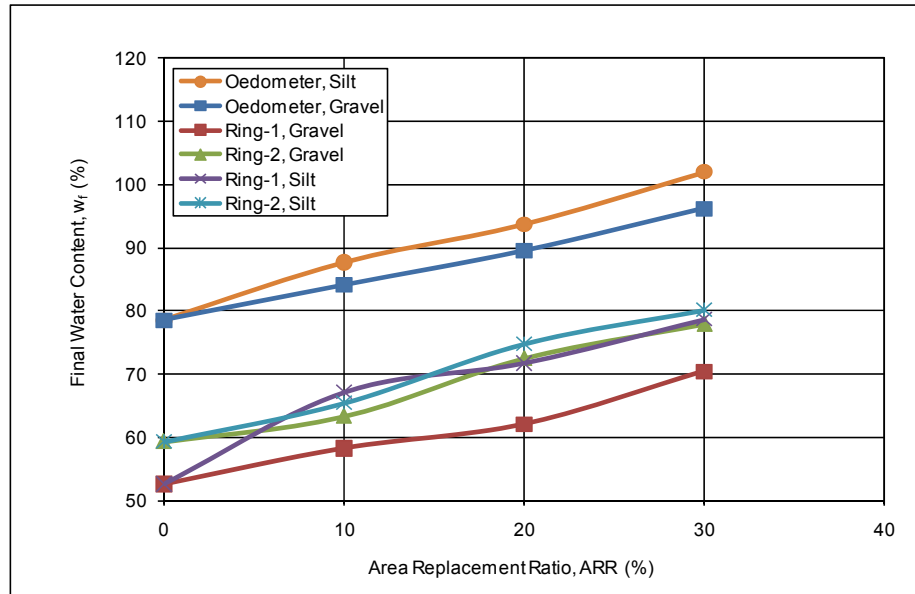


Figure 6. 62 Final Water Content vs. Area Replacement Ratio for Type-5 Soil under Vertical Pressure of 7 kPa (Phase-4, Stage (d))

In the light of the results of tests performed during this investigation, a comparison of the test methodologies are enlisted in Table 6.18.

Table 6. 18 Comparison of Test Methods Used during the Investigations

Test Type	Major Findings	Advantages	Disadvantages	Comments
Conventional Oedometer	Higher expansion values compared to CBR and Thin-Wall Ring	Easy to perform and available at every soil mechanics laboratory	<ul style="list-style-type: none"> <li>• Rigidity of the ring</li> <li>• Small sized samples that could not reflect the effects of discontinuities such as fissures and etc.</li> </ul>	<ul style="list-style-type: none"> <li>• Overestimates field behaviour; and its results shall not be used directly in predicting heave in practice.</li> <li>• Can be used for comparative purposes such as treatment estimations</li> </ul>
Modified CBR Mould	Lower expansion values compared to Oedometer	Larger sized samples compared to oedometer may reflect the effects of discontinuities more efficiently for undisturbed samples	<ul style="list-style-type: none"> <li>• Rigidity of the ring</li> <li>• Still may not reflect the actual field behaviour due to sample size</li> <li>• Not standardized and cannot be easily performed at all laboratories.</li> </ul>	Compared to oedometer tests, since similar results are obtained it can be used for comparative purposes such as treatment estimations
Thin-Wall Ring	Lower expansion values compared to Oedometer and CBR	<ul style="list-style-type: none"> <li>• Possibility of reflecting field conditions more efficiently due to flexible ring</li> <li>• Lateral swell pressure measurement</li> </ul>	<ul style="list-style-type: none"> <li>• May not reflect the actual field behaviour due to sample size</li> <li>• Not standardized and cannot be easily performed at all laboratories.</li> </ul>	<ul style="list-style-type: none"> <li>• The rigidity of the ring directly influences the measured lateral swell pressures as well as vertical swell percentages and its results shall not be used directly in practice.</li> <li>• Can be used for comparative purposes such as treatment estimations</li> </ul>

## **CHAPTER VII**

### **CONCLUSIONS**

The possible positive effects of trenches and/or columns backfilled with granular material, such as crushed stone or rock, on the swelling potential of expansive soils is investigated within the content of this study. The following main conclusions are drawn from the results of the tests performed for this purpose.

- a. The free swell oedometer and modified CBR mould tests performed on five different expansive clay samples with varying swell potential resulted in vertical swell treatment percentages of 17 to 27% for an area replacement ratio of 10%, 37 to 52% for an area replacement ratio of 20% and 51 to 72% for an area replacement ratio of 30%, with smaller values corresponding to soils having higher swelling potential. Despite the fact that the treatment percentage is observed to decrease with increasing swell potential, the resultant treatment is found to be still noteworthy revealing that opening a trench inside soil and backfilling it with a granular material, effectively improves the expansive behaviour where the attained values are two times higher than the replacement ratios, in average.
- b. Under an additional surcharge pressure of 25 kPa, the treatment percentages of granular material filled trenches in vertical swell are observed to be around 52 to 80% for an area replacement ratio of 10%, 57 to 91% for an area replacement ratio of 20% and 71 to 100% for an area replacement ratio of 30%. Therefore, it can be concluded that the presence of a lightweight structure or a manmade fill built over the soil

treated by granular material filled trenches further implements the treatment in vertical swell percentages.

- c. The thin wall ring tests performed with 7 kPa seating pressure showed average peak lateral swell pressure treatment percentages of 27% for an area replacement ratio of 10%, 54% for an area replacement ratio of 20% and 69% for an area replacement ratio of 30%. However, under an overburden pressure of 25 kPa, the decrease in peak lateral swell pressure is less accentuated which can be attributed to the contribution of vertical pressure in the lateral direction. The results of the thin wall ring tests showed that the subject treatment methodology also improves the expansive behaviour in lateral direction.
- d. From the results of the thin-wall oedometer tests, it was observed that the lateral swell pressure has reached to a peak and then decreased to an ultimate value which remained constant afterwards. This behaviour can be explained with the passive failure of expansive soil. For the test types with constant vertical stress, as the sample swells, the lateral swell pressure reaches to a peak, consecutively becoming the major principal stress which may cause a passive failure of the sample.
- e. The mechanism governing the proposed treatment methodology is observed to be mainly dependent on increased lateral strain ability of the soil due to the presence of voids in the fill material. This feature leads the passive failure condition to be reached at lower peak swell pressures. However, it is also anticipated that the friction between the soil and the trench filling material as well as the probable disturbance during opening of trenches may also affect the treatment performance but with a lower impact compared to filling of void spaces.
- f. The treated samples are observed to reach to their peak swell percentages more rapidly when compared to untreated expansive clay samples. This outcome is attributed to the behaviour of the granular soils

acting as a vertical drainage channel, hence facilitating intrusion of water into central parts of the soil sample.

- g. Coarse silt, used as a trench filling material or as a superficial layer on expansive soil during the investigations showed no additional distinct treatment ability neither in vertical nor in lateral swell.
- h. The results of the thin-wall oedometer tests performed on untreated expansive soil samples showed that the ratio of peak and ultimate lateral swell pressure is strongly dependent on the surcharge pressure for both peak and ultimate conditions. Lateral swell pressures (i.e.  $P_h/P_0$  ratio) decrease sharply with increasing overburden stresses.

#### **Recommendations for future research**

While it is believed that the main findings of the present study will still be valid, it is recommended that tests using undisturbed and larger samples or in-situ tests shall be performed on different expansive soils treated with numerous other granular soils having varying grain sizes and relative densities for future research. The effect of initial water content and initial dry unit weight of the expansive soil shall also be incorporated to the investigation program.

Based on the fact that the success of the methodology is simply based upon the introduction of a material providing lateral strain ability to the expansive soil system, tests shall be performed by using objects with predetermined void volume such as a grooved wooden cylindrical stick.

In case the future tests are decided to be performed under larger pressures, it should be kept in mind that there is a possibility of the granular material acting as a rigid member during the application of vertical pressures, thus affecting the loads shared by the soil and the granular material and the magnitude of swell pressures measured during the loading stages of the tests. Therefore, the results of swell tests under larger loads shall be evaluated with utmost caution.

For this particular investigation, the fundamental parameter used to define the treatment percentage is selected to be area replacement ratio which defines the amount of soil volume replaced by a granular material. Based on the fact that expansive clay cannot fill all the void volume of the granular fill due to granular material's particle arrangement, the amount of surface area of the granular material that is in contact with the expansive soil may also be effective in defining this parameter. Therefore, it is recommended that larger scale tests with different surface contact areas satisfying the same area replacement ratios, i.e. by using granular column groups with different diameters and spacing, shall be conducted to decide on which parameter better represents the treatment percentages.

## REFERENCES

- Adayat, T. and Hanna, T.H., (1991), "Performance of Vibrocolumns in Collapsible Soils", *Proceedings of the Indian Geotechnical Conference of Geotechnical Analysis, Practice and Performance*, Surat, India, pp. 383-386.
- Alamgir, M., (1989), *Analysis and Design of Plain and Jacketed Stone Columns in Clays*, M. Sc. Thesis, Department of Civil Engineering, BLET, Dhaka, Bangladesh.
- Al-Omari, R.R. and Hamodi, F.J., (1991), "Swelling Resistant Geogrid – A New Approach for the Treatment of Expansive Soils", *Geotextiles and Geomembranes*, Vol. 16, pp. 295-317.
- Al-Shamrani, M.A., Al-Mhaidib, A.I., (2000), "Swelling Behavior Under Oedometric and Triaxial Loading Conditions", in Shackelford, C.D., Houston, S.L., Chang, N.Y. (eds.), *Advances in Unsaturated Geotechnics*, Geotechnical Special Publication, ASCE, Vol. 99, pp. 344– 360.
- Al-Shamrani, M.A. and Dhowian, A.W., (2003), "Effect of Lateral Restraint Conditions on Predicted Heave of Expansive Soils", *Engineering Geology*, Vol. 69, pp. 63-81.
- Anagnostopoulos, C.A., (2006), "Physical and Engineering Properties of Cement Stabilized Soft Soil Treated with Acrylic Resin Additive", in: Al-Rawas, A.A. and Goosen, M.F.A (editors), *Expansive Soils: Recent Advances in Characterization and Treatment*, pp.405-415.

- AS 1289.7.1.1-2003, "Methods of Testing Soils for Engineering Purposes, Method 7.11: Soil Reactivity Test - Determination of the Shrinkage Index of a Soil", Shrink – Swell Index, Australian Standards.
- ASTM D1883 - 07e2, 2007, "Standard Test Method for CBR (California Bearing Ratio) of Laboratory-Compacted Soils", ASTM International, West Conshohocken, PA, 2003, DOI: 10.1520/D1883-07E02.
- ASTM D4546 – 08, 2008, "Standard Test Methods for One-Dimensional Swell or Collapse of Cohesive Soils", ASTM International, West Conshohocken, PA, 2003, DOI: 10.1520/D4546-08.
- Avşar, E., (2007), *Investigation of Swelling Anisotropy in Ankara Clay*, M.Sc. Thesis in Geological Engineering, Hacettepe University, Ankara, Turkey.
- Avşar, E., Ulusay, R. and Ergüler, Z.A., (2005), "Swelling Properties of Ankara (Turkey) Clay with Carbonate Concretions", *Environmental and Engineering Geosciences*, Vol.11, No.1, pp.73-93.
- Avşar, E., Ulusay R., Sönmez, H. (2009), "Assessment of Swelling Anisotropy of Ankara Clay", *Engineering Geology*, Vol. 105, pp. 24-31.
- Aytekin, M., (1992), *Finite Element Modeling of Lateral Swelling Pressure Distributions behind Earth Retaining Structures*, Doctoral Dissertation, Texas Tech University, Lubbock, Texas, USA.
- Aytekin, M., Wray, W.K. and Vallabhan, C.V.G., (1992), "Transmitted Swelling Pressures on Retaining Structures", *9th International Conference on Expansive Soils*, Dallas, Texas, pp. 32-43.
- Azam, S., (2006), "Large-Scale Oedometer for Assessing Swelling and Consolidation Behavior of Al-Qatif Clay", in: Al-Rawas, A.A. and



- Goosen, M.F.A (editors), *Expansive Soils: Recent Advances in Characterization and Treatment*, pp. 85-99.
- Baker, R. (1968), *The Effect of Thixotropy on Swelling Potential of Compacted Clay*, M.Sc. Thesis, Technion - Israel Institute of Technology, Haifa, Israel.
- Ben-Dor, E., Chabrilot S., Dematlê, J.A.M., Taylor, G.R., Hill J., Whiting M.L. and Sommer S., (2009), "Using Imaging Spectroscopy to Study Soil Properties", *Remote Sensing of Environment*, Vol. 113, Supplement 1, pp.S38-S55.
- Bhuvavajhala, K.R.P., (2000), "Strength Behavior of Expansive Soils Treated with  $\text{CaCl}_2$  and Lime", *Proceedings of Geo Eng 2000 – An International Conference on Geotechnical and Geological Engineering*, Melbourne, Australia, (online source at [www.lib.hpu.edu.ch](http://www.lib.hpu.edu.ch), accessed on February 10, 2012).
- Bishop, A.W. and Henkel, D.J., (1962), *The Measurement of Soil Properties in the Triaxial Test*, London: Edward Arnold Ltd.
- Bishop, A.W. and Wesley, L.D., (1975), "A Hydraulic Triaxial Apparatus for Controlled Stress Path Testing", *Geotechnique*, Vol.25, No.4, pp. 657-670.
- Blight, G.E. and Williams, A.B.B., (1971), "Cracks and Fissures by Shrinkage and Swelling", *Proceedings of 5th Regional Conference for Africa on Soil Mechanics and Foundation Engineering*, Angola, pp. 1-7.
- Brackley, I.J.A., (1975), "A Model of Unsaturated Clay Structure and its Application to Swell Behaviour", *Proceedings of 6th Regional Conference for Africa on Soil Mechanics and Foundation Engineering*, Durban, South Africa, pp. 71-79.

- Brackley, I.J.A., (1975), "Swell Under Load", *Proceedings of 6th Regional Conference for Africa on Soil Mechanics and Foundation Engineering*, Durban, South Africa, pp. 65-70.
- Chabrillat, S., Goetz, A.F.H., Krosley, L. and Olson, H.W., (2002), "Use of Hyperspectral Images in the Identification and Mapping of Expansive Clay Soils and the Role of Spatial Resolution", *Remote Sensing of Environment*, Vol.82, pp.431-445.
- Chen, F.H. and Huang, D., (1987), "Lateral Expansion Pressure on Basement Walls", *6th International Conference on Expansive Soils*, New Delhi, India, pp. 55-59.
- Chen, F.H., (1988), *Foundations on Expansive Soils*, Amsterdam: Elsevier Scientific Publishing Company.
- Croney, D. and Coleman, J.D., (1948), "Soil Structure in Relation to Soil Suction (pF)", *Journal of Soil Science*, Vol. 5, No. 1, pp. 75-84.
- Dhawan, P.K., Mathur, R. and Lal, N.B., (1982), "Effect of Lateral Confinement on Swell Pressure in Expansive Soils," *Highway Research Bulletin*, New Delhi, No. 17, pp. 49-60.
- Dhowian, A.W., Erol, A.O. and Youssef, A.F., (1990), *Evaluation of Expansive Soils and Foundation Methodology in the Kingdom of Saudi Arabia*, published by General Directorate of Research Grants Program, King Abdul-Aziz City for Science and Technology, Riyadh.
- Dhowian, A.W. and Al-Saadon, T.A. (2010), "Swell Behavior of Expansive Soils with Free Lateral Movement", accepted for publication in: *Journal of King Saud University*, Vol.22, Engineering Sciences No.2.

- Edil, T.B. and Alanazy, A.S., (1992), "Lateral Swelling Pressures", *7th International Conference on Expansive Soils*, Dallas, pp. 227-232.
- Elhady, H.A., (2007), "Properties of Treated Expansive Soil", *12<sup>th</sup> International Colloquium on Structural and Geotechnical Engineering*, Cairo, Egypt, 8 pages.
- El Sayed, S.T. and Rabba, S.A., (1986), "Factors Affecting Behavior of Expansive Soils in the Laboratory and Field—A Review", *Geotechnical Engineering*, Vol.17, pp. 89–107.
- El-Sohby, M.A. and Rabba, E.A., (1981), "Some Factors Affecting Swelling of Clayey Soils", *Geotechnical Engineering*, Vol.12, pp. 19-39.
- Ergüler, Z.A. and Ulusay, R., (2003), "A Simple Test and Predictive Models for Assessing Swell Potential of Ankara (Turkey) Clay", *Engineering Geology*, Vol.67, pp.331-352.
- Erol, A.O., (1987), *Expansive Soils and Foundation Methodology*, Short Course on Common Geotechnical Problems in Saudi Arabia, King Saud University, Riyadh, Saudi Arabia.
- Erol, A. O., Dhowian A. and Youssef, A., (1987), "Assessment of Oedometer Methods for Heave Prediction", *Proceedings of 6<sup>th</sup> International Conference on Expansive Soils*, New Delhi, India, pp. 99-103.
- Erol, A.O., Dhowian, A.M., Youssef, O. F., (1987), *Evaluation of Expansive Soils and Foundation Methodology in the Kingdom of Saudi Arabia*, Final Research Report No.SANCST AT.5-88, King Saud University, Riyadh, Saudi Arabia.

- Erol, A.O. and Ergun, U., (1994), "Lateral Swell Pressures in Expansive Soils", *8th International Conference on Soil Mechanics and Foundation Engineering*, New Delhi, India, pp. 1511-1514.
- Ertekin, Y., (1991), *Measurement of Lateral Swell Pressure with Thin Wall Oedometer Technique*, M.S. Thesis, in Civil Engineering, Middle East Technical University.
- FHA, (1974), *Guide to Use of the FHA Soil PVC Meter, Including Results of Nationwide Soil Tests and Correlation with Climatic Factors*, US Department of Housing and Urban Development, Publication No. 4075.15, US Government Printing Office, 27 pages.
- Fredlung, D.G. and Rahardjo, H., (1993), *Soil Mechanics for Unsaturated Soils*, New York: John Wiley and Sons.
- Fourie, A.B., (1989), "Laboratory Evaluating of Lateral Swelling Pressure", *Journal of Geotechnical Engineering*, Vol. 115, No. 1, pp. 1481-1485.
- Goetz, A.F.H., Chabrilat, S. and Lu, Z., (2001), "Field Reflectance Spectrometry for Detection of Swelling Clays at Construction Sites", *Field Analytical Chemistry and Technology*, Vol.5, No.3, pp. 143-155.
- Gourley, C.S., Newill, D. and Schreiner, H.D., (1993), "Expansive Soils", *TRL's Research Strategy*.
- Gundogdu, M.N.G., (1982), *Neojen Yaslı Bigadiç Sedimanter Baseninin Jeolojik, Mineralojik ve Jeokimyasal İncelenmesi*, PhD Thesis, Department of Geological Engineering, Hacettepe University, Ankara, Turkey (in Turkish).
- Hatipoğlu, U., (1993), *Lateral Pressures in Expansive Soils*, M.S.Thesis, in Civil Engineering, Middle East Technical University.

- Jacky, J., (1944), "The Coefficient of Earth Pressure at Rest", *Journal for the Society of Hungarian Architects and Engineers*, Vol. 78, No. 22, pp. 355-358.
- Jardine, R.J., Symes. M.J. and Burland, J.B., (1984), "The Measurement of Soil Stiffness in the Triaxial Apparatus", *Geotechnique*, Vol. 34, No. 3, pp. 323-340.
- Johnson, L.D. and Snethen, D.R., (1978), "Prediction of Potential Heave of Swelling Soils", *Geotechnical Testing Journal*, Vol.3, Issue 1, pp.117-124.
- Joshi, R.P. and Katti, R.K., (1984), "Lateral Pressure Development Under Surcharges", *Proceedings of 5<sup>th</sup>. International Conference on Expansive Soils, Adelaide, South Australia*, pp. 227-241.
- Kariuki, P.C., Woldai, T. and Van der Meer, F.D., (2004), "A Unified Swelling Potential Index for Expansive Soils", *Engineering Geology*, 72, pp. 1-8.
- Kariuki, P.C. and Van der Meer, F.D., (2004), "Effectiveness of Spectroscopy in Identification of Swelling Indicator Clay Minerals", *International Journal of Remote Sensing*, Vol. 25, No. 2, pp. 445-469.
- Kassif, G. and Zeitlen, J.G., (1962), "Behaviour of Pipes Buried in Expansive Clays", *Journal of Soil Mechanics and Foundation Engineering Division*, ASCE, Vol. 88, No. 2, pp. 133-148.
- Kassif, G and Baker R., (1969), "Swell Pressure Measured by Uni and Triaxial Techniques", *Proceedings of Seventh International Conference on Soil Mechanics and Foundation Engineering*, Mexico City, Vol. 1, pp. 215-218.

- Katti A.R. and Katti, R.K., (1996), "Procedure for Design and Construction of Shallow Foundations in Expansive Clayey Soils with CNS and MSM Technology", *Proceedings of National Seminar on Partially Saturated Soils and Expansive Soils*, Kakinada, India, pp. 5-14.
- Katti, R.K., (1978), "Search for Solutions to Problems in Black Cotton Soils", *First I.G.S Annual Lecture*, Indian Geotechnical Society at I.T.T., Delhi.
- Katti, R.K., (1979), "Search for Solutions to Problems in Black Cotton Soils", *Indian Geotechnical Journal*, Vol. 9, No. 1, pp. 1-80.
- Katti, R.K., Bhangale, E.S. and Moza, K.K., (1983), "Lateral Pressure in Expansive Soil with and without a Cohesive Non-Swelling Soil Layer, Application to Earth Pressures on Cross Drainage Structures in Canals and Key Walls in Dams", Final Report Part-I, submitted to Central Board of Irrigation and Power, New Delhi, Vol. 110, No. 21, 1-303 pp.
- Katti, R.K. and Katti A.R., (2008), "Physics and Engineering of Montmorillonitic Clay Leading to Discovery of C.N.S.L. Phenomenon", *12<sup>th</sup> International Conference on International Association for Computer Methods and Advances in Geomechanics (IACMAG)*, Goa, India, pp. 1227-1233.
- Katti R.K., Katti, D.R. and Katti A.R., (2002), *Behaviour of Saturated Expansive Soil and Control Methods*, revised and enlarged edition, Balkema: Swets and Zeitlinger Publishers, pp. 1132-1135.
- Komornik, A. (1962), *The Effect of Swelling Properties on Pile Foundations*, D. Sc. (Tech.) Thesis, Technion - Israel Institute of Technology, Haifa, Israel.
- Komornik, A. and Zeitlen, J.G., (1965), "An Apparatus for Measuring Lateral Soil Swelling Pressure in the Laboratory", *Proceedings of 6th International*

*Conference on Soil Mechanics and Foundation Engineering*, Vol.1, Canada, pp. 278-281.

Komornik, A. and David, D., (1969); "Prediction of Swelling Pressure of Clays", *Journal of ASCE, Soil Mechanics and Foundation Division*, SM No.1, pp.209-225.

Koteswara, R. D, Pranav, P.R.T. and Anusha, M., (2011(a)), "Stabilization of Expansive Soils with Rice Husk Ash, Lime and Gypsum – An Experimental Study", *International Journal of Engineering Science and Technology*, Vol.3, pp. 8076-8085.

Koteswara, R. D, Pranav, P.R.T. and Anusha, M., (2011(b)), "A Laboratory Study on the Utilization of GBFS and Fly Ash to Stabilize the Expansive Soil for Subgrade Embankments", *International Journal of Engineering Science and Technology*, Vol.3, pp. 8086-8098.

Lal, N.B. and Palit, R.M., (1969), "A New Dimension to the Measurement of Swell Pressure in Expansive Soils", *Proceedings of Symposium on Characteristics of and Construction Techniques in Black Cotton Soils*, College of Military Engineering, Poona.

Lambe T.W., (1960), "Compacted Clay Structure and Engineering Behaviour", *Transaction, ASCE*, Vol.125, pp. 682-756.

Lambe, T.W. and Whitman, R.V., (1969), "Soil Mechanics", New York: John Wiley and Sons.

McDowell, C., (1956), "Interrelationship of Load, Volume Change, and Layer Thickness of Soils to the Behavior of Engineering Structures," *Highway Research Board, Proceedings of the Thirty Fifth Annual Meetings*, Publication No 426, Transportation Research Board, Washington, D.C., pp. 754-772.

- McKeen, R.G., (1977), "Characterizing Expansive Soils for Design," presented at the Joint Meeting of the Texas, New Mexico, and Mexico Sections of the ASCE, Albuquerque, New Mexico, 23 pp.
- McKeen, R.G., (1980), "A Model for Predicting Expansive Soil Behavior," *Proceedings, 7th International Conference on Expansive Soils*, Dallas, Texas, The American Society of Civil Engineers (ASCE), New York, pp. 1-6.
- McKeen, R.G. (1981), "Field Studies of Airport Pavements on Expansive Clays", *Proceedings of Fourth International Conference on Expansive Soils*, Denver, Colorado, Vol. 1, pp. 242-262.
- Menzies, B.K., (1988), "A Computer Controlled Hydraulic Triaxial Testing System", in: *Advanced Triaxial Testing of Soil and Rock*, ASTM-STP 977, pp.82-94.
- Michel, J.C., Beaumont, A. and Tessier, D., (2000), "A Laboratory Method for Measuring the Isotropic Character of Soil Swelling", *European Journal of Soil Science*, Vol. 51, pp. 689-697.
- Mitchell, J.K., (1993), *Fundamentals of Soil Behavior*, 5<sup>th</sup>. Edition, New York: John Wiley & Sons.
- Muntahar, A.S., (2006), "Swelling Characteristics and Improvement of Expansive Soils with Rice Husk Ash", in: Al-Rawas, A.A. and Goosen, M.F.A (editors), *Expansive Soils: Recent Advances in Characterization and Treatment*, pp. 435-451.
- Nalbantoğlu, Z., (2006), "Lime Stabilization of Expansive Clays", in: Al-Rawas, A.A. and Goosen, M.F.A (editors), *Expansive Soils: Recent Advances in Characterization and Treatment*, pp. 371-384.



- Nayak, N.V. and Christensen, R.W., (1971), "Swelling Characteristics of Compacted, Expansive Soils", *Clays and Clay Minerals*, Vol.19, pp.251-261.
- Nelson, J.D. and Miller, D.J., (1992), *Expansive Soils, Problems and Practice in Foundation and Pavement Engineering*, New York: John Wiley and Sons.
- Ofer, Z., (1980), "Instruments for Laboratory and In - Situ Measurements of Lateral Swelling Pressure of Expansive Clays", *Proceedings of 4th International Conference on Expansive Soils*, Denver, Colorado, pp. 45-53.
- Ofer, Z. and Blight, G.E. (1985), "Measurement of Swelling Pressure in the Laboratory and In-Situ", *Transportation Research Record 1032: Evaluation and Control of Expansive Soils*, Transportation Research Board, Washington, D.C., pp. 15-22.
- Ofer, Z. and Komornik, A., (1983), "Lateral Swelling Pressure of Compacted Clay", *Proceedings of the 7th Asian Regional Conference on Soil Mechanics and Foundation Engineering*, Haifa, Israel, pp. 56-63.
- Özalp, H.K., (2010), *Determination of Lateral Swelling Pressure*, Ph.D. Thesis in Civil Engineering, İstanbul Technical University, İstanbul, Turkey.
- Özer, M., Ulusay, R., Işık, N.S., (2012), "Evaluation of Damage to Light Structures Erected on a Fill Material Rich in Expansive Soil", *Bulletin of Engineering Geology and the Environment*, Vol. 71, pp. 21-36.
- Parcher, J.V. and Liu P.C., (1965), "Some Swelling Characteristics of Compacted Clays", *Journal of the Soil Mechanics and Foundation Division*, ASCE, Vol. 91, No. 31, pp. 1-17.

- Phanikumar, B.R. and Rao, N.R., (2000), "Increasing Pull-Out Capacity of Granular Pile Anchor in Expansive Soils Using Base Geosynthetics", *Canadian Geotechnical Journal*, Vol. 37, pp. 870-881.
- Phanikumar, B.R. and Sharma, R.S., (2006), "Granular Pile Anchors – An Innovative Foundation Technique for Expansive Soils", in: Al-Rawas, A.A. and Goosen, M.F.A (editors), *Expansive Soils: Recent Advances in Characterization and Treatment*, pp.507-521.
- Phanikumar, B.R., Sharma, R.S., Rao, A.S. and Madhav, M.R., (2004), "Granular Pile Anchor Foundation (GPAF) System for Improving the Engineering Behavior of Expansive Clay Beds", *Geotechnical Testing Journal*, Vo. 27, No. 3, pp. 279-287.
- Popescu, M.E., (1986), "A Comparison between Behaviour of Swelling and Collapsing Soils", *Engineering Geology*, Vol.23, pp. 145-163.
- Rao, A.S. and Rao, M.R., (2008), "Swell Shrink Behavior of Expansive Soils under Stabilized Fly Ash Cushions", *Proceedings of the 12th International Conference of International Association for Computer Methods and Advances in Geomechanics (IACMAG)*, Goa, India, pp. 1539-1546.
- Richards, B.G., (1967), "Moisture Flow and Equilibria in Unsaturated Soils for Shallow Foundations", in: *Permeability and Capillarity of Soils*, STP 417, ASTM, Philadelphia, PA, pp. 4 –34.
- Richards, B.G., (1977), "Pressures on a Retaining Wall by an Expansive Clay", *Proceedings of 9th International Conference on Soil Mechanics and Foundation Engineering*, Tokyo, Japan, pp. 705-710.

- Richards, B.G and Kurzeme, M., (1973), "Observations of Earth Pressures on a Retaining Wall at Gouger Street Mail Exchange, Adelaide," *Australian Geomechanics Journal*, Vol. G3, No. 1, pp. 21-26.
- Robertson, A.M.G. and Wagener, F.V.M., (1975), "Lateral Swelling Pressures in Active Clay", *6th Regional Conference for Africa on Soil Mechanics and Foundation Engineering*, Durban, South Africa, pp. 107-114.
- Sapaz, B., (2004), *Lateral versus Vertical Swell Pressures in Expansive Soils*, MSc Thesis, METU Civil Engineering Department., Ankara, Turkey.
- Satyanarayana, B., (1969), "Behavior of Expansive Soil Treated or Cushioned with Sand", *Proceedings, 2<sup>nd</sup> International Conference on Expansive Clay Soils*, Texas A&M University, College Station, Texas, pp.308-316.
- Schneider, G.L, and Poor, A.R., (1974), "The Prediction of Soil Heave and Swell Pressures Developed by an Expansive Clay", *Construction Research Center, Research Report, No: TR-9-74*, University. of Texas at Arlington, 83 pp.
- Seco, A., Ramirez, F., Miqueleiz, L. and Garcia, B. (2011), "Stabilization of Expansive Soils for Use in Construction", *Applied Clay Science*, Vol. 51, p. 348-352.
- Seed, H.B., Mitchell, J.K. and Chan, C.K., (1962(a)), "Swell Pressure Characteristics of Compacted Clay", *Highway Research Board Bulletin* 313, National Research Council, Washington D.C., pp.12-39.
- Seed, H.B., Woodward, R.J. and Lundgren, R. (1962(b)), "Prediction of Swelling Potential for Compacted Clays", *Journal of Soil Mechanics and Foundation Division*, ASCE, Vol. 88, pp. 53-87.

- Shanker, B ., Ratnam, M.V. and Rao, A.S., (1987), "Multidimensional Swell Behaviour of Expansive Clays", *Proceedings of Sixth International Conference on Expansive Soils*, New Delhi, India, pp. 143-147.
- Sharma, R.S. and Phanikumar, B.R., (2005), "Laboratory Study of Heave Behavior of Expansive Clay Reinforced with Geopiles", *Journal of Geotechnical and Geoenvironmental Engineering*, Vol. 131, No. 4, pp. 512-518.
- Shiming, H., (1979), "Discussion on Some Problems of Expansive Soils", *Geotechnical Investigation and Surveying*, No. 4.
- Shiming, H., (1984), "An Experimental Apparatus for Three Dimensional Soil Expansion", *Proceedings of 8th Regional Conference for Africa on Soil Mechanics and Foundation Engineering*, Harare, pp. 139-142.
- Skempton, A.V., (1953), "The Colloid Activity of Clays", *Proceedings of the 3rd. International Conference on Soil Mechanics and Foundation Engineering*, Zurich, Vol. 1, pp. 57-61.
- Snethen, D.R., (1980), "Characterization of Expansive Soils using Soil Suction Data", *Proceedings of 4<sup>th</sup> International Conference of Expansive Soils*, Denver, Colorado, pp. 54.
- Snethen, D.R., (1984), "Evaluation of Expedient Methods for Identification of Potentially Expansive Soils", *5th International Conference on Expansive Soils*, Adelaide, South Australia.
- Snethen, D.R., Patrick, D.M., (1977), "An Evaluation of Expedient Methodology for Identification of Potentially Expansive Soils", in *MS Report No.FHWA-RE-77-94, NTIS, PB-289-164*, Soils and Pavement Laboratory, US Army Engineering Waterway Experiment Station, Vicksburg.

- Sridharan, A., Rao, A.S. and Sivapullaiah, P.V., (1986), "Swelling Pressure of Clays", *Geotechnical Testing Journal*, Vol. 9, No.1, pp. 24-33.
- Stavridakis, E.I., (2006), "Assessment of Anisotropic Behavior of Swelling Soils on Ground and Construction Work, in: Al-Rawas, A.A. and Goosen, M.F.A (editors), *Expansive Soils: Recent Advances in Characterization and Treatment*, pp.371-384.
- Subbarao, G.V.R., Siddartha, D., Muralikrishna T., Sailaja K.S. and Sowmya T., (2011), "Industrial Wastes in Soil Improvement," *ISRN Civil Engineering*, Vol. 2011, Article ID 138149, 5 pages.
- Sudhindra, C., Moza, K.K., (1987), "An Approach for Lateral Pressure Assessment in Expansive Soils", *Proceedings of 6th International Conference on Expansive Soils*, New Delhi, India, pp. 67-70.
- Tekin, M., (2005), *Model Study on Settlement Behaviour of Granular Columns under Compression Loading*, Ph.D. Thesis in Civil Engineering, Middle East Technical University, Ankara.
- Thomas, P.J., Baker, J.C. and Zelazny, L.W., (2000), "An Expansive Soil Index for Predicting Shrink-Swell Potential", *Soil Science Society of America Journal*, Vol.64, pp.268-274.
- Thomas, M.G., (2008), *Impact of Lateral Swell Pressure on Retaining Structure Design Using Expansive Cohesive Backfill*, M.Sc. Thesis in Civil Engineering, The University of Texas at Arlington.
- Tisot, J.P. and Aboushook, M., (1983), "Triaxial Study of Swelling Characteristics", *Proceedings of 7th Asian Regional Conference on Soil Mechanics and Foundation Engineering*, Haifa, Vol. 1, pp. 94–97.

- Tonoz, M.C., Gökçeoğlu, C. and Ulusay, R., (2003), "A Laboratory Scale Experimental Investigation of the Performance of Lime Columns in Expansive Ankara (Turkey) Clay", *Bulletin of Engineering Geology and Environment*, Vol. 62, pp. 62-91.
- Tonoz, M.C., Gökçeoğlu, C. and Ulusay, R., (2006), "Stabilization of Expansive Ankara Clay with Lime", in: Al-Rawas, A.A. and Goosen, M.F.A (editors), *Expansive Soils: Recent Advances in Characterization and Treatment*, pp. 318-339.
- Turker, D. and Çokça, E., (2006), "Effects of Addition of Fly Ash on Swell Potential of an Expansive Soil", in: Al-Rawas, A.A. and Goosen, M.F.A (editors), *Expansive Soils: Recent Advances in Characterization and Treatment*, pp. 453-463.
- TxDOT, (1999), "Test Procedure for Determining Potential Vertical Rise", *TxDOT Designation TEX-124-E Construction Division*, Texas Department of Transportation, 10 pp
- Van Der Merwe, D. H. (1964), "The prediction of heave from the plasticity index and percentage clay fraction of soils", *Civil Engineers in South Africa*, Vol.6, Issue 6, pp.103-107.
- Van Der Merwe, D.H., (1975), "Contribution to Specialty Session B, Current Theory and Practice for Building on Expansive Clays", *Proceedings of the 6th Regional Conference for Africa on Soil Mechanics and Foundation Engineering*, vol. 2. Durban, pp. 166–167.
- Venkataswamy, B., Gandhi, S.R., Srinivas, K.S. and Sanghavi, K.V., (2003), "Improvement of Expansive Clay by Deep in-Situ Technique, *ICG-2003 Geotechnical Engineering for Infrastructure Development*, pp. 311-314.

- Vijayvergia, V.N. and Ghazzaly, O.I., (1973), "Prediction of Swelling Potential for Natural Clays", *Proceedings of the Third International Conference on Expansive Soils*, Haifa, Vol.1, pp.227-236.
- Wattanasanticharoen, E., Puppala, A.J. and Hoyos, L.R., (2007), "Evaluations of Heaving Behavior of Expansive Soil Under Anisotropic Stress State Conditions", *Geotechnical Testing Journal*, Publication Pending.
- Weston, D.J., (1980), "Expansive Roadbed Treatment for South Africa", *Proceedings of Fourth International Conference on Expansive Soils*, Denver, Vol.1, pp.339-360.
- Windal, T. and Shahrour, I., (2002), "Study of the Swelling Behavior of a Compacted Soil Using flexible Odometer", *Mechanics Research Communications*, Vol. 29, No. 5, pp. 375-382..
- Yanıkömeroğlu, K., (1990), *Effect of Lateral Confinement on Swelling Behaviour*, M.Sc. Thesis in Civil Engineering, METU, Ankara, Turkey.
- Yılmaz, I., (2009), "Swell Potential and Shear Strength Estimation of Clays", *Applied Clay Science*, 46, pp.376-384.
- Yılmaz, I. and Kaynar, O., (2011), "Multiple Regression ANN(RBF,MLP) and ANFIS Models for Prediction Swell Potential of Clayey Soils", *Expert Systems with Applications*, 38, pp.5958-5966.
- Yitagesu F.A., Van der Meer, F. and Van der Werff, H., (2009), "Prediction of Volumetric Shrinkage in Expansive Soils (Role of Remote Sensing)", in Jedvolec, G. (editor), *Advances in Geoscience and Remote Sensing*, ISBN: 978-953-307-005-06, In Tech (online source at [www.intechopen.com/books/advances-in-geoscience-and-remote-sensing/prediction-of-volumetric-shrinkage-in-expansive-soils-role-of-remote-sensing-](http://www.intechopen.com/books/advances-in-geoscience-and-remote-sensing/prediction-of-volumetric-shrinkage-in-expansive-soils-role-of-remote-sensing-), accessed May 14, 2012).

## APPENDIX A

### RESULTS OF THIN-WALL RING TESTS PERFORMED ON UNTREATED TYPE- 3 AND TYPE 5 SOIL SAMPLES

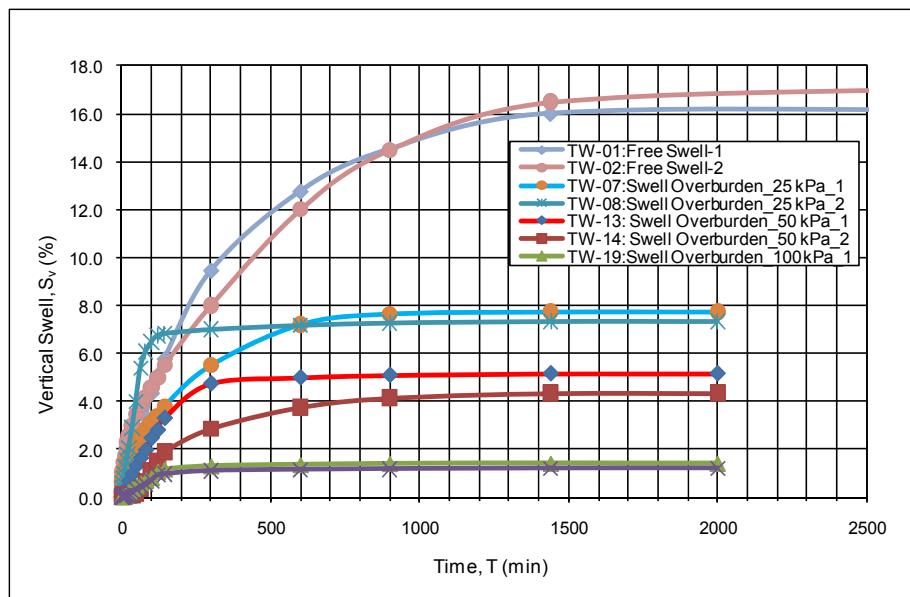


Figure A. 1 Vertical Swell Percentage vs. Time Relationship for Thin-Wall Ring Tests (Ring-1) Performed on Type-3 Untreated Soil Samples



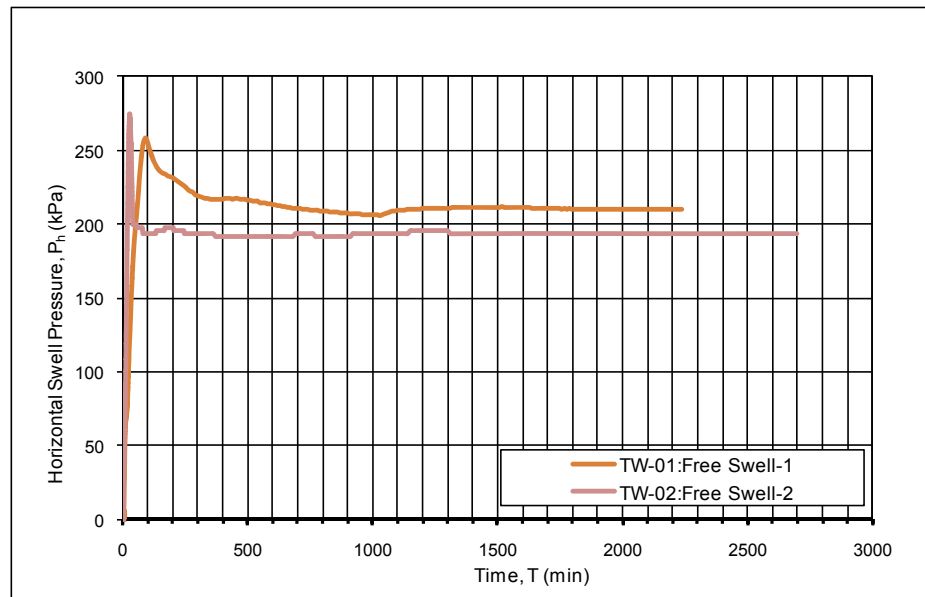


Figure A. 2 Lateral Swell Pressure vs. Time Relationship for Thin-Wall Ring Tests (Ring-1) Performed on Type-3 Untreated Soil Samples ( $P_s = 7$  kPa)

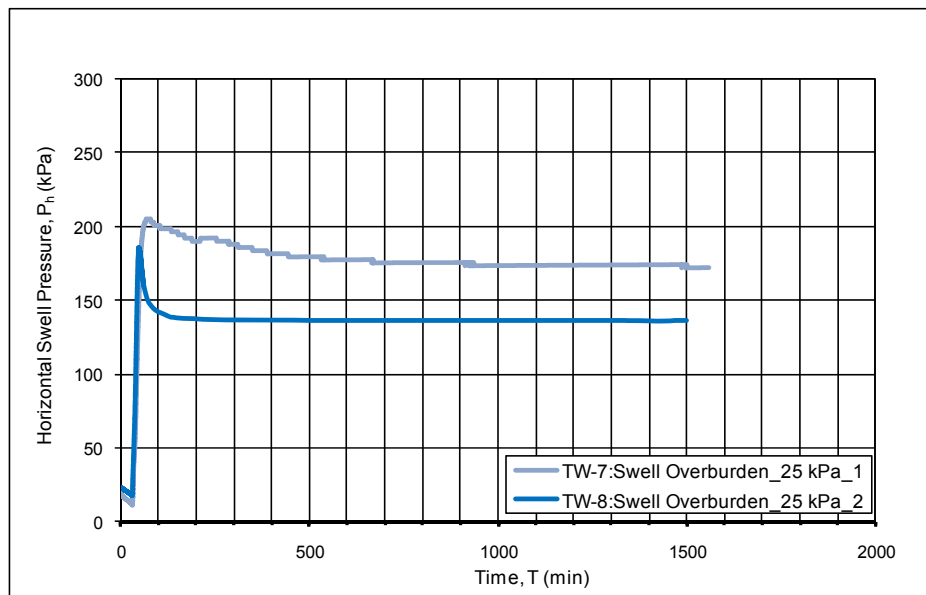


Figure A. 3 Lateral Swell Pressure vs. Time Relationship for Thin-Wall Ring Tests (Ring-1) Performed on Type-3 Untreated Soil Samples ( $P_o = 25$  kPa)

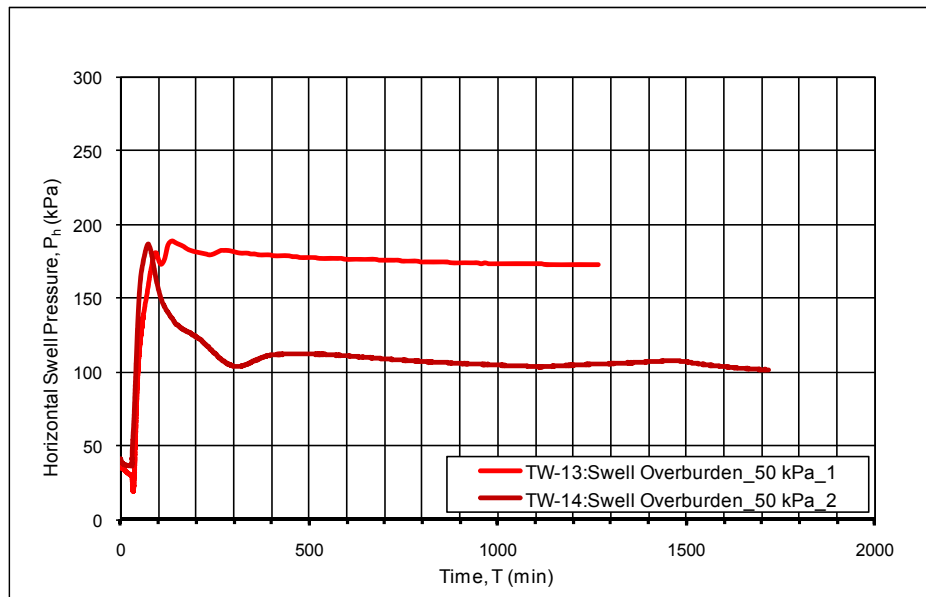


Figure A. 4 Lateral Swell Pressure vs. Time Relationship for Thin-Wall Ring Tests (Ring-1) Performed on Type-3 Untreated Soil Samples ( $P_o=50$  kPa)

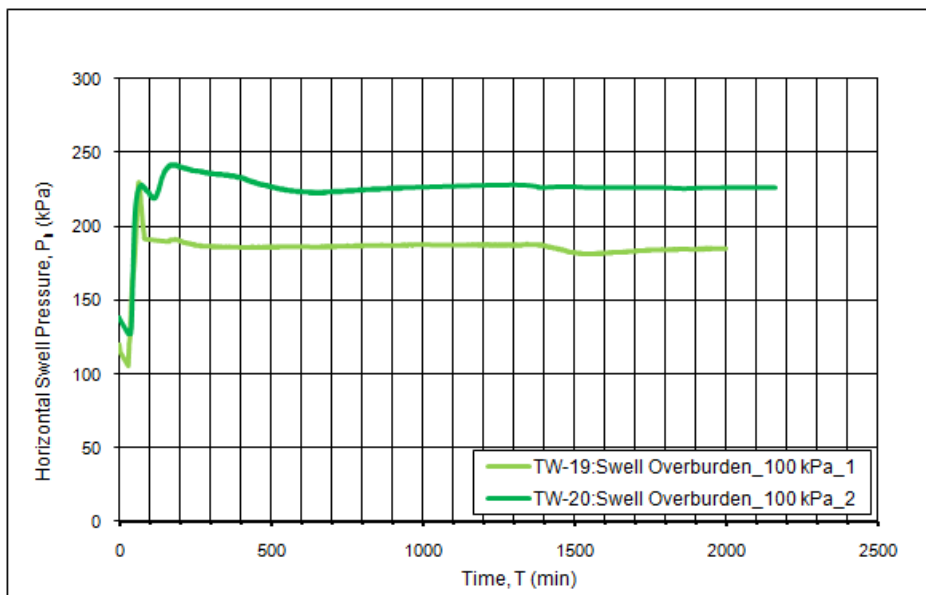


Figure A. 5 Lateral Swell Pressure vs. Time Relationship for Thin-Wall Ring Tests (Ring-1) Performed on Type-3 Untreated Soil Samples ( $P_o=100$  kPa)

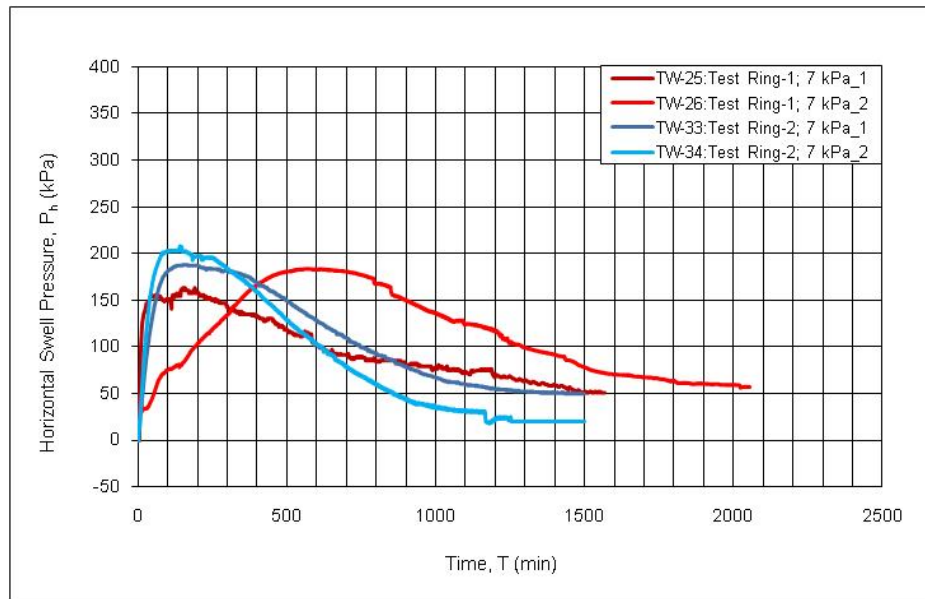


Figure A. 6 Lateral Swell Pressure vs. Time Relationship for Thin-Wall Ring Tests Performed on Type-5 Untreated Soil Samples ( $P_s=7$  kPa)

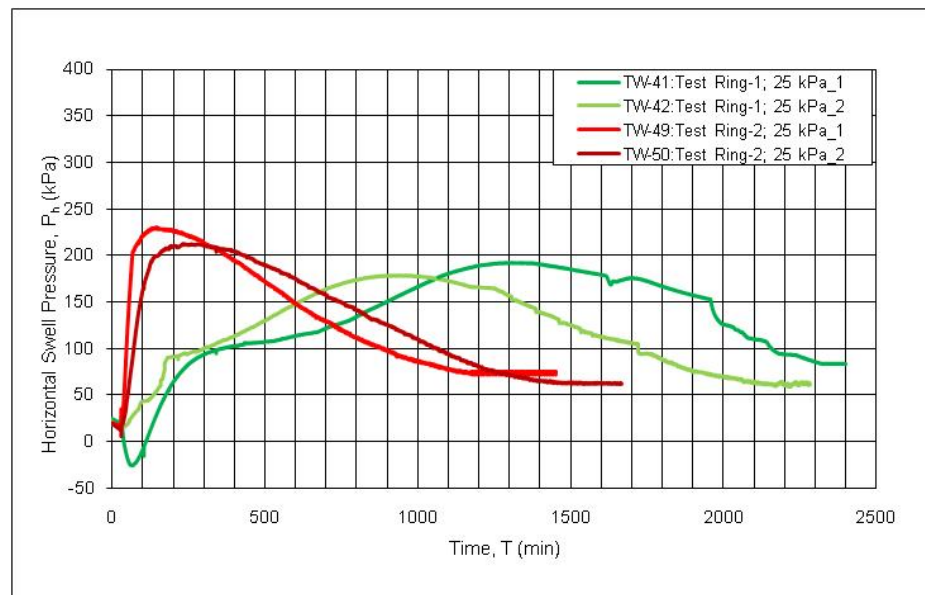


Figure A. 7 Lateral Swell Pressure vs. Time Relationship for Thin-Wall Ring Tests Performed on Type-5 Untreated Soil Samples ( $P_o=25$  kPa)

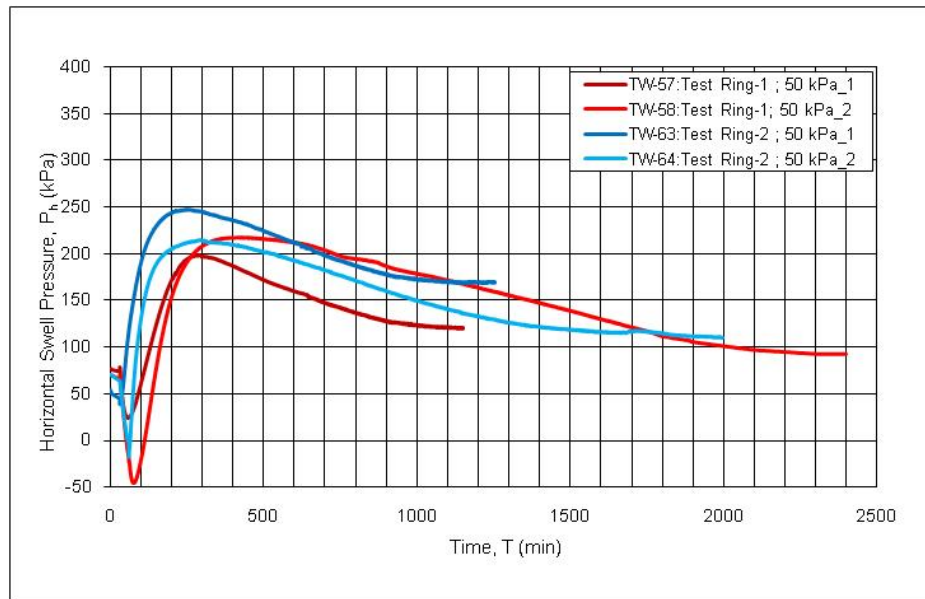


Figure A. 8 Lateral Swell Pressure vs. Time Relationship for Thin-Wall Ring Tests Performed on Type-5 Untreated Soil Samples ( $P_o=50$  kPa)

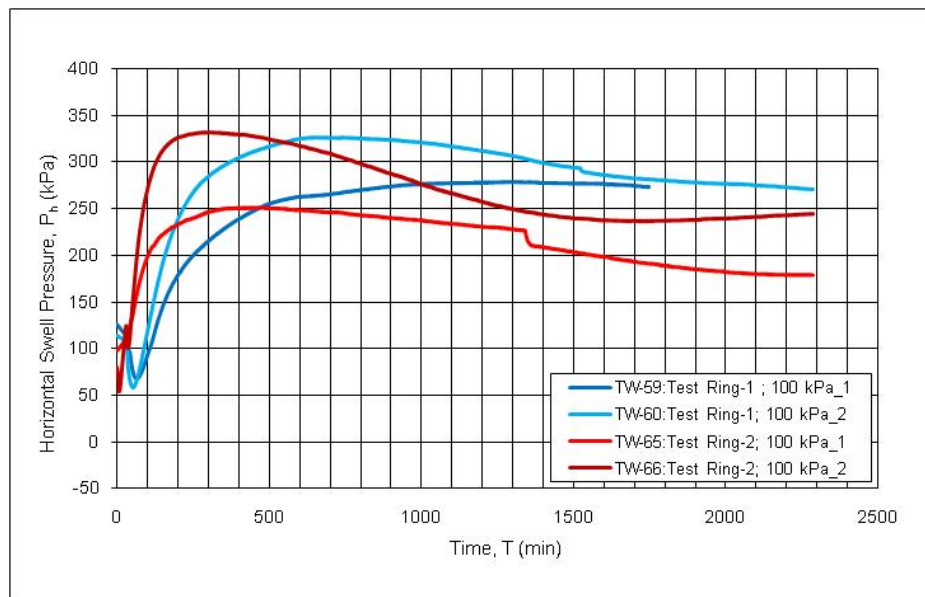


Figure A. 9 Lateral Swell Pressure vs. Time Relationship for Thin-Wall Ring Tests Performed on Type-5 Untreated Soil Samples ( $P_o=100$  kPa)

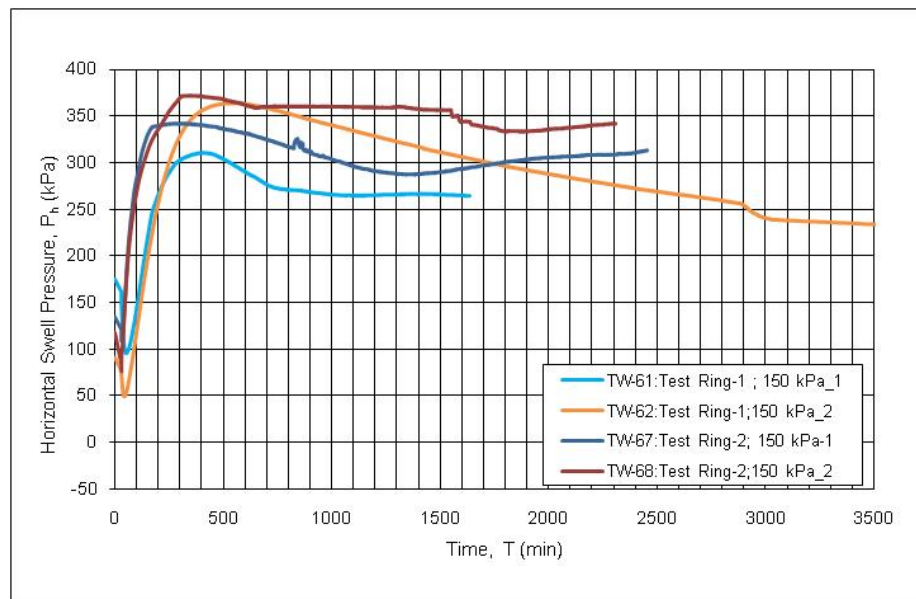


Figure A. 10 Lateral Swell Pressure vs. Time Relationship for Thin-Wall Ring Tests Performed on Type-5 Untreated Soil Samples ( $P_o=150$  kPa)

## APPENDIX B

### RESULTS OF THIN-WALL RING TESTS PERFORMED ON TREATED TYPE-3 SOIL SAMPLES

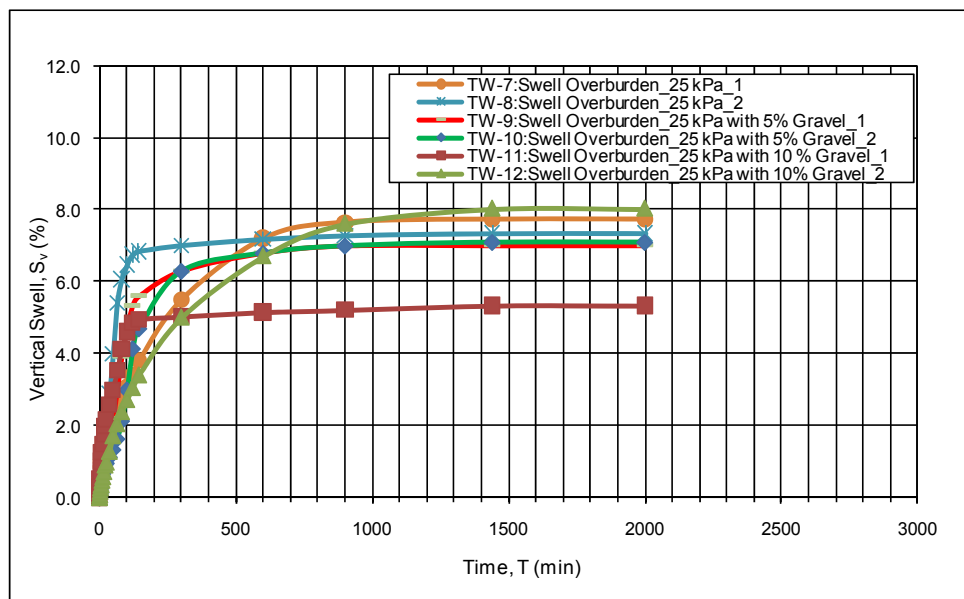


Figure B. 1 Vertical Swell Percentage vs. Time Relationship for Thin-Wall Ring Tests (Ring-1) Performed on Type-3 Soil with Different Treatment Percentages ( $P_o=25$  kPa)

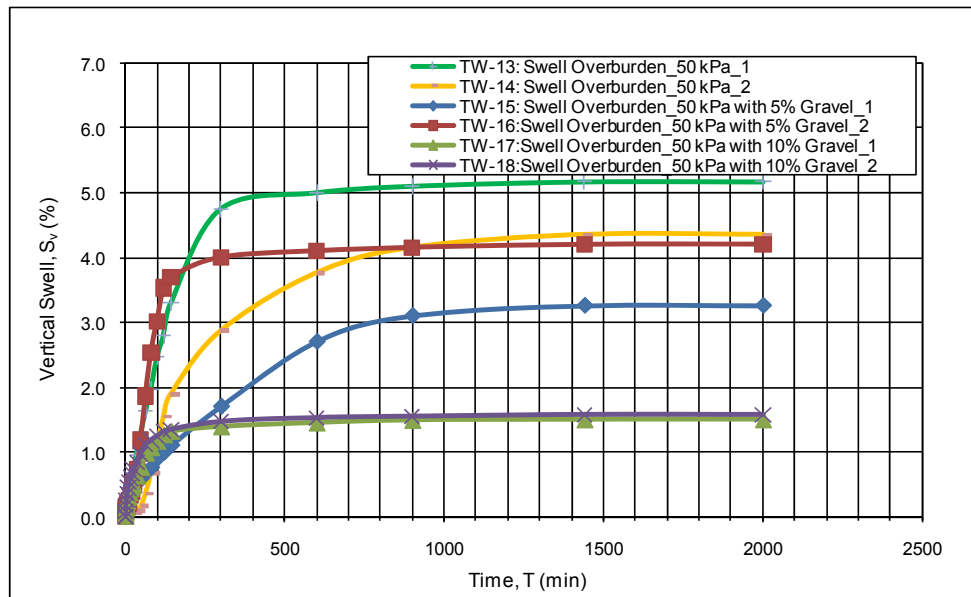


Figure B. 2 Vertical Swell Percentage vs. Time Relationship for Thin-Wall Ring Tests (Ring-1) Performed on Type-3 Soil with Different Treatment Percentages ( $P_o=50$  kPa)

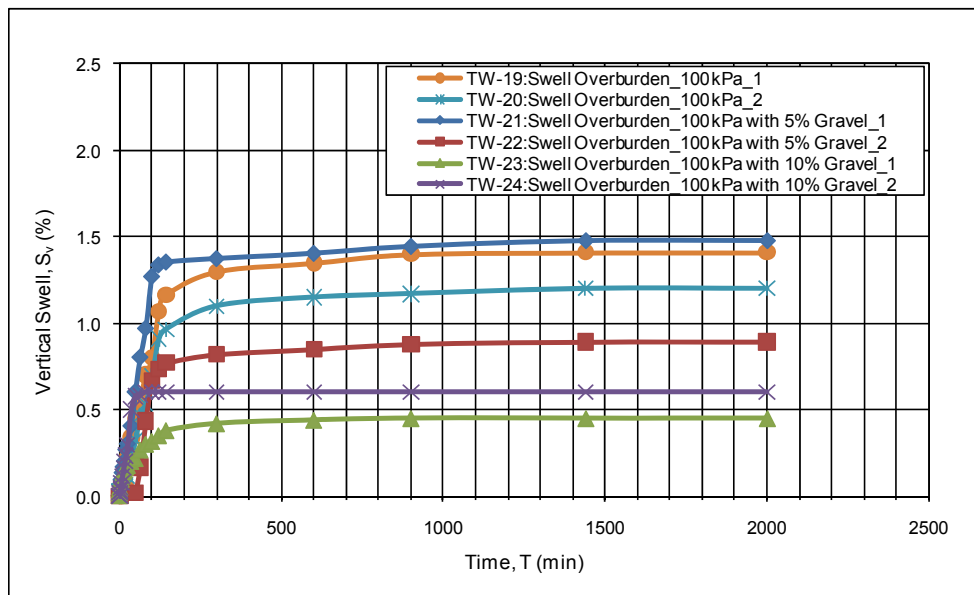


Figure B. 3 Vertical Swell Percentage vs. Time Relationship for Thin-Wall Ring Tests (Ring-1) Performed on Type-3 Soil with Different Treatment Percentages ( $P_o=100$  kPa)

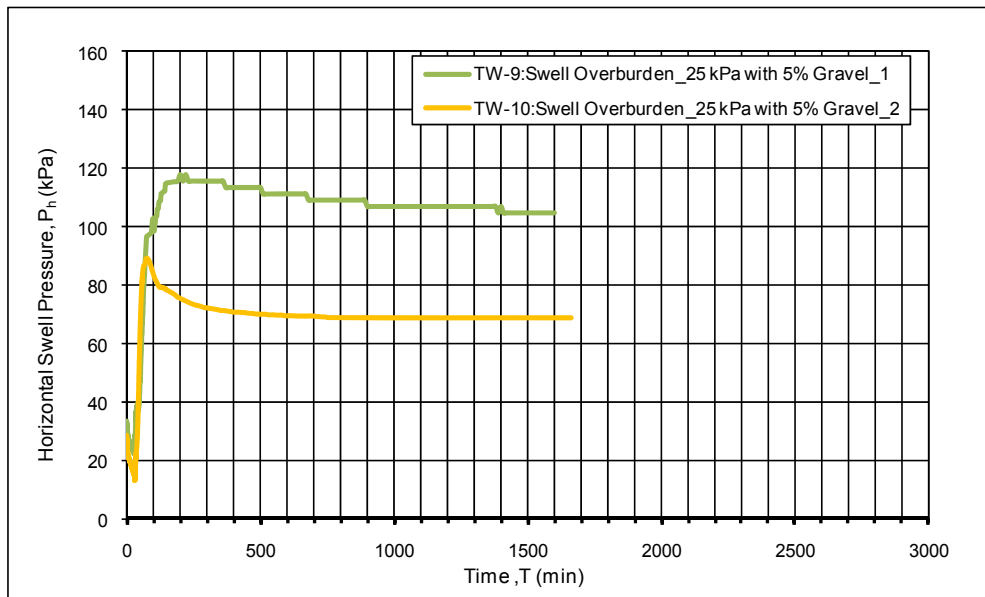


Figure B. 4 Lateral Swell Pressure vs. Time Relationship for Thin-Wall Ring Tests (Ring-1) Performed on Type-3 Soil Samples with ARR=5% ( $P_o=25$  kPa)

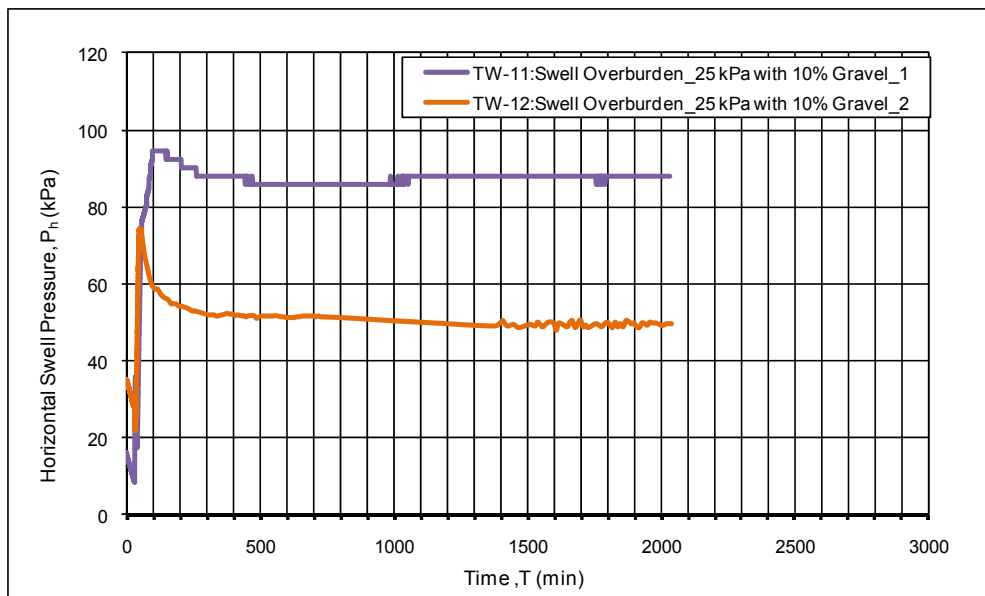


Figure B. 5 Lateral Swell Pressure vs. Time Relationship for Thin-Wall Ring Tests (Ring-1) Performed on Type-3 Soil Samples with ARR=10% ( $P_o=25$  kPa)



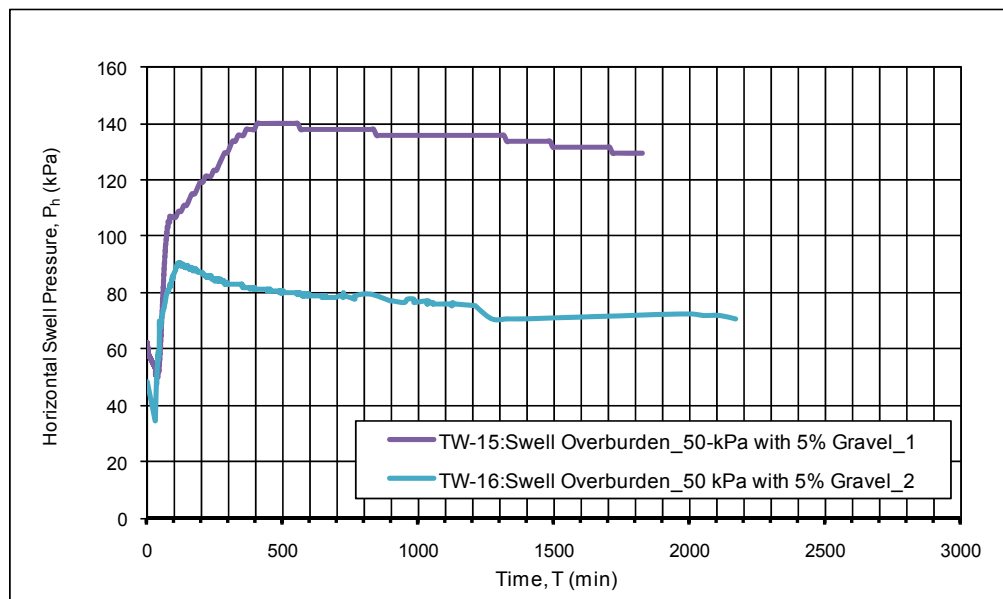


Figure B. 6 Lateral Swell Pressure vs. Time Relationship for Thin-Wall Ring Tests (Ring-1) Performed on Type-3 Soil Samples with ARR=5% ( $P_o=50$  kPa)

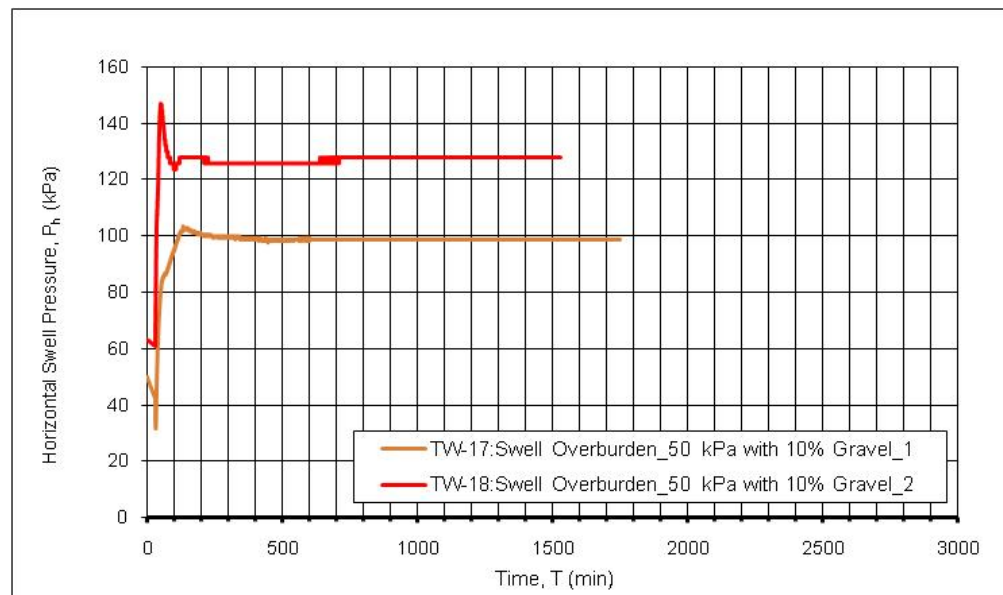


Figure B. 7 Lateral Swell Pressure vs. Time Relationship for Thin-Wall Ring Tests (Ring-1) Performed on Type-3 Soil Samples with ARR=10% ( $P_o=50$  kPa)

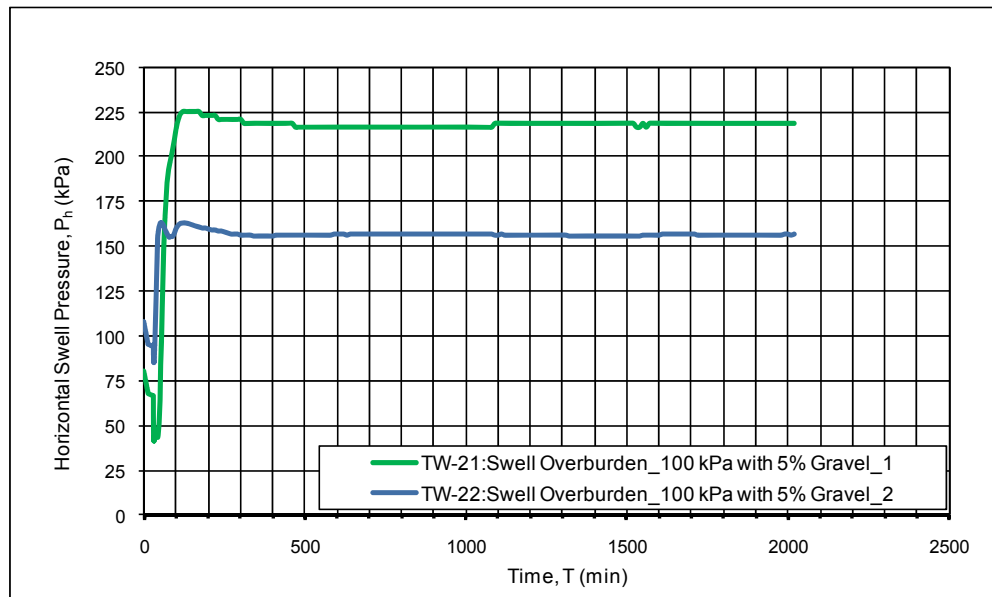


Figure B. 8 Lateral Swell Pressure vs. Time Relationship for Thin-Wall Ring Tests (Ring-1) Performed on Type-3 Soil Samples with ARR=5% ( $P_o=100$  kPa)

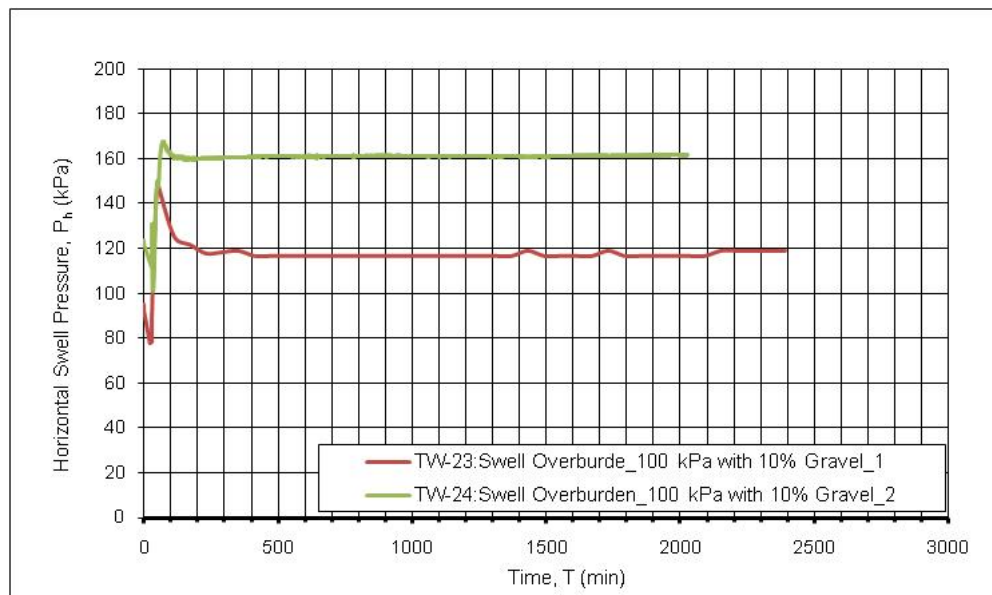


Figure B. 9 Lateral Swell Pressure vs. Time Relationship for Thin-Wall Ring Tests (Ring-1) Performed on Type-3 Soil Samples with ARR=10% ( $P_o=100$  kPa)

## APPENDIX C

### RESULTS OF THIN-WALL RING TESTS PERFORMED ON TREATED TYPE- 5 SOIL SAMPLES

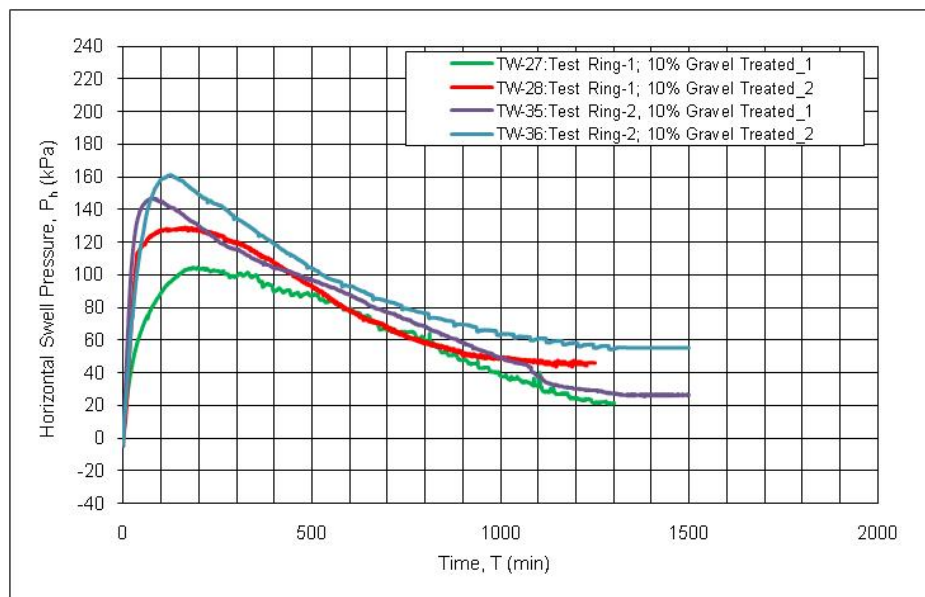


Figure C. 1 Lateral Swell Pressure vs. Time Relationship for Thin-Wall Ring Tests Performed on Type-5 Soil (10% Treated ;  $P_s=7$  kPa)

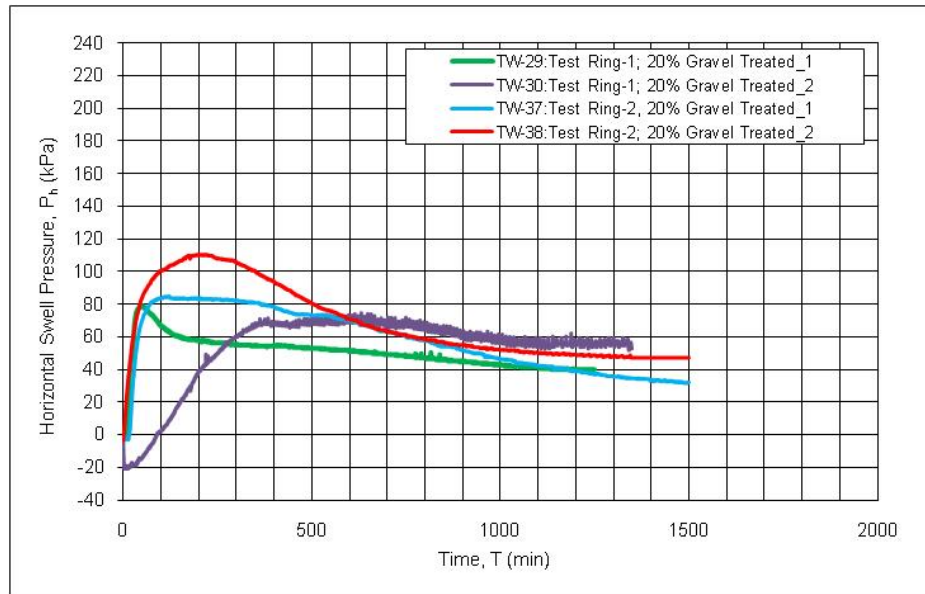


Figure C. 2 Lateral Swell Pressure vs. Time Relationship for Thin-Wall Ring Tests Performed on Type-5 Soil (20% Treated ;  $P_s=7$  kPa)

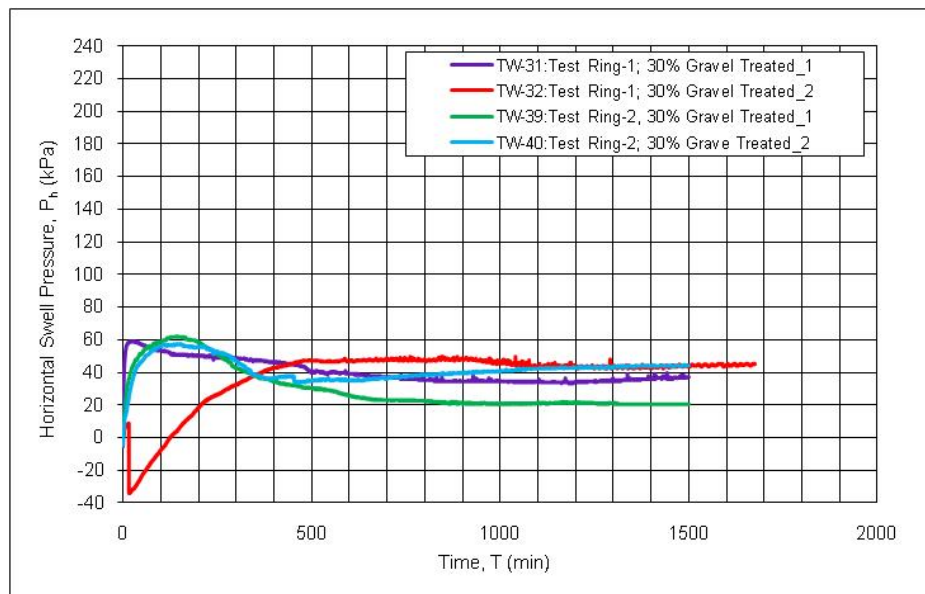


Figure C. 3 Lateral Swell Pressure vs. Time Relationship for Thin-Wall Ring Tests Performed on Type-5 Soil (30% Treated ;  $P_s=7$  kPa)

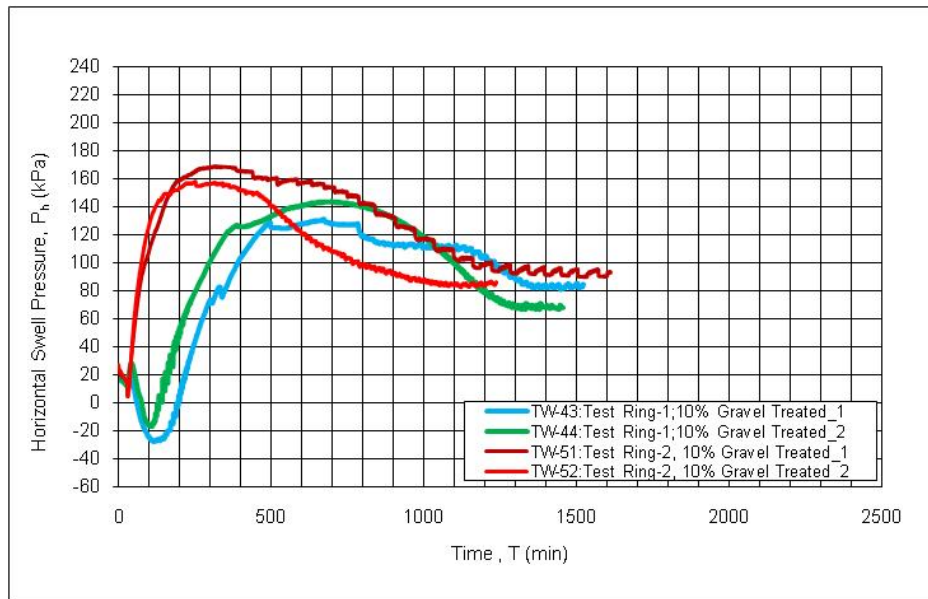


Figure C. 4 Lateral Swell Pressure vs. Time Relationship for Thin-Wall Ring Tests Performed on Type-5 Soil (10% Treated ;  $P_o=25$  kPa)

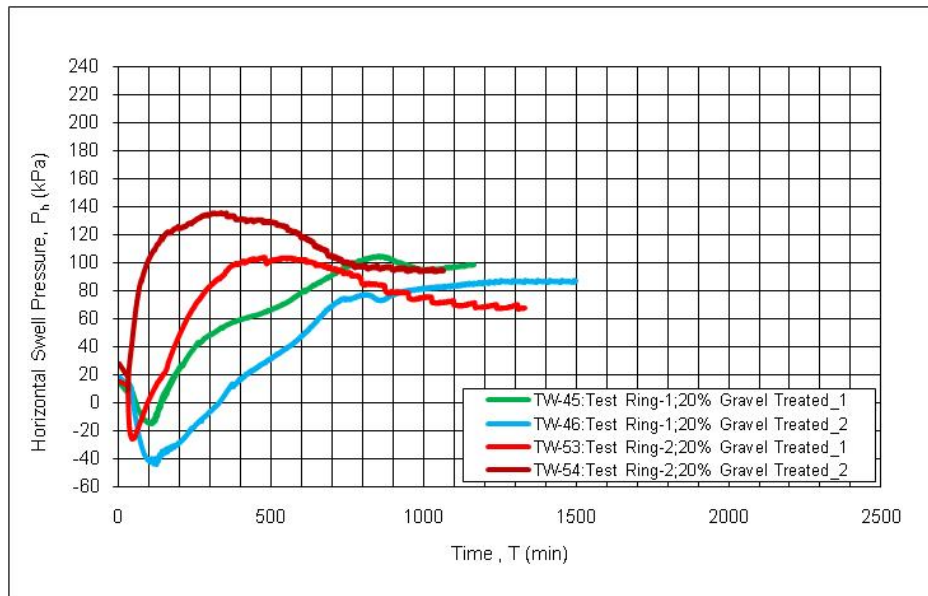


Figure C. 5 Lateral Swell Pressure vs. Time Relationship for Thin-Wall Ring Tests Performed on Type-5 Soil (20% Treated ;  $P_o=25$  kPa)

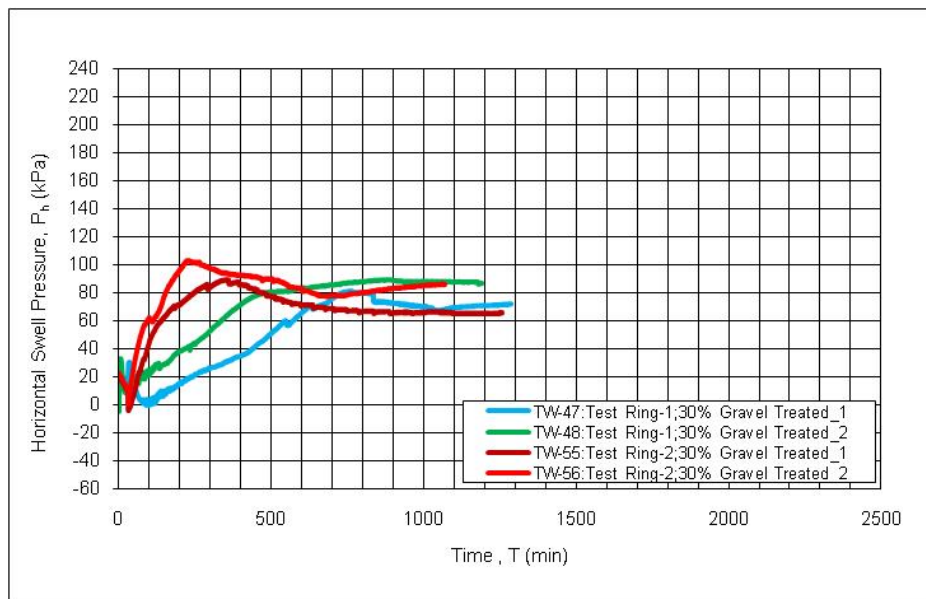


Figure C. 6 Lateral Swell Pressure vs. Time Relationship for Thin-Wall Ring Tests Performed on Type-5 Soil (30% Treated ;  $P_0=25$  kPa)

## APPENDIX D

### RESULTS OF THIN-WALL RING TESTS PERFORMED ON TYPE- 5 SOIL SAMPLES TREATED WITH SILT

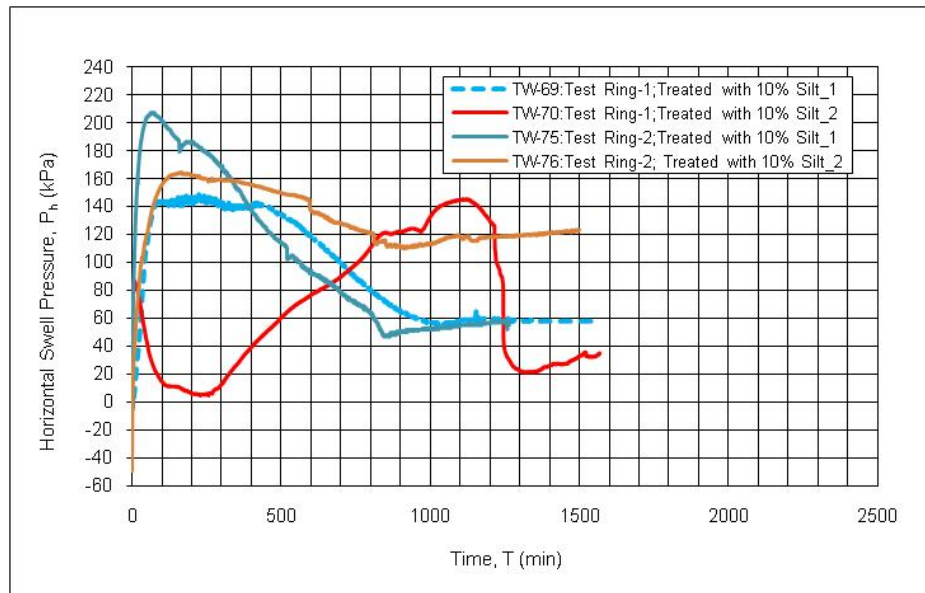


Figure D. 1 Lateral Swell Pressure vs. Time Relationship for Thin-Wall Ring Tests Performed on Type-5 Soil (10% Treated with Silt ;  $P_s=7$  kPa)

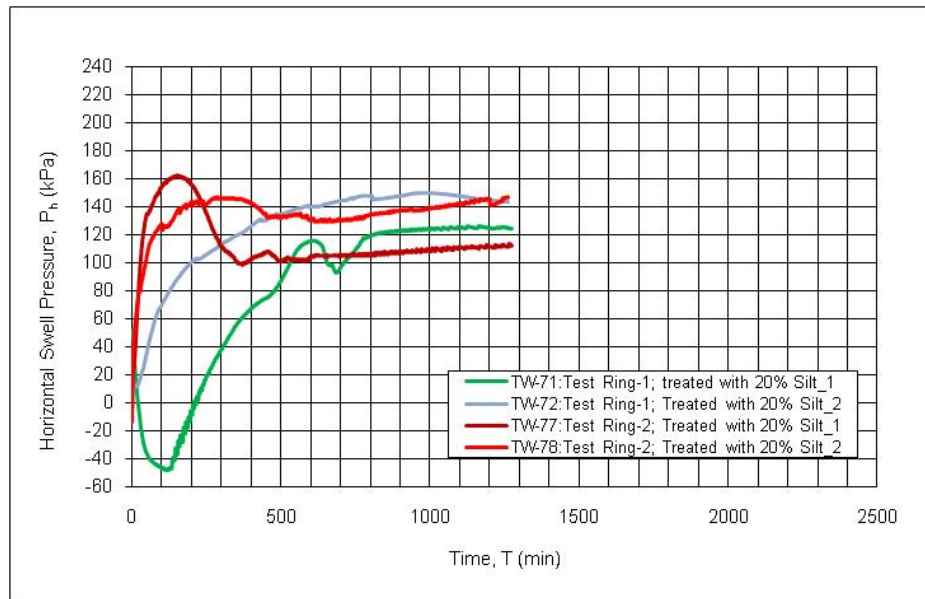


Figure D. 2 Lateral Swell Pressure vs. Time Relationship for Thin-Wall Ring Tests Performed on Type-5 Soil (20% Treated with Silt ;  $P_s=7$  kPa)

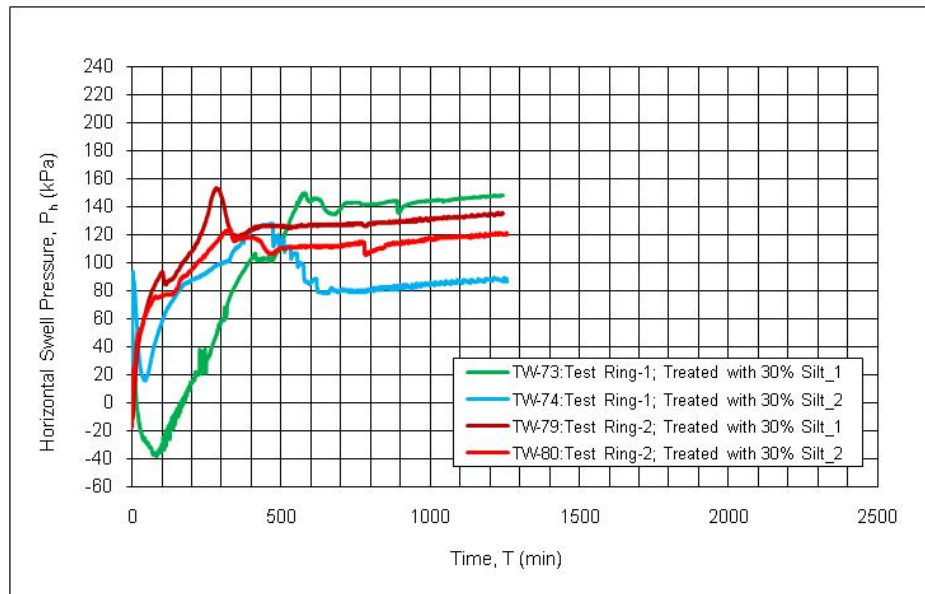


Figure D. 3 Lateral Swell Pressure vs. Time Relationship for Thin-Wall Ring Tests Performed on Type-5 Soil (30% Treated with Silt ;  $P_s=7$  kPa)



## APPENDIX E

### COMPARISON OF OEDOMETER AND MODIFIED CBR MOULD TEST RESULTS

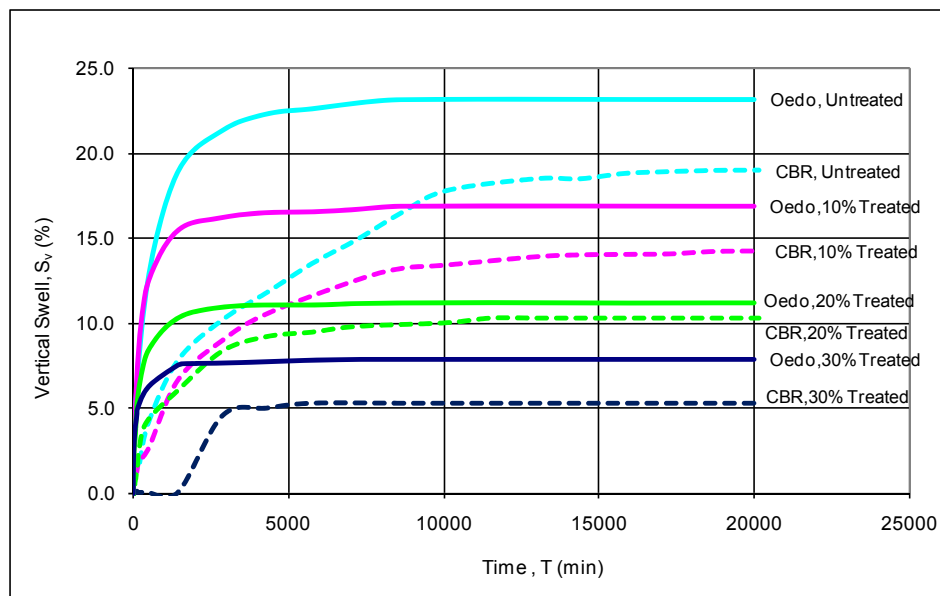


Figure E. 1 Vertical Swell Percentage vs. Time Relationship for Oedometer Tests and Modified CBR Mould Tests on Type-1 Soil Samples ( $P_s = 7$  kPa)

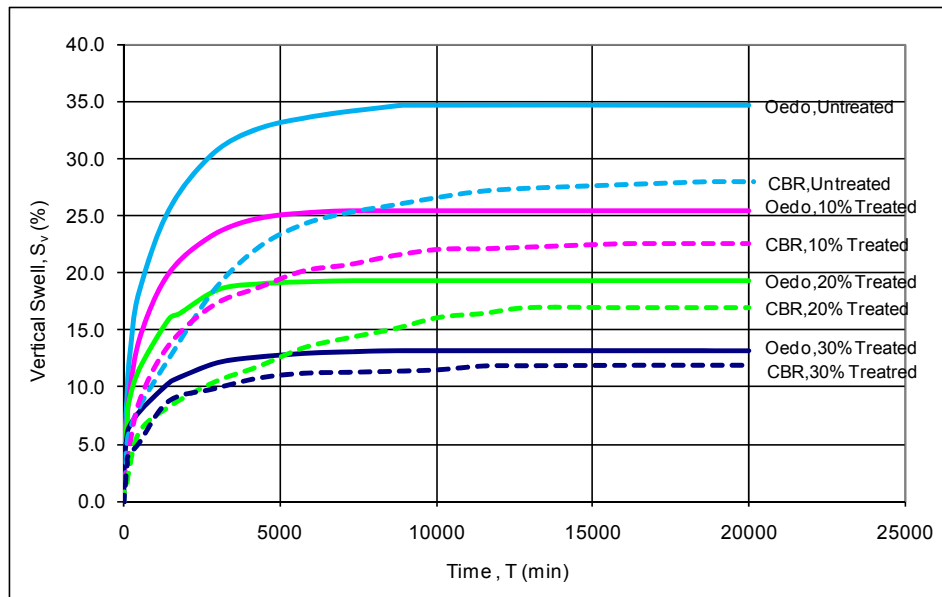


Figure E. 2 Vertical Swell Percentage vs. Time Relationship for Oedometer Tests and Modified CBR Mould Tests on Type-2 Soil Samples ( $P_s=7$  kPa)

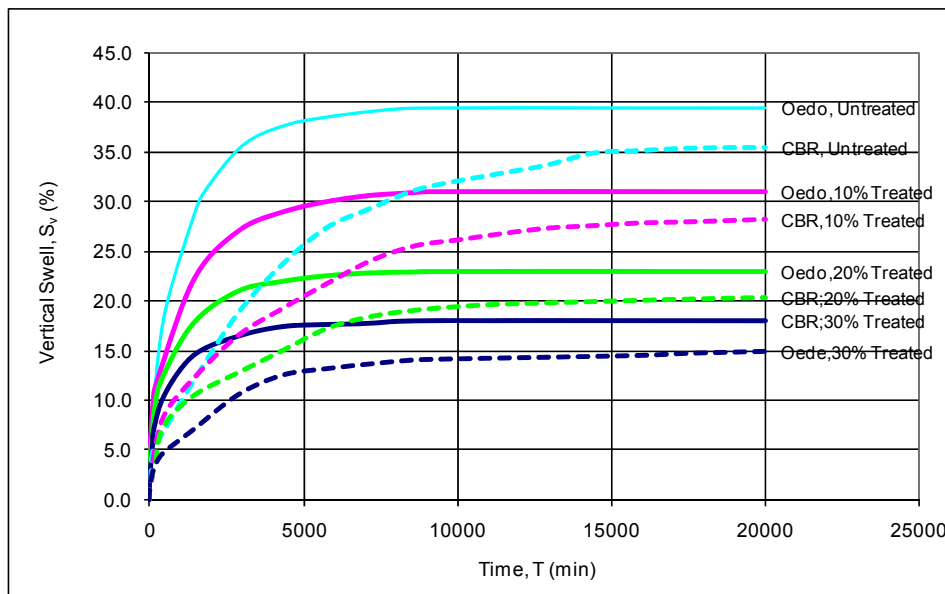


Figure E. 3 Vertical Swell Percentage vs. Time Relationship for Oedometer Tests and Modified CBR Mould Tests on Type-3 Soil Samples ( $P_s=7$  kPa)

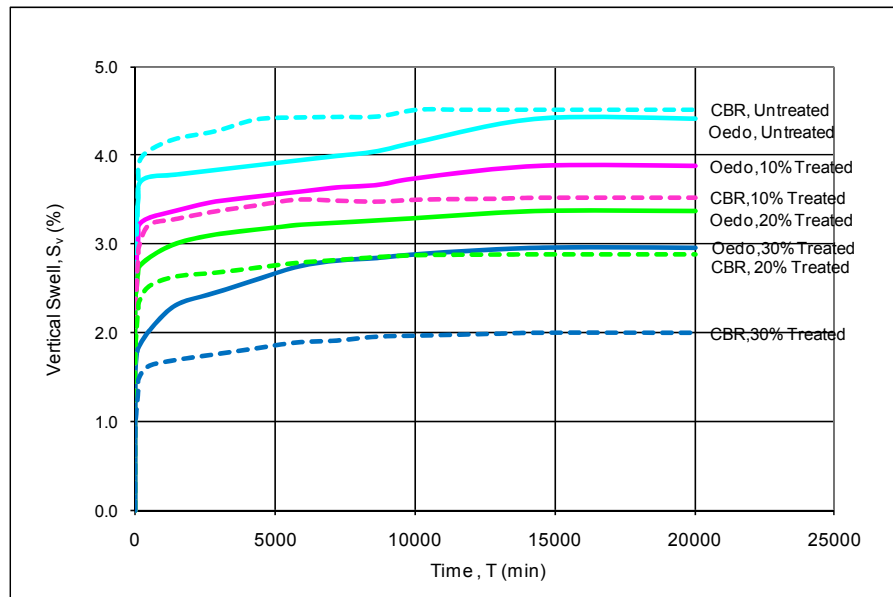


Figure E. 4 Vertical Swell Percentage vs. Time Relationship for Oedometer Tests and Modified CBR Mould Tests on Type-4 Soil Samples ( $P_s=7$  kPa)

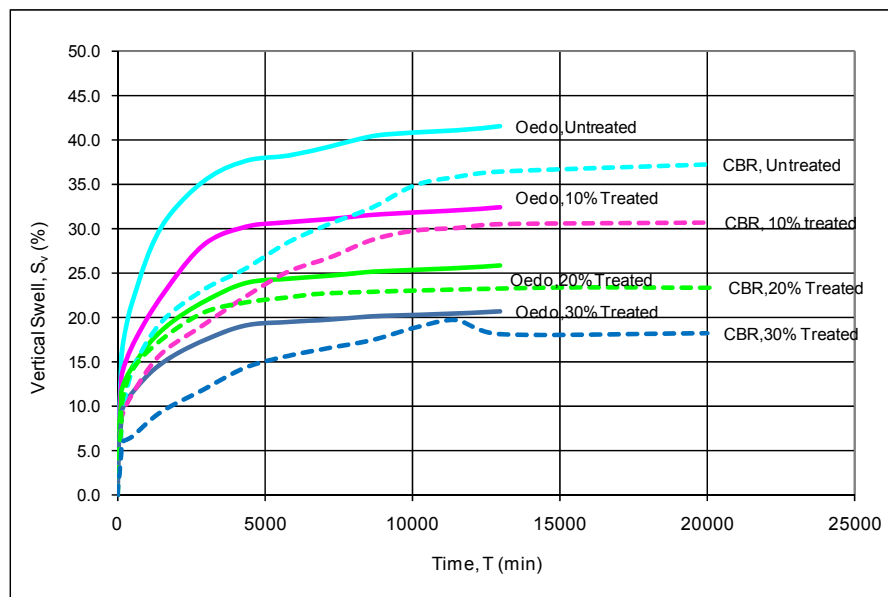


Figure E. 5 Vertical Swell Percentage vs. Time Relationship for Oedometer Tests and Modified CBR Mould Tests on Type-5 Soil Samples ( $P_s=7$  kPa)

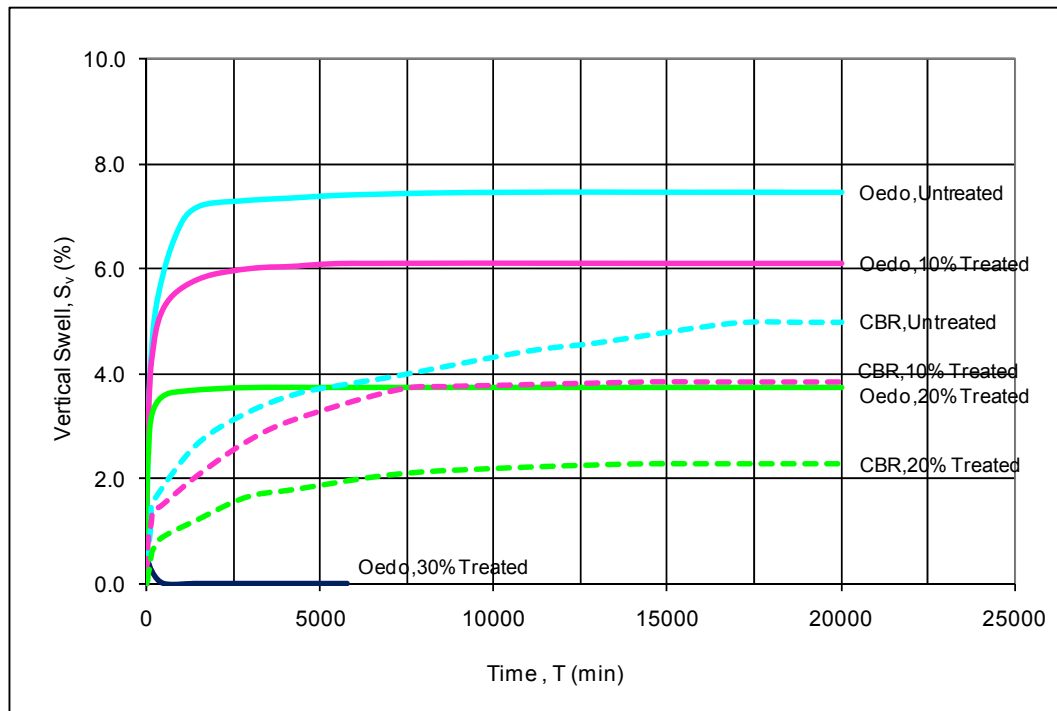


Figure E. 6 Vertical Swell Percentage vs. Time Relationship for Oedometer Tests and Modified CBR Mould Tests on Type-1 Soil Samples ( $P_0=25$  kPa)

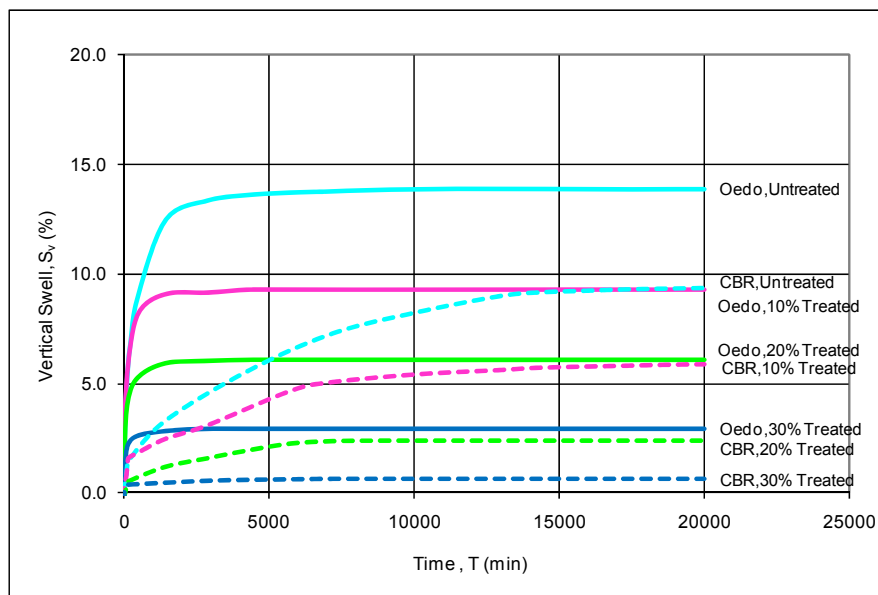


Figure E. 7 Vertical Swell Percentage vs. Time Relationship for Oedometer Tests and Modified CBR Mould Tests on Type-2 Soil Samples ( $P_0=25$  kPa)

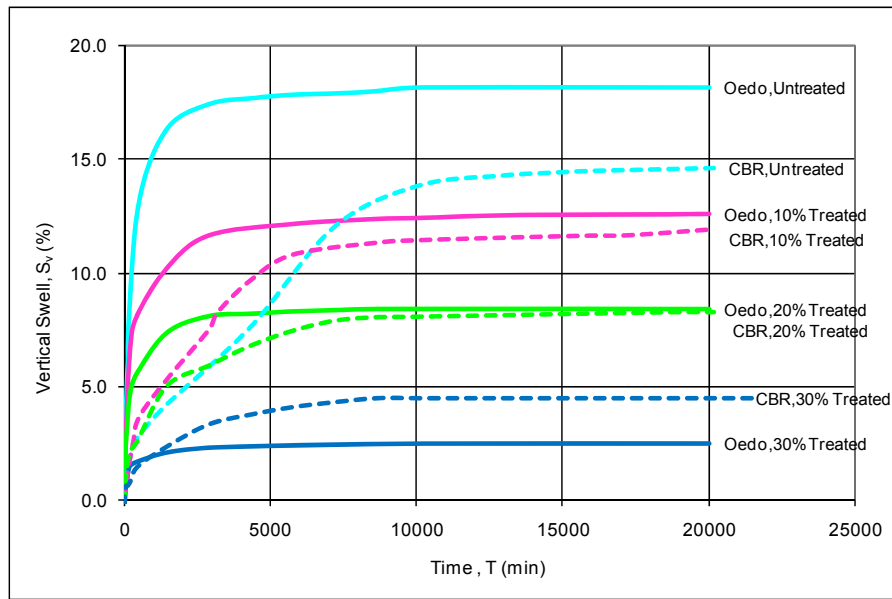


Figure E. 8 Vertical Swell Percentage vs. Time Relationship for Oedometer Tests and Modified CBR Mould Tests on Type-3 Soil Samples ( $P_0=25$  kPa)

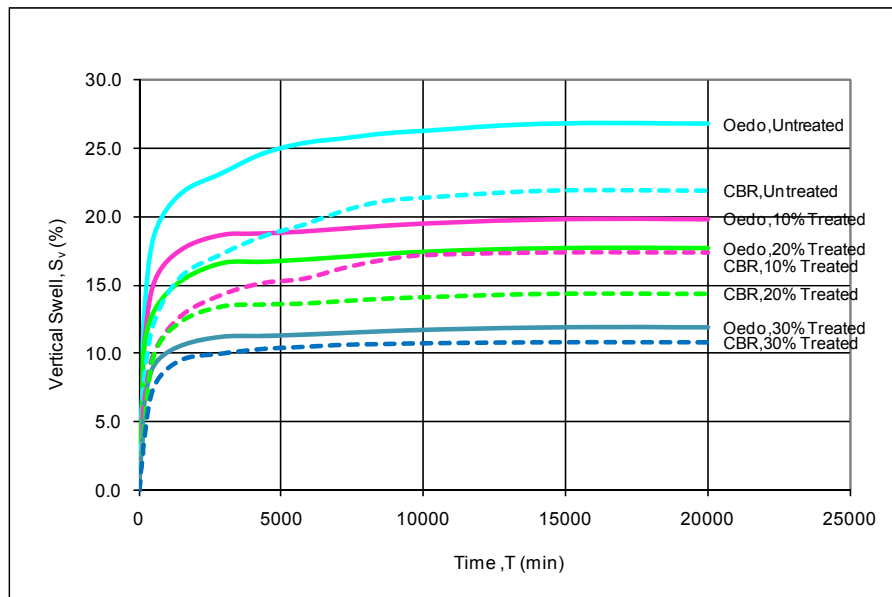


Figure E. 9 Vertical Swell Percentage vs. Time Relationship for Oedometer Tests and Modified CBR Mould Tests on Type-5 Soil Samples ( $P_0=25$  kPa)

## CURRICULUM VITAE

### PERSONAL INFORMATION

Surname, Name: Hergül, Timuçin  
Nationality: Turkish (TC)  
Date and Place of Birth: 30 October 1968, Bolu  
Marital Status: Married  
Phone: +90 312 236 44 50  
Fax: +90 312 236 44 60  
email: timucin@megamuhendislik.com.tr

### EDUCATION

Degree	Institution	Year of Graduation
MS	METU Civil Engineering	1994
BS	METU Civil Engineering	1990
High School	Konya Anadolu High School, Konya	1986

### WORK EXPERIENCE

Year	Place	Enrollment
2009-Present	MEGA Mühendislik, Müşavirlik	Geotechnical Engineer
2005-2009	AKSA Proje	Geotechnical Engineer
2000-2005	GEOMED Geoteknik Müşavirlik	Geotechnical Engineer
1999-2000	Military Service	
1997-1999	MG Strateji ve Planlama	Site Chief
1996-1997	TETCO Dwelling Construction, Israel	Site Chief
1995-1996	Karayolları Gn. Md., 17.Blg Md.	Geotechnical Engineer
1991-1995	METU Civil Engineering	Research Assistant

## **FOREIGN LANGUAGES**

Advanced English, Basic German

## **PUBLICATIONS**

Wasti, Y. and Hergül, T.,(1994)“An Experimental Study of the Performance of Geosynthetic Band Drains”, Geotextiles and Geomembranes, 13(10), 669-677 .

Hergül, T. and Wasti, Y.,(1994),”Geosentetik Şerit drenlerin Deneysel Bir Değerlendirmesi”, 5<sup>th</sup> National Conference on Soil Mechanics and Foundation Engineering, Vol.2, pp.455-67, METU, Ankara